Anaerobic Conversion of Primary Sludge to Resources in Microbial Electrochemical Cells

by

Dong Won Ki

A Dissertation Presented in Partial Fulfillment
of the Requirements for the Degree
Doctor of Philosophy

Approved April 2016 by the
Graduate Supervisory Committee:

Cesar Torres, Chair
Bruce Rittmann
Rosa Krajmalnik-Brown
Prathap Parameswaran
Sudeep Popat

ARIZONA STATE UNIVERSITY

May 2016

ABSTRACT

Microbial electrochemical cells (MXCs) serve as an alternative anaerobic technology to anaerobic digestion for efficient energy recovery from high-strength organic wastes such as primary sludge (PS). The overarching goal of my research was to address energy conversion from PS to useful resources (e.g. hydrogen or hydrogen peroxide) through bio- and electro-chemical anaerobic conversion processes in MXCs.

First, a new flat-pate microbial electrolysis cell (MEC) was designed with high surface area anodes using carbon fibers, but without creating a large distance between the anode and the cathode (<0.5 cm) to reduce Ohmic overpotential. Through the improved design, operation, and electrochemical characterization, the applied voltages were reduced from 1.1 to ~0.85 V, at 10 A m^{-2}. Second, PS conversion was examined through hydrolysis, fermentation, methanogenesis, and/or anode respiration. Since pretreatment often is required to accelerate hydrolysis of organic solids, I evaluated pulsed electric field technology on PS showing a modest improvement of energy conversion through methanogenesis and fermentation, as compared to the conversion from waste activated sludge (WAS) or WAS+PS. Then, a two-stage system (prefermented PS-fed MEC) yielded successful performance in terms of Coulombic efficiency (95%), Coulombic recovery (CR, 80%), and COD-removal efficiency (85%). However, overall PS conversion to electrical current (or CR) through pre-fermentation and MEC, was just ~16%. Next, a single-stage system (direct PS-fed MEC) with semi-continuous operation showed 34% CR at a 9-day hydraulic retention time. The PS-fed MEC also showed an important pH dependency, in which high pH (> 8) in the anode chamber improved anode respiration along with methanogen inhibition. Finally, H_2O_2 was produced in a PS-fed microbial electrochemical cell with a low energy requirement (~0.87 kWh per kg H_2O_2). These research developments will provide groundbreaking

knowledge for MXC design, commercial application, and anaerobic energy conversion from other high-strength organic wastes to resources.

DEDICATION

To my lovely soul mate, best friend, and better half, Sung Yeun Kim

And,

To my parents Jong Geun Ki and Yong Keum Jung who have guided and supported me with full of their dedication

ACKNOWLEDGMENTS

I did like mathematics but did not like too much of science when I was young because I was a real doubting Thomas. I remember telling my friends that I couldn't believe there was microbes, DNA, or something super small stuff because I've had not seen them on MY REAL EYES. Or it could be due to a little bit bad Korean education system forcing students to memorize more than to understand. So, I am thinking I became a very slow learner for every aspect of science. But, in a positive point, I have been enjoying understanding science longer in my life. When I first joined MXC team in SCEB, I was really impressed that lots of people (César, Sudeep, Prathap, etc.) had already equipped the micro-scale or even smaller size of the world on their minds, such as diffusion layer, proton gradient, or electron transport. Thinking the small world was very new to me and unfamiliar. I got used to gradually and accelerated after the amazing class "Advanced Environmental Biotechnology" by Dr. Rittmann, and his quote "think like microorganisms." I could say I am now an environmental biotechnologist.

I really must thank Dr. César Torres for his full of support and guidance in my PhD studies. He was a really problem-solver and decision maker on the project. He is one of the smartest, funniest, and humblest scientists that I have ever met. I was really lucky to meet him as my advisor in my life. I thank Dr. Bruce Rittmann to introduce me to César. And I've learned through his insightful questions to find out what is missing and what exact terminology I need to use. I also thank Dr. Rasa Krajmalnik-Brown for her kind acceptance being my committee member and advice in my dissertation. I thank Dr. Prathap Parameswaran for his support and teaching. I did not know too much of anaerobic technology in the beginning of my PhD. He was really good mentor and teacher in every aspect. I've learn a lot from him about not only my direct research but also his passion to research and relationship with others. I thank Dr. Sudeep Popat for

his guidance in my PhD study. He was my another mentor in microbial electrochemistry. Also, beginning my PhD, I was also really new to electrochemistry. I was really lucky to do several different electrochemical experiments with him.

I would like to thank my friends in SCEB. Especially, I thank Michelle for her cheers and passion as well as research input and great discussion. I thank Steven for his help of microscopic analysis for my last experiments. I thank Daewook for the help of qPCR experiments as well as his research and life advice from another Korean as senior. I thank Sean (Yenjung) for the help for lipid measurement. Also, chatting and discussion with him was a really good memory in the lab. I also thank Juan and Esra for their help to train me the sequencing analysis. I appreciate my all cubicle mates, Esra, Diana, Ibrahim, Rachel, Joe, and Brad and all the past members, also all 2nd floor crews. Lastly, I appreciate Diane and Carole for their support and reduce any stress about any non-research stuff. It was a really big comfort to me having them in the center. Especially, thank Carole for editing my several documents to get better shape. Thank you for my students, Julia and Scott for helping me lots of trifling matter in the lab and most importantly making lost of media bottles. I could meet many international scholars and thank them to have a good and enjoyable time.

Lastly I want to give my gratefulness to my family for their consistent pray, cheers, and support during my study over 5 years. Especially, I thank my parents for their sacrifice to get me better condition. Also, thank my sister- and brother-in-law family here in Arizona and also lovely niece, Sumin (Kailyn) Cheon to help stabilize here much better and all support. I appreciate my wife, Sungyeun Kim, for her full of love, support, and sacrifice. We have been through very well for the first project of our lives together for 6 years after the marriage and I wish our next chapters went much better together.

TABLE OF CONTENTS

LIST OF TABLES

LIST OF FIGURES

Figure Page

Figure Page

LIST OF ABBREVIATIONS

AD	Anaerobic digestion
ADS	Anaerobic digested sludge
AEM	Anion exchange membrane
ARB	Anode respiring bacteria
BES	2-bromoethanesulfonic acid
BMP	Biochemical methane potential
BOD	Biochemical oxygen demand
BSA	Bovine serum albumin
CE	Coulombic efficiency
COD	Chemical oxygen demand
CR	Coulombic recovery
EIS	Electrochemical impedance spectroscopy
FAME	Fatty acid methyl ester
FP	Focused Pulsed®
HRT	Hydraulic retention time
LSV	Linear sweep voltammogram
LCA	Life cycle analysis
MEC	Microbial electrolysis cell
MFC	Microbial fuel cell
MXC	Microbial electrochemical cell
OCP	Open circuit potential
OCV	Open circuit voltage
OTU	Operational taxonomic unit
PCoA	Principle coordinate analysis

PCOD	Particulate chemical oxygen demand
PEF	Pulsed electric field
PPE	Hydrogen peroxide production efficiency
PS	Primary sludge
qPCR	Quantitative (real-time) polymerase chain reaction
SCOD	Soluble chemical oxygen demand
SHE	Standard hydrogen electrode
SRT	Solid retention time
SSCOD	Semi-soluble chemical oxygen demand
TCOD	Total chemical oxygen demand
TMS	Thickened mixed sludge
TS	Total solids
TSS	Total suspended solids
TTF	Time-to-filter
VFA	Volatile fatty acids
VS	Volatile solids
VSS	Volatile suspended solids
WAS	Waste activated sludge
WWTP	Wastewater treatment plant
WtE	Waste to energy

CHAPTER 1

INTRODUCTION

1.1 Waste-to-resources

Under the law of mass conservation, all materials are recycled in the body of Earth. However, depending on the needs of Earth's humans, some concentrated materials or elements are used at a much faster rate, consequently requiring more energy, than natural recovery systems, and are wasted into a diluted environment (e.g., ocean, atmosphere or landfill), resulting in resource stress and depletion. Such resources include energy, water, and food. The most significant contribution to resource stress is that the overall world population has been increasing very fast, reaching over 7.4 x 10^6 as of February 2016 (Worldmeters, http://www.worldometers.info/world-population/). Cities or urban metropolitan area will accommodate ~70-80% of the world population by 2050 (Chandran, 2012), resulting in even more massive resource burdens.

Resource utilization to accommodate human needs yields enormous amounts of waste as by- or end-products. The paradigm of treating wastes has been changing from simple waste removal to resource recovery coupled to waste removal. Thus, wastes are not just wastes to be treated but resources to be collected. Sustainability engineers and scientists need to develop efficient and realistic resource recovery systems from wastes, especially with energy-neutral or energy-positive mechanisms.

Waste-to-Energy (WtE) or energy from waste (EfW) is the process that creates energy from a waste source, which could be semi-solid such as thickened sludge, liquid such as domestic sewage, or gas such as refinery gases (World Energy Council, 2013). Resource recovery has been most successfully applied to municipal solid waste (MSW) (Eurostat, 2013). Growing population and urbanization affects the rate of MSW

generation dramatically. The World Bank (2012) estimated that ~1.3 billion tonnes of MSW was generated in 2012, but they expect MSW generation rates to exceed urbanization rates and grow to ~2.2 billion tonnes per year by 2025 and 4.2 billion tonnes per year by 2050 (Mavropoulos, 2012). Increases in waste generation, energy costs and global energy requirements; growing concerns over environmental issues; and restricted landfill capacities have activated an increase in the global WtE market (Frost and Sullivan, 2011). Figure 1.1 shows the WtE conversion process (World Energy Council, 2013). Frost and Sullivan (2011) reported that the thermal WtE segment was expected to remain the largest fraction (~90%) of the total WtE market through 2015. Since that report, biochemical WtE has been rapidly gaining some of the market share (Frost and Sullivan, 2011) due to the environmental strain that accompanies thermal WtE. Life cycle analysis (LCA) reveals that incineration has a significant effect on climate change and acidification, and also has a significant impact on respiratory effects related to organic solvent exposure. Comparatively, the anaerobic digestion process has the least environmental impact among the WtE options (Zaman, 2009).

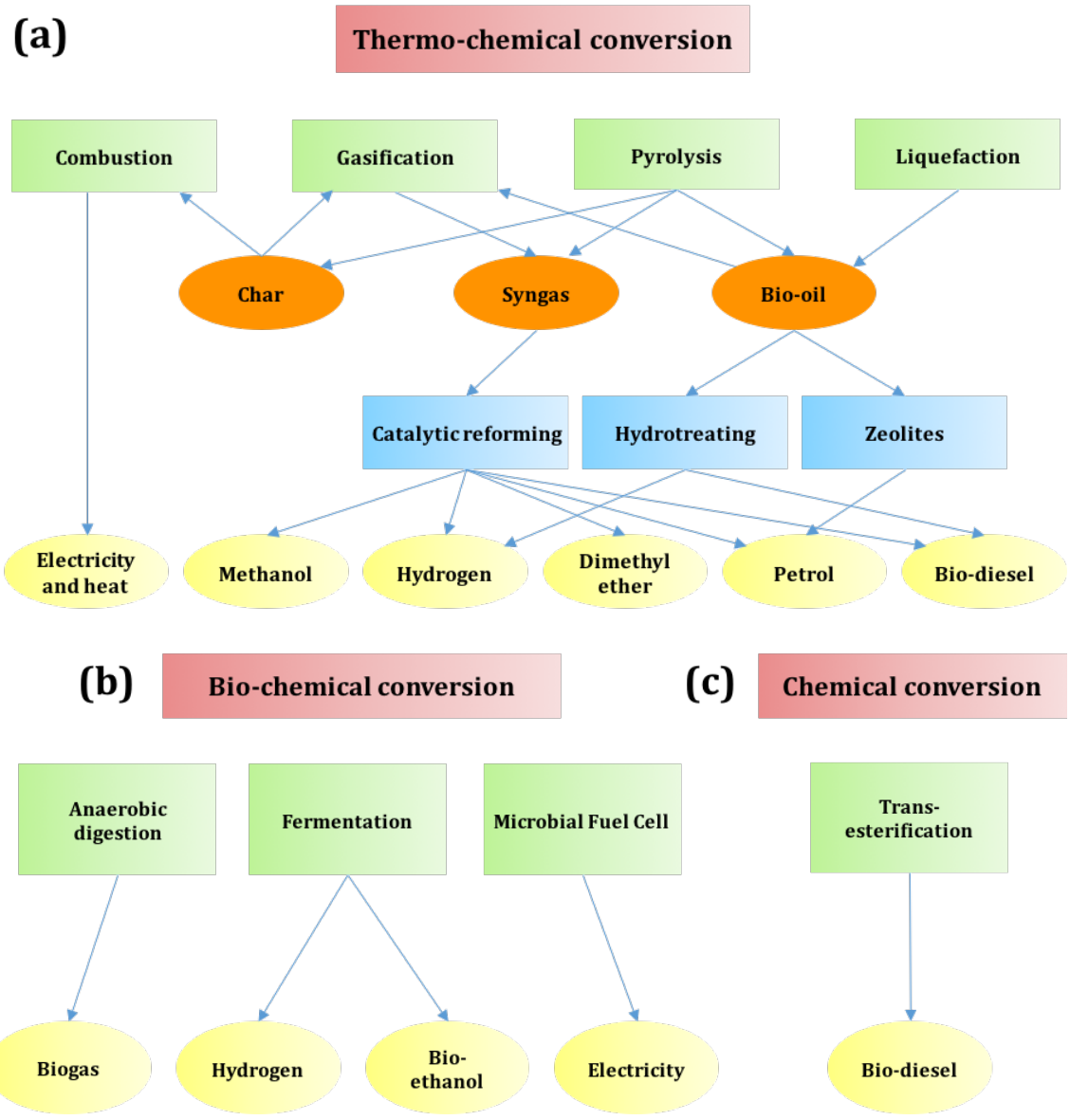

Figure 1.1 Routes of WtE segments. (a) thermo-chemical conversion, (b) bio-chemical conversion, and (c) chemical conversion. Source: World Energy Resources: Waste to Energy, World Energy Council 2013.

Wastewater treatment plants (WWTPs) are another point at which waste resources may be collected. The profound value of wastewater is better expressed when thought of as "wastes=resources" plus "water." However, for the past several decades, the development of wastewater treatment technologies has been predicated on

environmental pollution abatement before discharge into the water system. Moreover, such conventional wastewater treatment is energy-intensive for organics and nutrients removal (McCarty et al., 2011). Wastewater or sewage provides enormous potential for the recovery of chemicals, synthetic nutrients, fertilizers, bioplastics, value added fermentation products such as higher acids or alcohols, and clean water (Rulkens, 2008; Tyagi and Lo, 2013). Harvesting these resources will lead to a "sustainably engineered" water cycle, which will yield the same water quality that we have currently achieved without the current investment of copious amounts of energy and resources. Li et al. (2015) recently reported how we can generate profit from pollutants in wastewater, as shown in Figure 1.2.; an enterprise that could definitely amount to an energy-positive process with over 1.5 million dollars of profit per year. Zillertal, Strass WWTP, Austria is the best model of sustainable wastewater treatment with energy-positive operations (Wett et al., 2007; Water Environmental Research Foundation, 2010). In 2008, 20% more electrical energy was produced than required at this facility by developing methods that maximize organic carbon (or chemical oxygen demand, COD) diversion to digestion and biogas from sludges.

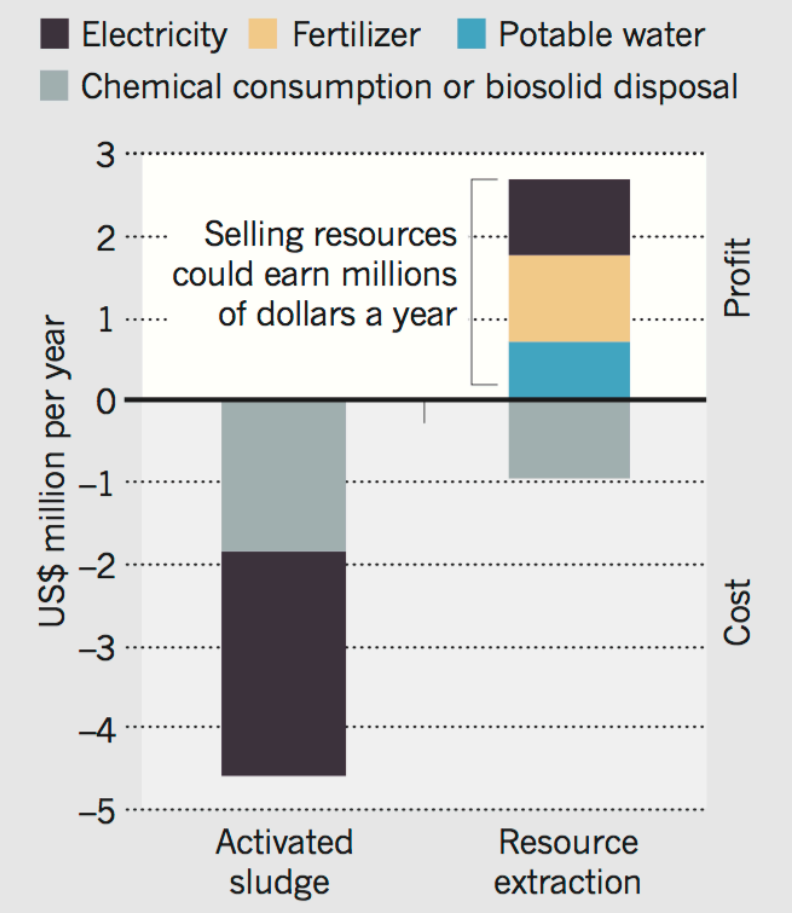

Figure 1.2 Pollutants to profits; capturing energy, nitrogen, phosphorus and water can turn wastewater treatment from a major cost into a source of profit (Estimates for a plant processing 100,000 m^3 of wastewater treatment per day). Source: Reuse water pollutant, Nature 2015.

1.2 Sludge as high strength organic waste

As explained in the previous section, organic carbon in wastewater can be transformed to biogas, such as methane, and utilized as combustible energy for operating WWTPs. Figure 1.3 shows the schematics of the typical wastewater treatment process in a WWTP. In two settlement tanks (primary and secondary), organic solids called sludges are gravitationally accumulated at the bottom of the tanks (and with the aid of chemical precipitation in certain WWTPs). Sizeable fractions of high-strength organic solids are present as primary sludge (PS) and waste activated sludge (WAS) in wastewater treatment plants (Metcalf & Eddy, 2003). PS and WAS together represent 80% of the organic carbon from influent wastewater (Shizas and Bagley, 2004). PS represents the majority fraction (66%) of organic carbon from influent wastewater.

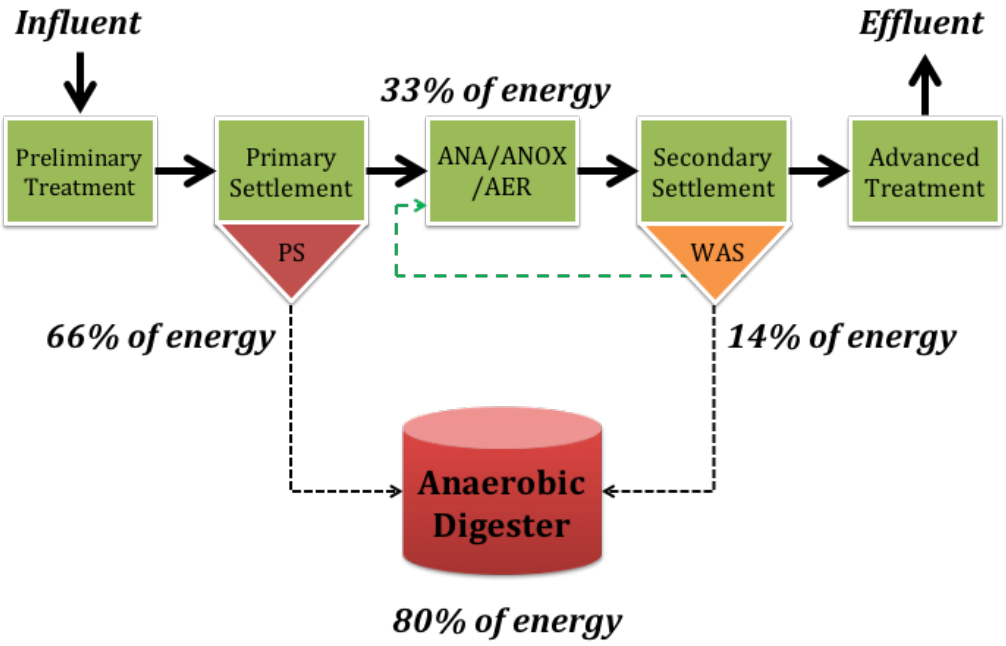

Figure 1.3 Schematics of the typical wastewater treatment process (Ana: anaerobic, Anox: anoxic, Aer: aerobic, PS: primary sludge, WAS: waste activated sludge) Here, the schematics also show the energy balance WWTP indicating 100% of energy as influent wastewater, 80% and 14% of energy as PS and WAS, respectively, collected in anaerobic digester, and 19% of energy loss as heat in the aerobic treatment.

It is important to exploit sludge characteristics to extract energy and nutrients from it. Sludge sources in a WWTP differ depending on the type of plant and its operational methods. Also, the characteristics vary according to seasons, the amount of aging (or different operational conditions, such as solid retention time, SRT), and the type of processing. In 1979, the US EPA reported the characteristics of different types of sludge based on their chemical profiles: untreated primary sludge, digested primary sludge, and untreated activated sludge (Table 1.1). Characteristics such as pH, alkalinity, and organic acid composition contribute to the success of anaerobic digestion. Also, knowing the volatile solid and nutrient (N, P, K, etc.) compositions will determine whether final products are disposed of or utilized as fertilizer. WAS particles contain living microorganisms such as bacteria, fungi, and protozoa that can feed on the incoming organics after primary clarifier application. WAS has ~10% more protein (by total dry solids, TS) than PS, and resists biological breakdown. On the other hand, PS is comprised of relatively non-cellular solids and includes more lipids and cellulose than WAS and is readily biodegradable, according to the Table 1.1.

Table 1.1 Typical chemical composition of untreated sludge and digested biosolids

Item	Untreated primary sludge		Digested primary sludge		Untreated activated sludge
	Range	Typical	Range	Typical	Range
Total dry solids (TS), %	5-9	6	2-5	4	0.8-1.2
Volatile solids (% of TS)	60-80	65	30-60	40	59-88
Grease and fats (%):					
Ester soluble	6-30	-	5-20	18	-
Ether extract	7-35	-	-	-	5-12
Protein (% of TS)	20-30	25	15-20	18	32-41
Nitrogen (N, % of TS)	1.5-4	2.5	1.6-3	3	2.4-5
Phosphorus (P_2O_5, % of TS)	0.8-2.8	1.6	1.5-4	2.5	2.8-11
Potash (K_2O, % of TS)	0-1	0.4	0-3	1	0.5-0.7
Cellulose (% of TS)	8-15	10	8-15	10	-
Iron (not as sulfide)	2-4	2.5	3-8	4	-
Silica (SiO_2, % of TS)	15-20	-	10-20	-	-
pH	5-8	6	6.5-7.5	7	6.5-8
Alkalinity (mg/L as $CaCO_3$)	500-1500	600	2500-3500	3000	580-1100
Organic acids (mg/L as acetate)	200-2000	500	100-600	200	1100-1700
Energy content (kJ/kg TSS)	23,000-29,000	25,000	9000-14,000	12,000	19,000-23,000

Source: Wastewater Engineering: Treatment and Reuse 4th Edition, Metcalf & Eddy, 2003.

1.3 Microbial electrochemical cell as transformative tool to produce useful resources

1.3.1 Overview

Microbial electrochemical cell (MXC) technology (or bioelectrochemical systems, BES) is a relatively new research area that has been gaining momentum over the last decade in the treatment of wastewater and/or production of useful resources (Torres, 2014). Figure 1.4 shows the schematics of reactions that take place in microbial electrochemical cells. In brief, an organic substrate, also referred to as an electron donor, can be used for biofilm synthesis on the anode. We call the specific microorganisms that adhere to and grow on the anode as anode-respiring bacteria (ARB) (Torres et al., 2007). ARB are the agents of microbial catalysis and they are capable of transferring electrons to the electrode, preferring the anaerobic condition near the anode. They use a minimum number of electrons for their growth and transfer the rest to the anode through the oxidation of the original electron donors. The journey of electrons from the electron donor typically ends up with final electron acceptors at the cathode by either oxygen or water in the case of a microbial fuel cell (MFC) for oxygen reduction or a microbial electrolysis cell (MEC) for hydrogen production, respectively (Figure 1.4). To meet electron neutrality between the two chambers, ions can move across the ion exchange membrane (cation or anion). The reactions at each electrode yield pH changes: decreasing pH in the anode and increasing pH in the cathode. These are important parameters for maintaining ideal condition for anode respiration as well as minimizing energy loss in microbial electrochemical cells. I discuss this more detail in Chapter 3.

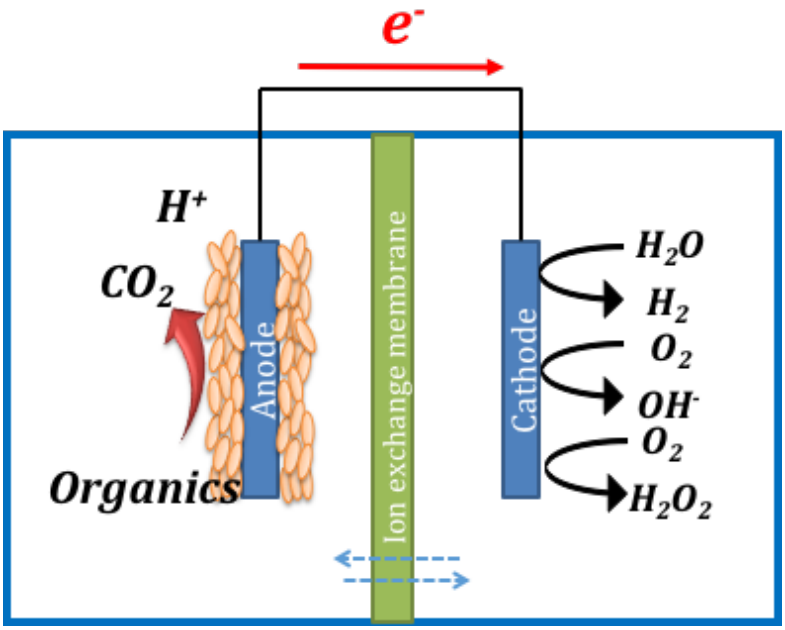

Figure 1.4 Schematics of bio- and electro-chemical reactions in microbial electrochemical cells

1.3.2 Anode-respiring bacteria

The reason why ARB are the specific microorganisms of choice for use in MECs is that their respiration systems employ solid electron acceptors such as metal oxides, carbon and metal electrodes as opposed to other microbes that utilize soluble electron acceptors such as oxygen, nitrate, and sulfate. We find representative ARB, from the genera *Geobacter* or *Shewanella*, in the natural environment (typically in soils and sediments). In order to respire metals or minerals found in their environments, they have evolved specific electron transport mechanisms called extracellular electron transfer (EET), that we can exploit as they are able to convey electrons from cells in our MEC biofilms to the surface of the solid electron acceptor (anode) (Caccavo et al., 1994; Frankel and Bazylinski, 2003; Lovley et al., 2011; Venkateswaran et al., 1999; Weber et al., 2006) via sequential redox processes from the cell membranes to the anode (Bond et al., 2012; Hernandez and Newman, 2001; Torres et al., 2010). *Geobacter* and

Shewanella are the representative ARB that have been studied extensively (Kim et al., 1999; Lovley et al., 2011; Lovely and Nevin, 2013). Researchers have optimized performance, as characterized by high current density, by using acetate as the electron donor in anaerobic condition to cultivate ARB on the anode and have found that *Geobacter* sp. flourish in MXCs if the desirable potential is provided (Torres et al., 2009). However, depending on operational conditions like substrate type, temperature, pH, etc., there are different types of ARB that can be employed. Knowing and understanding microorganisms is the key parameter for engineers to optimize reactor conditions and thus maximize performance. In addition, discovering new ARB and incorporating them into symbiotic ecosystems with other microorganisms are where the field of microbial electrochemistry is evolving (Miceli et al., 2012). Table 1.2 shows a list of known ARB from the literature.

Table 1.2 Lists of anode-respiring bacteria ([a]mediator-less and [b]–needed) modified with Logan (2009) and Guo et al. (2012) (continued on the next page).

[a]Anode-respiring bacteria	Classification*	Comments	References
Acidiphilium sp.3.2 Sup5	Alphaproteobacteria	Current at low pH and in the presence of oxygen in a poised potential system	Borole et al., 2008
Aeromonas hydrophilia (A3)	Deltaproteobacteria		Pham et al., 2003
Clostridium butyricum	(Phylum) Firmicutes	First gram-positive bacterium shown to produce electrical current in an MFC	Park et al., 2001
Desulfobulbus propionicus	Deltaproteobacteria		Holmes et al., 2004
Desulfovibrio desulfuricans	Deltaproteobacteria	Reduced sulphate when growing on lactate; resazurin in the medium was not thought to be a factor in power production	Zhao et al., 2008
Desulfuromonas acetoxidans	Deltaproteobacteria	Identified in a sediment MFC community and shown to produce power	Bond et al., 2002
Escherichia coli	Gammaproteobacteria	Found to produce current after long acclimation times	Zhang et al., 2006

Table 1.2 (continued) Lists of anode-respiring bacteria ([a]mediator-less and [b]–needed) modified with Logan (2009) and Guo et al. (2012)

[a]Anode-respiring bacteria	Classification*	Comments	References
Geobacter metallireducens	Deltaproteobacteria	Shown to generate electricity in a poised potential system	Bond et al., 2002
Geobacter sulfurreducens	Deltaproteobacteria	Generated current without poised electrode	Bond et al., 2003
Geopsychrobacter electrodiphilus	Deltaproteobacteria	Psychrotolerant	Holmes et al., 2009
Geothrix fermentans	(Phylum) Acidobacteria	Produced an unidentified mediator	Bond & Lovley, 2005
Klebsiella pneumonia L17	Gammaproteobacteria	The first time this species produced current without a mediator	Zhang et al., 2008
Ochrobactrum anthropic YZ-1	Alphaproteobacteria	An opportunistic pathogen, such as *P. aeruginosa*	Zuo et al., 2008
Pichia anomala	(Kingdom) Fungi	Current generation by a yeast	Prasad et al., 2007

Table 1.2 (continued) Lists of anode-respiring bacteria ([a]mediator-less and [b]–needed) modified with Logan (2009) and Guo et al. (2012)

[a]Anode-respiring bacteria	Classification*	Comments	References
Pseudomonas aeruginosa	Gammaproteobacteria	Produced low amounts of power through mediators such as pyocyanin	Rabaey et al., 2004
Rhodoferax ferrireducens DX-1	Betaproteobacteria	Used glucose	Claudhuri et al., 2003
Rhodopseudomonas palustris	Alphaproteobacteria	Produced high power densities of 2.72 W/m^2 compared with an acclimated wastewater inoculum (1.74 W/m^2)	Xing et al., 2008
Shewanella oneidensis DSP10	Gammaproteobacteria	Achieved a high power density (2 W/ m^2 or 500 W/m^3) by pumping cells grown in a flask into a small (1.2 mL) MFC	Ringeisen et al., 2007

Table 1.2 (continued) Lists of anode-respiring bacteria ([a]mediator-less and [b]–needed) modified with Logan (2009) and Guo et al. (2012)

[a]Anode-respiring bacteria	Classification*	Comments	References
Shewanella oneidensis MR-1	Gammaproteobacteria	Various mutants identified that increase current or lose the ability for current generation	Bretschger et al. 2007
Shewanella putrefaciens IR-1	Gammaproteobacteria	Direct proof of electrical current generation in an MFC by a dissimilatory metal-reducing bacterium	Kim et al., 1999
Thermincola sp.strain JR	(Phylum) Firmicutes		Wrighton et al., 2008

Table 1.2 (continued) Lists of anode-respiring bacteria ([a]mediator-less and [b]–needed) modified with Logan (2009) and Guo et al. (2012)

[b]Anode-respiring bacteria	Classification*	Comments	References
Actinobacillus succinogenes	Gammaproteobacteria	Neutral red or thionin as electron mediator	Park et al., 1999
Desulfovibrio desulfuricans	Gammaproteobacteria	Sulphate/sulphide as mediator	Park et al., 1997
Erwinia dissolvens	Gammaproteobacteria	Ferric chelate complex as mediators	Vega and Fernandez, 1987
Escherichia coli	Gammaproteobacteria	Mediators such as methylene blue needed	Schröder et al., 2003
Gluconobacter oxydans	Alphaproteobacteria	Mediator (HNQ, resazurin or thionine) needed	Lee et al., 2002
Klebsiella pneumoniae	Gammaproteobacteria	HNQ as mediator	Rhoads et al., 2005
Lactobacillus plantarum	(Phylum) Firmicutes	Ferric chelate complex as mediators	Vega and Fernandez, 1987

Table 1.2 (continued) Lists of anode-respiring bacteria ([a]mediator-less and [b]–needed) modified with Logan (2009) and Guo et al. (2012)

[b]Anode-respiring bacteria	Classification*	Comments	References
Proteus mirabilis	Gammaproteobacteria	Thionin as mediator	Thurston et al., 1985; Choi et al., 2003
Pseudomonas aeruginosa	Gammaproteobacteria	Pyocyanin and phenazine-1-carboxamide as mediator	Rabaey et al., 2004
Shewanella oneidensis	Gammaproteobacteria	Anthraquinone-2,6-disulfonate (AQDS) as mediator	Ringeisen et al., 2006
Streptococcus lactis	(Phylum) Firmicutes	Ferric chelate complex as mediators	Vega and Fernandez, 1987

* Classification of ARB are mostly Class level except some Phylum and Kingdom level noticed in the column.

1.3.3 Energy losses in MXCs

Fuel cell technology deals with customizing electron-harvesting systems that convert chemical into electrical energy in particular environments. Typical chemical fuel cells use hydrogen to produce electrical energy or electricity. As an MXC is one form of chemical fuel cell, most fuel cell principles are the same. Energy transformation of chemical fuel is stepwise from anode to cathode. Electrons from donor substrate are transferred to the anode, and the captured electrons flow from the anode to the cathode through an external circuit by the difference in the electrochemical potential or potentiostat. At the cathode, the oxidants (O_2 or H_2O) are reduced to the hydroxide ions ($4e^-$ oxygen reduction reaction) or hydrogen gas ($2e^-$ water splitting reaction) in fuel cells or electrolysis cells, respectively. Over the half-reactions at each anode and cathode, energy losses (or overpotentials) occur in fuel cells. These energy losses represent serious challenges in reactor design and operation. There are three major losses in fuel cells: activation, concentration, and ohmic (O'Hayre et al., 2009). Activation energy loss is the energy required to overcome activation energy barriers across the interface between electrode and electrolyte to generate net current. Concentration energy loss is derived from the concentration gradient between bulk solution and the surface of the electrode . Ohmic energy loss is caused by 1) electrical resistance to current in electrodes and connecting wire and 2) transfer of counter ions for charge neutrality in electrolytes and membranes. Ionic Ohmic loss is usually > 90% of total Ohmic losses. The electronic and ionic Ohmic losses are determined by following equations:

$$\eta_{Ohm-electronic} = i \times R_{ext} \quad (1.1)$$

$$\eta_{Ohm-ionic} = j \times (R_{electrolyte} + R_{membrane}) \quad (1.2)$$

where, $\eta_{\text{Ohm-electronic}}$ is the Ohmic loss in electrodes and connecting wire (V), i is current (A), R_{ext} is the external resistance (Ω), $\eta_{\text{Ohm-ionic}}$ is the Ohmic loss in electrolyte and

membrane (V), j is current density (A/cm²), $R_{electrolyte}$ and $R_{membrane}$ are the area specific resistances in liquid electrolyte and membrane, respectively (Ω·cm²). Here, in ionic Ohmic losses (or Ohmic overpotential), the current flow unit is changed into flux form (mass/area·time) as current density since the ions transport along the planar membrane. As most of fuel cells have good conductors, electronic Ohmic loss is typically negligible. However, we need to consider ionic Ohmic losses with or without a membrane when using real wastewater since the conductivity of wastewater is typically low, ~1 mS/cm (Taylor and Gardner, 2007). Moreover, reactors should be designed with a very short distance between the anode and cathode to reduce Ohmic losses. The different form of Ohmic loss is shown in the following equation:

$$\eta_{Ohm-ionic-electrolyte} = \frac{j \times d}{\kappa} \quad (1.3)$$

where d is the distance for ion travel (cm) between anode and cathode, and κ is the conductivity of the electrolyte (S/cm). Figure 1.5 shows the variance of Ohmic overpotential calculated with equation (1.3) depending on current density in the MXC, wastewater or electrolyte solution conductivity, and the distance between the anode and cathode. For this reason, Popat and Torres (2016) highlighted that distance between anodes and cathodes should be in the millimeter (mm) instead of centimeter (cm) range. MXCs are more effective in treating high-strength organic wastes, such as sludges in wastewater, than they are at treating low-strength organic wastes like domestic wastewater (McCarty et al., 2011) due to higher conductivity or alkalinity (Table 1.1).

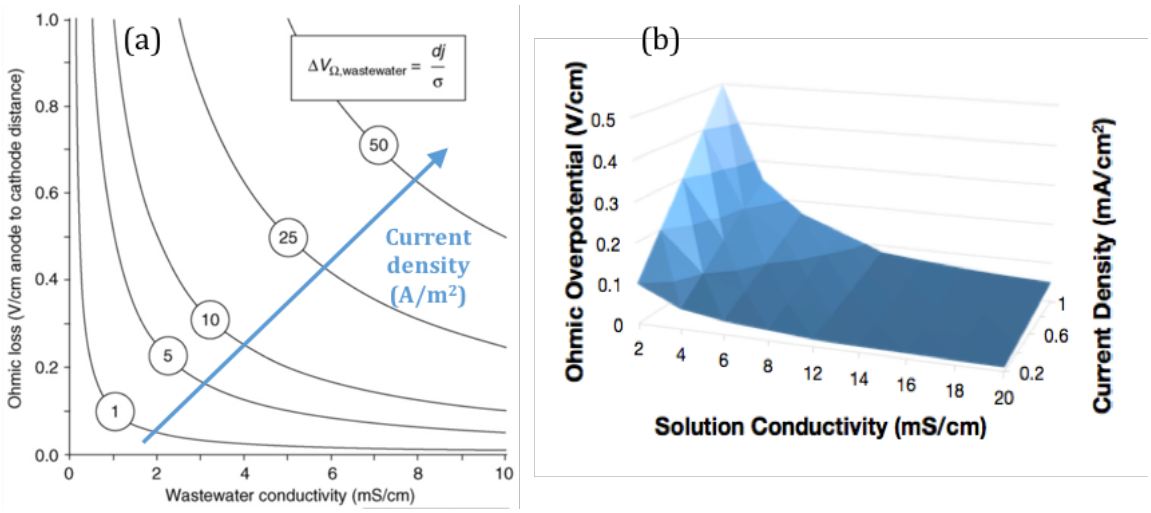

Figure 1.5 Ohmic loss (electrolyte) in microbial electrochemical cells as shown in Rozendal et al., (2008) (a) and Popat and Torres (2016) (b). These graphs illustrate the calculated Ohmic loss (electrolyte) per centimeter of distance between anode and cathode depending on electrolyte solution conductivity and current density.

Thus, MXC system design requires additional bio- and electro-chemical development in order to maximize the efficiency of the anaerobic conversion process when complex organic substrates are used. For example, a high-surface area anode promotes syntrophies between ARB and other anaerobic microbes by providing more space for them to adhere in close proximity to one another. Also, reduced spacing between anode and cathode results in less Ohmic loss within an MXC. Understanding reactor design as well as operation parameters will provide important guidelines for further optimization of MXCs.

1.3.4 MXC applications – emerging options for wastewater treatment and resource recovery

As shown in Figure 1.4, captured electrons at the anode can then be used for power production in microbial fuel cells (MFCs) or hydrogen production at the cathode with an additional voltage in microbial electrolysis cells (MECs). MFCs and MECs are

the most popular options studied in MXC applications (Borole et al., 2011; Logan et al., 2006). In the case of MFCs, we can theoretically obtain ~1.1 V of energy coupled with acetate oxidation at the anode and oxygen reduction at the cathode (Logan et al., 2006). However, as explained by the energy losses in the above section, we obtain only ~0.2-0.4 V (Cheng and Logan, 2011; Logan, 2009). Also, oxygen diffusion hinders viable organic loss for electrical energy production even though removal of wastewater COD increases (Ge et al., 2013; Angosto et al., 2015; Zhuang et al., 2012). In the case of MECs, there is no concern of oxygen diffusion, but energy losses (or overpotentials) are applied in the same way as MFCs. Thus, we need to apply more energy than theoretically required. However, valuable hydrogen gas production may be able to offset energy losses because hydrogen is a promising energy-carrier, having high energy content and minimal pollution potential. For example, the heat of combustion of hydrogen is higher than that of methane: 142 kJ/mol of e^- for H_2 and 100 kJ/mol of e^- for CH_4. Even though we consider H_2 to be a promising future energy source, it is currently challenging to link it to wastewater treatment due to storage and transportation safety issues.

Other emerging options for wastewater treatment and useful resource recovery involve the production of caustic solution and hydrogen peroxide (Rabaey et al., 2010; Rozendal et al., 2009; Borole et al., 2011). Production of caustic in the cathode using MXCs is a cost-effective and novel method with removal of organic pollutants of the wastewater in the anode, but also presents logistical challenges since the products must be transported out of wastewater treatment plants. Hydrogen peroxide (H_2O_2) production in MXCs is a very fascinating option because H_2O_2 can disinfect or pre-treat wastewater on-site. Existing facility units such as UV or addition of iron represent tertiary treatments known as advanced oxidation processes (AOPs). However, conventional H_2O_2 production methods are energy-intensive and use potentially

carcinogenic compounds as catalysts, which may threaten human health (Pletcher, 1999; Campos-Martin et al., 2006). Therefore, H_2O_2 generating MXC technology benefits society by: 1) treating wastewater, 2) converting renewable energy, 3) producing a useful, safe, and environmentally friendly resource (H_2O_2), and 4) generating reusable water with a built-in disinfectant (H_2O_2). Rozendal et al. (2009) first reported this concept using acetate as the substrate and a carbon cloth gas diffusion electrode as an air-cathode. Cathodic batch operation yielded ~0.13 wt% of H_2O_2 with an energy requirement of ~0.93 kWh/kg H_2O_2.

There are many limitations when studying H_2O_2 production in microbial electrochemical cells. H_2O_2 can decompose much faster at a certain condition, for example, high pH (>12) and/or metal ion presence. Since H_2O_2 itself is a strong oxidant that generates even stronger radicals (e.g. $OH^{\cdot}$), it is important to use compatible membrane, container, and cathode materials. For example, Stadie (2015) reported that homogeneous membranes (e.g. FAA) cannot withstand H_2O_2 exposure and are, thus, not recommended. H_2O_2 production and preservation is not easy in an MXC due to its inherent characteristics of self-decay and form change in response to pH fluctuations at the cathode. The theoretical H_2O_2 production reaction is

$$O_2 + 2e^- + 2H^+ \rightarrow H_2O_2$$

However, if the proton supply (H^+) is insufficient, the reaction follows this route, instead:

$$O_2 + H_2O + 2e^- \rightarrow HO_2^- + OH^-$$

where two anions are produced, causing an increase in pH in the cathode chamber. The pK_a of H_2O_2 is 11.75 at standard temperature and pressure (STP). Thus, at high pH (> 12), the form of H_2O_2 is mainly HO_2^-, which is more susceptible to water attack without

stabilizers. Thus, maintaining cathode pH (< 10) is important to achieve higher H_2O_2 concentrations and cathodic efficiency.

1.4 Research questions, objectives, and dissertation outline

My dissertation addresses energy conversion from high-strength organic wastes to electrical current in microbial electrochemical cells to establish a viable decentralized wastewater treatment system focusing on valuable chemical (H_2O_2) production. But, treatment of real, large-scale wastewater streams using H_2O_2-producing microbial electrochemical cells is in its early-stages due to significant research gaps. In order to reduce the gaps, we need to understand the following three important research areas: wastes (e.g., sludge) to electricity conversion, optimization of bio- and electro-chemical anaerobic conversion processes, and H_2O_2 production from sludge in MXCs. Figure 1.6 shows the schematics of my dissertation research segments.

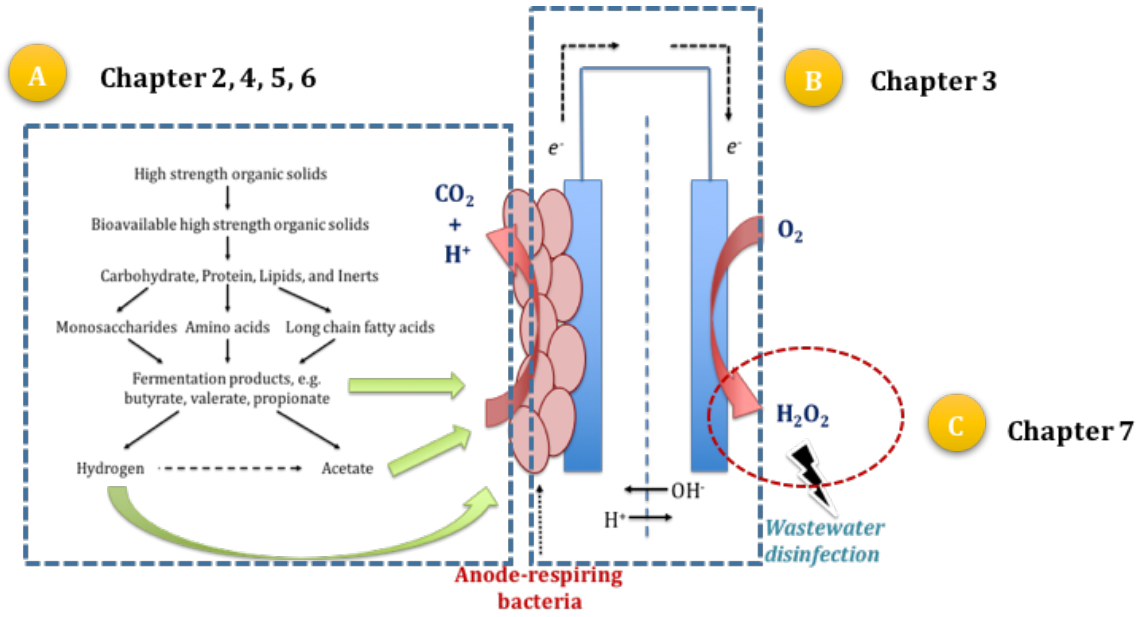

Figure 1.6 Microbial electrochemical cells (MXCs) technology combined with anaerobic energy conversion and hydrogen peroxide (H_2O_2) production.

A. Anaerobic energy conversion processes of high-strength organic wastes in MXCs - Chapter 2, 4, 5, and 6

Scientific knowledge about energy conversion from high-strength organic wastes (e.g. sludge) into electric energy in MXCs is minimal. Since ARB are significantly faster than methanogens at consuming VFAs (Torres et al., 2010), hydrolysis can be the rate-limiting step in the MXC anaerobic conversion process. To improve the rate of hydrolysis, pre-treatment technologies may be applied, including mechanical, thermal, alkaline, ultrasonication, and microwave pre-treatments (Cho et al., 2012; Eskicioglu et al., 2006; Kim et al., 2003; Park et al., 2004; Pilli et al., 2011). Pre-fermentation ahead of MXC loading can also be considered as a pre-treatment along with solids stabilization and useful substrate selection such as VFAs (Choi and Ahn, 2014; Yang et al., 2013). However, transformation of complex organic wastes in batch and (semi-) continuous settings is not well understood in MXCs. Therefore, long-term, (semi-) continuous operation using high-strength organic wastes is a pressing need that will promote consistent electron capture from waste and, consequently, MXC scale-up. Here, I chose primary sludge (PS) as a representative complex organic biomass (or collection of high-strength organic solids). I selected pulsed-electric-field (PEF) as my pre-treatment technology because it has been studied with great success in treating waste activated sludge (WAS), reducing solids volume, and providing a sustainable carbon source for denitrification (Lee, 2010; Salerno et al, 2009).

B. MXC design, operation, and electrochemical characterization - Chapter 3

MXC system design requires additional bio- and electro-chemical development in order to maximize the efficiency of the anaerobic conversion process. For example, a high-surface area anode could promote syntrophies between ARB and other anaerobic microbes by providing more space for them to adhere in close proximity to one another.

Also, reduced spacing between anode and cathode results in less Ohmic loss within an MXC as I explained in the above section (1.3.3). Understanding reactor design as well as operation parameters will provide important guidelines for further optimization of MXCs.

C. H_2O_2 production using PS in MXCs - Chapter 7

H_2O_2 production is thermodynamically feasible through 2-electron oxygen reduction reaction at the cathode in MFCs (Rozendal et al., 2009). If H_2O_2-producing microbial electrochemical cells were to be applied to the wastewater treatment process, the use of H_2O_2 can be versatile such as tertiary wastewater treatment with ultraviolet irradiation or iron (advanced oxidation process, AOP), pretreatment of influent sludge, or disinfection of digested sludge. However, H_2O_2 production in MXCs is a relatively rudimentary research topic to reveal the operational condition especially with PS as the original electron donor.

I, therefore, pose several questions to be answered in my research. First, how much do our newly designed MXCs improve their performance in terms of energy investment, capture, and loss? Second, how much does PEF treatment affect PS hydrolysis to enhance bioavailability and energy capture? Third, can pre-fermentation and PEF treatment affect energy recovery from PS in MXCs? Fourth, is the direct addition of PS to MXCs reliable and durable for long term operation and able to recover enough energy from PS? Finally, can hydrogen peroxide be produced in MXCs using PS as an electron source?

Chapter 2 focuses on the energy sources found in various wastewater streams. I deliver a general background on high-strength organic wastes and explain, through a literature summary, how solid wastes transform to viable soluble organics, and thus to

useful energy, with anaerobic technologies including anaerobic digesters (AD) and microbial electrochemical cells (MXCs).

Researchers have been using different MXC designs for each of the individual research aims, but we must consider important performance challenges for practical applications. One of the main performance challenges in MXCs is the low voltage efficiency in comparison to other fuel and electrolysis cells. To improve the voltage efficiency, I developed a new flat-plate MEC that allows a high surface area for the anode using carbon fibers, while maintaining a minimal distance between the anode and the cathode. I characterized the applied voltages in flat-plate MECs as individual overpotentials, such as activation, Ohmic, and concentration overpotentials, to optimize and increase voltage efficiency using commercially available materials and adding carbon dioxide to the cathode. I present these in Chapter 3, which was published in *Chemical Engineering Journal* (Ki et al., 2016).

PS is a renewable and sustainable energy source, but pre-treatment is often required to accelerate hydrolysis of organic solids. PEF treatment has been proven effective for WAS, but its impact on PS is not known (Salerno et al, 2009; Lee et al, 2010). Therefore, I evaluated the impacts of PEF pre-treatment of PS on energy recovery by methanogenesis and fermentation to volatile fatty acids (VFAs). I present these in Chapter 4, which was published in *Environmental Engineering Science* (Ki et al., 2015).

Pre-fermentation ahead of MXC, as a two-stage system, would be a good means to increase the conversion of high-strength organic wastes (e.g., PS) to simple organic acids, which are the substrates available to the anode-respiring bacteria (ARB) that capture the electrons from the organic substrates as electric current. However, practical application of pre-fermentation followed by an MXC needs to be evaluated for long-term continuous operation, even though the concept of pre-fermentation was supported by

previous batch studies (Choi and Ahn, 2014; Mahmoud et al., 2014; Yang et al., 2013). I have investigated the combination of PEF pre-treatment and semi-continuous pre-fermentation of PS to produce volatile fatty acids (VFAs) as the electron donor for microbial electrolysis cells (MECs). I present these in Chapter 5, which was published in *Bioresource Technology* (Ki et al., 2015).

Direct addition of PS to MXCs, as a single-stage system, could be a simple process compared to the two-stage system described in Chapter 5. Under anaerobic conditions, methanogenesis always governs as the major electron sink and competes with ARBs that capture electrons as electrical currents (Parameswaran et al., 2009). Therefore, I evaluated energy recovery in the forms of methane and electrical current from PS directly added to MECs in batch and semi-continuous, long-term operation. Also, I evaluated the importance of pH in the anode in terms of energy recovery and effluent sludge quality. I present these in Chapter 6, which will be submitted to *Water Research*.

Chapter 7 combines all lessons obtained from Chapters 3-6 to demonstrate production of hydrogen peroxide (H_2O_2) in the cathode chamber with direct addition of PS into the anode chamber in flat-plate microbial electrochemical cells. This chapter will be submitted to a peer-review journal.

Chapter 8 is a summary of my research and explains the significance of my work.

CHAPTER 2

BACKGROUND ON HIGH-STRENGTH ORGANIC WASTES

2.1 What are high-strength organic wastes?

The definition of high-strength organic waste (or wastewater) is somewhat obscure because there is no specific range of standardized characteristics. Typically, ultimate biochemical oxygen demand (BOD_L), total suspended solids (TSS), and fat, oil, and grease (FOG) are used as parameters for determining high-strength organic wastes. These values vary widely; BOD_5 levels range from 100-3685 mg/L, TSS from 142-4375 mg/L, and FOG from 50-14,958 mg/L (Jantrania, 1991; Lowe et al., 2007; Matejcek et al., 2000; Siegrist et al., 1984). Based on the literature, Hegar defines standard high-strength wastewater as higher than 2500 (±750) mg/L of BOD_5, 1200 (±360)mg/L of TSS, and 300 (±90) mg/L of FOG. On the other hand, some wastewater, such as brewery wastewater and sugar beet juice wastewater, contain more bioavailable organics like alcohol and sugar with less solids.

Since the high-strength waste streams are concentrated, higher values generally indicate higher solids content and/or longer carbon chains, which will ultimately be degraded or broken down through multiple steps during anaerobic digestion. In this study, I define high-strength organic wastes as having chemical oxygen demand (COD) concentrations higher than ~3900 (±1200) mg/L, corresponding to 2500 mg/L of BOD_5 because 64% of typical domestic wastewater consists of a biodegradable COD fraction (Metcalf & Eddy, 2003). My definition excludes most domestic wastewater (300~500 mg COD/L) from the high-strength waste designation.

Wastewater generated by swine, food processing, pulp and paper production, breweries, and different types of sludges (primary, waste activated or secondary, algae, anaerobic digested, saline domestic sewage) are possible high-strength organic wastes.

2.2 Anaerobic food web

High-strength organic wastes are promising sources of renewable energy since the total amount of waste keeps increasing with time and continuous population growth (UN-Habitat., 2010). As I explained in Chapter 1, in order to convert high-strength organic wastes into useful energy and resources, various bio-chemical (e.g. anaerobic digestion), thermo-chemical (e.g. gasification), and mechanical-chemical (e.g. ultrasonication) methods can be applied (Tyagi and Lo, 2013). The most successful technique currently employed by the wastewater treatment market is anaerobic digestion (AD). Even though the transformations from one step to the next vary with the source of each waste, the basic, stepwise processes are the same and result in the production of a biogas mixture containing mostly methane (CH_4) and carbon dioxide (CO_2), with traces of other gases (eq. 2.1) (Tezel et al., 2011).

$$C_cH_hO_oN_nS_s + yH_2O \rightarrow xCH_4 + nNH_3 + xH_2S + (c-x)\,CO_2 \qquad (2.1)$$

$$x = 1/8\,(4c + h - 2o - 3n - 2s)$$

$$y = 1/4\,(4c + h - 2o + 3n + 3s)$$

The resultant methane can be converted into other energy forms, such as heat and electricity, within a wastewater treatment plant. Methane production from complex wastes follows a process with four major phases in the anaerobic environment (Figure 2.1): 1) hydrolysis, 2) acidogenesis, 3) acetogenesis, and 4) methanogenesis (Rittmann and McCarty, 2001).

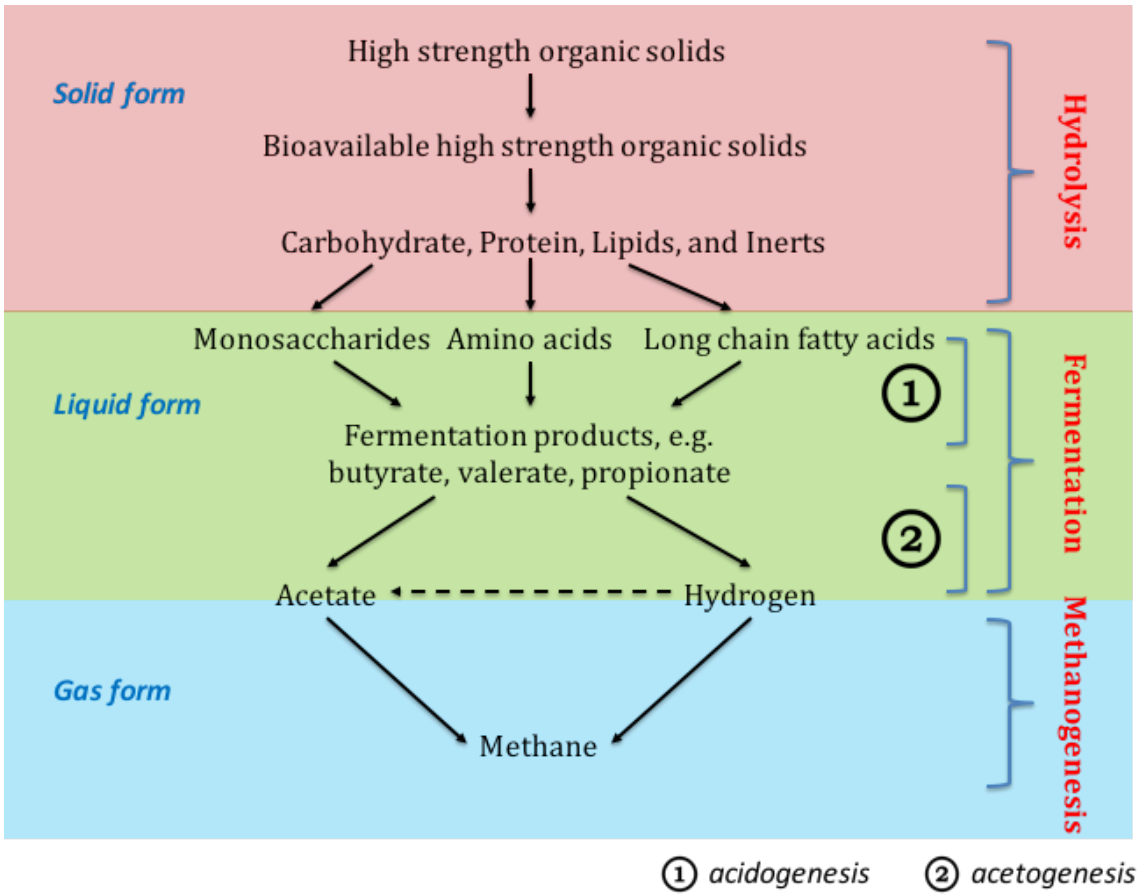

Figure 2.1. Anaerobic energy conversion process to produce methane in anaerobic digestion

2.2.1 Hydrolysis

Hydrolysis is the first step during which complex organic compounds such as polysaccharides, proteins, and lipids (fats and greases) are hydrolyzed, to soluble products by extracellular enzymes. In the hydrolysis step, high-strength organic solids such as particulate biomass disintegrates into a bolus of bioavailable but still particulate carbohydrates, proteins, and lipids, as well as particulate and soluble inert materials (Vavilin et al. 2008). Through this step, solid surface area increase, and so does thus the hydrolysis rates of the principle components such as particulate carbohydrates, proteins, and lipids. Then, the particulate carbohydrates, proteins, and lipids are enzymatically

hydrolyzed to monosaccharides, amino acids, and long chain fatty acids, respectively. The rates of hydrolysis for the particulate macromolecules are different due to differences in their extracellular enzymes (hydrolases): cellulases, proteinases, and lipases, respectively (Stryer, 1988). Hydrolysis is known as the rate-limiting step in an anaerobic food web or anaerobic degradation process. Therefore, it often governs the whole process for biogas production in AD, as an example. This necessitates long detention times, usually greater than 30 days, needed to approach full conversion of municipal sludges in AD processes. To increase the accessibility of complex biomass structures to microbial activity and thus to enhance the hydrolysis rate, an assortment of pre-treatment technologies are applied. I cover pre-treatment technologies in more detail later in this Chapter. Thus, hydrolysis is often a major energy-demanding step, but it also provides many opportunities for improving and optimizing the overall process efficiency through research and development.

2.2.2 Fermentation

Fermentation is the second step of the anaerobic energy conversion process. It is further divided into i) acidogenesis and ii) acetogenesis. Acidogenesis is the next phase wherein fermenting bacteria convert hydrolyzed products to hydrogen, carbon dioxide, acetate, and higher carbon chain (> 2) volatile fatty acids (VFAs) and alcohols. Acetogenesis then results in the production of acetate from short-chain organic acids and alcohols produced by acidogenesis. In this step, hydrogen and carbon dioxide are also generated. In fermentation, soluble organic compounds serve as both electron donors and electron acceptors (Rittmann and McCarty, 2001). The final products of fermentation, which are hydrogen, carbon dioxide, and acetate, are the precursors of the next step in the process: methanogenesis. Acetate, is the key product of acidogenesis and acetogenesis (~20% and ~42% produced by each process, respectively) needed for

methanogens to produce methane during AD or ARB to produce electrical energy in MXCs, (McCarty and Smith, 1984). Taken together, total acetate production is 72% by the fermentation process. However, hydrogen partial pressure should be maintained at low concentrations, $H_2 < 10^{-4}$ atm, for conversion of intermediates (e.g., propionate and butyrate) to acetate, otherwise the reaction will not proceed (McCarty and Smith, 1986). This indicates that a well-balanced, syntrophic relationship among anaerobic microbes will provide ideal outcomes in AD and MXCs.

2.2.3 Methanogenesis in anaerobic digestion

Anaerobic digestion (AD) as a mature technology has a long history. The first digestion plant treating sewage sludge was built in Bombay, India in 1859 (Meynell, 1976). In 1895, biogas from a "carefully designed" sewage treatment facility was used to fuel street lamps in England (McCabe and Eckenfelder, 1957). The first commercial demonstration of AD was carried out in Germany, in 1927 (Ferry, 1993). Microbiological knowledge, enhanced by the ability to identify specific anaerobic microorganisms, boosted the development of AD and promoted methane production since 1930s (Buswell and Hatfield, 1936).

Methanogenesis is the last phase in the anaerobic conversion process during which 1) acetoclastic (or acetate-utilizing) and 2) hydrogenotrophic (or hydrogen-utilizing) methanogens consume acetate, carbon dioxide, and hydrogen to produce methane gas as the final end product (eq. 2.2-2.3).

$$CH_3COOH \rightarrow CH_4 + CO_2 \quad (2.2)$$

$$4H_2 + CO_2 \rightarrow CH_4 + 2H_2O \quad (2.3)$$

Methanogens are included in *Euryarchaeota*, which is a sub-branch of the *Archaea* kingdom. Understanding methanogenic *Archaea* is the key to controlling the AD process. Since methanogens are strict obligate anaerobes, any anaerobic condition

provides a good habitat for their growth, such as the stomachs of ruminant animals, marine sediments, peat lands, and anode chambers in MXCs. The physiology of methanogens classify into two types: rods (*Methanobacterium and Methanobacillus*) and spheres (*Methanococcus*, *Methanothrix*, and *Methanosarcina*). Acetate-utilizing methanogens are *Methanosarcina* and *Methanothrix*, and hydrogen-utilizing methanogens are *Methanobacterium, Methanobacillus, and Methanococcus*.

Acetate can also be formed by acetogens (or homo-acetogens) using CO_2 and H_2 within the anaerobic process shown in Figure 2.1 and eq. 2.4. The resulting acetate can be used for methane production by hydrogen-utilizing methanogens.

$$4H_2 + CO_2 \rightarrow CH_3COOH + 2H_2O \qquad (2.4)$$

In the anaerobic food web or anaerobic energy conversion process, methanogens work together with hydrolytic and fermentative microorganisms even though individual microbial species have very specialized and unique roles and needs. Each has an ideal set of growth parameters and their environment must be tuned so that all thrive. Typical AD operation conditions are 20-25 days of solid retention time (SRT), a mesophilic temperature of ~37°C, and pH 6.8-7.6. Alkalinity and toxicity are the critical parameters of operation dictated by the methanogens (Rittmann and McCarty, 2001). Reactor design and AD operation should be conceptualized from the perspective of developing and nurturing a synergistic ecosystem.

2.3 Pre-treatment

Pre-treatment of high-strength solid wastes enhances the overall rate of anaerobic energy conversion. There are a variety of technologies invented and tested to improve digestion performance. Heat, chemical, mechanical, and electrical methods are the most popular for sludge treatment. The advantages of pre-treatments are 1) increase of the surface area of solid particles and thus increase of solubilization by enzymatic hydrolysis, 2) improvement in biogas production, and 3) reduction of volatile solids (VS). Thermal pre-treatment employs temperatures higher than 100 °C (Haug et al. 1978; Pickworth et al. 2005; Chauzy et al. 2007; Kim et al. 2003; Eskicioglu et al., 2006). Acid or alkaline chemicals as well as strong oxidants (e.g. ozone and hydrogen peroxide) have been using for chemical pre-treatment (Haug et al. 1978; Kim et al. 2003; Kim et al., 2007; Li et al., 2008). Ultrasonication and microwaves are commonly applied as mechanical treatments (Khanal et al. 2007; Nickel and Neis, 2007; Kim et al. 2003; Wolff et al. 2007). Pulsed-electric-field (PEF) as an electrical method of pre-treatment is applied for sludge treatment (Rittmann et al., 2008; Salerno et al., 2009; Lee et al., 2010). Also, various combinations of these pre-treatment technologies have been studied (Vlyssides and Karlis, 2004; Kim et al. 2003). However, further optimization and economic analysis is needed for successful implementation of each of these pre-treatment technologies. Many publications show significant improvement in AD performance with several pre-treatment technologies. However, these methods have not been widely adopted in full-scale operations because the net benefits have not been proven (Rittmann et al., 2008). Investment in and installation of new units as well as the addition of extra energy and/or chemicals present serious operating problems due to toxic by-products, odors, corrosion, or maintenance and have hindered efforts for scaling-up to full capacity and commercialization. Here, I describe the background of

PEF pre-treatment technology in more detail because I utilize this technology in the research presented in Chapters 3 and 5.

2.3.1 Pulsed-electric-field (PEF) technology

PEF technology uses a high-energy pulsed electric field (>10 kV) with a rapid rise and fall (within a micro-second) to disrupt cellular membranes and walls, complex organic solids, and macromolecules (Rittmann et al., 2008). PEF technology has been utilized in molecular biology for electroporation, which uses an electric field to force pores in cellular membranes to reversibly open, enabling the movement of plasmids and DNA into cells for medical therapies (Madigan et al., 2003). Also, PEF is widely used for sterilization or pasteurization as a form of thermal processing in the food industry (Töpfl, 2006; Zhang, 2007). Since early 2000, PEF has been used in wastewater treatment, mostly for the processing of biosolids (Koners et al., 2004; Choi et al., 2006; Kopplow et al., 2004; Loeffler et al., 2001). OpenCEL™, now a research development initiative of Trojan Technologies (http://www.trojantechnologies.com/our-businesses/opencel/), enhanced the technique for full-scale application with continuous treatment on a flow-through basis, called Focused Pulsed (FP) technology. A full-scale unit was installed at the Northwest Water Reclamation Plant (NWWRP) in the city of Mesa, Arizona and started operating in March of 2007 (OpenCEL). Figure 2.2 shows the schematics of sludge treatment flow within the FP unit.

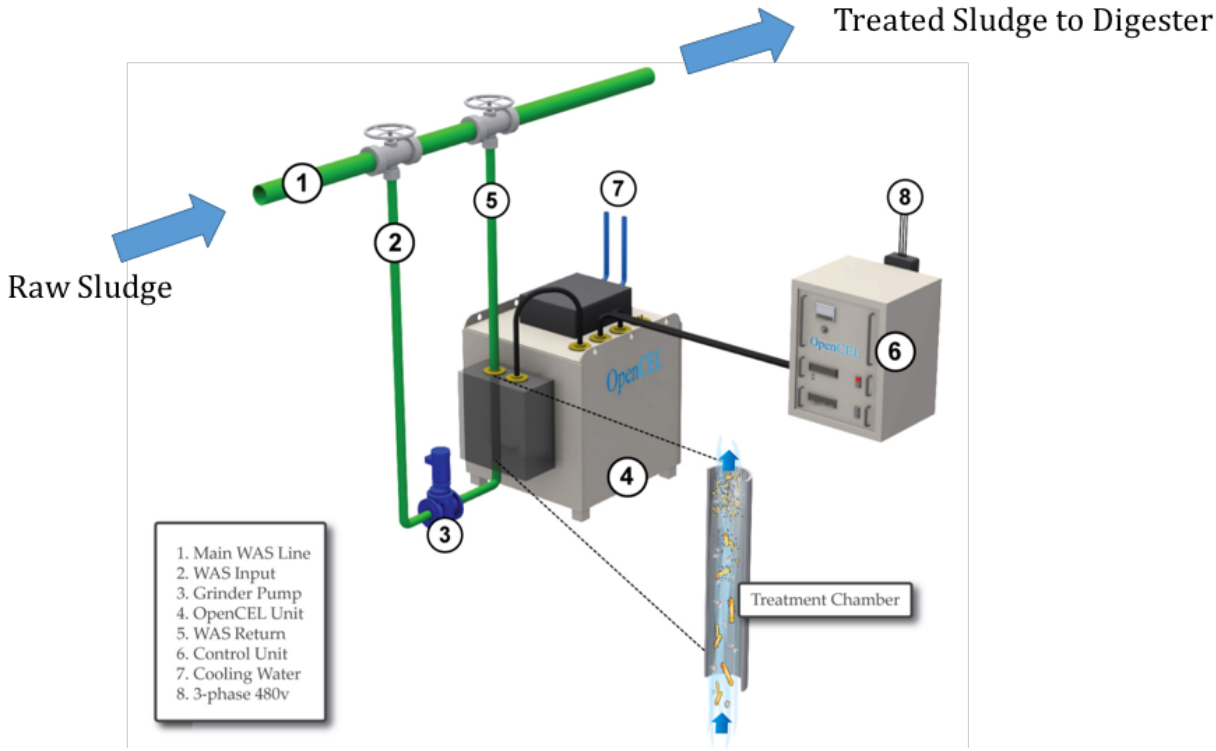

Figure 2.2 Schematics of sludge treatment in a Focused Pulsed (FP) unit by OpenCEL™ (Rittmann et al., 2008).

PEF (or FP) technology has been applied to cellular solid wastes such as waste activated sludge (WAS), pig manure (PM), or photosynthetic microorganisms (*Synechocystis* PCC 6803, *Scenedesmus*) because PEF attacks the basic building blocks of cell membranes and walls, which are composed of phospholipids and peptidoglycans, respectively (Choi et al., 2006; Salerno et al., 2009; Sheng et al., 2011; Lai et al., 2014). Phospholipids and peptidoglycans are very vulnerable to exposure to strong electric fields because they are polar molecules that contribute to a net negative charge on the outer surfaces of cells.

Depending on the treatment intensity, the solubilization and biogas production in batch methanogenic digesters are different (Salerno et al., 2009). Parameters that affect the intensity are electric field strength (or applied voltage), treatment time, specific time

and pulse geometry, treatment temperature, and sample characteristics (e.g., conductivity, air bubbles and particles). Eq. 2.5 shows the calculation of treatment intensity for FP units (Salerno et al., 2009; Lee et al., 2010).

$$Treatment\ Intensity = K \cdot \frac{V^2 \cdot D \cdot f \cdot \sigma \cdot HRT}{L^2} \quad (2.5)$$

Where

Treatment Intensity = kWh/m^3,

K = a constant for unit conversion,

V = applied voltage (V = J/C = kg·m^2/C·sec^2),

D = pulse width (sec /pulse),

f = pulse frequency (pulse/sec),

σ = sample conductivity (S/m = sec·C^2/kg·m^3),

L = distance between electrode (m), and

HRT = residence time in the pulsed electric field (sec).

Salerno et al. (2009) reported that higher intensities applied to WAS resulted in more dissolved organics including dissolved organic carbon (DOC) and SCOD as well as higher methane gas production, ranging from 1.1 to 19.8 kWh/m^3. When using the FP alpha unit, ~30 kWh/m^3 are typically used to treat WAS, PS, PM and photosynthetic microorganisms (Lee et al., 2010; Lai et al., 2014; Ki et al., 2015). PEF is considered a disintegration technology since solid contents do not vary between control and PEF-treated samples in terms of total and volatile suspended solids (TSS and VSS); and treatment intensity does not affect these results (Lai et al., 2014; Ki et al., 2015; Salerno et al., 2009). This is because even though the particle size distribution of the cell biomass changed it did not effect TSS and VSS measurement using a 1.2 um glass fiber filter. However, the increase of methane gas production resulted from the increase of viable organics emitted by the disintegrated particles as soluble COD. Figure 2.3 shows

examples of FP treatment on solid wastes, noting some damaged cells in WAS and *Syntechocystis*.

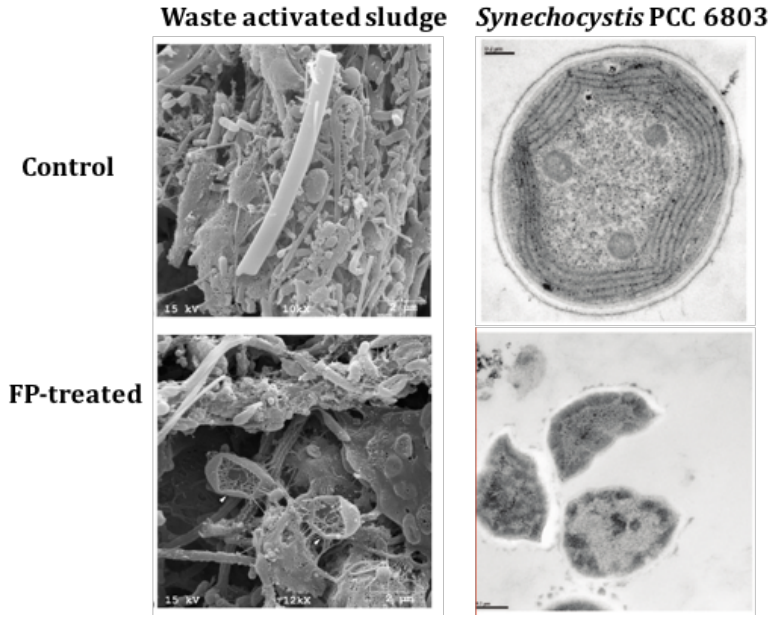

Figure 2.3 Scanning electron microscopy (SEM) and transmission electron microscopy (TEM) images of control and PEF-treated WAS (left) and *Synechocystis* (right) from Salerno et al. (2009) and Sheng et al. (2011).

PEF treatment has been proven effective for WAS and photosynthetic microorganisms, but its impact on PS alone is not known. Detailed explanations and evaluation of PEF's effect on PS are discussed in Chapter 3 and 4.

CHAPTER 3

REDUCED OVERPOTENTIALS IN MICROBIAL ELECTROLYSIS CELLS THROUGH IMPROVED DESIGN, OPERATION, AND ELECTROCHEMICAL CHARACTERIZATION[1]

3.1 Introduction

Microbial electrochemical cells (MXCs) represent a promising technology for the recovery of energy from waste organics either as electrical power or for production of useful chemicals such as hydrogen (H_2), hydrogen peroxide (H_2O_2) and many others (Logan et al., 2006; Rozendal et al., 2006; Rozendal et al., 2009; Rabaey et al., 2010; Nevin et al., 2011). In MXCs, anode-respiring bacteria (ARB) oxidize waste organics, and generate an electrical current on the anode (Torres et al., 2007; Lee et al., 2008; Vologni et al., 2013). In the simplest form of anode respiration, acetate, a common product of anaerobic metabolism, is used as the electron donor (equation 1).

$$CH_3COO^- + 4H_2O \Rightarrow 2HCO_3^- + 9H^+ + 8e^- \quad (1)$$

At the cathode, these electrons reduce oxygen (O_2) to water or H_2O_2 in microbial fuel cells (MFCs) (equation 2), or water to H_2 in microbial electrolysis cells (MECs) (equation 3), which requires a small voltage input (Rozendal et al., 2006; Lee et al., 2010).

$$O_2 + 4H^+ + 4e^- \Rightarrow 2H_2O \text{ or } O_2 + 2H^+ + 2e^- \Rightarrow H_2O_2 \quad (2)$$

$$2H_2O + 2e^- \Rightarrow H_2 + 2OH^- \quad (3)$$

One of the major limitations still hindering the application of MXCs is the low voltage efficiency (Rabaey et al., 2010; Harnisch and Schröder, 2010). In the case of MFCs, a theoretical maximum of 1.1 V is available when coupling acetate oxidation at the

[1] This chapter was published in altered format as Ki D, Popat SC, Torres CI. 2016. Reduced overpotentials in microbial electrolysis cells through improved design, operation, and electrochemical characterization. Chemical Engineering Journal 287, 181-188.

anode to O_2 reduction at the cathode. Yet, at current densities of > 5 A m^{-2}, only < 0.3 V is produced, representing > 0.8 V of overpotential (Sun et al., 2012; Hoskins et al., 2014; Torres, 2014). Similarly, although the theoretical applied voltage in MECs is only 0.14 V, the actual applied voltage can be as high as 1.2 V, representing close to 1 V of overpotential (Zhang et al., 2010; Tartakovskyet al., 2011; An and Lee, 2013; Sleutels et al., 2013). Such large overpotentials are in stark contrast with most other fuel cells or electrolysis cells, where orders of magnitude higher current densities are possible at lower overpotentials (Wang et al., 2011; Ursúa et al., 2012). There is thus a need to consider design and operation tactics for MXCs that help reduce the overall overpotential in the system.

Overpotentials in electrochemical systems are always classified into three major types: activation, Ohmic, and concentration overpotentials (O'Hayre et al., 2006). Activation overpotential is related to the activation barrier for a given electrochemical reaction, and the properties of the catalysts in overcoming the activation barrier. In the case of the anode reaction in MXCs, activation overpotential relates to the energy lost in the oxidation of the electron donor by the ARB to metabolism. Likewise, cathode activation overpotential relates to the energy loss at cathode during reduction of O_2 to water or H_2O_2 in MFCs or of water to H_2 in MECs. Ohmic overpotential is related to the transport of ions between the anode and the cathode, and depends on the conductivity of the electrolyte. In the case of MXCs, low conductivity solutions are used for the growth of ARB, and thus this results in high Ohmic overpotential if the distance between the two electrodes is large. Thus, to reduce Ohmic overpotential, it is imperative that I reduce distances between the anode and the cathode, as previously suggested by many other studies (Liu and Logan, 2004; Pham et al., 2006; Liu et al., 2010; An and Lee, 2013).

Concentration overpotential is related to Nernstian and activation losses resulting from not being able to maintain the concentrations of reactants on the electrode surface as well as not removing products from the electrode surface at a fast enough rate. The most common form of concentration overpotential acknowledged for MXCs is due to the pH imbalance that results between the two electrodes when using a membrane to separate the electrodes (Rozendal et al., 2006; Torres et al., 2008). For every pH unit the cathode pH is higher than the anode pH, a Nernstian concentration overpotential of ~ 60 mV results. We showed recently that even when bulk concentrations are the same, for e.g. in the absence of a membrane, differences in electrode surface concentrations can still lead to a high concentration overpotential (Popat et al., 2012).

In this study, I aim to systematically characterize and reduce all overpotentials in an MEC. Although I use an MEC here, the results should directly apply to all other MXCs that use a microbial anode with an inorganic catalyst-based cathode. I started with a logical design for the MEC with reduced distance between the anode and the cathode, and high surface area electrodes. From thereon, based on the characterized individual overpotentials, I modified the materials and the operating conditions I used to reduce the overall overpotential and thus the applied voltage. I show here how it is possible to reduce applied voltages in MECs at a current density of 10 A m^{-2}, from 1.1 V to ~ 0.85 V, thus representing only ~ 0.7 V of overpotential. I also provide a perspective on ways to reduce further overpotentials as well as a limit to the overall voltage efficiency possible in MXCs.

3.2 Materials and methods

3.2.1 MEC design and operation

I designed modular flat-plate MECs each with two anodes and two cathodes. I provide a schematic and photos in Figure 3.1. Briefly, the anodes were made of carbon fibers (24K Carbon Tow, FibreGlast, OH, USA) that were woven around a titanium plate that served as current collector (each anode was 10 cm x 10 cm, geometric area of 100 cm^2). A photograph of an assembled anode is shown in Figure 3.1c. The two anodes shared a common chamber. I used stainless steel meshes (Type 314, McMaster-Carr, USA) or nickel meshes (Ni 200, Unique Wire Weaving Co., Inc., USA) as the cathodes, and each cathode had a separate individual chamber. I cleaned the assembled anodes with 1 M nitric acid for 3 hours, 1 M acetone for 12 hours, 1 M ethanol for 3 hours, and deionized water (18 MΩ) overnight before using them. I equipped the anode chamber with a reference electrode (Ag/AgCl, MF-2052, Bioanalytical Systems, Inc., USA), which was at a ~2 cm distance from each anode. All potentials I report throughout are converted to vs. standard hydrogen electrode (SHE) using a conversion factor of +0.27 V. I determined this conversion factor as previously described for the medium I fed to the MECs (Torres et al., 2009). I used the anion exchange membranes AMI-7001 (Membrane International, Glen Rock, NJ) or Fumasep FAA (FuMa-Tech, Germany) to separate the anode and the cathode chambers. I maintained the distance between the anode and cathode at < 0.5 cm. The anode chamber volume was ~0.5 L and the cathode chamber volume (individual) was ~0.1 L (or 0.2 L total). The anode was fed with acetate as the electron donor (see medium composition below), while the cathode was fed with a 100 mM solution of NaCl or NaOH.

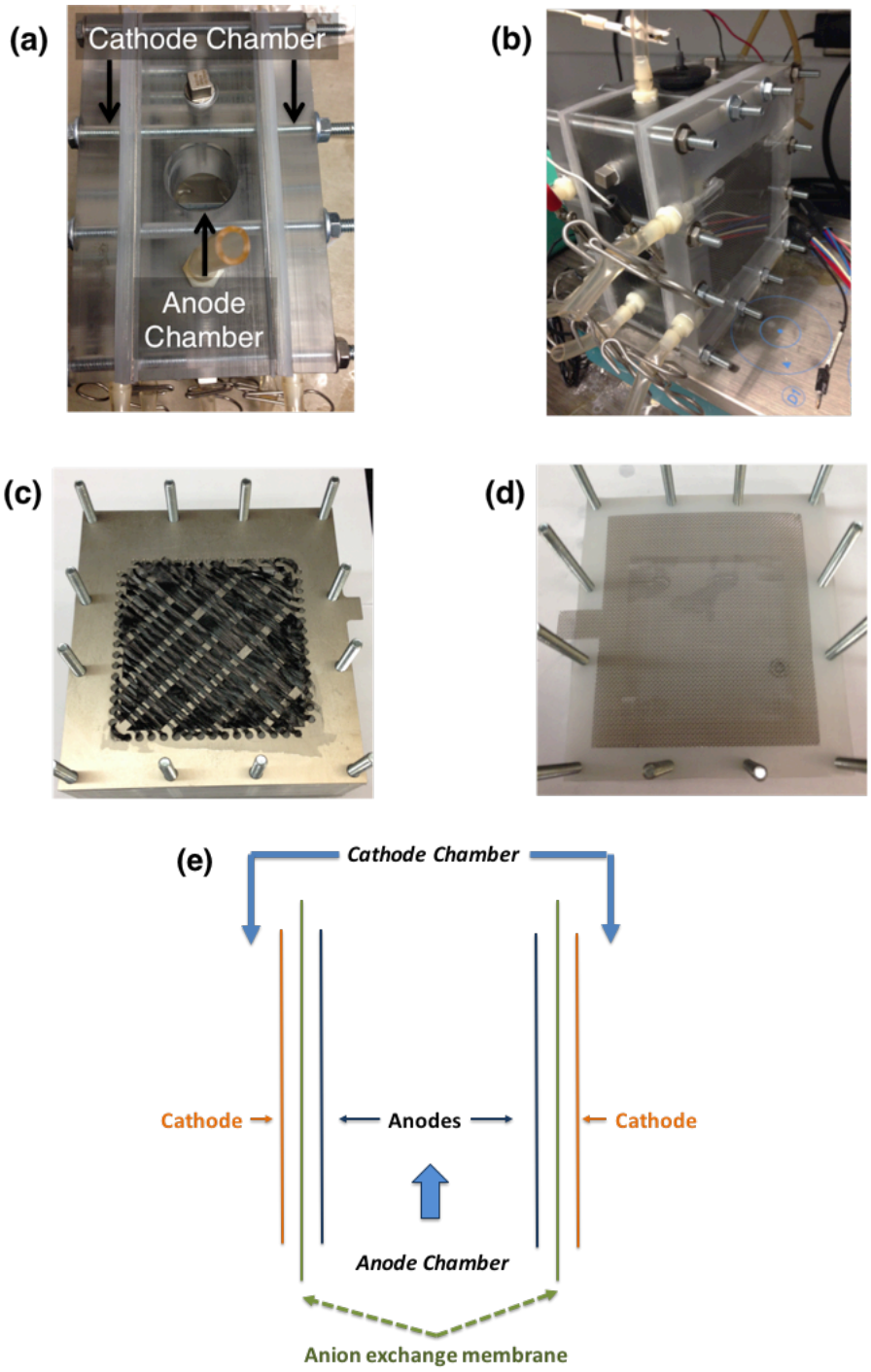

Figure 3.1. Pictures of modular flat-plate MEC (a) top view of the MEC with configuration of anode and cathode chambers, (b) assembled flat-plate MEC, (c) carbon fiber anode woven with titanium current collector, and (d) SS cathode, and (e) Schematic of two anodes and two cathodes in a modular flat-plate MEC.

I inoculated the MECs with a mixture of anaerobic digested sludge (2 mL, obtained from Mesa Northwest Wastewater Reclamation Plant in Mesa, AZ, USA) and the effluent from a continuously fed MEC in our laboratory fed with acetate as the electron donor (248 mL). I operated the MECs in batch mode initially, followed by continuous flow of the anode medium at a rate of 0.3-0.5 mL min^{-1}, resulting in a hydraulic retention time of 16.7-27.8 h. The anode feed consisted of 50 mM acetate, 100 mM phosphate buffer (PBS, 85 mM of KH_2PO_4 and 15 mM of Na_2HPO_4), 14 mM ammonium chloride, and trace minerals (Torres et al., 2007). The pH of the medium was ~7.6. I operated the MECs in a temperature-controlled room at 30 °C. I sparged the anolyte and catholyte with ultra-high purity nitrogen gas (>99.999%) to remove O_2 before feeding to each chamber. For experiments where I added CO_2 to the cathode (see text in Results and Discussion), I used 100% CO_2 that was sparged into an external chamber containing the catholyte. The CO_2 flow rate was 250 mL min^{-1} and I recirculated the catholyte within the cathode chambers at 20 mL min^{-1} flow rate (Figure 3.2). I set the anode potential at -0.03 V with a multi-channel potentiostat (VMP3, BioLogic Science Instruments, Knoxville, TN), and recorded current, and anode and cathode potential every two minutes. This anode potential was selected on the basis of a previous study that has shown that the potential is oxidizing enough to allow optimum growth of known ARB (Torres et al., 2009).

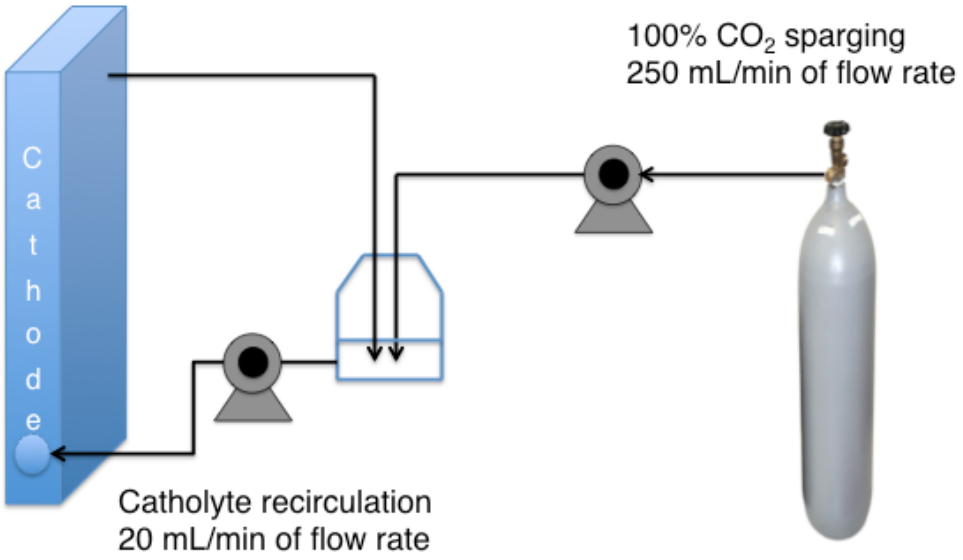

Figure 3.2. Schematic for CO_2 addition to cathode.

After a stable current was obtained, I developed *j-V* curves using chronoamperometry starting from the open circuit potential up to the anode potential resulting in the highest saturation current densities, stepping the potential 25 mV for each data point. I waited ~10 minutes for steady current at each potential before stepping up the anode potential. At the end of each experiment, I performed electrochemical impedance spectroscopy (EIS) measurements at 100 kHz with an amplitude of 10 mV, while using the anode as the working electrode and the cathode as the counter and reference electrode to determine the Ohmic resistance between the anode and the cathode. The Ohmic resistance used was an average value from 20 measurements. I also performed *iR* correction for all anode and cathodes potentials by doing EIS measurements in the same way as described above but with the anode or the cathode as the working electrode and the Ag/AgCl reference electrode as the reference.

3.2.2 Electrochemical impedance spectroscopy of MEC cathodes

To characterize the performance of the cathodes I used in the MECs during operation (with or without addition of CO_2 to the cathode), I performed potentiostatic

EIS measurements at each condition at various cathode potentials. I used an amplitude of 10 mV, with a frequency range of 100 kHz to 10 mHz. I took six data measurements per decade of frequency. I fit the Nyquist plot data using an equivalent circuit model containing two charge transfer resistances in series with an Ohmic resistance. For each cathode potential, I report a total area-specific resistance, which is the sum of the two charge transfer resistances.

3.2.3 Tests for selection of materials for enhanced MEC performance

3.2.3.1 Characterization of anion exchange membranes

I characterized various commercially available AEMs (Table 3.1) to use in our MECs when adding CO_2 to the cathode. I used AEMs since it has been showed that when electroneutrality is maintained by transport of OH^- from the cathode chamber to the anode chamber, either directly or via carbonate and/or bicarbonate species, the pH on the anode can be maintained close to 7 (Torres et al., 2008; Fornero et al.,2010). For the AEM characterization, I used electrochemical cells containing two chambers filled with 100 mM $NaHCO_3$. I performed EIS on the cell with one stainless steel rod (≈9 cm^2, 5 mm diameter) as the working electrode, and another as the counter and reference electrode, using a frequency of 100 kHz and an amplitude of 10 mV. This allowed measurement of the Ohmic resistance between the two electrodes for the various AEMs. I also performed EIS analysis without a membrane to obtain the Ohmic resistance just from the liquid electrolyte used, thus making it possible to determine the resistance to ion transport from the AEMs only from subtraction. I show a list of the membranes tested in Table 3.1 along with their thickness and pH stability range.

Table 3.1. List of membranes tested, including their supplier and physical properties.

Type	Membrane	Supplier	Thickness (mm)	pH
Heterogeneous	AMI-7001	Membranes International, USA	0.50-0.51	1-10
	Excellion I-200	SnowPure, USA	0.32-0.34	NR
Homogenous	Fumasep FAA	FuMa-Tech, Germany	0.13-0.15	6-13
	Fumasep FAB	FuMa-Tech, Germany	0.10-0.13	0-14
	A201	Tokuyama, Japan	0.028	0-14

3.2.3.2 Characterization of cathode materials

For testing and comparing the performance of different cathodes for use in the MECs, I used a flat-plate two-chamber electrochemical cell having the same volume (100 mL) for each chamber. I used a stainless steel mesh electrode (Super-Corrosion-Resistance Type 316 Stainless Steel Mesh, SS [20 x 20 wires/inch] (McMaster-Carr, USA) or a nickel mesh electrode, Ni 200 [70 x 70 wires/inch] (Unique Wire Weaving Co., Inc., USA) of size 7 cm x 7 cm (49 cm^2 projected area) as the cathodes. I provide more information on the two materials in Table 3.2. I used AMI-7001 as the membrane, and the same Ni mesh electrode as the counter electrode for all tests. For the electrolyte, I used 100 mM NaOH solution in both chambers.

Table 3.2. Properties of cathode meshes tested in this study.

	Nickel	SS
Item	Nickel 200	Super-Corrosion-Resistance Type 316
Wire mesh (Wires/In.)	70 x 70	20 x 20
Wire diameter (In.)	0.004	0.018
Width opening	0.0103	0.032
% Open area	51.8	41
Cost ($/ft^2)	22.76	14.2
Company	UNIQUE WIRE WEAVING Co., Inc.	McMaster-Carr

I performed linear sweep voltammetry (LSV) on the cathodes at 30 °C at a scan rate of 10 mV s^{-1}. Before performing LSV, I measured the Ohmic resistance by EIS and applied *iR* correction during the LSV. I repeated the LSV for at least three times for each material.

3.3 Results and discussions

3.3.1 Characterization of overpotentials in MECs

I first performed chronoamperometry to obtain *j-V* curves for an MEC constructed with stainless steel mesh cathodes (SS-1) and AMI-7001 membranes (Figure 3.3a, Experiment 1 in Table 3.3). I performed at least two replicate measurements to obtain the curves for each condition and show only one representative set here. All replicates followed the same trend and an additional representative set is shown in Figure 3.4.

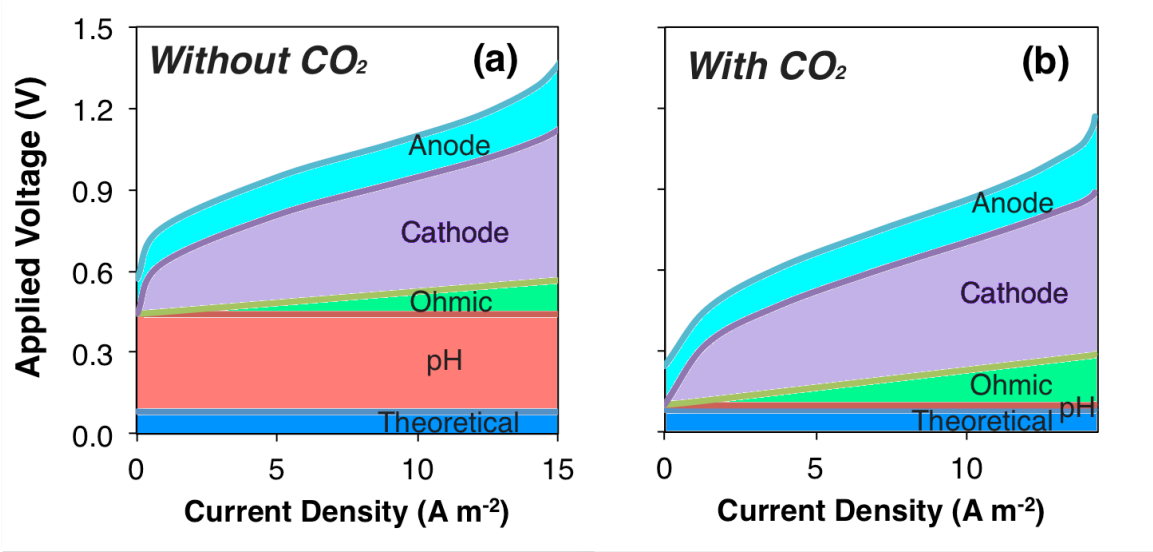

Figure 3.3. Characterization of the applied voltage in the flat-plate MEC with AMI-70001 membrane and stainless steel mesh cathode (a) without and (b) with CO_2 addition to cathode (Experiment 1 and 2, respectively). I performed chronoamperometry to plot *j-V* curves after producing high current densities (> 15 A m^{-2}) in the MEC.

Table 3.3. Operational conditions for flat-plate MEC.

	AEM	Cathode	CO_2 addition to cathode
Experiment 1	AMI-7001	Stainless Steel	No
Experiment 2	AMI-7001	Stainless Steel	Yes
Experiment 3	Fumasep FAA	Nickel	No
Experiment 4	Fumasep FAA	Nickel	Yes

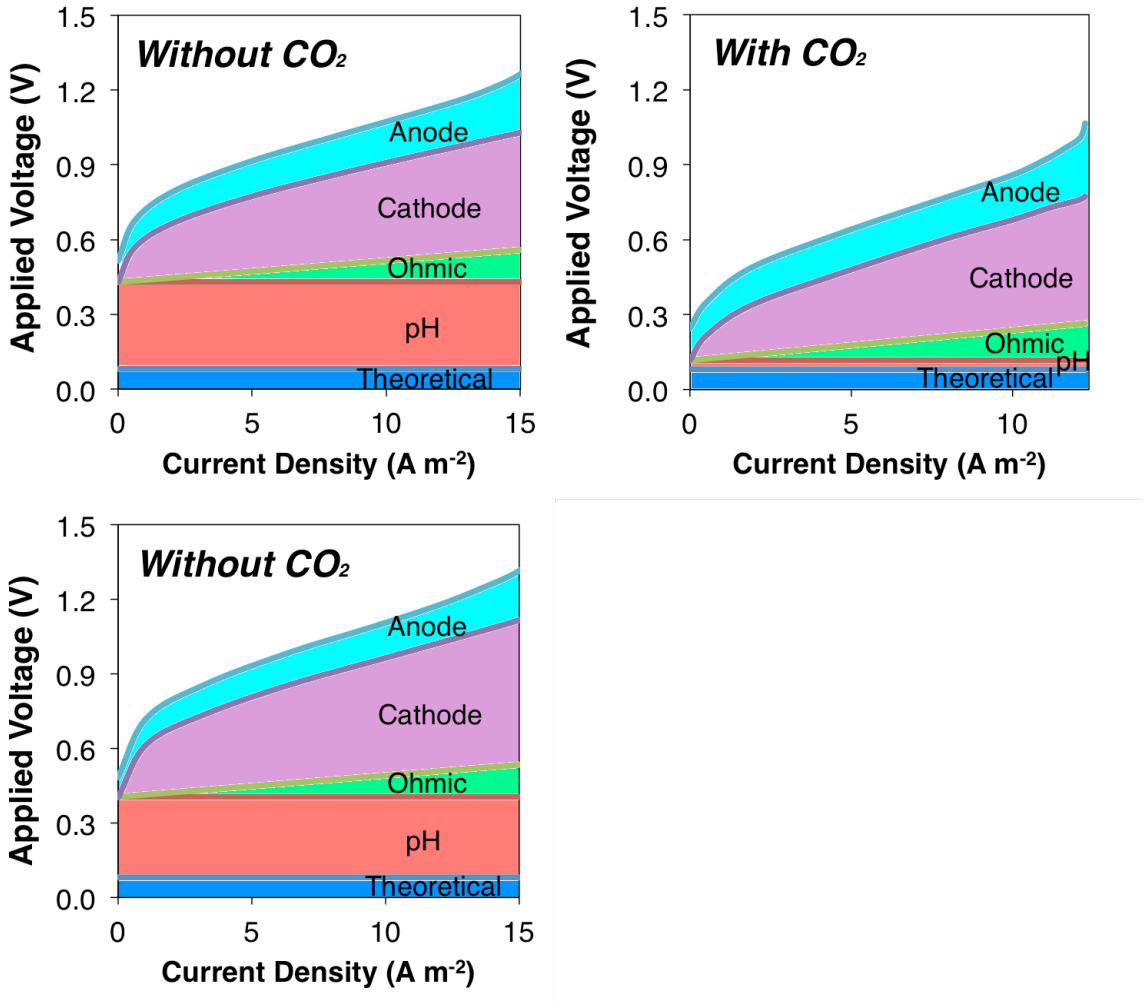

Figure 3.4. Replicate *j-V* curves for Figure 3.3.

I divided the total overpotential into four individual overpotentials: (i) anode overpotential resulting from ARB metabolism, (ii) Ohmic overpotential, which is related to ion transport between the anode and the cathode, (iii) concentration overpotential related to an increase in the cathode chamber pH due to low concentration of H^+ or high concentration of OH^-, and (iv) cathode overpotential, which includes cathode activation losses and potentially any concentration losses related to different local concentrations of reactants and products from the bulk electrolyte. The overall applied voltage in the MECs is then the sum of all overpotentials and the theoretical applied voltage necessary, as per the following equation.

$$E_{ap} = E_{Th} + \eta_{pH} + \eta_{Ohmic} + \eta_{ca} + \eta_{an} \quad (4)$$

where E_{ap} is the applied voltage, E_{Th} is the theoretical voltage necessary, η_{Ohmic} is the Ohmic overpotential, η_{pH} is the concentration overpotential due to increased cathode pH, η_{ca} is the cathode overpotential, and η_{an} is the anode overpotential. The applied voltage (E_{ap}) was the difference between the anode and cathode potentials measured with the potentiostat. The theoretical voltage (E_{Th}) is the energy needed to overcome the thermodynamic barrier for H_2 production in MECs. I calculated this with the Nernst equation with known acetate and bicarbonate concentrations, and pH,

$$E_{Th} = E_{ca} - E_{an} = \left(E^0_{ca} - \frac{RT}{2F}\ln\frac{pH}{[10^{-7}]^2}\right) - \left(E^0_{an} - \frac{RT}{8F}\ln\frac{[CH_3COO^-]}{[HCO_3^-]^2[10^{-7}]^9}\right) \quad (5)$$

where E_{ca} and E_{an} represent the theoretical cathode and anode potential from the Nernst equation.

I calculated concentration overpotential related to a high cathode pH (η_{pH}) by measuring the observed pH difference between bulk liquid in the anode and cathode, and using the relationship of 60.1 mV of overpotential per one unit that the cathode pH is higher than the anode pH at 30 °C. I determined Ohmic overpotential from the Ohmic resistance (R_{Ohmic}; Ohm cm^2) measured using EIS.

$$\eta_{Ohmic} = j \cdot R_{Ohmic} \quad (6)$$

I calculated the anode overpotential from the following equation,

$$\eta_{an} = E_{an,observed} - E_{an} \quad (7)$$

I assumed that the remainder of the applied voltage is due to the cathode overpotential.

For the *j-V* curve shown in Figure 3.3 and 3.4, I used 100 mM NaOH as the catholyte. This in itself creates the concentration overpotential due to a high cathode pH. However, this was out of convenience for the experimental protocol. Even for MECs that are operated with NaCl electrolyte or buffers, the increase in cathode pH is a widely observed phenomenon (Rozendal et al., 2008; Sleutels et al., 2009; Nam and Logan, 2912). I show in Figure 3.5 how the cathode pH increases over time up to almost 13 if I use a 100 mM NaCl solution at the cathode.

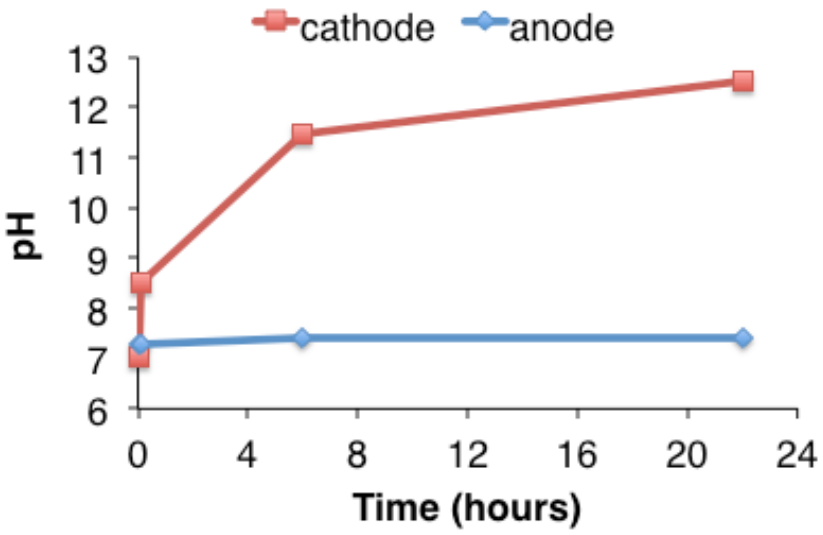

Figure 3.5. pH increase in flat-plate MEC cathode. pH in cathode fed with 100 mM NaCl increased up to >12.5 within 24 hours at ~10 A m^{-2}.

As shown in Figure 3.3a, at a high current density (~10 A m^{-2}) where the total applied potential was 1.092 ± 0.017 V, the cathode has the largest fraction of the

overpotential (0.429 ± 0.040 V), followed by the concentration overpotential due to a high cathode pH (0.344 ± 0.019V), the anode overpotential (0.153 ± 0.012 V), and the Ohmic overpotential (0.085 ± 0.002 V). Energy losses associated with the anode are usually not avoidable because they relate to the concentration gradients of reactants and products in the anode biofilm (substrate and proton), intracellular potential losses (ARB metabolism), and the extracellular potential losses (EET to anode) (Lee and Rittmann, 2010; Torres et al., 2010). The anode overpotential is typically 0.1-0.3 V depending on the current density (Lee and Rittmann, 2010; Jeremiasse et al., 2010). This is reflected in the Nernst-Monod equation used for modeling ARB, in which the mid-point potential, which results in half the maximum current density production, is only ~0.1 to 0.15 V more positive of the theoretical anode potential for many pure and mixed cultures (Yoho et al., 2014; Torres et al., 2008; Torres et al., 2008). In this case, the anode overpotential (0.153 ± 0.012 V) is within range of what is known for ARB with an efficient metabolism and EET mechanism. Therefore, I should focus on the energy losses from concentration overpotential due to a high cathode pH and cathode overpotential to improve the voltage efficiency.

3.3.2 Effect of CO_2 addition to the cathode

The pH imbalance between the anode and the cathode in MXCs always results in a higher pH at the cathode (Rozendal et al., 2006; Popat et al., 2012). Since an increase in one pH unit decreases the redox potential for the hydrogen evolution reaction by 60.1 mV (at 30 °C), this results in a large concentration overpotential. In the case shown in Figure 3.3a, the pH difference between the two chambers was 6.0 units, and so the concentration overpotential was 0.361 V. We have previously tested a strategy whereby adding CO_2 to the cathode can reduce the pH, and thus reduce the concentration overpotential in air-cathode MFCs which include the oxygen reduction reaction (Popat et

al., 2012; Torres et al., 2009). I tested this strategy for our flat-plate MEC design. In MECs with a liquid catholyte, hydroxide ion (OH^-) can be combined with the added CO_2 to form bicarbonate (HCO_3^-) and/or carbonate (CO_3^-) anions (Figure 3.6). These anions dissolved in catholyte will buffer the pH close to their pK_a values of 10.3 and 6.3 for the HCO_3^-/CO_3^- and CO_2/ HCO_3^- couples, respectively. This is advantageous in decreasing the pH-related concentration overpotential. A previous study shows that the pHs of catholytes were ~5.9 and ~6.5 of non-buffer and buffer solution with CO_2 addition to cathode in MFC (Fornero et al., 2010).

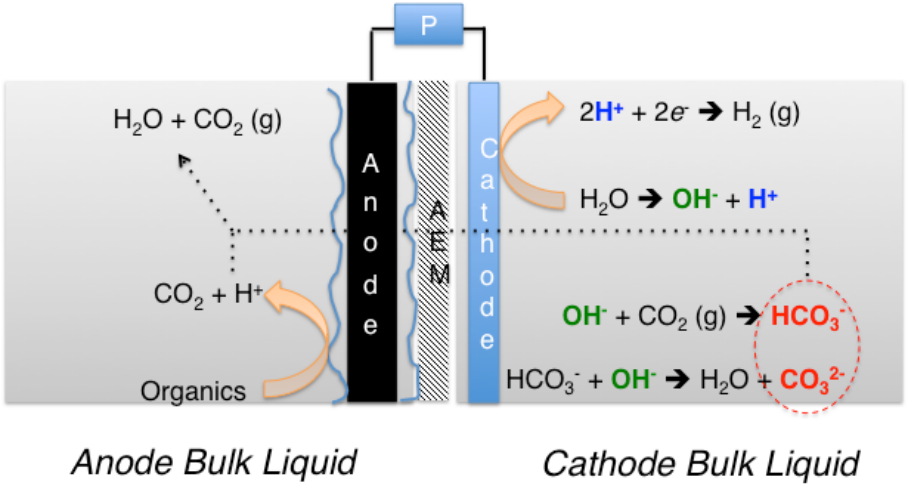

Figure 3.6. Mechanism of CO_2 in decreasing the concentration overpotential.

I show in Figure 3.7 the effect of adding CO_2 to the cathode on the applied voltage and the cathode pH at a high current density (~18.5 A m^{-2}). As soon as I introduced CO_2 into the cathode chambers of the MEC, the applied voltage decreased from 1.285 to 1.083 V. This represents a decrease in the overpotential of 0.202 V. The cathode pH decreased by roughly 5 units. This should result in a decrease in the applied voltage of ~ 0.301 V. While the change I observe is smaller than this, it could be due to a higher local cathode pH than that measured in the bulk solution of the cathode chambers. This overpotential could then thus be included in the cathode overpotential for which I do not distinguish

between the activation losses and the concentration overpotential due to higher surface pH than bulk solution. I have observed such phenomenon in MFC cathodes before (Popat et al., 2012). Nonetheless, I confirmed that adding CO_2 to the cathode represents a great opportunity to reduce significantly the applied voltage in MECs. This improvement is greater than the previous report in air-cathode MFCs (Torres et al., 2008), which shows the improvement of the operational voltage of the MFC by 0.08 and 0.12 V with 5 and 10% of CO_2 addition to the MFC cathode, respectively. The larger improvement I observed could be due to higher concentration of CO_2 (100%) added to the cathode in our study.

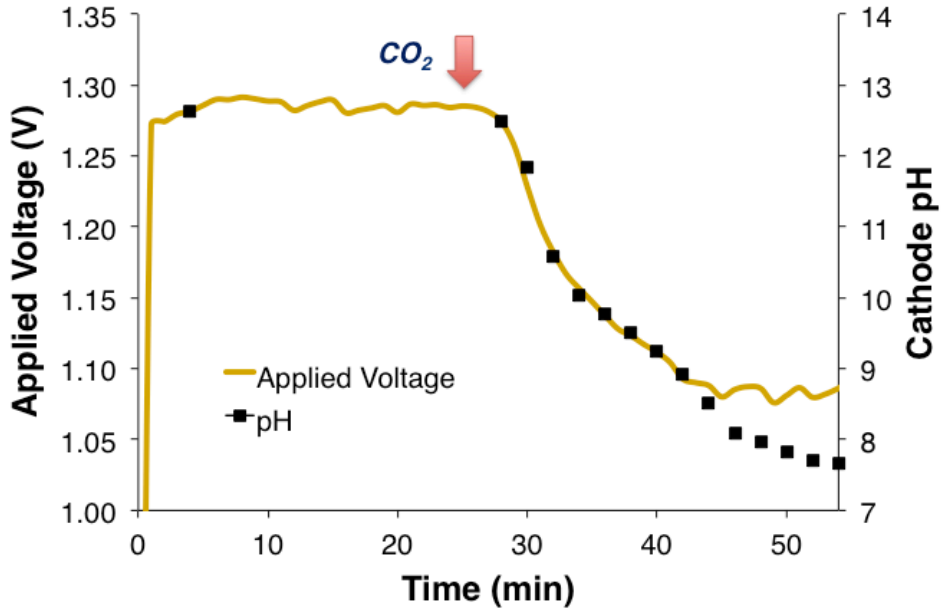

Figure 3.7. Decrease in applied voltage and cathode pH with CO_2 addition to cathode. Current density was 18.5 ± 0.3 A m^{-2}.

To further confirm that the benefit of CO_2 is primarily on the pH, and not necessarily on the cathode activation overpotential, I performed EIS measurements on the cathode, at various cathode potentials. Through these measurements, I determined the overall cathode resistance at each potential. The results from these measurements

are shown in Figure 3.8. In Figure 3.8a, I show the cathode potential vs. the cathode area-specific resistance, from which it is apparent that the main impact of CO_2 is on changing the cathode potential at which a given current density is obtained. However, the overall shape of the curve remains similar, suggesting that the catalyst properties have not changed. This is exemplified further in Figure 3.8b, where the current density vs. the cathode area-specific resistance relationship stays the same irrespective of adding CO_2. These results indicate that CO_2 only affects the performance by decreasing the pH in the cathode chamber without resulting in any cathode catalytic changes.

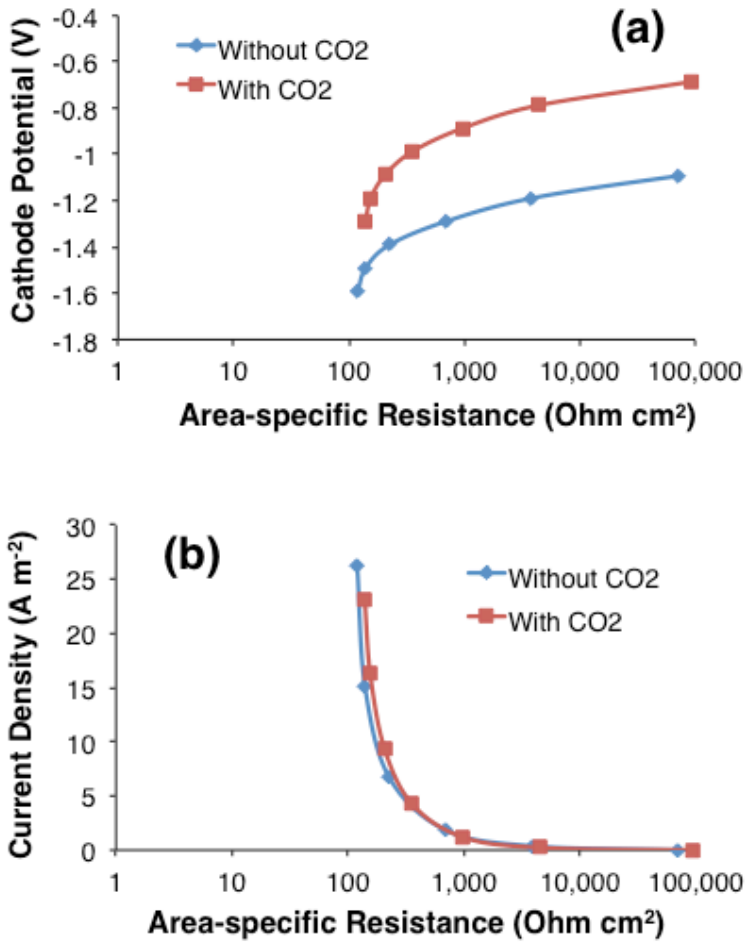

Figure 3.8. Effect of CO_2 on the cathode catalytic reaction: (a) cathode potential vs. the cathode area-specific resistance, (b) current density vs. the cathode area-specific resistance.

Next I characterized the flat-plate MEC the same way as in Figure 3.1a, but this time while continuously adding CO_2 to the cathode chambers (Experiment 2). A comparison of the complete characterization with (Figure 3.3b) and without CO_2 is shown in Figure 3.3. Adding CO_2 to the cathode chamber almost completely eliminated pH-related concentration overpotential (only 0.027 ± 0.013 V). At a current density of 10 A m^{-2}, I reduced the total applied voltage from 1.092 to 0.859 V, which is amongst the best reported performances for MECs in literature (An and Lee, 2013; Tartakovsky et al. 2011; Sleutels et al., 2013; Zhang et al., 2010). There are few studies having exceptional high current densities (> 16 A m^{-2}) with 1 V of applied voltage (Jeremiasse et al., 2010; Sleutels et al., 2009). The high performance might result from a good reactor design with a high rate of flow through recirculation of anolyte and catholyte (hydraulic retention times [HRTs] ≈ 1~2 minutes). The recirculation helps mass transport of reactants and products to and from anode and cathode; this might be one of the reasons for their high performance. The energy usage for high rate of recirculation with pump was not evaluated.

Even though the overall overpotential was reduced with addition of CO_2 to the cathode chamber, the Ohmic overpotential increased, and this is likely due to a shift in the predominant species being transported through the AEM from OH^- to carbonate or bicarbonate. I next focused on decreasing this Ohmic overpotential to ensure the maximum benefit of adding CO_2 for pH control. In addition, this leaves cathode overpotential as the major overpotential in the system (0.457 ± 0.023 V), and thus I focused also on testing other cathode catalysts with the aim of reducing the overall applied voltage.

3.3.3 Material selection for reducing the Ohmic and cathode overpotentials

3.3.3.1 Membranes

I show in Figure 3.9 the area specific resistance to ion transport for five different AEMs in 100 mM bicarbonate solution. While AMI-7001 is a standard AEM that have been used in various laboratory MXC studies (Parameswaran et al., 2009; Fornero et al., 2010; Liu et al., 2010), it had the largest resistances to transport of bicarbonate of all the membranes I tested. The FAA, FAB, and A201 membranes provided significantly less resistance to bicarbonate transport compared to the AMI-7001 and I-200 membranes. The result is consistent with the type of membrane, i.e. "homogeneous" or "heterogeneous." Heterogeneous membranes (AMI-7001 and I-200) have a backing material, providing greater mechanical strength but an increase in thickness and thus higher ion transport resistance. On the other hand, homogeneous membranes (FAA, FAB, and A201) are the opposite since they are made from finer resin particles, thus resulting in thinner and flexible membranes with lower resistance (Vyas et al., 2001; Güler, 2010) (see Table 3.1 for thicknesses for each membrane). Since FAA has also better stability at higher pH compared to AMI-7001 (Table 3.1), I selected FAA as the membrane to replace AMI-7001 in the next phase of our MEC testing.

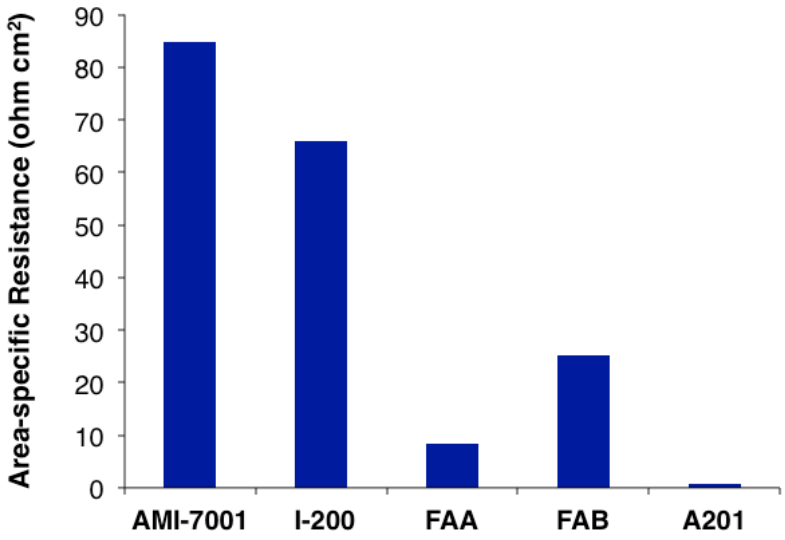

Figure 3.9. Resistances of various membranes tested in 100 mM $NaHCO_3$.

3.3.3.2 Cathodes

Even though CO_2 has a benefit in decreasing the concentration overpotential, the cathode overpotential also represents one of the major overpotentials. A Pt-based cathode can decrease the cathodic activation losses most effectively, but Pt is expensive. Thus, there have been many studies to develop efficient catalysts for reducing cathodic activation overpotential with non-noble metals (Jeremiasse et al., 2010; Krstajić et al., 2011; Hu et al., 2009; Couper et al., 1990). Many reports show that nickel or Ni-based cathodes are effective in decreasing the hydrogen evolution reaction overpotential (Jeremiasse et al., 2010; Selembo et al., 2010; Hu et al., 2010). Therefore, to decrease the cathode overpotential by selecting a good low-cost catalyst, I chose a commercially available Ni mesh, and tested its performance against the SS mesh as a comparison (Figure 3.10). The nickel mesh (Ni 200) had less overpotential compared to the SS mesh especially at high current density. At 10 A m^{-2}, cathode potential is higher by 0.12 (± 0.002) V with Ni 200 mesh indicating a lower activation barrier to produce H_2. This could be because of higher catalytic activity of pure nickel vs. in an alloy, such as in

stainless steel, or related to the specific configuration I used for the meshes (for e.g. open area, mesh size etc. – see Table 3.2).

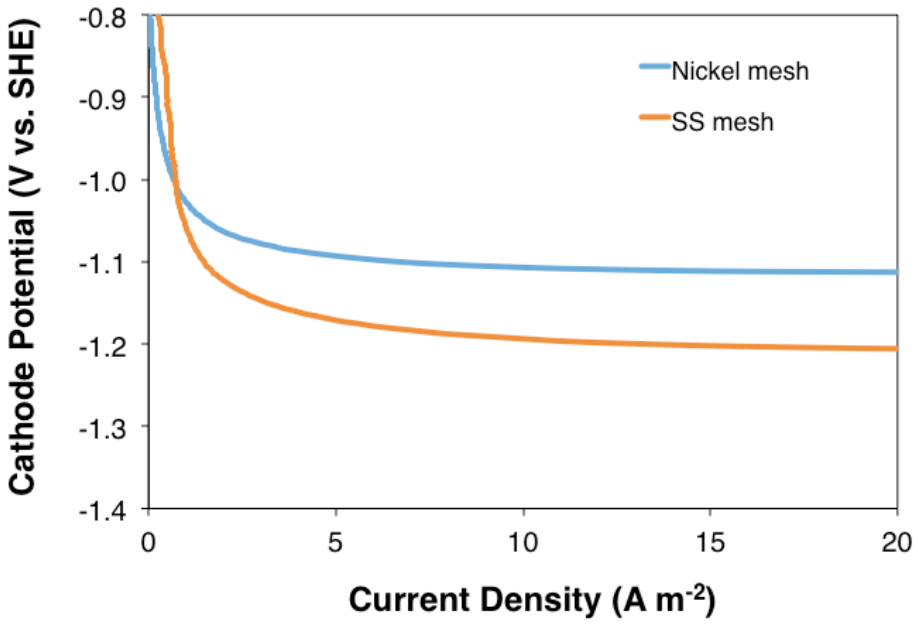

Figure 3.10. Linear sweep voltammograms (LSVs) of stainless steel and nickel mesh cathodes at pH 13.

3.3.4 Characterization of overpotentials in MEC with improved materials

With the Ni mesh cathode and FAA membrane, I performed the same characterization experiments for the MEC as I did with the MEC with SS mesh cathode and AMI-7001 membrane, both without and with adding CO_2 to the cathode chambers (Experiment 3 and 4, respectively). Figure 3.11 shows the *j-V* curve with the applied voltage separated into the various overpotentials. I also summarize each individual overpotential at 10 A m^{-2} in Table 3.4.

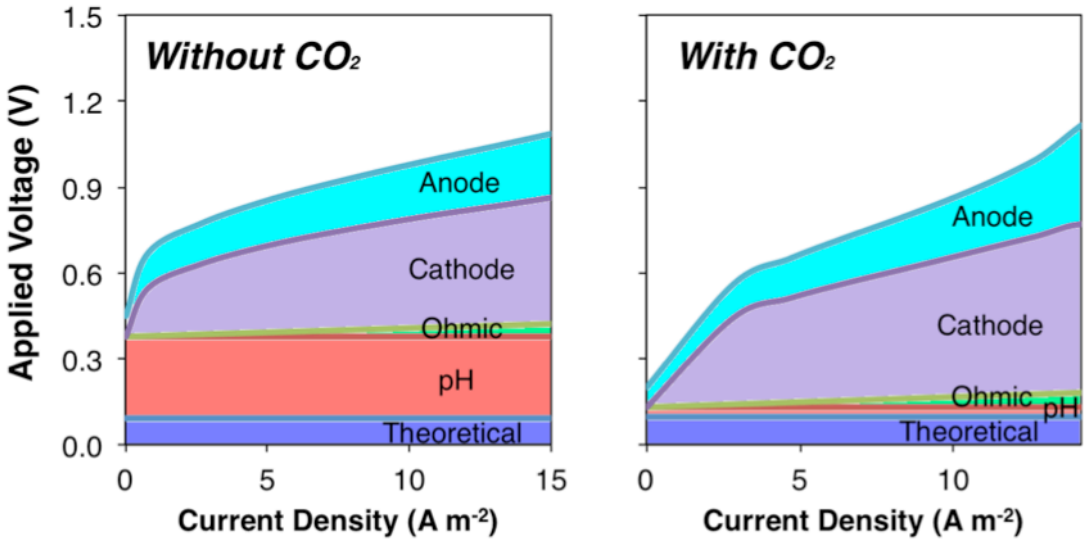

Figure 3.11. Characterization of applied voltage in flat-plate MEC with FAA membrane and nickel mesh cathode (Experiment 3 [left] and Experiment 4[right]). All replicates followed the same trend and an additional representative set is shown in Figure 3.12.

At 10 A m^{-2}, the total overpotential without adding CO_2 to the cathode was 0.989 ± 0.017 V, a significant decrease over the values obtained before the materials improvement (1.092 ± 0.017 V). The FAA membrane decreased the Ohmic overpotential by ~ 52 mV from 0.085 ± 0.002 V with AMI-7001 to 0.033 ± 0.004 V at 10 A m^{-2}. The cathode overpotential decreased from 0.429 ± 0.040 V to 0.405 ± 0.036 V. The FAA membrane allowed for a slightly lower pH in the cathode chamber, which also resulted in a decrease in the concentration overpotential due to a higher cathode pH (0.279 ± 0.011 V overpotential with FAA vs. 0.344 ± 0.019 V overpotential with AMI-7001). The overall reduction in the applied voltage however was smaller than the improvements in these overpotentials, because the anode overpotential was slightly higher at 0.199 ± 0.013 V vs. 0.153 ± 0.012 V.

When adding CO_2 to the cathode chambers, the applied voltage at 10 A m^{-2} was 0.888 ± 0.022 V, which does not represent an improvement over the previous MEC

before including new materials (0.859 ± 0.001 V). This was despite improvement in the Ohmic overpotential, which decreased from 0.125 V ± 0.007 to 0.035 ± 0.003 V with the FAA membrane. The largest part of the overpotential (0.513 ± 0.021 V) in this case was from the cathode overpotential. There are several possible reasons for this. It is possible that there was a local high pH on the cathode surface, despite a lower bulk pH with adding CO_2, which could result in a higher cathode overpotential, which includes any losses due to local concentration gradients.

Table 3.4. Individual overpotential characterized in flat-plate MEC at 10 A m^{-2} with and without CO_2 addition to different cathodes (SS and Ni).

Overpotential	SS without CO_2	SS with CO_2	Ni without CO_2	Ni with CO_2
Anode	0.153 (± 0.012)	0.168 (± 0.016)	0.199 (± 0.013)	0.210 (± 0.014)
Cathode	0.429 (± 0.040)	0.457 (± 0.023)	0.405 (± 0.036)	0.513 (± 0.021)
Ohmic	0.085 (± 0.002)	0.125 (± 0.007)	0.033 (± 0.004)	0.035 (± 0.003)
pH	0.344 (± 0.019)	0.027 (± 0.013)	0.279 (± 0.011)	0.032 (± 0.002)
Theoretical	0.081 (± 0.000)	0.081 (± 0.000)	0.091 (± 0.001)	0.098 (± 0.001)
Total	1.092 (± 0.017)	0.859 (± 0.001)	0.989 (± 0.017)	0.888 (± 0.022)

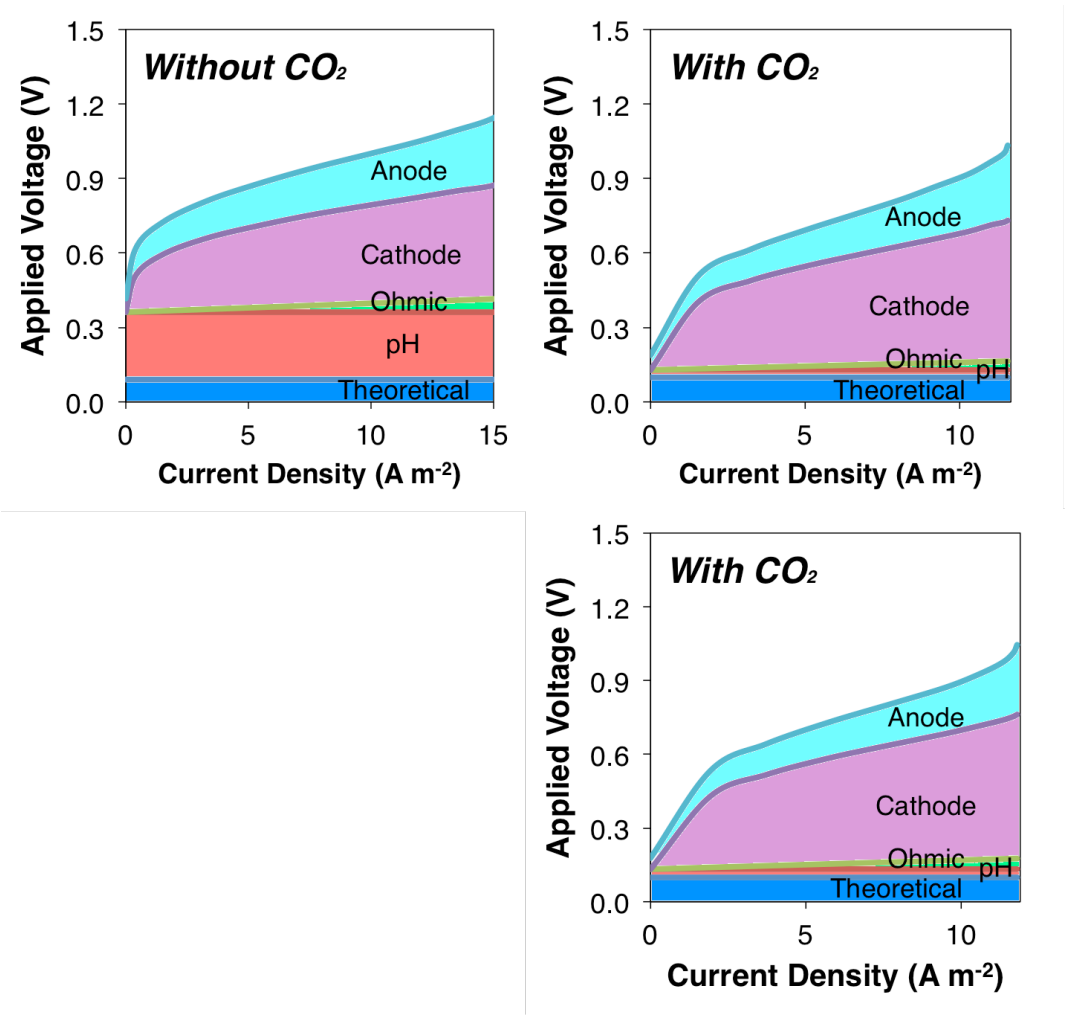

Figure 3.12. Replicate *j-V* curves for Figure 3.11

In addition, the characterization with CO_2 added to the cathode was done after several days of operation of the MEC, which could have resulted in inhibition of the nickel catalyst. It has previously been reported that with long-term operation (> 1 month) with a Ni foam cathode, the overpotential increased, but the exact mechanisms of this change in performance are not known (Jeremiasse et al., 2010). One possible mechanism is the formation of nickel hydride, which has been shown to diminish the catalytic properties of Ni (Hu et al., 2009). In addition, another possible cause could be the decrease of active surface area due to either the H_2 or CO_2 bubbles trapped in the

mesh (Figure 3.13), which were evident while operating the cathode in this fashion. This would result not only in higher activation losses due to reduced surface area, but also possibly concentration overpotential due to accumulation of H_2 on the reaction surface.

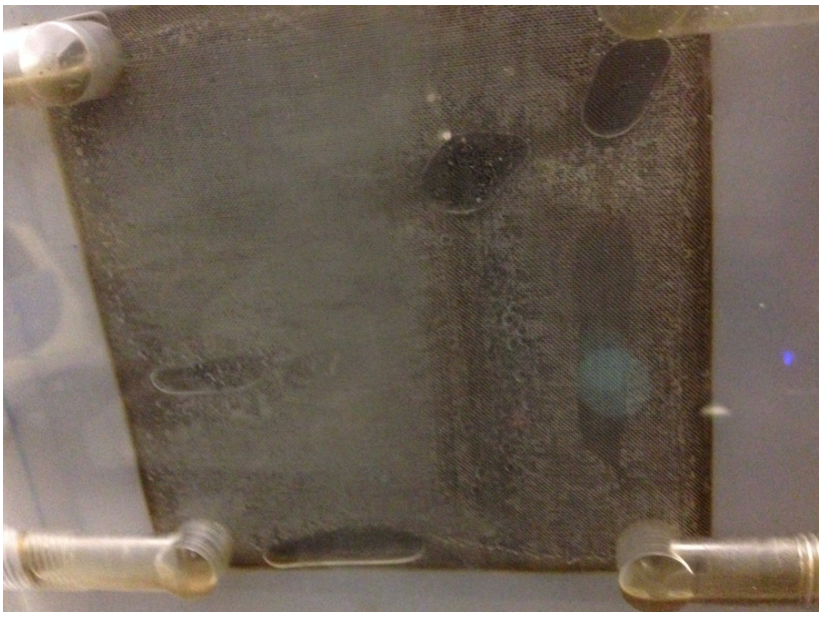

Figure 3.13. Trapped gas bubbles on the cathode surface when using Ni 200 at high current density (> 10 A m^{-2}).

3.4 Implications

I characterized the applied voltage in flat-plate MECs as individual overpotentials from different phenomena. This is of great theoretical and practical importance in order to optimize design and increase voltage efficiency. In our flat-plate MECs, low overpotentials at high current densities were observed with (i) high-surface area anode, (ii) commercially available cathodes and membranes, and (iii) CO_2 addition to the cathode.

Overpotentials arising from each different phenomenon in MECs would vary based on the materials (e.g. membrane, microbial and inorganic catalysts, and solution properties and concentrations) and reactor designs. Different researchers use their own materials and design preferences for achieving their performance goals. However, the type of characterization I present here can serve as a first step to compare the voltage efficiency among various studies.

CO_2 (100%) addition to the cathode eliminated concentration overpotential due to a high cathode pH, just like in air-cathode MFCs as shown earlier (Popat et al., 2012; Torres et al, 2009). I want to note here that while I used a two-chambered MEC where pH difference between the anode and cathode is directly apparent due to the use of a membrane, I have shown that local gradients could also cause a Nernstian concentration overpotential at the cathode in single-chambered systems, which can be decreased or eliminated using CO_2 (Popat et al., 2012). Recycle of the CO_2 produced in the anode from oxidation of organics would be the ideal scenario. In the present study, I use the optimum system using pure CO_2 and fast recirculation with pump. However, how CO_2 is returned from the anode to the cathode needs to be optimized further, especially when dealing with real wastes at the anode.

Homogeneous membrane (FAA) could decrease the Ohmic overpotential with better ionic transport. Especially, the lower membrane resistance was beneficial to allow the membrane to facilitate anions transport (OH^-, HCO_3^-, CO_3^{2-}) with CO_2 addition. However, among the overpotentials I categorized, Ohmic overpotential was the smallest, especially at lower current density (< 5 A m^{-2}). Since current densities when fed with real wastewater could be relatively smaller compared to synthetic medium, I may employ heterogeneous membranes or separators due to the small Ohmic overpotential, as they are mechanically stronger for real wastewater, and economically feasible. I estimate that in any case it should not be difficult to minimize the Ohmic overpotential to < 0.1 V.

The cathode overpotential is still a major problem in our reactor design when I used the commercially available mesh-type cathodes without using any precious metal, as well as widely recognized by many studies (Rozendal et al., 2006; Popat et al., 2012; Rozendal et al, 2008; Zhao et al., 2006). Even though I reduced the concentration overpotential due to a high cathode pH through addition of CO_2, local concentration gradients could still cause a Nernstian concentration overpotential. Overcoming this would require optimizing mass transport between the anode and the cathode further, possibly through using novel designs and/or improved hydrodynamics at the local surfaces. In traditional electrolysis cells, cathode overpotential, although being the highest of all overpotentials, is significantly less than in MECs. I estimate that the cathode overpotential in MECs through further optimization could possibly be reduced to ~ 0.2 V.

Considering all the improvements that can be made, as well as the 0.1-0.3 V of overpotential needed at the anode, I estimate that the total applied voltage in MECs at high current densities (e.g. > 10 A m^{-2}) could be reduced to ~0.7 V. This should thus be the goal of all future optimization studies that hope to address the scalability of MECs.

CHAPTER 4

EFFECT OF PULSED ELECTRIC FIELD (PEF) PRETREATMENT ON PRIMARY SLUDGE FOR ENHANCED BIOAVAILABILITY AND ENERGY CAPTURE[2]

4.1 Introduction

The amount of sludge generated by wastewater treatment has been increasing over time (Rulkens, 2008). In the past, sludges from wastewater treatment plants were disposed of through incineration, landfill application, surface disposal, and ocean disposal (Lim et al, 2014; Spinosa and Vesilind, 2003). However, since 2012, ocean dumping has been prohibited, according to the London Convention for control of sea pollution. Moreover, the cost of sludge disposal often is more than 50% of the total cost to operate a wastewater treatment plant (Rulkens, 2008). Therefore, alternatives that minimize sludge for disposal are key needs for sustainable wastewater treatment. Simultaneous reduction of sludge amounts and with resource capture provide the ideal approach of sludge management (Rittmann, 2008).

Waste activated sludge (WAS) and primary sludge (PS) together represent 80% of the organic carbon from the influent wastewater (Shizas and Bagley, 2004). Hence, they present an excellent opportunity to capture the sludges' renewable energy either 1) directly as renewable methane through methanogenesis or electric current in microbial electrochemical cells (MXCs) or 2) as fermented soluble volatile fatty acids, which can be utilized as internal substrate for denitrification and phosphorus removal. Slow solids hydrolysis is a key factor limiting energy capture (Rittmann et al, 2008; Velasquez-Orta et al, 2011; Wang et al, 2009), and sludge pre-treatment that makes hydrolysis of the

[2] This chapter was published in altered format as Ki D, Parameswaran P, Rittmann BE, Torres CI. 2015. Effect of pulsed electric field (PEF) pretreatment on primary sludge for enhanced bioavailability and energy capture. Environmental Engineering Science 32(10), 831-837.

sludges' organic solids more rapid will increase the capture of resources while minimizing the solids for disposal (Lalaurette et al, 2009).

Various pretreatment techniques have been used to increase hydrolysis rates: e.g., heat treatment, ultrasonication, acid or alkaline chemicals treatment, microwave, and combinations of those techniques (Cho et al., 2012; Eskicioglu et al., 2006; Haug et al., 1978; Kim et al., 2003; Park et al., 2004; Pilli et al., 2011). These pretreatment techniques have not yet been adopted successfully at full scale due to high capital cost, energy use, and chemical consumption. A new alternative is Focused Pulsed® (FP) treatment, which has been studied for improvement of anaerobic digestion in wastewater treatment plants (Lee and Rittmann, 2011; Lee et al., 2010; Rittmann et al., 2008; Salerno et al., 2009; Zhang et al., 2009). FP works on the principle of pulsed electric fields (PEF), and it has been specifically adapted for sludge pretreatment. PEF has been shown to increase methane gas production from anaerobic digestion of waste activated sludge and subsequent reduction of biosolids (Salerno et al., 2009; Rittmann et al., 2008). It also has proven advantageous as an electron donor for denitrification at WWTPs (Lee et al., 2010).

The initial target for PEF pretreatment was WAS (Salerno et al., 2009). While WAS consists mostly of stabilized cell biomass, PS contains relatively more bioavailable crude lipids, proteins, and carbohydrates. PS represents a sizeable fraction of total solids that are generated in a wastewater treatment plant (up to 60% by volume) and sent to the anaerobic digester (Metcalf and Eddy, 2002). Also, PS characteristics vary depending on the seasons and location. PEF treatment of PS alone has not been investigated to-date, although thickened mixed sludge (TMS) (1:1 mixture of PS and WAS) has shown modest improvements with PEF treatment (Ritmann et al., 2008) in a full-scale anaerobic digester.

In this study, I first assess the effect of PEF treatment of PS on sludge characteristics and microbial inactivation. Next, I evaluate the effects of PEF treatment on methanogenesis through biochemical methane potential (BMP) assays. I also perform batch fermentation experiments with and without PEF treatment, using methanogen-inhibited conditions, to evaluate the production of organic acids as an electron donor and carbon source for a range of wastewater applications, such as denitrification, enhanced biological phosphorous removal, and MXCs.

4.2 Materials and Methods

4.2.1 PEF treatment of primary sludge (PS)

Primary sludge was collected from the primary clarifier underflow at the Mesa Northwest Wastewater Reclamation Plant (MNWWRP) in Mesa, Arizona, USA. I treated 30 liters of the PS in the FP alpha unit (OpenCEL/Trojan Technologies, London, ON, Canada) located at the Swette Center for Environmental Biotechnology (SCEB) (Tempe, AZ). System and key process variables are described in previous studies (Lee et al., 2010; Salerno et al., 2009), and more details about FP can be obtained at www.opencel.com. I maintained a sample conductivity of 0.175 mS/cm during FP treatment. With a field-strength of 30kV, the treatment intensity (TI) was 33 kWh/m^3 (Salerno et al., 2009).

4.2.2 BMP and Fermentation

Biochemical methane potential (BMP) tests were performed based on previous studies (Angelidaki et al., 2009; Owen et al., 1979). BMP reactors were set up with a 200-mL working volume in 250-mL serum bottles. Anaerobic digested sludge (ADS) from a well operating anaerobic digester in MNWWRP served as the inoculum after degassing in a 37°C shaker for four days. Triplicate control and PEF-treated PS samples were mixed with ADS in the volumetric ratio of 3:7 (ADS:sample), and buffer and nutrient supplements were added, as described in Angelidaki et al. (2009). Butyl rubber septa and aluminum caps were used for sealing the serum bottles after N_2-gas sparging for 10 minutes to establish anaerobic conditions. The bottles were incubated at 30°C on a shaker table (150 rpm). Negative controls contained the ADS and basal medium alone. Methane gas produced from the ADS inoculum was subtracted from the production from control and PEF-treated PS. The COD of the produced CH_4 was calculated from

$$1\ \text{mL}\ CH_4\ \frac{1\ mmol\ CH_4}{24.86\ mL}\ \frac{8\ meq\ e^-}{mmol\ CH_4}\ \frac{8\ mg\ COD}{meq\ e^-}\ =\ 2.57\ mg\ COD\ \text{at 30 °C}$$

I performed three serial enrichments for PS fermentation with an ADS inoculum that was selectively inhibited for methanogenesis using 50 mM of 2–bromoethanesulfonic acid (BES) (Parameswaran et al., 2011). The first enrichment consisted of a 1:1 volume ratio of PS:ADS and was operated for 15 days, after which 10% of the reactor contents by volume were transferred to a subsequent serum bottle with PS for two more serial enrichments with batch operation times of 15-20 days. At the end of three serial enrichments for control or PEF-treated PS, I performed batch fermentation experiments with the enriched inoculum (10% v/v) for a period of 28 days and with 50 mM BES. The serial enrichment of fermentative bacteria was performed to evaluate the impact of PEF treatment on the kinetics of volatile fatty acids production from PS.

4.2.3 Determining the hydrolysis rate based on methane production

When hydrolysis is the rate-limiting step, the rate of CH_4 production in batch BMP tests can be used to estimate hydrolysis kinetics (Bolzonella et al, 2005; Pavlostathis and Giraldo-Gomez, 1991). First-order hydrolysis kinetics in terms of CH_4 production in a batch reaction is given by:

$$M = M_{max} [1 - \exp (-k_{hyd} t)] \quad (1)$$

where M= cumulative methane production from the BMP assay at time t (mL)

M_{max} = ultimate methane yield from BMP assay at the end of the incubation time (mL)

k_{hyd} = first-order hydrolysis-rate constant (day^{-1})

Equation 1 provides an accurate representation of the BMP results when a) hydrolysis is the rate-limiting step, b) the maximum methane production at the end of the batch tests (M_{max}) represents the total concentration of hydrolyzable COD at the beginning of the tests, and c) hydrolysis kinetics can be represented as first order in the concentration of hydrolysable COD.

Rearranging equation 1 yields

$$\ln [1-\{M/M_{max}\}] = -k_{hyd}\, t \qquad (2)$$

which is a straight line with a slope whose magnitude is the hydrolysis rate constant (k_{hyd}). I obtained k_{hyd} by performing linear regression of $\ln [1-\{M/M_{max}\}]$ versus t.

4.2.4 Analytical methods

The amount of gas was measured with a frictionless glass syringe (PERFEKTUM, Popper and Son, NY) inserted into the septum until its pressure was equal to atmospheric. Gas composition was by sampling the gas phase using a 500-µL gas-tight syringe and performing gas chromatography and thermal conductivity detection (GC-TCD, GC 2010, Shimadzu) after separation on a packed column (Shincarbon ST 100/120, 2m, Restek, Bellefonte, PA). N_2 was the carrier gas with a constant pressure and flow rate of 5.4 atm and 10 mL/min, respectively. I employed temperatures of 120, 145, and 150 °C for injection port, column, and detector, respectively, and the current was 45 mA. Methane (CH_4), hydrogen (H_2), and carbon dioxide (CO_2) were detected by GC-TCD. Calibration was performed using an analytical grade gas standard (CH_4: CO_2: H_2 = 40%: 30%: 30%, Matheson Tri-Gas, Twinsburg, Ohio).

PS characteristics were assayed with total chemical oxygen demand (TCOD), semi-soluble COD (SSCOD), total suspended solids (TSS), volatile suspended solids (VSS), NH_3-N, volatile fatty acids (VFAs), and soluble proteins. Semi-soluble (SS) means that COD analysis was performed on the permeate after filtration through a 1.2-µm glass-fiber filter (WhatmanTM, UK), as described in Lee et al. (2010). COD and NH_3-N were measured using HACH kits and spectrophotometer (DR2700, HACH, Loveland, CO). Soluble proteins were analyzed with the BCA method (Brown et al., 1989), using a BCA protein assay kit (Sigma-Aldrich, St. Louis, MO). Bovine serum albumin (BSA) was used for the standard calibration curves of protein measurement. I used two methods to

measure VFAs: HACH VFA kit and HPLC. For initial VFA characterization, I used HACH kit. For analysis of other VFAs from the fermentation bottles, an HPLC was used for separation of the acids, as described in Parameswaran et al. (2009).

The statistical differences of PS-TCOD conversion to CH_4 and VFAs between control and PEF treatment were evaluated using the Mann-Whitney U test by SPSS 22 (IBM, Armonk, New York) for BMP and Fermentation.

4.3 Results and Discussions

4.3.1 Primary sludge characteristics after PEF treatment

Table 4.1 shows the comparison of primary sludge before and after FP treatment. TCOD and suspended solids have similar concentrations in both cases, which means that FP did not cause net oxidation of volatile solids. However, soluble components such as SSCOD, VFAs, and proteins increased in PEF-treated primary sludge by 78~86%, since microbial cell membranes and walls and macromolecules were disrupted. The increases of soluble organics were modest for PS compared to WAS, which showed a 4800% increase of SCOD with a lower treatment intensity, ~19.8 kWh/m^3 (Salerno et al., 2009). The very low fraction of SSCOD-to-TCOD in control and PEF-treated PS (less than 3%) indicates that hydrolysis of the organic solids in PS was the main source of the methane and VFAs production. PEF treatment also increased the sample temperature from 29°C to 49°C, although Sheng et al. (2011) showed that similar temperature increases were not responsible for changes of sludge characteristics.

Table 4.1. Primary sludge characteristics before and after PEF treatment

Parameters	Control	PEF treated	Change (%)
TCOD (mg COD/L)	18,100 (± 92)	18,300 (± 424)	1.4
SSCOD (mg	257 (± 3)	459 (± 2)	79
SSCOD/TCOD (%)	1.4	2.5	79
TSS (mg/L)	13,500	13,400 (± 102)	-0.7
VSS (mg/L)	10,300 (± 19)	10,200 (± 67)	-0.9
Protein (mg/L)[a]	54 (± 1.2)	99 (± 0.9)	86
VFAs (mg COD/L)	84	150	79
Temp. (°C)	29	49	-
pH	6.7	6.9	-

[a] Protein as bovine serum albumin (BSA)

4.3.2 Stability of PEF-treated PS under psychrophilic conditions

A significant benefit of PEF treatment of PS could be microbial inactivation. Sheng et al. (2011) showed that PEF treatment inactivated the cyanobacterium *Synechocystis* PCC 6803, based on culture plating. Here, I evaluated microbial inactivation by monitoring for changes in soluble COD, VFAs, and volatile suspended solids for control and PEF-treated PS during storage at 4°C. Figure 4.1 shows that control PS underwent rapid degradation during storage at 4°C: SSCOD increased to about 2000 mg/L after 50 days of storage. In contrast, PEF-treated PS maintained stable SSCOD values of around 500 mg/L for the entire 54 days. The increase in SSCOD for the control PS was accompanied by a decrease in the VSS, while PEF-treated PS had a constant VSS concentration. Degradation also could be measured as VFAs, shown in Figure 4.2. Only the control PS had VFA production, predominantly propionate. Inactivation by PEF was repeatable, as shown by data for a second trial (Figure 4.3). Hydrolytic bacteria in PS could be spore or non-spore forming, given the complexity of

PS. Spore-forming bacteria could resist inactivation by PEF, while other bacteria (e.g., non-spore forming hydrolytic bacteria, fermenters) in PS could be inactivated. However, the microbial inactivation with PEF at 4°C indirectly indicates that the fraction of spore-forming hydrolytic bacteria was very limited for hydrolysis of PS, since PEF-treated VSS was stable during long-term storage (Figure 4.1).

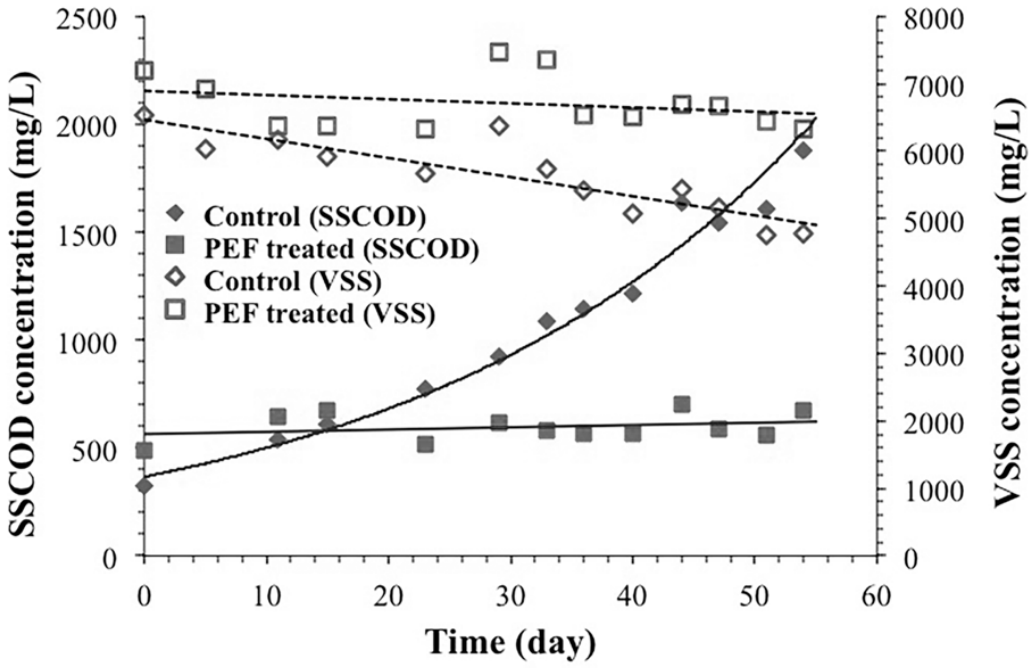

Figure 4.1. Changes of SSCOD and VSS concentrations of control and PEF-treated PS during storage at 4°C. Solid and dotted lines, used to highlight trends, were generated using the Trendline function in MS Excel.

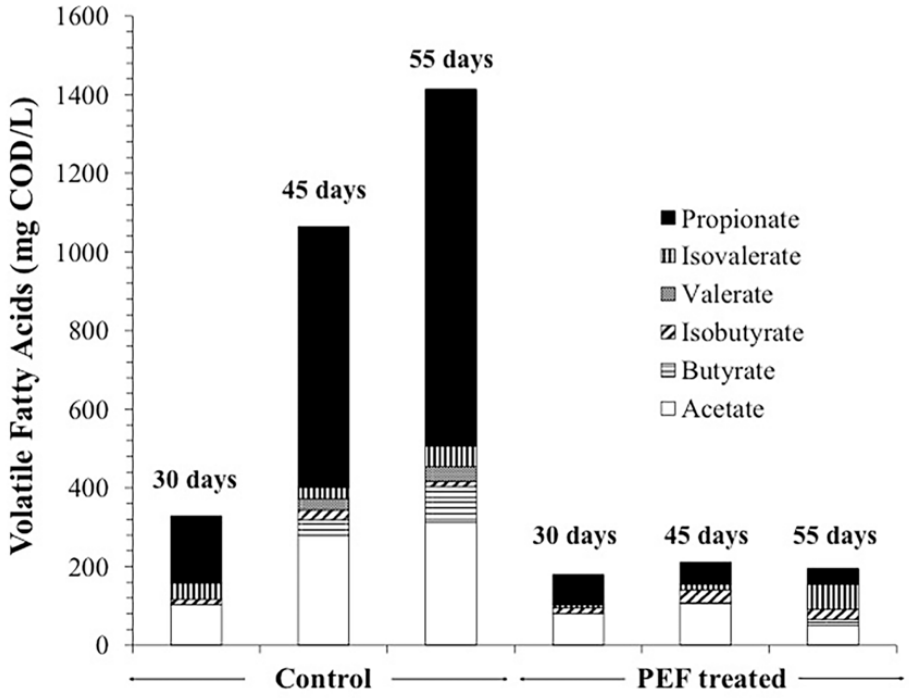

Figure 4.2. VFAs profiles of control and PEF-treated PS during storage at 4°C. The number of days on top of each bar graph corresponds to the time since storage began.

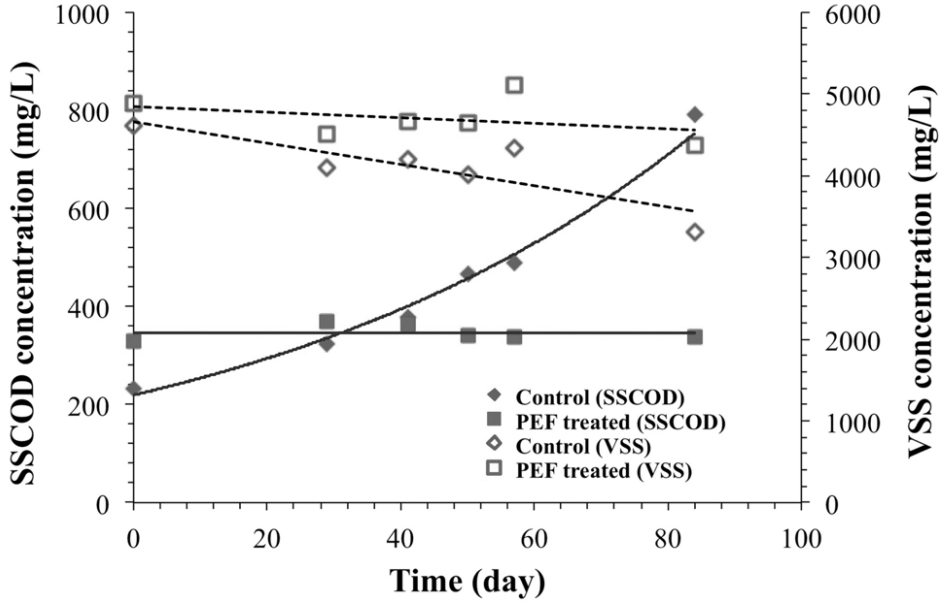

Figure 4.3. Inactivation of PEF treated PS compared to control PS in which had increase of soluble COD concentration and decrease of VSS concentration with time in the storage of psychrophilic condition with primary sludge.

4.3.3 Biochemical methane potential (BMP)

As shown in Figure 4.4, the initial rate of methane production in BMP assays was rapid for control and PEF-treated PS over ~10 days, after which the rate decreased. Even though the trends for control and PEF-treated PS are similar, the CH_4-production rate was higher for PEF-treated PS between 3 to 14 days, when particle hydrolysis likely played a major role for controlling the rate of methanogenesis. At the end of the BMP assay, the PEF-treated PS had yielded 8% more methane, and its fractional COD conversion increased from 32% to 34.5%, an 8% relative increment; the difference of CH_4 conversion from PS-TCOD was significant between control and PEF (p-value < 0.05).

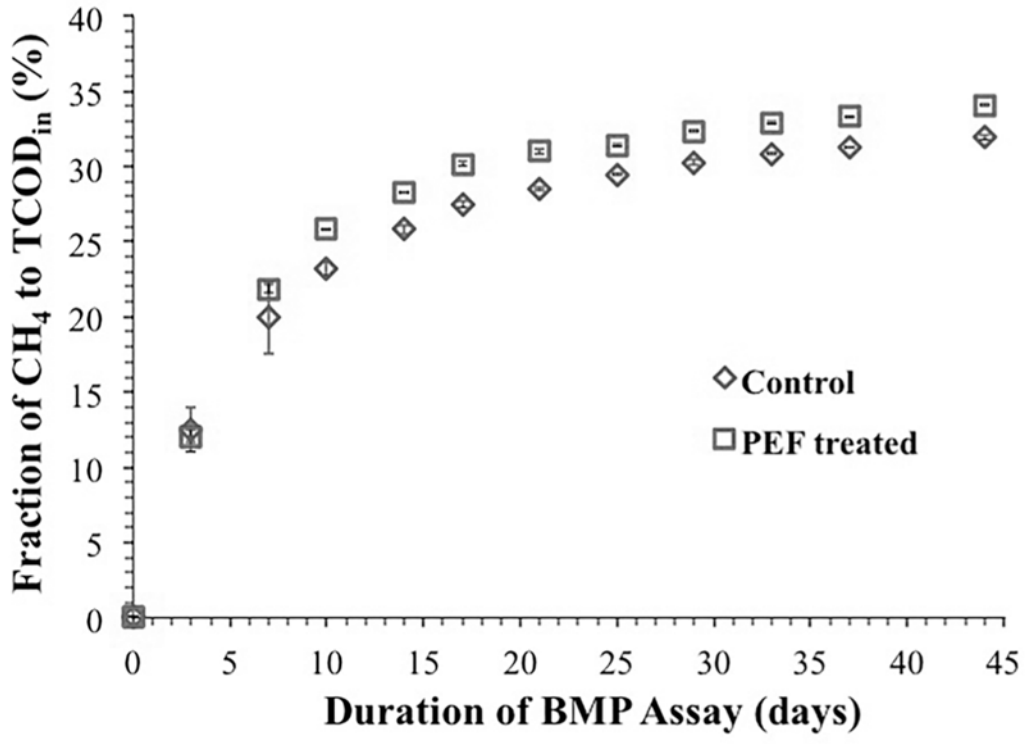

Figure 4.4. Cumulative CH_4 results for control and PEF-treated PS in BMP assays as a fraction of the TCOD of the starting PS.

Using the first-order model (equations 1 and 2), I computed the hydrolysis rate constants ($k_{hyd\text{-}BMP}$) as 0.105 (± 0.005) and 0.119 (± 0.012) (day^{-1}) for control and PEF-treated PS, respectively. Other studies place the PS-hydrolysis rate constants in a similar range, between 0.09 and 0.17 (day^{-1}) (Elbeshbishy et al., 2012; Ferreiro and Soto, 2003), with local differences arising due to differences in operational condition (e.g., temperature), particle size of the PS solids, and compositions of carbohydrate, protein, and lipid. The 13% increase in hydrolysis rate coefficient for PEF-treated PS, compared to control PS, may explain the increment to CH_4 conversion within the initial 14 days. Methane production from control PS slowly caught up with the PEF-treated PS between 14 and 44 days, resulting in the small decline in the relative increase in CH_4 production, to 8%. These trends indicate that PEF-treated PS may be modestly effective at only short solid retention time (SRT).

4.3.4 Fermentation with methanogen inhibition

Figure 4.5 shows the results of batch fermentations over 30 days with 50 mM BES added to inhibit methanogenesis. The 1st and 2nd enrichments showed similar results for total VFAs and pH. The initial lag time with PEF-treated PS fermentation reactors might have resulted from lower microbial activity after PEF treatment, even though PEF increased the initial soluble COD. This might have caused lower rates of hydrolysis and fermentation in the initial stage. On the other hand, untreated (control) PS had an undisturbed starting population of indigenous fermenters in the PS, plus those from the inoculum. Therefore, the control could have had quicker VFA production by consuming soluble organics from easily hydrolysable solids. After around 10 days, the pH declined to less than 5.5, and total VFAs stabilized. PEF-treated PS always had pH 0.1 to 0.2 units lower than control PS, one indication of higher fermentation efficiency to

VFAs. After a short lag period, the PEF-treated PS showed slightly, but consistently higher concentration of total VFA.

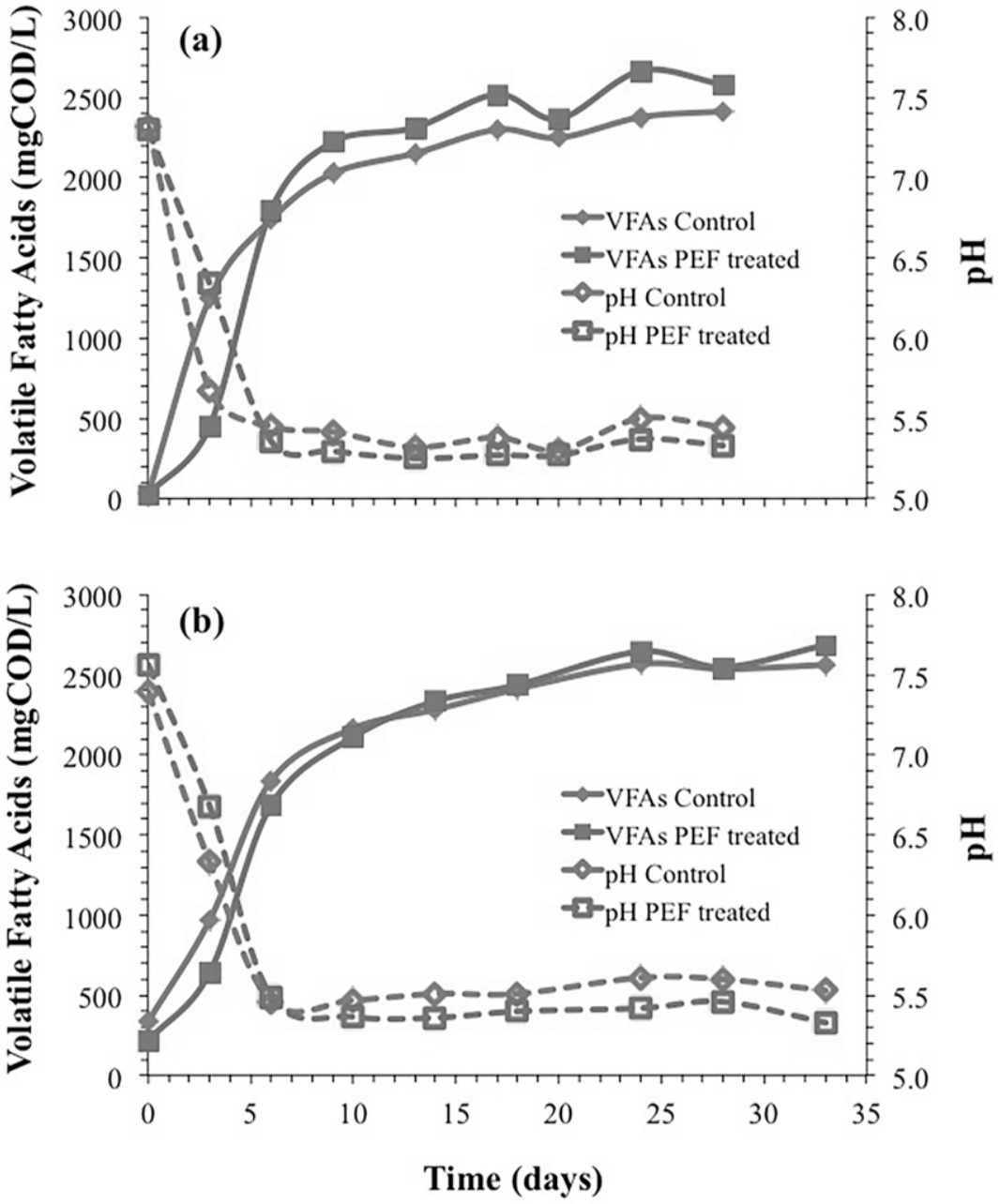

Figure 4.5. pH and volatile fatty acids (VFAs) concentrations produced in the fermentation batch bottles: (a) 1st enrichment fermentation and (b) 2nd enrichment fermentation.

Based on the VFA production, I also computed the hydrolysis rate constants ($k_{hyd\text{-}fermentation}$) using first-order model: 0.204 (± 0.009) and 0.254 (± 0.089) (day^{-1}) for control and PEF-treated PS, respectively. Thus, PEF-treated PS showed a 24% increase in hydrolysis rate coefficient, compared to control PS, over 10 days. Higher k_{hyd} based on fermentation compared to BMP is consistent to Pratt et al. (2012). At the end of batch fermentation, the PEF-treated PS had accumulated 7% more VFAs, and its fractional COD conversion (gVFA-COD/$gTCOD_{in}$) increased from 13 to 14%, a 7% relative increment; the difference of VFAs conversion from PS-TCOD was significant between control and PEF (p-value < 0.05). Though the relative increment after PEF treatment by fermentation is similar to the one in BMP assay, the actual magnitude of ~13% conversion in fermentation is much lower, compared to ~30% in BMP during 30 days operation. Hydrolysis and fermentation may have been limited due to three reasons. First, PS may have a substantial fraction of organic solids that resist hydrolysis (Rulkens, 2008; Jones et al., 2008). Second, the low pH after 10 days may have inhibited hydrolytic bacteria (Veeken et al., 2000). Third is feedback inhibition by the fermentation products (Pratt et al., 2012; Raposo et al., 2006).

Even though VFAs accumulation with time had similar trends to methane production in BMP assays, total VFAs produced in control and PEF-treated PS started to stabilize earlier (between 6 to 10 days), compared to BMP (after 10 days) (Figure 4.4 and 2.5). Correspondingly, I also show in Figure 4.6 that acetate production in all cases (control and PEF-treated PS of the 1st and 2nd enrichments) stabilized in less than 10 days of batch operation. On the other hand, other fatty acids (propionate, butyrate, iso-butyrate, valerate, and iso-valerate) increased to the end of the batch experiments (Figure 4.7). These results support a possible thermodynamic feedback inhibition of β-

oxidation that converts longer fatty acids (e.g., butyrate) to acetate (Rittmann and McCarty, 2001; McCarty and Smith, 1986).

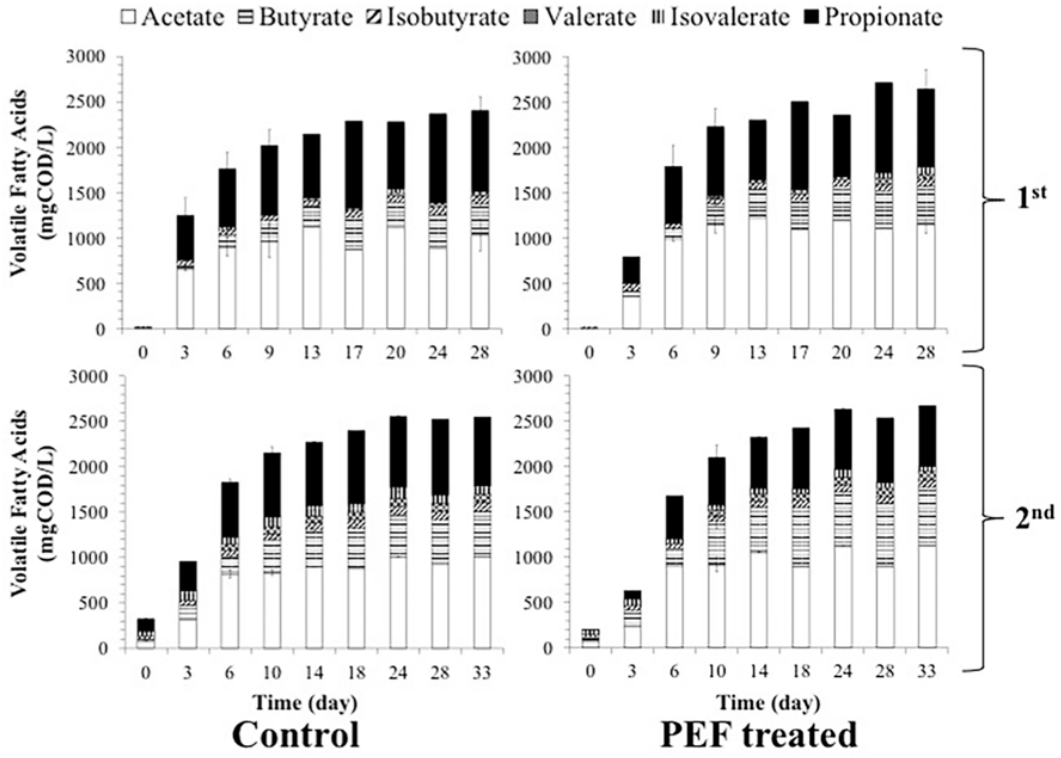

Figure 4.6. Changes of VFAs profiles during the 1st and 2nd enrichment fermentations for control and PEF-treated PS.

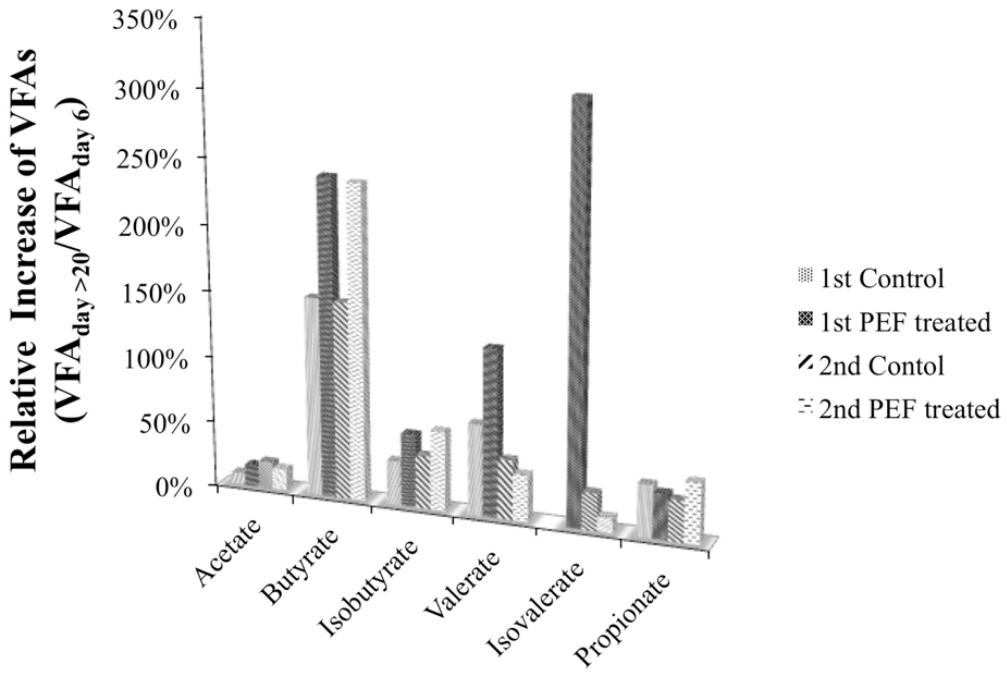

Figure 4.7. Relative increase of volatile fatty acids (VFAs) with the ratio of the average VFAs over 20 days to VFA at day 6**.**

4.3.5 Is PEF treatment effective for PS only?

Table 4.2 shows that the methane-production rate (MPR) for PEF-treated sludges were 1.6, 1.7, and 1.1 times higher than the respective controls for thickened mixed sludge (50:50 ratio of WAS:PS), WAS alone, and PS alone, respectively. This highlights that WAS contributed significantly to the positive impacts observed with FP treatment of thickened mixed sludge (Rittmann et al., 2008). Consistent with the impact of PEF on methane production are the much larger increases in soluble COD after FP treatment of WAS (4800%) (Salerno et al., 2009), compared to PS (79%) (Table 4.1). This large difference results from the severe disruption of WAS flocs and bacterial cells (Salerno et al., 2009). In contrast, PS has relatively more non-cellular organic solids, and the organic solids are more readily biodegradable. Thus, PEF treatment of PS did not result in a big increase in SSCOD or a large increment of methane production. The VFAs after

fermentation of sludges could generate sustainable electron donors for emerging technologies such as microbial electrochemical cells, denitrification, or advanced biological phosphorus removal (Choi and Ahn, 2014; Lee et al., 2010; Tong and Chen, 2007). Similar to the modest improvement of methane production using PEF-treated PS, PEF treatment did not result in a large increment of VFAs accumulation from PS. However, our study points to the value of evaluating different ratios of PS and WAS for anaerobic digestion and fermentation to VFAs.

Table 4.2. Comparisons of methane production rate with different sludge types in anaerobic digestion

Sludge type	Methane production rate (L/kg VS/ day)		Ratio of MPR increase	Reference
	Control	PEF treated		
WAS + PS (1:1)	794	1270	**1.6**	Rittmann et al. (2008)
Only WAS	8.6	14.8	**1.7**	Salerno et al. (2009)
Only PS	0.61	0.68	**1.1**	This study

4.4 Conclusion

PEF treatment of PS resulted in efficient microbial inactivation and modest improvements in the bioavailability of organic solids in PS. COD-conversion efficiencies by methanogenesis and fermentation marginally increased by 8% and 7%, respectively, at the end of batch experiments. Hydrolysis rate coefficients increased by 13% and 24%, as well. These results support that the maximum benefit to energy capture and solids reduction for wastewater-treatment sludges should be achieved by PEF treatment of WAS, rather than PS. This points to the value of optimizing ratios of PS: WAS for PEF treatment, whether the goal is methanogenesis or fermentation to VFAs.

CHAPTER 5

EFFECTS OF PRE-FERMENTATION AND PULSED-ELECTRIC-FIELD TREATMENT OF PRIMARY SLUDGE IN MICROBIAL ELECTROCHEMICAL CELLS[3]

5.1 Introduction

Wastes containing high concentrations of organic solids, such as primary and waste activated sludge, black water, and livestock manure, offer potential for energy recovery. These wastes can be stabilized using anaerobic digestion (AD) that produces methane, which is combusted to heat digesters and buildings or to generate electrical power (McCarty et al., 2011). Microbial electrochemical cells (MXCs), a new anaerobic biotechnology, convert organic compounds to electricity or other valuable products, e.g., hydrogen gas and hydrogen peroxide (Rittmann et al., 2008a; Rozendal et al., 2009; Torres et al., 2010). Domestic and animal wastewaters and landfill leachate have been tested for MXC feasibility (Liu et al., 2004; You et al., 2006; Mahmoud et al., 2014).

While primary sludge (PS) generated during municipal wastewater treatment is a readily accessible source of organic solids, a major bottleneck for using PS for energy recovery is the slow hydrolysis of particulate organics (Rittmann and McCarty, 2001; Ristow et al, 2005, Cokgor et al., 2009). Two-stage AD – hydrolysis followed by methanogenesis – has been evaluated for several decades as a means to accelerate hydrolysis to improve methane generation and solids destruction (Ghosh, 1987; Bhattacharya et al., 1996; Ghosh et al., 1995). Likewise, various pretreatment methods may be able to augment the rate and extent of hydrolysis of particulate organics: e.g.,

[3] This chapter was published in altered format as Ki D, Parameswaran P, Popat SC, Rittmann BE, Torres CI. 2015. Effects of pre-fermentation and pulsed-electric-field treatment of primary sludge in microbial electrochemical cells. Bioresource Technology 195, 83-88.

mechanical, thermal, alkaline, ultrasonication, and microwave pre-treatments (Cho et al., 2012; Eskicioglu et al., 2006; Kim et al., 2003; Park et al., 2004; Pilli et al., 2011).

In this study, I evaluate semi-continuous pre-fermentation of PS as a method to produce volatile fatty acids as electron donor for microbial electrolysis cells (MECs). Pre-fermentation ahead of an MEC should be a good means to increase the conversion of particulate organics to simple organic acids. These organic acids are the substrates available to the anode-respiring bacteria (ARB) to produce electric current (Torres et al., 2009; Rosenbaum et al., 2010; Choi and Ahn, 2014; Mahmoud et al., 2014; Yang et al., 2013). Testing pre-fermented PS liquor in single-chamber air-cathode microbial fuel cells (MFCs), Yang et al. (2013) obtained a good performance in terms of Coulombic efficiency and soluble COD removal. Choi and Ahn (2014), also using a single-chamber air-cathode MFC, showed advantages for sludge reduction and electricity production (increased current and power densities). Mahmoud et al. (2014) investigated fermentation of landfill leachate, producing acid metabolites (mostly acetate) that were utilized in a dual-chamber MEC to allow significant increases in its performance compared to raw leachate. While the concept of pre-fermentation was supported by these batch studies, practical application of pre-fermentation followed by an MXC needs to be evaluated for long-term continuous operation.

I also evaluate the effect of pulsed-electric-field (PEF) pre-treatment on electron recovery from PS in the two-stage system of pre-fermentation and MEC. In particular, PEF is an emerging sludge pre-treatment technology that has been applied to increase the biogas production and volatile solids reduction in anaerobic digesters and to generate sustainable electron donors for denitrification (Lee and Rittmann, 2011; Rittmann et al., 2008b; Alder et al., 2009; Lee et al., 2010). PEF has been shown effective in waste activated sludges, but no previous studies exist on PS treatment alone

with PEF. Up to now, no study evaluated the impacts of PEF treatment of PS for energy capture in an MXC system. I evaluate the impact of PEF pre-treatment in conjunction with pre-fermentation.

5.2 Materials and Methods

5.2.1 Primary sludge (PS) characterization

I collected PS from the primary clarifier underflow at the Mesa Northwest Wastewater Reclamation Plant (MNWWRP) in Mesa, Arizona, USA. I pretreated a fraction of the collected PS with PEF using the Focused Pulsed® (FP) *alpha* unit (OpenCEL/Trojan Technologies, London, ON, Canada) located at the Swette Center for Environmental Biotechnology (Lee et al., 2010; Salerno et al., 2009). I diluted the PS ~1.3-fold with distilled water to achieve a conductivity of 0.175 mS cm^{-1}, and I applied a treatment intensity of 33 kWh m^{-3} during PEF treatment (Salerno et al., 2009). Control and PEF-treated PS were stored in a 4°C cold room and used as feedstock for semi-continuous fermentation experiments. Their characteristics (e.g., suspended solids, chemical oxygen demands) are shown in Tables 5.1 and 5.2.

Table 5.1. Influent primary sludge characterization in each condition

Average (unit: mg/L)

	under methanogen inhibition (BES)						without methanogen inhibition (No BES)					
	6 day HRT - 6 day SRT		3 day HRT - 3 day SRT		2 day HRT - 2 day SRT		3 day HRT - 3 day SRT		6 day HRT - 15 day SRT		3 day HRT - 15 day SRT	
	Control	PEF treated	Control	PEF treated	Control	PEF treated	Control	PEF treated	Control	PEF treated	Control	PEF treated
TCOD	10100 (±625)	11100 (±834)	10300 (±518)	11300 (±1063)	10870 (±895)	11400 (±967)	9410 (±633)	9760 (±369)	10900 (±399)	9350 (±111)	12200 (±47)	11800 (±231)
SSCOD	632 (±227)	589 (±81)	1270 (±248)	604 (±68)	1680 (±179)	605 (±59)	352 (±101)	501 (±50)	513 (±52)	681 (±188)	347 (±139)	483 (±1)
TSS	6930 (±318)	7620 (±439)	6150 (±306)	7670 (±462)	5480 (±281)	7290 (±189)	6390 (±8)	6440 (±327)	7530 (±506)	5990 (±177)	8730 (±21)	7600 (±40)
VSS	6060 (±318)	6640 (±399)	5310 (±199)	6580 (±103)	4910 (±226)	6480 (±169)	5500 (±157)	5560 (±324)	6600 (±444)	5250 (±206)	7260 (±26)	6550 (±107)

Table 5.2. Characteristics for influent of pre-fermentation reactors at 3 day SRT (=HRT) in order to collect centrate for MEC batch experiment

Average (unit: mg/L)

	Control	PEF
TCOD	7500 (±300)	8300 (±600)
SSCOD	380 (±110)	350 (±20)
TSS	4700 (±300)	5400 (±500)
VSS	4300 (±200)	4900 (±400)
BOD_5	3100 (±200)	3600 (±200)

5.2.2 Fermentation set up and operation

The fermentation reactors were started in batch mode with a 180-mL working volume in 250-mL serum bottles; anaerobic digested sludge (ADS) from MNWWRP was the inoculum. Three serial enrichments of batch fermentation were performed under selective methanogenic inhibition using 50 mM 2-bromoethanesulfonic acid (BES). At the end of batch fermentations, I carried out semi-continuous fermentation at 6-, 3-, and 2-day solid retention times, SRTs (= HRTs, hydraulic retention times). Each condition was maintained for 5x SRTs to ensure steady state.

After this operation, I operated the fermentation reactors at a 3-day SRT (=HRT) without any methanogen inhibitor. To improve hydrolysis of PS, I later increased the SRT to 15 days and operated with two different HRTs (6 and 3 days) by adding the appropriate amount of the concentrated solids back into the reactor after centrifugation. For example, I maintained a 15-day SRT and 6-day HRT by the following five steps: 1) remove 30 mL of mixed liquor from the 180-mL volume in the fermentation reactor (giving a 6-day HRT), 2) discard 18 mL, 3) centrifuge the remaining 12 mL (giving a 15-day SRT) at 3220 x g (Eppendorf Centrifuge 5810 R, USA), 4) mix the solids pellets with

fresh PS to a total final volume of 30 mL, and 5) add the resultant PS mixture into the reactors.

5.2.3 MEC set up and operation

I used a flat-plate microbial electrolysis cell (MEC), which avoids oxygen intrusion that typically occurs in microbial fuel cells (MFCs) and leads to undesirable and difficult-to-quantify electron losses (Torres et al., 2009). The components of the MEC are shown in Figure 5.1. The MEC had two anodes within a common anode chamber (0.3-0.35 L in volume) and two cathodes in two individual cathode chambers, 0.1-0.2 L each on either side of the anode chamber. The differences of anode and cathode volumes resulted from the membrane bending or warping when anolyte and catholyte were added with syringes. The anodes were made of carbon fiber (24K Carbon Tow, Fibre Glast, OH, USA) woven into a titanium frame that was the current collector. The carbon fiber, already woven with the current collector before MEC assembly, was washed in the following order (An and Lee, 2013): 1 N nitric acid for 3 hours, 1 N acetone for 12 hours, 1 N ethanol for 3 hours, and finally 18 MΩ deionized water. The cathodes were stainless steel meshes (SS, type 316, mesh 80 x 80, 0.0055" of wire diameter, McMaster-Carr, USA), and the separators were anion exchange membranes (AMI-7001, Membranes International, Glen Rock, NJ, USA). Each anode, cathode, and membrane has projected area of 100 cm^2, for a total of 200 cm^2 of projected area for the anode, the cathode, and the membrane.

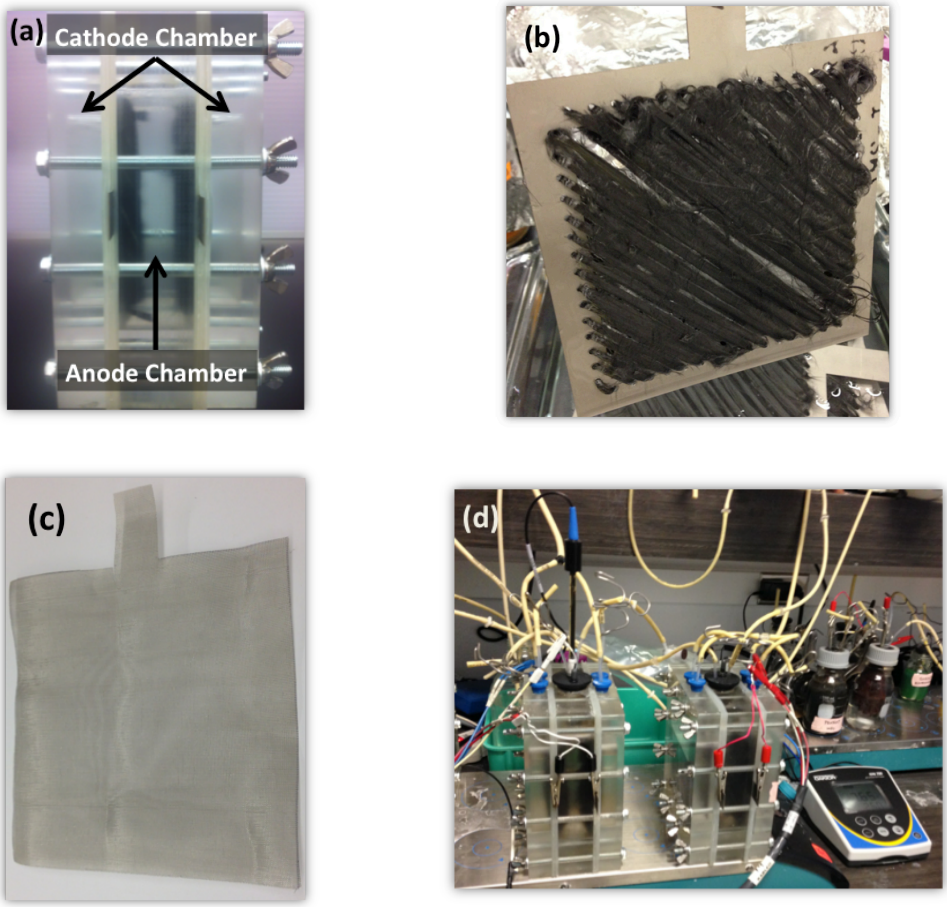

Figure 5.1. Pictures of flat-plate MECs. (a) Assembled MECs, (b) carbon fiber anode woven with titanium current collector, (c) SS cathode, and (d) MEC reactors equipped with a pH probe when fed with primary sludge.

For ARB acclimation, I inoculated the MEC with anaerobic digested sludge (from MNWWRP) and the effluent from an MEC that has been continuously operated with acetate medium. The MEC anode was operated first with acetate medium in batch mode until the current was greater than 5 A m^{-2}. I then changed to continuous mode with acetate. The acetate medium consisted of 50 mM acetate, 100-mM phosphate buffer (85% Na_2HPO_4 and 15% KH_2PO_4), 14 mM ammonium chloride, and trace minerals (Lee et al., 2008). The anode potential was poised -0.3 V (vs. Ag/AgCl) with a potentiostat (VMP3, BioLogic Science Instruments, Knoxville, TN) to create non-limiting conditions

for ARB kinetics (Torres et al. 2008). After I operated the MEC with the acetate medium for two months, I allowed acetate to deplete in batch operation and changed the feed to the pre-fermented centrate. I conducted two batch runs with acetate prior to the control and PEF-treated centrate batch MEC runs to ensure that MEC anodes had similar conditions.

Figure 5.2 is a schematic of the MEC experiments using fermented PS "centrate," which was generated by centrifuging (3220 x g) and then filtering (GF/C, Whatman®, UK) fermentation effluent. The centrate was composited for ~10 days to obtain enough liquid volume to be fed to the MEC anode chamber (~ 0.5 L), and it was stored in 4°C refrigerator prior to use. The centrate pH and alkalinity were ~6 and 300 mg/L as $CaCO_3$. Before being fed to the MEC, centrate pH was measured and adjusted to ~7 by adding sodium hydroxide. A pH probe was installed in the center of the anode chamber (Figure 5.1d), and the pH was maintained between 6.5 and 8.5 with manual addition of sodium hydroxide (1 M) or hydrochloric acid (1 M), as needed.

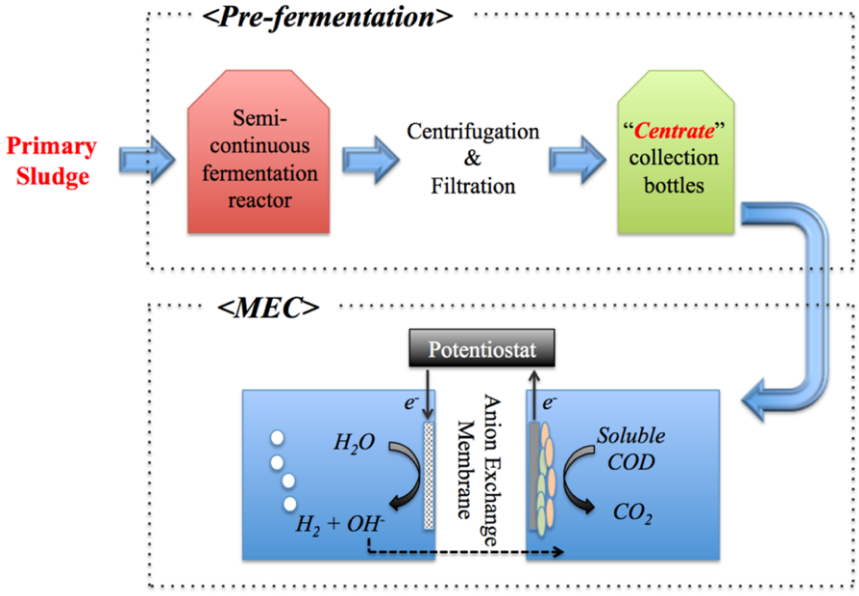

Figure 5.2. Schematic of the linkage between semi-continuous fermentation of PS and current capture from the fermentation centrate using an MEC.

5.2.4 Analytical methods

The volume of produced biogas was measured with a frictionless glass syringe (PERFEKTUM, Popper and Son, NY) by injecting it through the septum on the fermentation reactor and letting the gas pressure equilibrate with atmospheric pressure. Gas composition was analyzed with a gas sample taken with a 500-µL gas-tight syringe and using a gas chromatograph equipped with a thermal conductivity detector (GC-TCD, GC 2010, Shimadzu) and a packed column (Shincarbon ST 100/120, 2 m, Restek, Bellefonte, PA). N_2 was the carrier gas with a constant pressure and flow rate of 5.4 atm and 10 mL/min, respectively. Temperatures were 120, 145, and 150°C for injection port, column, and detector, respectively, and the current was 45 mA. Calibration was done with an analytical grade gas standard (CH_4: CO_2: H_2 = 40%: 30%: 30%, Matheson Tri-Gas, Twinsburg, Ohio).

PS characterization involved measuring total chemical oxygen demand (TCOD), semi-soluble COD (SSCOD) (defined as COD of the permeate filtered through a 1.2-µm GF/C filter), total suspended solids (TSS), volatile suspended solids (VSS), and volatile fatty acids (VFAs). COD was measured using spectrophotometric methods by HACH kit and spectrophotometer (DR2700, HACH, Loveland, CO). For the separation and quantification of VFAs from the fermentation experiments, an HPLC equipped with an AMINEX HPX-87H column was employed according to the conditions described in Parameswaran et al. (2009).

5.2.5 Calculations

The current density expressed in A m^{-2} was calculated based on the projected area of the anode.

Electron-equivalent mass balance on the fermentation reactors was expressed as mgCOD L^{-1}:

$$TCOD_{influent} = TCOD_{effluent} + CH_4 + Other$$

$$= PCOD_{effluent} + SCOD_{effluent} + CH_4 + Other \quad (1)$$

where $TCOD_{influent}$ is the measured input PS total COD concentration, $TCOD_{effluent}$ is the measured effluent TCOD concentration, $SCOD_{effluent}$ is the measured semi-soluble COD concentration, $PCOD_{effluent}$ is the computed particulate COD (difference between $TCOD_{effluent}$ and $SCOD_{effluent}$), CH_4 is the COD equivalent of the methane gas (mL),

$$1\ mL\ CH_4 \frac{1 mmol\ CH_4}{24.86\ mL} \frac{8\ meq\ e^-}{mmol\ CH_4} \frac{8 mg\ COD}{meq\ e^-} = 2.57\ mg\ COD\ at\ 30\ °C \quad (2)$$

and Other is any unaccounted COD sinks.

The electron-equivalent mass balance for MEC operation was also based on COD equivalents:

$$COD_{initial} = electrical\ current + COD_{final} + COD_{unaccounted} \quad (3)$$

where $COD_{initial}$ is the measured mgCOD of the input centrate, electrical current is the COD equivalent of the Coulombs accumulated during the batch operation,

$$1\ Coulomb\ of\ current \frac{1e^- eq}{96485\ C} \frac{8g\ COD}{e^- eq} \frac{1000\ mg}{g} = 0.083\ mg\ COD \quad (4)$$

COD_{final} is the measured mgCOD at the end of batch MEC, and $COD_{unaccounted}$ is any unaccounted COD.

Coulombic efficiency (CE, the fraction of electrons recovered as electrical current at the anode of an MXC compared to the electrons removed from the substrate) and Coulombic recovery (CR, the fraction of electrons recovered as electrical current at the anode of an MXC compared to the total influent electrons in the substrate) were calculated based on Equations 5 and 6, along with the conversion of Equation 4:

$$CE\ (\%) = \frac{electrical\ current}{(COD_{initial} - COD_{final})} \times 100 \quad (5)$$

$$CR\ (\%) = \frac{electrical\ current}{COD_{initial}} \times 100 \quad (6)$$

Volatile-Solids Destruction was computed based on the averaged change of VSS concentration for each SRT;

$$Volatile\ Solids\ Destruction\ [VSD](\%) = \frac{(VSS_{in} - VSS_{out})}{VSS_{in}} \times 100 \quad (7)$$

5.3 Results and Discussions

5.3.1 Semi-continuous fermentation with methanogen-inhibited conditions

I showed volatile solids destruction (VSD) results at each SRT for both control and PEF-treated PS (Figure 5.3). In control PS, the VSD decreased with shorter SRTs from 27% at 6 days to 14% at 3 day SRT. On the other hand, VSD was maintained at around 25% at 3 day SRT for PEF-treated PS (1.8 fold higher than control), indicating its greater biodegradability. However, both control and PEF-treated PS showed only 4% VSD at 2 day SRT, likely due to washout of fermenters and the need for appropriate active biomass.

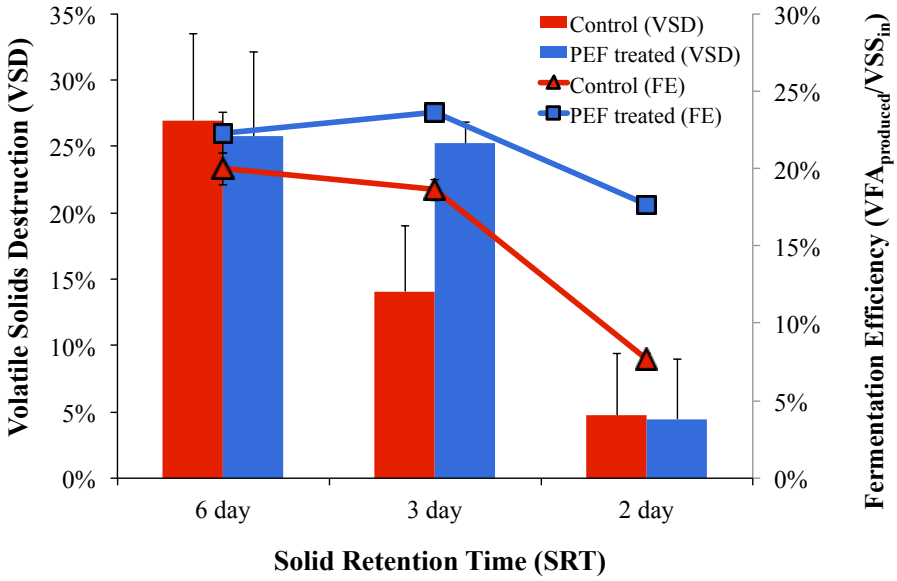

Figure 5.3. Volatile Solids Destruction (VSD) and fermentation efficiency (FE) (defined as the ratio of $VFA_{produced}/VSS_{in}$) in control and PEF-treated PS, at different solid retention times (SRTs)

This study shows that a relatively longer HRT (=SRT) of 6 days led to the highest fermentation efficiency or FE ($VFAs_{produced}/VSS_{in}$) of 20% in the control PS reactor, while PEF treatment shortened it to 3 days, with an FE of 23%. The VFAs - acetate, butyrate,

and propionate - are the dominant VFAs in the effluent of the semi-continuous fermentation reactors (Figure 5.4). The proportion of acetate increased, while that of butyrate decreased when the SRT became shorter, for both control and PEF-treated reactors. Propionate decreased in the control reactors with shorter SRT, while the opposite trend was observed in PEF-treated reactors.

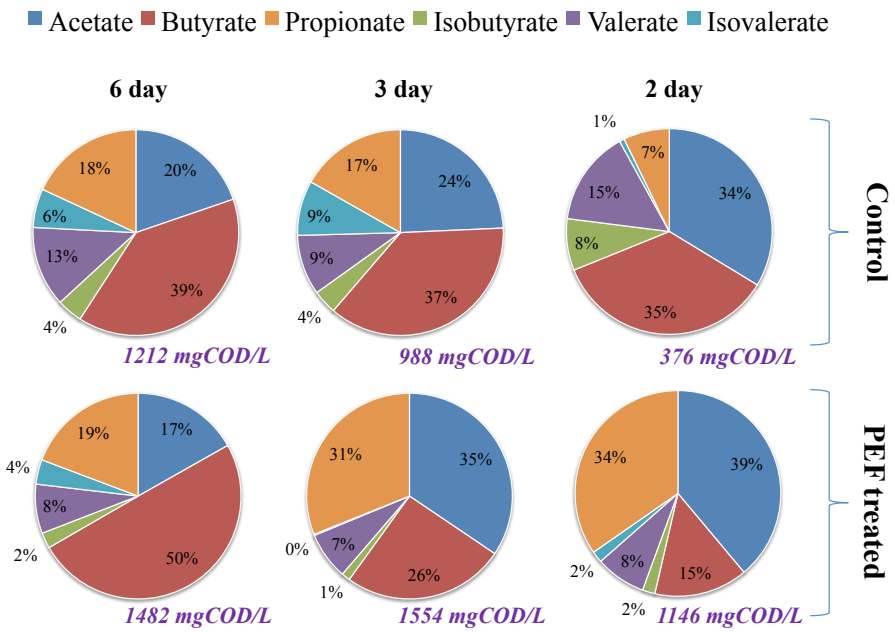

Figure 5.4. Volatile fatty acids (VFAs) produced and its proportion after stabilization of each SRT (Total VFA concentrations at the bottom of pie charts represent the average of duplicate measurements.)

PEF-treated PS fermentation at 3-day SRT (= HRT) was the optimum for allowing efficient hydrolysis from PS organic solids and achieving higher VSD and FE (Figure 5.3).

5.3.2 Optimizing the semi-continuous pre-fermentation stage without methanogen-inhibited conditions

I performed a comprehensive evaluation of the pre-fermentation SRT (= HRT) with methanogenic inhibition in Figure 5.3 and 5.4. From this analysis, I concluded that

3-day is the shortest SRT allowing efficient hydrolysis from PS organic solids: ~25% of volatile solids destruction and ~23% fermentation efficiency. Thus, I evaluated SRTs of 3 and 15 days without inhibition of methanogenesis.

The distribution of VFAs and methane produced at the different HRTs and SRTs tested in the fermentation reactors is shown in Figure 5.5. The 3-day SRT resulted in much more VFAs accumulation (by 1.4~2.5 fold) and less methane production (by 2~7.5 fold). While the longer SRT increased overall hydrolysis of PS, a significant fraction of VFAs available for feeding to the MECs was diverted to methane gas. Furthermore, the increase in SRT did not bring about a large increase in the overall TCOD removal as VFAs or methane, suggesting a higher fraction of recalcitrant compounds in the PS studied. Based on the semi-continuous fermentation experiments, the 3-day SRT (= HRT) was the best condition tested for pre-treatment of PS before MEC.

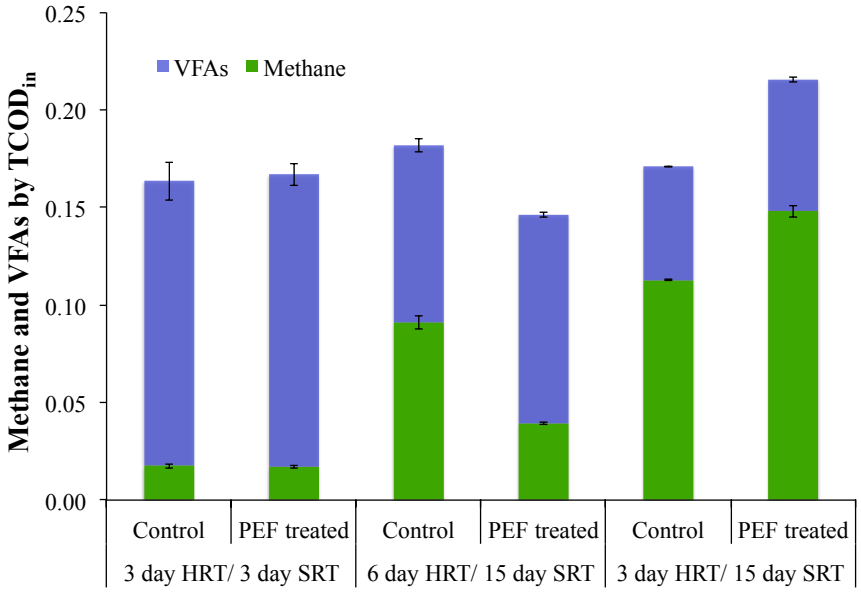

Figure 5.5. Steady-state fermentation efficiencies to VFAs and methane (g COD of the product normalized to $TCOD_{in}$) for the different fermentation condition (SRT and HRT). The initial $TCOD_{in}$ values ranged from 9400 to 12000 mgCOD L^{-1} and are tabulated in Table 5.1.

Fermentation reactors fed with control and PEF-treated PS had similar FEs (~17% by $TCOD_{in}$), indicating that the impact of PEF was not manifested by methane and total VFAs productions. However, PEF exacerbated methanogenesis for the 15-day SRT, probably due to lack of washout of methanogens, although the difference also might be associated with a longer adaptation time, as the experiments were done sequentially in the same bottle.

5.4.3 Centrate characterization from pre-fermentation reactors

Based on the trends in Figure 5.5, I repeated the fermentation studies with a 3-day SRT to generate enough effluent for operating the centrate-fed MECs. I show in Figure 5.6a COD mass balances for these 3-day fermentations. The fraction of produced methane and VFAs (~15% by $TCOD_{in}$) in both fermentations was similar to the results (~17% by $TCOD_{in}$) in Figure 5.5, confirming minimal impact of PEF on these parameters. Around 15% of $TCOD_{in}$ was converted to semi-soluble COD (centrate) and, thus, available to be an electron donor in the MEC. The semi-soluble COD was mainly VFAs, at 57% and 76% of SSCOD in control and PEF-treated centrates, respectively. Acetate was the dominant VFA in both cases, followed by propionate. PEF treatment increased the fraction of acetate in total VFAs by ~35%, compared to control (Figure 5.6b). This indicates that PEF led to selective enrichment of a microbial community that promoted acetate accumulation, as observed in anaerobic digesters after PEF treatment (Zhang et al, 2009).

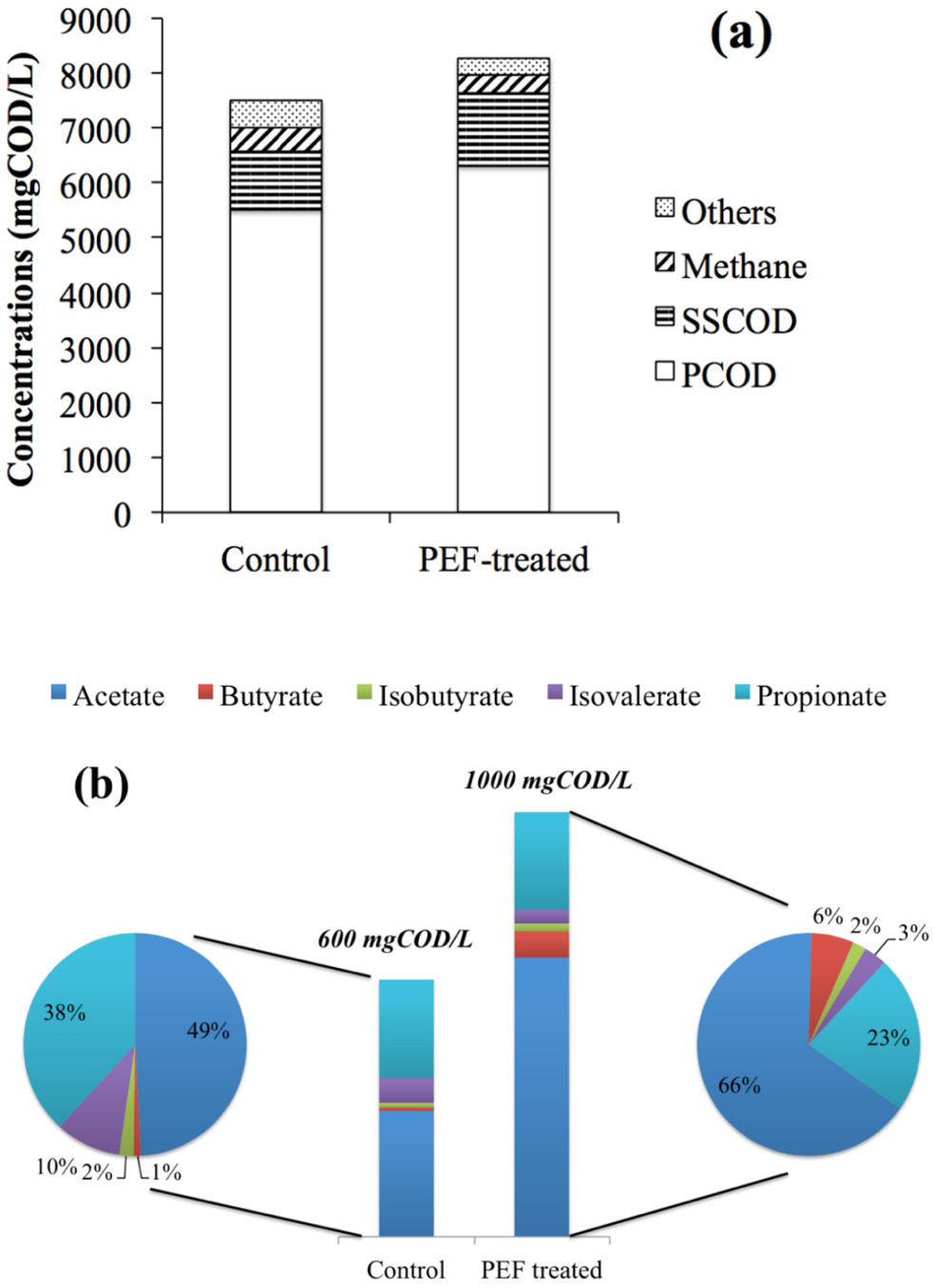

Figure 5.6. Detailed characterization of the performance of pre-fermentation reactors operated with a 3-day SRT. (a) COD mass balance for control and PEF-treated PS. (b) Volatile fatty acids (VFAs) profiles and total VFAs concentrations as COD.

5.3.4 Performance of the MECs fed control and PEF-treated PS centrate

I show in Figure 5.7a the current densities and the Coulombs recovered as COD in MECs fed with control and PEF-treated PS centrate. With the pH maintained near neutral, the current densities increased to as high as 1.3 and 3.1 A m^{-2} for control and PEF-treated centrate, although they declined to the background current by ~1.5 and 2.0 days, respectively. Correspondingly, VFAs were hardly detected at the end of both batch experiments: control: 47 (± 1) mg COD L^{-1}, PEF-treated: 0 mg COD L^{-1}. The higher concentrations of SSCOD and VFAs and, particularly, the 2.6-fold larger acetate mass in the PEF-treated centrate (88 versus 230 mg COD applied) led to the 2.4-fold higher peak current density. Since anode-respiring bacteria prefer acetate as their electron donor (Torres et al., 2007; Lee et al., 2008; Liu et al., 2005; Oh and Logan, 2005), the selective accumulation of acetate in PEF-treated PS centrate probably was the factor for the much faster rate of anode respiration in the MEC.

Higher initial SSCOD was important for allowing the PEF-treated PS centrate to have a faster rate of electron recovery. Because the volume of the anode chamber for the PEF-treated centrate was larger (0.35 versus 0.30 L), the starting mass of SSCOD was greater for the PEF-treated centrate: 459 versus 315 mg SSCOD. Integration of the currents in Figure 5.7a indicates that the Coulombs recovered were 360 and 232 mg COD for PEF-treated and control centrates, respectively. The 55% larger input of SSCOD with the PEF-treated centrate is consistent with the 55% more electrons captured as current.

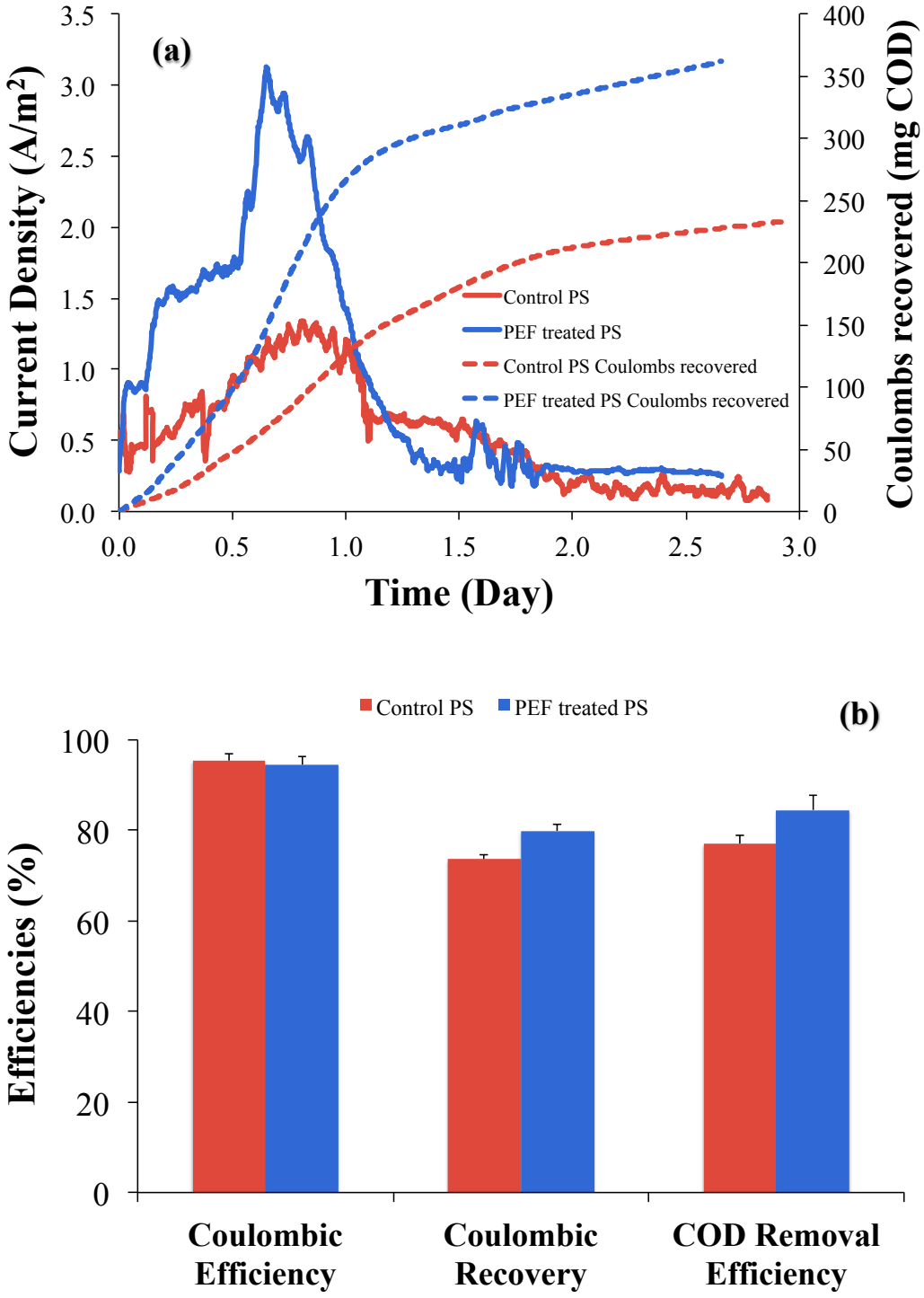

Figure 5.7. Performance of MECs fed with control and PEF-treated PS centrate operated with pH control: (a) current density and Coulombs recovered as mg COD and (b) efficiencies by normalized to the initial centrate SSCOD.

In Figure 5.7b, the MECs fed control and PEF-treated PS centrate gave good performance in terms of CE, CR, and COD removal: 95, 74, and 77% for control and 95, 80, and 85% for PEF, respectively (p value < 0.05 for CR and COD removal between the two MECs). Thus, the ARB could use the centrate's SSCOD efficiently as an electron donor. Although PEF pre-treatment had a strong positive effect on the maximum current density (Figure 5.7a), it gave only a small increase in CR and COD removal and had no effect on CE.

Table 5.3 summarizes the electron flows from SSCOD in centrate, as well as from the original TCOD of the PS. Although only 14 or 16% of PS TCOD ended up as the centrate's SSCOD after pre-fermentation, most of the SSCOD was recovered as current in the MEC (74% and 80% for control and PEF-treated, respectively). Between control and PEF-treated, PEF treatment had modest improvement of CR by 6% although the absolute CR was 34% higher in PEF-treated centrate fed MEC, which is likely due to ~1.5 (or ~1.9) times more SSCOD (or acetate) fed in the MEC as described earlier. Correspondingly, 7% lesser SSCOD in PEF-treated centrate fed MEC was detected at the end of the batch (23% and 16% for control and PEF-treated, respectively).

Table 5.3. Summary of COD flows in mg L^{-1} of the pre-fermented centrate fed MEC and normalized to the initial centrate SSCOD in the MEC and to the input PS TCOD in the two-stage system

	Control			PEF-treated		
	COD (mg L^{-1})[a]	Fraction by $SSCOD_{in}$ (%)[b]	Fraction by $TCOD_{in}$ (%)[c]	COD (mg L^{-1})[a]	Fraction by $SSCOD_{in}$ (%)[b]	Fraction by $TCOD_{in}$ (%)[c]
Initial centrate SSCOD	1050 (±16)	100	14	1310 (±27)	100	16
Final centrate SSCOD	241 (±1)	23	3	202 (±25)	16	2
Final centrate PCOD	51	5	0	52	3	0
Current as COD	774	74	10	1040	80	13
Unaccounted COD	-14	-1	0	9	1	0

[a)] Anode volume was 0.3 and 0.35 L for control and PEF-treated PS centrate fed MEC

[b)] Fraction by initial centrate SSCOD of the MEC stage

[c)] Fraction by starting TCOD in the PS of the pre-fermentation stage (control PS: 7500 (± 300) mgCOD L^{-1}, FP-treated PS: 8300 (± 600) mgCOD L^{-1})

5.4 Conclusion

I evaluated semi-continuous pre-fermentation of PS as a means to enhance electron recovery as current in an MEC. Pre-fermentation with a 3-day SRT (= HRT) led to more VFA accumulation and less methane production. Although PEF treatment before fermentation did not alter the production of VFAs and methane for the 3-day SRT, it yielded more of the most desirable fermentation product, acetate. This resulted in higher maximum current density in the batch MEC experiments. Over the full duration of the MEC batch experiments, CE, CR, and COD-removal efficiency were high for the pre-fermented centrate and hardly affected by PEF pre-treatment.

CHAPTER 6

MAXIMIZING COULOMBIC RECOVERY FROM PRIMARY SLUDGE BY CHANGING RETENTION TIME AND pH IN A FLAT-PLATE MICROBIAL ELECTROLYSIS CELL[4]

6.1 Introduction

Anaerobic digestion (AD) is a mature and integrated environmental biotechnology within wastewater treatment plants to achieve sludge reduction and simultaneous energy recovery as methane (CH_4). This combustible gas can be used to heat digesters and buildings, and produce electrical power (McCarty et al., 2011). Sludge reduction is important in order to decrease solids transportation costs from treatment plants (Lukicheva et al., 2009). Also, for land application as a fertilizer, sludge treatment must follow the guideline, 40 CFR 503 of the USEPA requirements, as per which at least 38% of volatile solids reduction during AD should be achieved to result in production of Class B biosolids (US EPA, 2000).

As an emerging alternative option to AD, microbial electrochemical cells (MXCs) can be used to treat high-strength wastes such as municipal sludge (McCarty et al., 2011; Popat and Torres, 2016). Anode-respiring bacteria (ARB) are an essential component of MXCs, and are able to transfer electrons from oxidation of organic compounds directly to a solid electrode. This results in electron capture as current, at a rate and extent faster than methanogenesis (Torres et al., 2010). Electron diversion from wastes to the anode, instead of methane, can provide diverse products, such as electrical power and hydrogen peroxide with oxygen reduction reaction in the cathode in microbial fuel cells (MFCs), and hydrogen with hydrogen evolution reaction in the cathode in microbial electrolysis cells (MECs) (Rittmann et al., 2008; Rozendal et al., 2008).

[4] This chapter was prepared as a manuscript and will be submitted for publication.

MXC studies fed with sludge have shown successful results with regard to solids reduction; over 38% volatile solids reduction has been reported in several studies (Ge et al., 2013; Wang et al., 2013; Belafi-Bako et al., 2014). However, there remains a need for improvement in Coulombic recovery and efficiency, CR and CE, which represents the fraction of electrons from the influent and the removed chemical oxygen demand (COD) demand resulting in electrical current (Xiao et al., 2014; Ge et al., 2013). Lower CR or CE in the literature has been reported mainly due to electron diversion to methane instead of the anode. For example, Ge et al. (2013) reported larger energy recovery in biogas than electrical power in primary sludge (PS)-fed MFCs which acted as a "modified anaerobic digester"; methane-to-current energy ratio was 12.4. Indeed, there are several studies that show that combining anaerobic digester with MXCs could improve biogas production (Koch et al., 2015; Vrieze et al., 2014; Arends and Verstraete, 2012; Tartakovsky et al., 2011; Vijayaraghavan and Sagar, 2010; Weld and Singh, 2011; Sasaki et al., 2011; Sasaki et al., 2010; Rabaey et al., 2005). Especially, Vrieze et al. (2014) showed increase of methane production as well as remediation of a failed anaerobic digester after inserting electrodes in the digester; this was due to more methanogenic biomass retention on electrodes.

Despite the benefits of anaerobic digestion, electron loss from organic substrates to methane is not the ultimate goal in an MXC, where there is potential to produce other products of higher economic value, such as those listed above. Thus, suppressing methanogenesis is a major requirement to effectively take advantage of the flexibility of MXCs. To minimize methane production in MXCs, several methanogenic suppression methods have been tested with: 1) periodic aeration in the anode chamber (Chae et al., 2010; Rabaey et al., 2010), 2) addition of chemical inhibitors, such as 2-Bromoethanesulfonate (BES) (Chae et al., 2010; Xiao et al., 2014; Zhuang et al., 2012;

Parameswaran et al, 2010) or alamethicin (Zhu et al., 2015), and 3) pH control (Yuan et al, 2011; Zhuang et al., 2010). pH control, in particular, is important for methanogenesis as well as anode respiration. In addition, another important parameter that could be used is solid and/or hydraulic retention time (SRT and HRT), since lower SRT (or HRT) can cause washout of methanogens (Rittmann and McCarty, 2001). Most of MXC studies reported in the literature using sludge were in batch operation, and there is only one study that reported continuous operation with PS in MFCs for long-term investigation at a fixed HRT (9-day or 14-day) (Ge et at., 2013).

In addition to operational conditions, reactor design could also be another factor for low CR in MXC fed with sludge, with more electron diversion to methane. For example, high-strength solids could lead to significant clogging of the anode surface area and membranes (Ge et al., 2013; Arends and Verstraete, 2012), retaining more methanogenic biomass. In order to minimize solids clogging and enhance electron recovery in MXCs, some studies have recently evaluated the impact of pre-fermentation stage ahead of an MXC (Yang et al., 2013; Choi and Ahn, 2014; Abourached et al., 2014; Ki et al., 2015a). Pre-fermentation enables the accumulation of volatile fatty acids, which are preferred substrates for ARB in MXCs. Most of these studies involved a batch fermentation and air-cathode MFC process configuration (Yang et al., 2013; Choi and Ahn, 2014; Abourached et al., 2014), showing good performance in terms of CE and soluble COD removal. In Chapter 5, I extended this concept further with semi-continuous pre-fermentation plus batch MECs fed with pre-fermented PS centrate (Ki et al., 2015a). In brief, the optimum condition of pre-fermentation stage was 3-day solid retention time, SRT (= HRT, hydraulic retention time). When fed with the PS centrate, the soluble COD conversion to electrical current was very high, with 95, 80 and 85% of CE, CR, and COD removals, respectively, in batch MECs. However, the total energy

conversion from influent solid PS from the pre-fermentation stage + MEC was just ~16%, and volatile suspended solid (VSS) reduction was ~25%. This indicates that the two-stage pre-fermentation + MEC improved the efficiency of the MEC stage, but at the expense of very low total electron recovery from the PS and incomplete solids destruction.

In this study, I aimed to maximize CR and minimize methane in a primary sludge-fed MEC by controlling operational conditions with a design that contains high-surface area carbon fiber anodes in a flat 2D configuration to minimize clogging. This MEC design was evaluated in Chapter 3 and shown to have a high voltage efficiency as well (Ki et al., 2016). I first evaluated electron balances from PS in a single-stage MEC system, in semi-continuous operation, for an extended period of time (~300 days). I also evaluated the importance of HRT and pH in the anode chamber with respect to electron distribution between electrical current and methane. Finally, I discuss sludge treatment performance with regards to solids reduction and dewaterability.

6.2 Materials and Methods

6.2.1 Primary sludge (PS)

I collected PS from Northwest Water Reclamation Plant (NWWRP) in Mesa, AZ, USA and Greenfield Water Reclamation Plant (GWRP), in Gilbert, AZ, USA for batch and semi-continuous experiments, respectively. I treated PS with the pulsed electric field (PEF) unit (the FP *alpha* unit) and stored in a temperature controlled room at 4 °C, as described in Ki et al. (2015b), to prevent psychrophilic fermentation and degradation of raw PS during cold storage (Ki et al., 2015a; Ki et al., 2015b).

6.2.2 MEC reactor set up and operation

I built flat-plate microbial electrolysis cells (MECs) having one anode chamber in the center flanked by two cathode chambers on either side. The reactor design including all materials was the same outlined in Ki et al. (2016). In brief, anode volume was ~500 mL, and the cathode at each side was ~50 mL. Carbon fibers and stainless steel meshes were used as anode and cathode electrodes, respectively. Anion exchange membranes (AEM, AMI-7001, Membranes International, Glen Rock, NJ, USA) were used as a separator between the anodes and cathodes. The anode, cathode, and membrane projected areas were 100 cm^2 each, which corresponded to a projected anode area to volume ratio of 40 m^2 m^{-3} reactor. The design of anode surface area (200 cm^2) for 500 mL of anode volume was based on the calculation of the expected current density from PS, along with the targeted HRTs (Appendix A.1).

Anaerobic digested sludge and biofilm scraped from a pre-acclimatized acetate-fed MEC were used for inoculating the MEC. I operated the MEC first with acetate medium (50 mM acetate, 100 mM phosphate buffer, 14 mM ammonium chloride, and trace minerals as described in Ki et al., 2015a) in continuous mode for approximately 2 months. The anode potential was poised at -0.3 V (vs. Ag/AgCl) with a potentiostat

(VMP3, BioLogic Science Instruments, Knoxville, TN). Before changing the feed to PS, the MEC was operated with two cycles of acetate-fed batch until depletion of the substrate.

I operated MECs in semi-continuous mode with a stirrer mixing system starting from 15-day HRT to 12-, 9-, and 6-day HRT. After that, I resumed operation at 12-day HRT to observe the effect of pH. When fed fresh PS in the MECs with everyday feeding at each HRT, I measured the pHs of the effluent PS and maintained the MEC anode between 7 and 8.5 with sodium hydroxide addition (5M NaOH).

When operating with 12-day HRTs again with neutral and high pHs, I developed *j-V* curves with chronoamperometry starting from open circuit potential of the anode to the anode potential resulting in the highest current densities, while stepping the potential from 30 to 100 mV for each data point. I performed the *j-V* experiments in triplicates in each case when the current density reached to the maximum on each day of PS-feeding at 12-day HRTs.

6.2.3 Analytical methods

PS characterization included measurement of total chemical oxygen demand (TCOD), semi-soluble COD (SSCOD), biochemical oxygen demand (BOD), total suspended solids (TSS), volatile suspended solids (VSS), ammonia (NH_3-N), total phosphorus (T-P), and alkalinity. COD, NH_3-N, T-P, and alkalinity were measured using spectrophotometric methods by HACH kit and spectrophotometer (DR2700, HACH, Loveland, CO). Semi-soluble COD was measured on the permeate after filtration through a 1.2-µm glass-fiber filter (Whatman™, UK), as described in Ki et al. (2015a). TSS, VSS and BOD_5 were measured according to Standard Methods (APHA, 2012). Dewaterability of the MEC digested sludge was evaluated using the Time-to-filter (TTF) test (APHA, 2012). In brief, I placed 10 mL of sludge sample onto the filtration device

with Whatman No. 1 (47 mm diameter) connected to the graduated Falcon Tubes inside the vacuum flask. After the sample was added to the filter paper and waited 10 min, I turned on the pump with a vacuum pressure 52~56 cm Hg. I recorded the time to collect each mL of filtrate until 5 mL. TTF tests were performed in triplicates at room temperature. Conductivities of PS influent and effluent of different pHs at 12-day HRT were measured using Waterproof Multiparameter PCS Testr 35 (Oakton Instrument, Vernon Hills, IL).

In semi-continuous operation, I attached a 500-mL bottle to the headspace of the anode chamber to measure biogas volume and composition. After stable operation was achieved at each HRT, I measured the gas volume and composition every day for one cycle of each HRT. At the 12-day HRT with high pH, hydrogen (H_2) gas at the cathode was also collected and measured using a 1 L bottle. I used a 500-µL gas-tight syringe (PERFECTUM, New Hyde Park, NY) to measure gas composition with gas chromatography and thermal conductivity detection (GC-TCD, GC 2010, Shimadzu) after separation on a packed column (Carboxen™ 1010 PLOT, Supelco, Bellefonte, PA). Argon was the carrier gas with a constant pressure and flow rate of 42.3 kPa and 10 mL/min, respectively. I employed temperatures of 150, 80, and 220 °C for injection port, column, and detector, respectively, and the current was 41 mA. Methane and carbon dioxide were also detected by GC-TCD. Calibration was performed using an analytical grade gas standard (CH_4: CO_2: H_2 = 40%: 30%: 30%, Matheson Tri-Gas, Twinsburg, Ohio).

6.2.4 Calculations

Electron balances were made based on TCOD as described in previous studies (Ki et al., 2015a). Details are provided in Appendix A.2. CE, CR, cathodic H_2 recovery (or cathodic conversion efficiency, the ratio of electrons donated to H_2 normalized to the

electrons transferred in the circuit from the anode to the cathode) were calculated, as described in the previous studies (Lee et al. 2009; Ki et al., 2015a).

6.3 Results and Discussions

6.3.1 PS fed semi-continuous MEC operation

I first operated a PS fed batch MEC and show detailed performance information in the Appendix A.2. Batch operation showed a CR of 56% and 53% for two experiences lasting 30 and 45 days, respectively. Then, I operated the MECs semi-continuously with different HRTs (6~15 days) starting with 15-day, to 12-, 9-, 6-, and 12-days again, this time with neutral and high pH conditions, as shown in Figure 6.1. PS used for semi-continuous operation contained ~8 g COD L^{-1} and ~3.6 g VSS L^{-1}. Current densities at steady-state for each HRT are represented in Figure 6.1 and showed an increasing trend with decreasing HRT: from 0.35 (± 0.06) A m^{-2} at 15-day HRT to 2.21 (± 0.28) A m^{-2} at 9-day HRT. Note the trend in current production during each feed with time, starting at a high current density, then decaying as COD is consumed. At 6-day HRT, the current density did not increase further than 2.2 A m^{-2}, which was the maximum current density during the semi-continuous mode of operation in our study. During the repeat 12-day HRT experiment with pH control, the maximum current densities were not significantly different compared to the earlier 12-day HRT regime, as shown in Figure 6.1 and Table A.2.

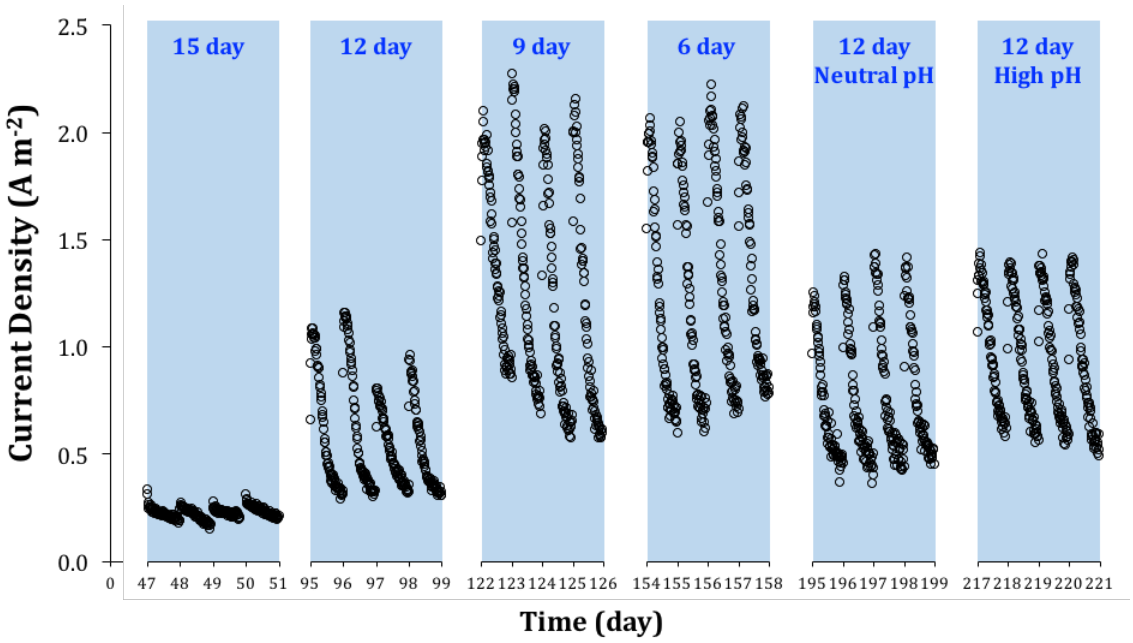

Figure 6.1. Current density with time at different HRTs during semi-continuous MEC operation. The gaps in time between different HRTs were the adaptation periods. Data shown in this figure correspond to the the last 4 days of operation for each HRT when current had already stabilized.

6.3.2 Electron diversion to electrical current and methane at different HRTs

I performed electron balances during the last 6-15 days of operation for each HRT during which the MEC showed a stable performance. A minimum of 6 measurements were averaged to generate Figures 6.2a. Electron balances indicate that MEC semi-continuous operation for various HRTs (15 to 6 days) achieved over 60% of TCOD removal and over 40% overall conversion to either methane or Coulombs, which is similar to the BOD_5 to TCOD ratio of the influent PS. This reaffirms that MECs work efficiently in anaerobic energy conversion from particulate wastes, and provide complete stabilization of the PS. However, CR was low at 13% for 15-day HRT as a result of large methanogenic activity (33% of electrons). Thus, the MEC behaved largely as an AD at this HRT. However, CR increased to 28 and 34% for 12- and 9-day HRTs, respectively,

with decreasing methane fractions. Thus, lower HRT seem to favor ARB activity by increasing loading and possibly washing out methanogens. This typically happened in AD with poor methanogenic performance below 8-day SRT, as shown in the literature (Miron et al., 2000; Lee et al., 2011). This approach of methanogenic control for MXCs has not been reported before to our knowledge. At 6-day HRT, even though the current density was similar to 9-day HRT, methane and Coulombs recovery decreased to a combined total of ~41%, which might result from washout of directly viable organics as well as active microbial biomass for hydrolysis and fermentation. Nonetheless, VSS destruction was 59% well above the regulatory limit for production of Class B biosolids.

Apart from the effect of the HRT on the PS conversion, manually controlled pH conditions were different at each HRT, as reported in Figure 6.2b and Table A.2. To further understand the impact of pH on electron recovery as current and methane alone, as a function of HRT, I normalized the recovery as shown in Figure 6.2b. I could clearly see the increase in CR and decrease of methane recovery with increasing pH. To elucidate further the significance of pH on electron recovery from PS in the MECs, I performed 12-day HRT experiments again at a neutral pH (~7.3) and a higher pH (~8.1). At the 12-day HRT with high pH in the anode, I operated the MEC for 21 days until the outcomes (e.g., current density, methane, and, effluent COD) were reproducible and repeatable (Figure 6.1 and 6.2). The results during stable operation in different pHs are discussed in the next section.

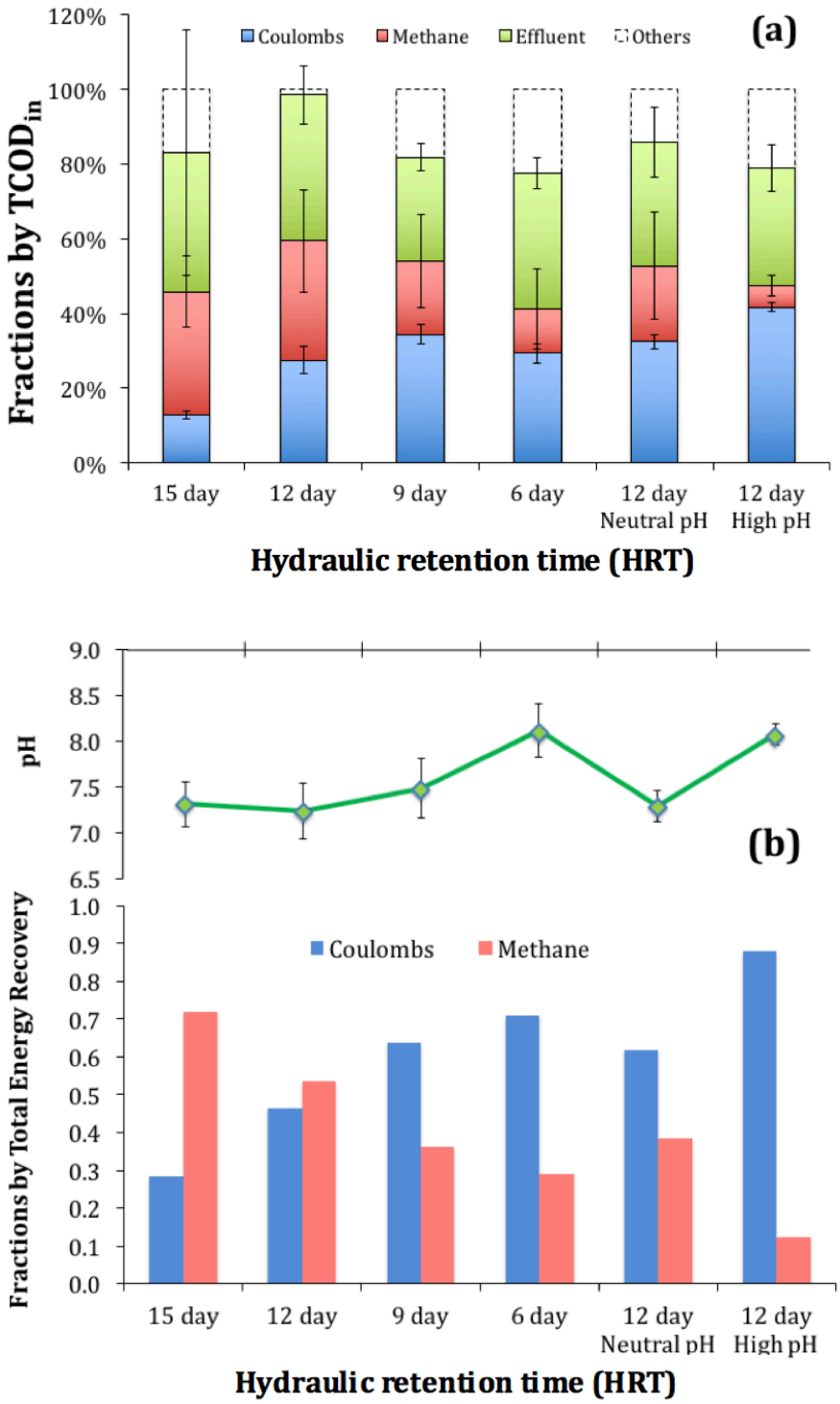

Figure 6.2. Electron balance of semi-continuous MECs fed with PS at each balance (a), and electrical current and methane fractions normalized by total energy recovered from PS-$TCOD_{in}$ (b)

6.3.3 Importance of pH management

Even though HRT was important for electron recovery as Coulombs instead of methane, pH was also an important factor. Especially, when MXCs are fed with high-strength wastes such as PS, a pH drop can occur due to the rapid fermentation of organics and the produced CO_2 as a result of anode respiration. Also, if production and accumulation of volatile fatty acids due to rapid fermentation of PS occurs greater than its consumption by ARB and other microbes, the pH can drop as well. This could be one of the primary drivers of changing CO_2 speciation. Thus, this study with different HRT experiments served as the basis for the optimum pH range (7-8.5) to be maintained in the MEC anode (Figure 6.2b and Table A.2).

At 12-day HRT again after 6-day HRT operation with neutral pH, ~7.3, the CR was ~33% and the methane fraction was ~20% (Figure 6.2a). An increase in anode pH to ~8.1 (high pH) at the same 12-day HRT resulted in a sharp increase in CR to ~42% with decrease of methane recovery to ~6% (Figure 6.2a). This indicates that methanogenic activity was sharply inhibited at higher pH > 8.0, enabling higher CR. Based on the analysis of total electron fractions in Figure 6.2b, the Coulombs recovered increased at high pH by 26%, and correspondingly the methane recovery decreased by 26%.

I observed a strong negative correlation between increasing pH (in the range of 7.94 to 8.54) and methanogenesis (Figure 6.3a). However, CR stabilized and did not increase in the pH range of 7.94 and 8.27, with even a decrease in CR at a higher pH of 8.54, probably due to a pH inhibition on ARB metabolic activity.

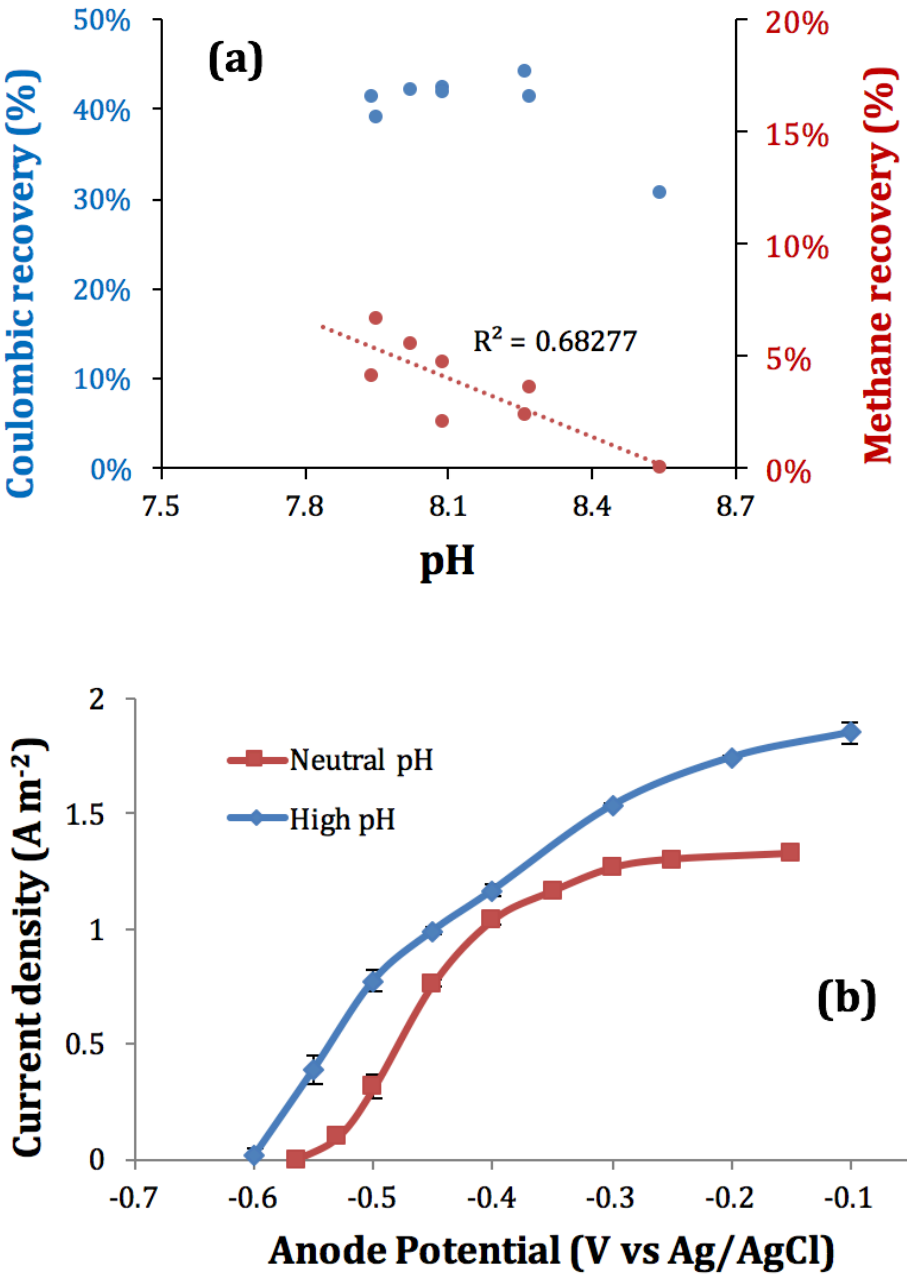

Figure 6.3. Effect of pH on the electron recovery and *j-V* response. (a) Relationship between Coulombic and methane recovery and pH of the anode chamber. (b) Comparison of the *j-V* response for high and neutral pH at stabilized condition of 12-day HRT.

In Figure 6.3b, I show the effect of pH on the *j-V* response during steady-state operation at 12-day HRT. At neutral pH (~7.3) condition, the *j-V* response saturated over a narrow range of anode potential. At high pH (~8.1), the *j-V* curve did not saturate completely. The shift in pH not only resulted in a shift in open circuit potential (OCP) (Appendix A.3), but also a shift of the catalytic curve of ARB to the left as also shown in Figure A.4, where I normalized the currents by the maximum current densities, resulting in a better CR. Also, the better CR was expected from higher current densities in high pHs than neutral pHs, even though the maximum current densities in each condition were similar by 1.2-1.4 A m^{-2} (Figure 6.1 and A.5).

6.3.4 Sludge treatment: reduction and dewaterability

Sludge treatment is the most important goal of anaerobic technology (e.g., AD) while extracting useful energy from them. TCOD removal and sludge reduction (by VSS) for all HRTs are shown in Table 6.2. TCOD and VSS reduction were ~70% and ~60%, respectively. Similar amount of VSS reduction of sewage sludge in an MFC was reported - 63% and 55% without and with BES (methanogen inhibitor), respectively - for 37-day batch operation (Xiao et al., 2014). Vologni et al. (2013) reported that 32% and 24% of PS-VSS reduction without and with pH control, which were 6.2 and 7.0 at initial pHs of batch operation. In the continuous operation by Ge et al. (2013), 37-51% of TCOD removal and 51-57% of VSS reduction from the first-stage MFC unit fed with PS at 7-day SRT despite a very low CE, ~2%. In our batch tests during 30 and 45 days' operation in MEC, VSS reductions were 68 and 76% (Table A.1). At 6-day HRT operation, I still had high VSS reduction of ~60% with high CE of 46%. On the other hand, typical VS (or VSS) reduction in AD is ~50% and it changes depending on SRTs/HRTs and the initial sludge composition: 56% VS reduction at a 15-day SRT (Tchobanoglous et al., 2002), 35% from PS at a 20-day HRT (Ghyoot and Verstraete, 1997), 62% from waste activated

sludge at a 15-day HRT, and 40-50% from sewage sludge (Cao and Pawłowski, 2012). Lee et al. (2011) reported the effect of SRT (4-20 days) on methanogenesis in AD of thickened mixed sludge showing sludge reduction of 34 to 50% from lower to higher SRT. This indicates a smaller extent of hydrolysis of organic solids as well as washout of methanogens in lower SRT (especially lower than 10 days). Compared to AD system, I especially showed very high performance of sludge reduction even at low HRT (6 day). Even though electron distribution was changed with HRT and pH, I consistently obtained similar solid reduction with varying HRTs.

Table 6.1. Change of PS-TCOD and VSS concentration in the anode chamber at different HRTs

	HRTs	TCOD (mgCOD/L)	VSS (mg/L)	TCOD removal (%)	VSS reduction (%)
Influent	-	8045 (± 109)	3635 (± 273)	-	-
Effluent	15 day	2890 (± 1841)	1644 (± 705)	64 (± 23)	55 (± 21)
	12 day	3019 (± 724)	1669 (± 266)	62 (± 9)	54 (± 11)
	9 day	2413 (± 279)	1433 (± 100)	70 (± 4)	61 (± 9)
	6 day	2622 (± 399)	1482 (± 193)	67 (± 5)	59 (± 10)
	12 day neutral pH	2322 (± 245)	1465 (± 174)	71 (± 3)	60 (± 10)
	12 day high pH	2296 (± 236)	1421 (± 149)	71 (± 3)	61 (± 10)

I performed time-to-filter (TTF) tests for PS influent and effluents at 12-day HRT for both neutral and high pHs to assess the effect of MEC treatment on sludge dewaterability, and compared with anaerobic digested sludge (ADS) (Figure 6.4). To

make similar condition of PS effluent as TCOD, I diluted ADS ~19 times; TCOD and VSS were 2370±10 mg/L and 1770±30 mg/L, respectively. TTF value of the influent PS was 3.6 min, while the filtrate collection times were reduced significantly to 1.7 min for the neutral pH, which is more than 2-fold faster than the feed PS. At high pH, sludge dewaterability of the digested PS improved to 0.5 min, which is 7.3- and 3.3-fold faster than the feed PS and neutral pH effluent, respectively. I show similar results of ADS with PS effluent at neutral pH. Improvement of dewaterability with high pH is likely due to the decomposition of sludge structure with release of bound water and extracellular polymeric substances from sludge (Zhou et al., 2014). Similar results of dewaterability enhancement were observed with anaerobic digested sludge at high pHs (Apul et al., 2010). This is the first report for primary sludge dewaterability effluent used in MXC, an important factor to measure sludge stabilization. These results highlight the benefit of treating effluent sludge at 12-day HRT at high pH condition.

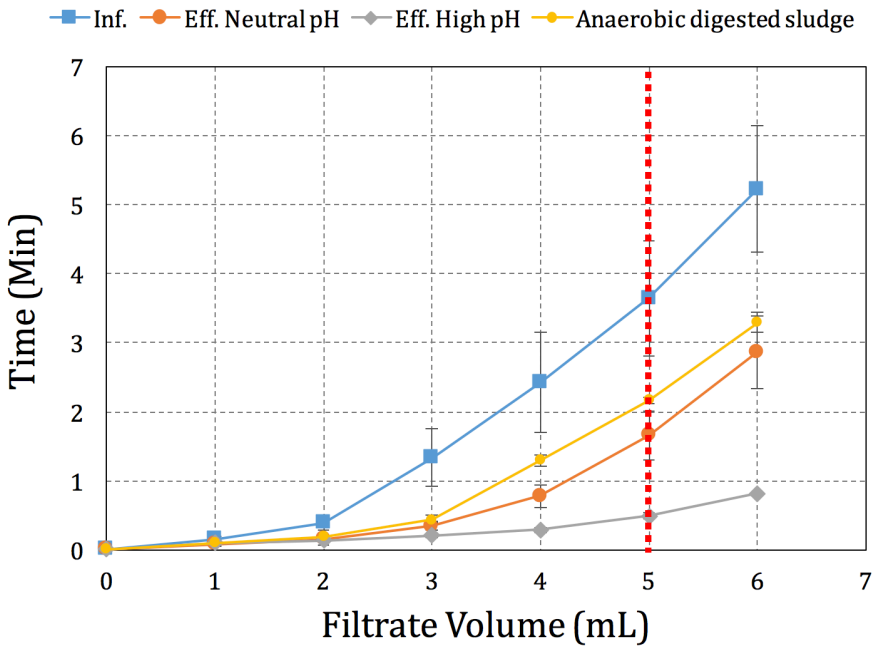

Figure 6.4. Time-to-filter (TTF) test of PS influent and effluent at 12-day HRT. A vertical dotted red line indicates 50% of initial loaded sample volume filtrated.

6.3.5 MXC design and long-term operation

The design of MXC is important to have better performance of current production as well as wastewater treatment. The increase of transport rates is the key for successful MXC design (Popat and Torres, 2016). The transport processes include the fluxes of electron donor and acceptor, the ionic flux, the acidity and alkalinity fluxes at anode and cathode respectively, the electron transport flux at the biofilm, and the reactant/product crossover flux in MXCs. Here in our study, I designed and used i) high-surface area anodes with carbon fiber woven on titanium pates (as a 2-D structure) and ii) close distance between anode and cathode. The anodes did not have a 3-D structure for biofilm growth, such as the brush anode most popularly used in literature, but still higher surface areas than flat-surface anode (e.g. carbon felt). Our MECs enabled to minimize Ohmic losses (or Ohmic overpotential), which is one of the key limitations of MXCs (Ki et al., 2016; Popat and Torres, 2016; McCarty et al., 2011), while still resulting in very high current densities when fed with acetate medium (Ki et al., 2016).

The MEC design I used contributed to high H_2 production: the rates measured at 12-day HRT and high pH experiments were 0.373 m^3 H_2 m^{-3} day^{-1} by anode chamber volume and 1.234 L H_2 g VSS^{-1} day^{-1} by influent PS-VSS. The electrical energy input calculated with ~1.1V of applied voltage was 2.7 kWh m^{-3} H_2, which is lower than typical energy input for water electrolysis, 5.6 kWh m^{-3} H_2. Cathodic H_2 recovery and CE were 93 (± 15) and 61 (± 6) %, respectively, thus overall H_2 recovery from PS was 57 (± 11) %, which is higher than 40 to 60% cathodic H_2 recovery in previous studies using municipal wastewater with dual-chamber MECs (Ditzig et al., 2007; Heidrich et al., 2013).

I performed long-term MEC operation directly fed with PS for ~300 days with ~75 days of two-consecutive batch and ~221 days of semi-continuous, without reactor

downtime and absence of replacement of reactor parts. It was surprising that membrane had no severe fouling issue during the long-term operation. At the end of semi-continuous operation, when I opened after 12-day HRT at high pH, I could see that the PS solids did not penetrate through the anode to the membrane side, probably resulting in long-term operation without membrane failure in the MEC system. This indicates our anode design was successful for anode respiration as well as PS hydrolysis in long-term operation, and for minimization of membrane deterioration (Figure A.9).

6.4 Conclusions

This study demonstrates electron balances in the efficiently-designed flat-plate MEC fed with PS for HRTs between 6- and 15-days. The maximum current densities reached over 2 A m^{-2} in 6- and 9-day HRTs, while CR was the highest 9-day HRT (34%). Maintaining pH over 8 in the anode chamber reduced electron diversion to methane, thus increasing CR. PS-fed MECs yielded high sludge reduction by ~60% at all HRTs, indicating lower HRT still led to energy recovery and sludge reduction. As a first report of electron balances in long term semi-continuous MEC operation using PS for ~300 days, this study demonstrated that Coulombic recovery and sludge treatment can be improved using an MXC with optimum design and operational conditions.

CHAPTER 7

H_2O_2 PRODUCTION IN MICROBIAL ELECTROCHEMICAL CELLS FED WITH PRIMARY SLUDGE[5]

7.1 Introduction

Hydrogen peroxide (H_2O_2) is a useful chemical due to its strong oxidative properties, coupled with its low molecular weight and high energy content. Also, H_2O_2 is environmentally attractive as its reaction products consist solely of water or oxygen. Approximately 2.2 million metric tons of H_2O_2 are produced annually (Campos-Martin et al., 2006). It is a versatile chemical that is currently utilized in a variety of industrial processes including the electronics industry, paper and pulp bleaching, bleaching of textiles, production of color safe detergents, treatment of wastewater, chemical synthesis, and extraction and separation in the mining and metal industries (Campos-Martin et al., 2006).

The conventional method for H_2O_2 production, the Anthraquinone Oxidation (AO) process, is expensive due to the extreme conditions needed (e.g. high pressure and temperature), as well as the need to remove impurities. Moreover, anthraquinone and its derivatives are threats to human health being known potential carcinogens (Pletcher, 1999; Campos-Martin et al., 2006).

As an alternative method for H_2O_2 production, electrochemical technologies have been proposed and actively studied since early 1990s (Otsuka and Yamanaka, 1990; Yamanaka and Otsuka, 1991; Alcaide et al., 1998; Yamanaka and Otsuka, 1998; Mclean et al., 2002; Yamanaka and Murayama, 2008). Chemical fuel cells such as polymer electrolyte membrane fuel cells (PEMFCs) and alkaline fuel cells (AFCs) can produce

[5] This chapter was prepared as a manuscript and will be submitted for publication.

H_2O_2 at up to ~10% (wt) with platinum as the anode catalyst for hydrogen oxidation and carbon along with metal-porphyrin derivatives as cathode catalyst for oxygen reduction to H_2O_2 (Yamanaka et al., 2008; Yamanaka et al., 2010). Microbial electrochemical technologies also can produce H_2O_2 at the cathode, but not at the high concentrations achieved in chemical fuel cells (Rozendal et al., 2009). The highest H_2O_2 concentration produced in microbial electrochemical cells (MXCs) is 0.9 % (wt) (Modin and Fukushi, 2013). Using H_2O_2 generated on site within a wastewater treatment infrastructure for cleaning membranes in membrane-based treatment systems, treatment of greywater, pre-treatment of sludge, or post-treatment of sludge as polishing step, is an attractive application of such MXCs.

To the best of our knowledge, nine studies for H_2O_2 production in MXC have been reported in recent years (Rozendal et al., 2009; Fu et al., 2010; Modin and Fukushi, 2012; Modin and Fukushi, 2013; Arends et al., 2014; Chen et al., 2014; Chen et al., 2015; Sim et al., 2015; Li et al., 2016); this excludes studies where the aim was to perform Fenton oxidation at the cathode where H_2O_2 is generated and consumed *in situ* (Zhang et al., 2015). Depending on the type of electrochemical cell and its operation, the concentration as well as production rate of H_2O_2 varies. After the first study (Rozendal et al., 2009), research for H_2O_2 production in MXC has been focused on the materials for cathodes, membranes, or as well as operation including improving oxygen diffusion (Stadie, 2015; Sim et al., 2015; Li et al., 2016). Most of these studies are done with synthetic wastewater (e.g. acetate or glucose).

On the other hand, H_2O_2 production with real wastewater has been reported in only four studies (Modin and Fukushi, 2012; Modin and Fukushi, 2013; Arends et al., 2014; Sim et al., 2015). Compared with synthetic wastewater (mostly acetate) as substrate for the MXC anode, H_2O_2 production with real wastewater has very poor

performance in terms of concentrations produced and the rates of production, with especially a high energy input (> 2 kWh per kg H_2O_2). This brings up the importance of reactor design and operation to improve voltage efficiency as I studied in Chapter 3 and 6. Also, cathodic conversion (or Coulombic) efficiency or H_2O_2 production efficiency (PPE), which stands for fraction of cumulative Coulombs as current used and measured for H_2O_2 production, was variable ranging from 5% to 70% (Modin and Fukushi, 2012; Modin and Fukushi, 2013; Arends et al., 2014; Sim et al., 2015).

In Chapter 3, 5, and 6, I studied and optimized the flat-plate MECs with the characterization of overpotentials and primary sludge (PS) conversion for hydrogen (H_2) production. Thus, the approach I have used in this study aims to assess the anodic and cathodic performance including PS conversion, PPE, and voltage efficiency between MEC and H_2O_2-producing microbial electrochemical cell (H_2O_2 cell). I also used PS as a real wastewater for main electron donor at the anode, since PS can have the possibility of larger net electron capture to the anode and thus generation of enough H_2O_2 at the cathode. I used the same design of flat-plate MEC but slightly modified for H_2O_2 production with passive air diffusion to compared with MEC.

7.2 Materials and methods

7.2.1 Design and operation of microbial electrochemical cells

I operated a flat-plate microbial electrochemical cell separated with anion exchange membrane (AEM), AMI-7001 (Membranes International, Inc.) with the same design as used in Chapter 3, 5, and 6 for microbial electrolysis cells (MECs), with one anode chamber shared between two anodes, and two separate cathode chambers for two cathodes (Ki et al, 2015a; Ki et al., 2016). For H_2O_2 production, anode and anode chamber are the same as MEC, but the cathode chamber consisted of a serpentine flow cell having a ~120 mL volume located between the AEM and cathode. Detail parts, configuration, and assembly of H_2O_2 cell are provided in Appendix B (Figure B.1). For cathode fabrication for H_2O_2 production, I use carbon cloth cathode (GDL-CT, Fuel Cells Etc, TX, USA) with a 30% PTFE microporous layer (MPL). I coated Teflon PTFE DISP 30 with 2 layers of 16 mg/cm^2 on the air-exposed size of the cathode for 15 minutes at 200 °C and 1 hour at 280 °C. I coated Vulcan carbon powder at a loading of 0.5 mg cm^{-2} with 0.83 mL cm^{-2} of Nafion as the ionmer (D521 Dispersion, Fuel Cell Store, TX, USA) on the liquid-exposed side of the cathode. The cathode sizes ~79 cm^2. The distance between the anode and cathode was ~1 cm. I included a reference electrode (Ag/AgCl, MF-2052, Bioanalytical Systems, Inc., USA), which was at a ~2 cm distance from each of the anodes. I used a multi-channel potentiostat (VMP3, BioLogic Science Instruments, Knoxville, TN) to control the anode potential at -0.3 V (versus Ag/AgCl) and and recorded current, and anode and cathode potential every two minutes with the software (EC-Lab v. 10.37).

Originally, the MECs were started with ARB acclimation with typical acetate media described in Chapter 3 and 5 (Ki et al., 2015a; Ki et al., 2016). After ~4 months of operation, I changed substrate from acetate to PS. I operated ~15 months with different condition: batch and semi-continuous modes (Chapter 6). Then, the MEC was opened to

take samples to analyze the microbial community and reassembled to conduct ~4 months further with 12- and 9-day HRTs. The background electrolyte of the cathode (catholyte) for MEC was sodium hydroxide (NaOH) of 100 mM concentration. After the MEC operation, I opened the reactor again to change to H_2O_2-production mode. I maintained the same operational condition in the anode by 9-day HRT with one-day feeding cycle. I flowed catholyte continuously in the serpentine cathode chamber with ~1.5 hour HRT for 18 days, then changed in batch mode with one-day cycle. I collected catholyte sample around 1 mL at 1.5, 3, 6, 12, and 24 hours to measure pH and H_2O_2 concentration. Catholyte in H_2O_2-production mode was 50 mM NaOH.

7.2.2 Primary sludge

I collected PS from Greenfield Water Reclamation Plant (GWRP), in Gilbert, AZ, USA. I treated PS with lab scale pulsed electric field (PEF) unit (the FP *alpha* unit) and stored in the temperature controlled room at 4 °C before use to prevent psychrophilic fermentation and degradation of raw PS during cold storage (Ki et al., 2015a; Ki et al., 2015b).

7.2.3 Analytical methods

I characterized PS for total chemical oxygen demand (TCOD), semi-soluble COD (SSCOD), total suspended solids (TSS), and volatile suspended solids (VSS) according to Standard Methods (APHA, 2012). Semi-soluble COD was filtrate using vacuum pump through a 1.2-μm glass-fiber filter (Whatman™, UK), as describe in Ki et al. (2015b). I used colorimetric methods to determine H_2O_2 concentration of catholyte from the cathode chamber (Graf and Penniston, 1980). Briefly summarizing, the chemical solutions and samples were prepared in 1.5 mL cuvettes in the following order: 10 μL of sample (including H_2O_2 standard), 2 mL of HCl (50 mM), 0.2 mL of KI (1 M), 0.2 mL of ammonium molybdate (1M) in H_2SO_4 (0.5 M), and starch solution (1%) as indicator. H_2O_2 measurement were performed at 570 nm of wavelength using a Cary 50-Bio UV-

Visible spectrophotometer (Varian, Palo Alto, CA). Total alkalinity was measured using spectrophotometric methods by HACH kit and spectrophotometer (DR2700, HACH, Loveland, CO).

7.2.4 Calculations

I calculated Coulombic recovery (CR), Coulombic efficiency (CE), and H_2O_2 production efficiency (PPE). CR and CE were calculated as described in the previous studies (Lee et al., 2009; Ki et al., 2015b). PPE for H_2O_2 production was calculated with the measured H_2O_2 concentration, the recorded cumulative Coulombs as electrical current using Eq. (1),

$$H_2O_2\ production\ \ efficiency\ (\%) = \frac{n \times F \times C_{H2O2} \times V}{\int_0^t Idt} \times 100 \quad (1)$$

where n is the number of moles equivalent to moles of H_2O_2 (n=2, here), F is the Faraday constant (96,485 Coulombs mol^{-1}), C_{H2O2} is the measured concentration of H_2O_2 (mol L^{-1}), V is the volume of cathode chamber.

7.2.5 Microbial ecology

I collected biomass samples for bacterial activity and microbial community in MEC and H_2O_2 cell mode: anode suspension (AnS), anode biofilm of chamber side (BfC), and anode biofilm of membrane side (BfM) on the carbon fiber electrodes. For suspension samples, I centrifuged to obtain pellets for DNA extraction. I prepared for 0.17~0.27 gram of biomass and inserted in the bead tubes provided by a Power Soil DNA extraction kit (MoBio laboratories, Inc., Carlsbad, CA). Following the instruction of the kit for DNA extraction, I quantified the DNA concentration with Nanodrop spectrophotometer. The extracted DNAs were stored at -20 °C before pyroseqencing process.

I sent the extracted DNA to the Microbiome Analysis Laboratory (http://krajmalnik.environmentalbiotechnology.org/microbiome-lab.html) for Illumina MiSeq at Arizona State University. Amplicon sequencing of the V4 region of the 16SrRNA gene was performed with the barcoded primer set 515f/806r designed by Caporaso et al. (2012). Data received from the testing laboratory were analyzed using QIIME (Caporaso et al., 2010) after discarding sequences shorter than 25 bp, longer than 450 bp, or labeled as chimeric sequences. After screening, primer sequences were trimmed off, and taxonomic classification was performed using RDP classifier (Cole et al., 2009) at the 80%-confidence threshold. The total number of sequence reads for each sample after screenings were: MEC AnS=58,557, MEC BfC =64,681, MEC BfM=56,365, H_2O_2 cell AnS= 35,928, H_2O_2 cell BfC=58,902, and H_2O_2 cell BfM=55,570.

7.3 Results and discussions

7.3.1 Primary sludge characteristics and efficiencies

I conducted semi-continuous operation fed with PS in two different modes (MEC and H_2O_2 cell) by the same HRT (9-day). Table 7.1 shows the COD and SS characterization of influent and effluent PS on the stabilized condition. I can see all characteristic parameters of the effluent PS in H_2O_2 cell were higher than those in MEC. This results in decrease of COD removal efficiency in H_2O_2 cell by 27% compared to MEC (Figure 7.1). This is likely due to inhibition of methanogenesis since the gas volume produced in the anode chamber significantly decreased in the H_2O_2 cell, compared to MEC (Appendix B, Table B.1). This inhibition could be a result of H_2O_2 and oxygen by diffusion through the membrane from the air-cathode during the second phase of operation.

Table 7.1. Characteristics of PS influent and effluent for 9-day HRT in MEC and H_2O_2 cell mode

	MEC		H_2O_2 cell	
	Influent	Effluent	Influent	Effluent
TCOD	7450 (±330)	2860 (±20)	7700 (±90)	3940 (±40)
SSCOD	370	280	420 (±20)	340 (±20)
TSS	4260 (±40)	1880 (±20)	4590 (±140)	2650 (±70)
VSS	3740 (±20)	1680 (±10)	3890 (±130)	2210 (±60)

CRs were similar in both MEC and H_2O_2 cell by ~30%, while the Coulombic efficiency increased from 48% in MEC to 64% in H_2O_2 cell, mainly because of lower COD removal efficiency. Most of MEC studies using air-cathode reported very high COD

removal efficiency and low CE because oxygen diffused from air degrade viable organics faster than ARB utilize them (Ge et al., 2013; Angosto et al., 2015; Zhuang et al., 2012). However, the opposite trends of our study result from the efficient design having large surface area carbon fiber anode with flat-plate MEC. The woven anode of membrane side and the heterogeneous membrane (AMI-7001) might help blocking or reducing oxygen crossover from cathode to PS in anode. Also, the rate of oxygen diffusion could be significantly lower than the actual demand to loose PS-COD to oxygen.

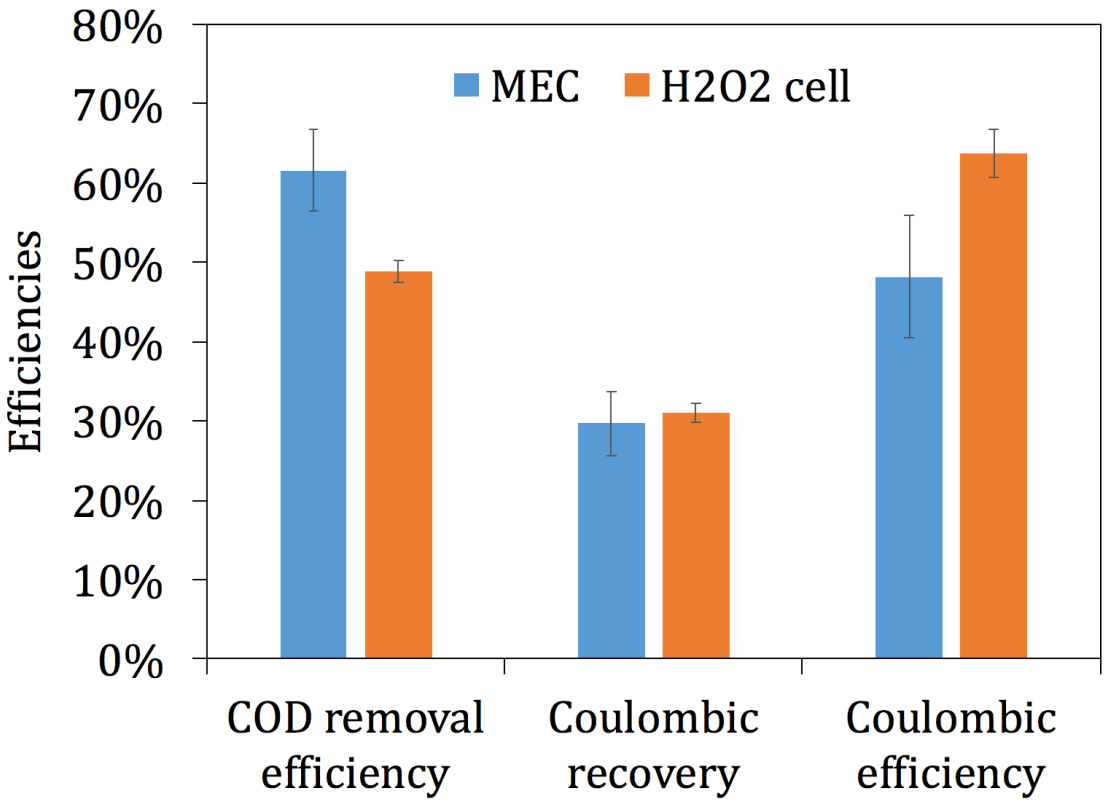

Figure 7.1. Comparisons of results of COD removal efficiencies, CR, and CE in the two different operational mode: MEC and H_2O_2 cell.

7.3.2 Microbial phylotypes relevant to community structure and function

Figure 7.2 shows the taxonomy of microbial communities classified at the order level in 6 samples of anode suspension (AnS) and biofilms of the MEC and H_2O_2 cell; the biofilm samples were taken at the chamber side (BfC) and membrane side (BfM) of the

anode. Microbial communities were different at each location from the MEC reactors. AnS and BfC had very similar communities in MEC and H_2O_2 cell, while BfM were significantly different. The most dominant phylotype in AnS were *Bacteroidales*, which are well-known bacteria for hydrolysis and fermentation of complex organics (Chapter 6, Appendix A; Rismani-Yazdi et al., 2013; Jia et al., 2013). Microbial community of suspended biomass in PS-fed MEC in this study has almost similar to the previous results (Chapter 6, Appendix A). *Desulfuromonadales* and *Desulfobacterales* were dominant in the biofilm on the anode of chamber side, and especially *Geobacter*, unclassified *Pelobacteraceae*, and unclassified *Desulfobulbaceae* were dominant at the genus level. These organisms have been typically found in the anode (Chapter 6, Appendix A; Torres et al., 2009; Jia et al., 2013; Kiely et al., 2011; Wang et al., 2014).

Of special interest is the difference of microbial communities between MEC BfM and H_2O_2 cell BfM. *Natranaerobiales* were the most abundant phylotype in MEC BfM, and especially *Dethiobacter* (Family *Anaerobrancaceae*) and unclassified *Anaerobrancaceae* were the largest fractions at the genus level by 23 and 25%, respectively. *Dethiobacter alkaliphilus,* which is 96% similarity to the representative sequence in the MEC BfM, was known as obligate anaerobes using hydrogen as electron donor and thiosulfate, elemental sulfur, and polysulfide as electron acceptors in high pH (~10) and high salt (~0.6 M of sodium) with (Sorokin et al., 2008). On the other hand, *Oceanospirillales* and *Rhizobiales* were the predominant in H_2O_2 cell BfM, and especially *Halomonas* and *Parvibaculum* were the largest fractions at the genus level by 17 and 16%, respectively. *Halomonas* species are aerobes living in saline condition. In particular, some species such as *Halomonas salaria* sp. and *Halomonas denitrificans* sp. has yellow or brown-yellow color (Kim et al., 2007), which are the similar appearance of the anode (membrane side) at the end of the experiments (shown in Appendix B Figure B.2). *Parvibaculum lavamentivorans* DS-1 are also aerobes and of interest

microbes degrading synthetic laundry detergent (e.g. linear alkylbenzenesulfonate, LAS) (Schleheck et al., 2011). The AEM (AMI-7001) polymer consists of benzene, carbon oxides, sulfur oxides, styrene, and fluoride, with a functional group of quaternary ammonium, which especially is used as surfactants (Alami et al., 1993; Kern et al., 1994; Danino et al., 1995). This suggests some surfactant chemicals from the AEM might be degraded with H_2O_2 or radicals and released into the anode of membrane side, and *Parvibaculum* sp. were able to grow on the anode fiber of membrane side. It is worthy to note that there were not only significant differences in the community, but also the Live/Dead ratios on BfM samples (shown in Appendix B). Also, Principal Coordinate Analysis (PCoA) as provided in Appendix B Figure B.4 corroborated the similarities of AnS and BfC and differences of BfM in MEC and H_2O_2 cell.

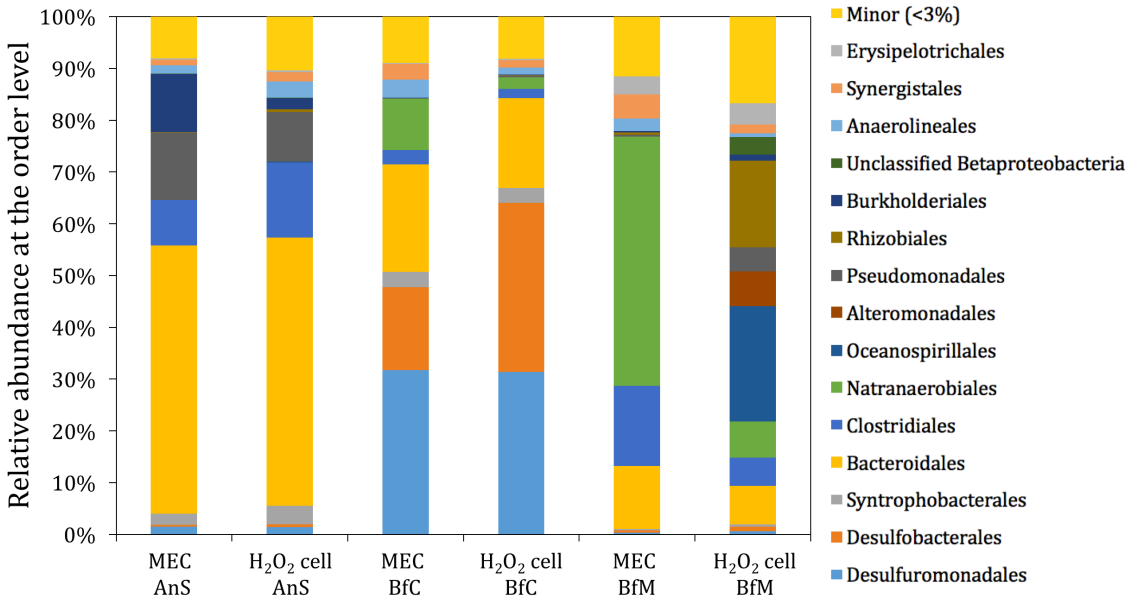

Figure 7.2. Microbial community structure at the order level for anode suspension (AnS), biofilm of chamber side (BfC), and biofilm of membrane side (BfM) in MEC and H_2O_2 cell operation.

There are two common results in microbial communities of BfM from MEC and H_2O_2 cell - 1) totally different community structures from BfC and 2) major microbes

being able to grow in high salt or high alkalinity condition. First, even though the materials (carbon fibers) were the same and even connected with the same conductive materials (titanium frame), the communities on each side of the anode (chamber versus membrane direction) were significantly different. Second, due to the catholyte (NaOH) used in MEC and H_2O_2 cell, high-salt or -pH tolerant microbes were dominant (e.g., *Oceanospirillales* or *Natranaerobiales*)

The difference of microbial community between MEC BfM and H_2O_2 cell BfM are related to oxygen availability; anaerobes were dominantly found in MEC BfM, while aerobes were in H_2O_2 cell BfM, indicating oxygen came into the catholyte through air-cathode and into the anode of membrane side diffused through the AEM. Oxygen might penetrate to the anode chamber, but there was no significant change on BfC samples nor any change in ARB function (similar Coulombic recovery ~30% in Figure 7.1).

7.3.3 Voltage efficiencies between MEC and H_2O_2 cell

In Figure 7.3, I show total overpotentials (η_{tot}) in H_2O_2 cell were lower by ~150 mV than the MEC. Since I poised the anode potential at -0.3 V (vs Ag/AgCl) during the experiments in both cases, I can assume the anode overpotential (η_{an}) could be the same as ~0.26 V or even lower. The remaining parts (η_{rem}) are the sum of Ohmic (η_{Ohmic}), cathode (η_{cat}), and pH-related concentration overpotentials (η_{pH}) as shown in Chapter 3. The differences of η_{rem} were likely due to changes of each overpotential. The distance between anode and cathode increased ~0.5 cm; thus I can expect the increase of η_{Ohmic} by 18 mV assuming 1 A m^{-2} of current density and 2.73 mS cm^{-1} of conductivity (based on the current density profile shown in Appendix B Figure B.2 and conductivity measurements of PS effluent in Chapter 6) and using Ohm's law. Based on the pH measurement of anode and cathode, which discuss more in the later section in H_2O_2 cell, the pH difference was ~5.8 in MEC (Ki et al., 2016) and 3.4~5.6 in H_2O_2 cell between

anode and cathode chamber, thus 12~142 mV of η_{pH} could be decreased in H_2O_2 cell. Cathode overpotential, which is typically the largest fraction among overpotentials, could be rest of them. Thus, based on the above numbers η_{cat} of H_2O_2 cell could be lower by 26~156 mV than MEC. This indicates that the designed flat-plate MEC with a modification for H_2O_2 production still has a good voltage efficiency.

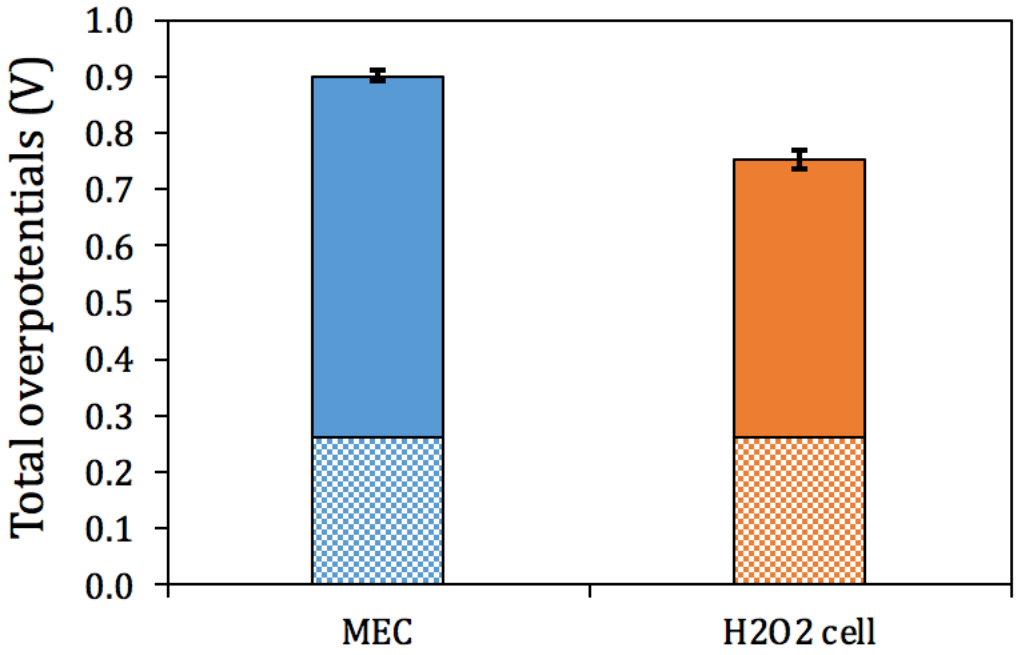

Figure 7.3. Total overpotentials in MEC and H_2O_2 cell. Since I fixed anode potential, -0.3 V (versus Ag/AgCl) in both MECs and assumed theoretical potential, -0.56 V with acetate in PS, ~0.26 V can be expected as anode overpotential (hatched sections). The remaining parts show the rest of overpotentials including Ohmic, cathode, and pH-related concentration overpotentials.

7.3.4 H_2O_2 production and cathode conversion efficiency

In Figure 7.4, I show H_2O_2 concentrations (theoretical and measured) and H_2O_2 production efficiency (PPE) based on Eq (1). Theoretical H_2O_2 assumes all of the cumulative charge (or Coulombs) measured is utilized for production of H_2O_2. I can observe that the H_2O_2 concentration increased up to ~200 mg L^{-1} by 3 hours and then

decreased to ~121 mg L^{-1} by 24 hours. The theoretical H_2O_2 increased linearly up ~2300 mg L^{-1}, indicating PS conversion to electrical current was successfully maintained in the anode, but the PPE kept decreasing with time from 72 % (1.5 hours) to 5 % (24 hours).

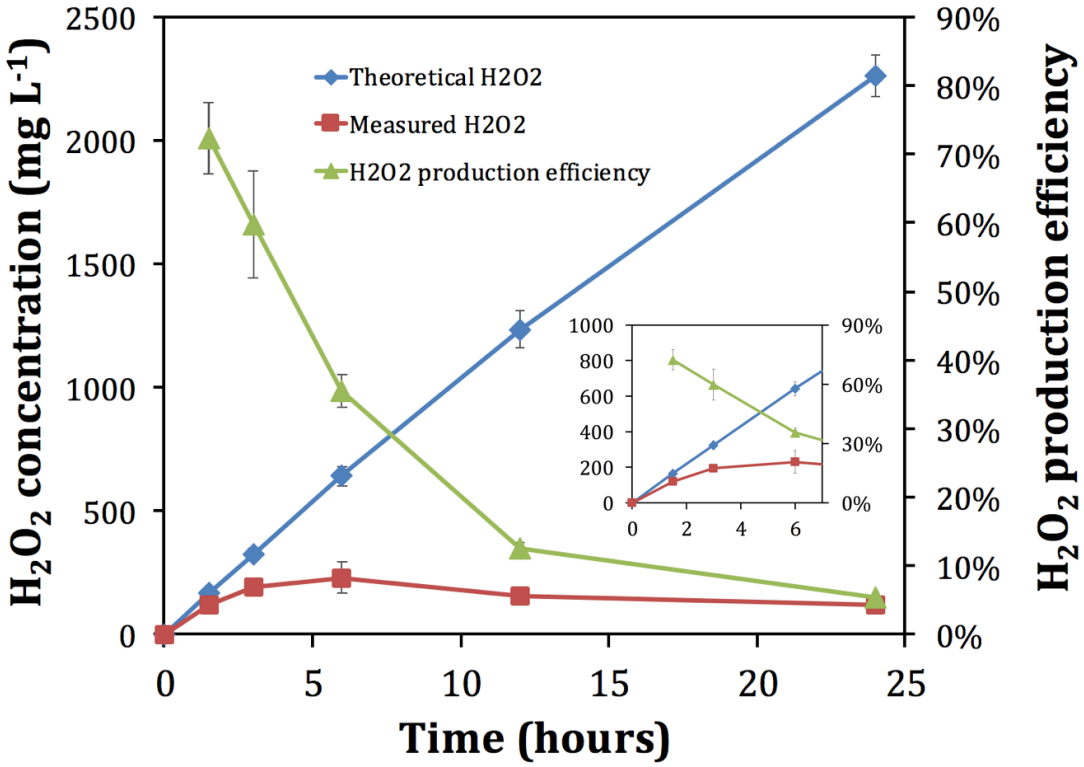

Figure 7.4. Results of cathode batch operations: 1) theoretical and 2) measured H2O2 concentrations based on 100% conversion from cumulative coulombs and detection method, respectively, and 3) H_2O_2 production efficiency (number of measurements, N=3). Inset shows zoomed sections of the first 6 hours' operation in the H_2O_2 cell.

Catholyte pH in the H_2O_2-producing cathode decreased with time from ~12.6 (0 hour) to 10.4 (24 hour) (Figure 7.5). The decrease of pH might be two possible reasons; 1) OH^- diffusion from cathode to anode through AEM because of concentration gradients (high OH^- concentration (pH ~12.6) in cathode to low OH^- concentration (pH ~7) in anode), and 2) bicarbonate (HCO_3^-) diffusion from anode to cathode through AEM. HCO_3^- were formed by carbon dioxide (CO_2) oxidized from organics and OH^- crossed over from cathode as well as manually spiked sodium hydroxide (NaOH), which is for

better anode respiration of ARB with maintaining anodic pH around neutral (7-8.5). Increased HCO_3^- could diffuse to cathode, where HCO_3^- changed to carbonate (CO_3^{2-}) because of pK_a (~10.3), resulting in pH drop due to the proton (H^+), as shown in Appendix B Figure B.5.

Figure 7.5 shows alkalinity and pH in one-day batch cycles (triplicates). Based on the measured total alkalinity and pH of the catholyte, different alkalinity species (CO_3^{2-}, HCO_3^-, and OH^-) changed with time. Within 3 hours, CO_3^- drastically increased along with decrease of OH^-. After that, HCO_3^- gradually increased because of pK_a of HCO_3^- /CO_3^{2-}. Initial catholyte total alkalinity was 2220 mg L^{-1} as $CaCO_3$ and incremented up to ~3000 mg L^{-1} because of manually added sodium hydroxide in the anode, indicating possible mechanisms as explained above are correct.

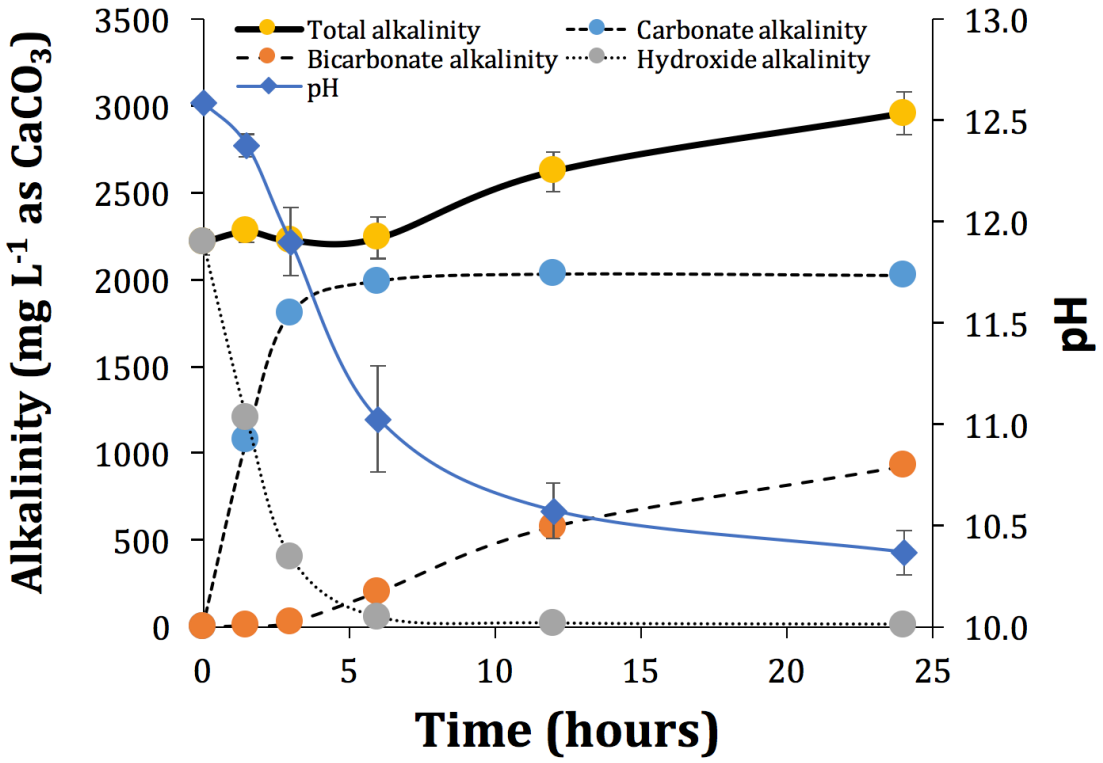

Figure 7.5. pH and alkalinity of catholyte in batch operation of H_2O_2 cell

A decrease in H_2O_2 concentrations means that H_2O_2 generated at the cathode did not accumulate with time, indicating a faster decay rate. There are several possibilities of H_2O_2 decay: 1) metal ions diffusion from anode in PS, 2) membrane degradation with consumption of H_2O_2, and 3) interference with carbonate ions . Direct movement of metal ions is likely not too much because I used anion exchange membrane. There was no membrane deterioration or chemical deposits after running 27 days in H_2O_2 cell fed with PS (Figure B.6) unlike the previous study by Modin et al. (2012). Lee et al. (2000) reported that peroxide is less stable in carbonate solution (Na_2CO_3) and rate of decomposition of H_2O_2 was ~9-fold faster than caustic solution (NaOH) at pH 10~10.6, 30~50 ˚C, and 1.5~3 M of ionic strength. Exact mechanism of H_2O_2 decay with carbonate ions have not been explained so far. I also performed H_2O_2 decay tests to confirm the H_2O_2 decay with the similar condition of theoretical H_2O_2 and carbonate concentration, showing H_2O_2 decomposed quickly with time during ~1 day operation in sodium carbonate solution. Detail results are provided in the supporting information (Figure B.7). Other than those possibility, produced H_2O_2 also has a potential to diffuse to anode chamber like oxygen diffusion in air-cathode microbial fuel cells, which cause a decrease of H_2O_2 concentration.

7.3.5 Outlook

Our results show a promising proof-of-concept study to produce H_2O_2 from PS. However, there are several important notes to improve efficiency and make this system more practical. First, MXC design should be key for the overall energy efficiency including maintaining short distance between anode and cathode, appropriate ionic solutions, enough surface area of bio- and physicochemical-catalysts in anode and cathode, etc. In 6-hour operation with production of ~230 mg H_2O_2 L^{-1}, cathode potential was around -0.5 V (versus Ag/AgCl) with fixed anode potential, -0.3 V (versus Ag/AgCl), which indicates around 0.2 V of applied voltage, resulting in ~0.87 kWh per

kgH_2O_2 with ~1 A m^{-2} of current density. This energy requirement for H_2O_2 production is relatively lower compared to other studies; 2.5-78 kWh per kgH_2O_2 using real wastewater (Modin and Fukushi, 2012; Modin and Fukushi, 2013; Arends et al., 2014, and Sim et al., 2014), and ~0.93, 3, and 0.659 kWh per kgH_2O_2 using synthetic wastewater, acetate (Rozendal et al., 2009; Modin and Fukushi, 2013; Chen et al., 2015, respectively). Detail comparisons of H_2O_2 cell using real wastewater were provided in supplementary data (Table B.2). Lower energy input compared to other studies proves higher voltage efficiency in the optimized flat-plate MECs.

Second, I determined that lower PPE was a function of retention time of H_2O_2 in the cathode chamber, and not a function of any anodic reaction. Lower PPE cause the overall cathodic product recovery as H_2O_2 much lower by ~3.2% (CE: 64% and PPE: 5% after 24 hours) in H_2O_2 cell than one as H_2 by ~43% (CE: 48% and PPE: 90%, which is based on the result in Chapter 6). Continuous flow of catholyte may result in a decrease of final H_2O_2 concentration, suggesting more studies necessary to evaluate the optimum operation. Based on this study and on-going research fed with acetate medium by Michelle Young, I suggest ~4 hour HRT.

Third, a faster rate of anode reaction, or high current density, is necessary. Improvement of current directly relates with an increase of H_2O_2 concentration. Here, the maximum current density was ~1 A m^{-2} (or ~20 mA) fed with PS in semi-continuous operation. Flat-plate MECs fed with acetate typically have ~10 A m^{-2} with generation of ~0.3% (wt.) H_2O_2, which is corresponding to ~3000 mg L^{-1} of H_2O_2 (Figure B.8). High-strength organic wastes have better opportunities because of dense organic contents, but are related not only with the downstream reaction of anaerobic energy conversion as anode respiration in MEC but also with the upstream reactions as hydrolysis and fermentation. To increase the hydrolysis, which is known as rate-limiting process, pre-treatment technologies can be applied.

7.4 Conclusions

In comparison with overpotentials of MEC and H_2O_2 cell, I showed that reactor design is important in the applied voltage (~0.2 V) that energy input for H_2O_2 production (~0.87 kWh per kgH_2O_2) of this study was the best performance among other studies of H_2O_2-producing microbial electrochemical cells. PPE was governed by a function of retention time in the cathode because of the degradation of H_2O_2. This is the first demonstration of H_2O_2 production using PS in the flat-plate and dual-chambered MEC. Maximum H_2O_2 concentration was achieved ~230 mg/L in 6 hours of batch operation.

CHAPTER 8

SUMMARY AND RECOMMENDATIONS FOR FUTURE RESEARCH

8.1 Summary

The research that I have conducted throughout this dissertation is anaerobic energy conversion from primary sludge (PS) as a high-strength organic waste to collect useful resources (e.g. H_2 or H_2O_2) using microbial electrochemical cells (MXCs). Before attempting energy conversion from PS in MXCs, I first developed a new MXC. I aimed, in Chapter 3, to improve the design and operation of microbial electrolysis cells (MECs) to achieve current densities >10 A m^{-2} with reduced applied voltages, using a thorough analytical framework involving electrochemical techniques such as chronoamperometry, voltammetry, and electrochemical impedance spectroscopy. This is because one of the main performance challenges in MXCs is the low voltage efficiency in comparison to other fuel and electrolysis cells. I developed a design that provides high anode surface area using carbon fibers without creating a large distance between the anode and cathode (<0.5 cm) to reduce Ohmic overpotential. I determined that Ohmic overpotential at current densities >10 A m^{-2} remained <0.1 V, even when using an anion exchange membrane to separate the anode and the cathode. I observed the largest overpotential from cathode related phenomena. The increase in pH in the cathode chamber, often to ~13, results in >0.3 V of Nernstian concentration overpotential. I showed that this overpotential became negligible when CO_2 was added to the cathode. I also tested two different cathode materials (stainless steel and nickel) to compare the cathode activation overpotentials. Overall, through our design and operation improvements, I was able to reduce the applied voltages from 1.1 to ~0.85 V, at 10 A m^{-2}. The results also provide important guidelines for further optimizations of MXCs.

PS is a renewable and sustainable energy source, but pretreatment is often required to accelerate hydrolysis of organic solids. Pulsed electric field (PEF) treatment has been proven effective for waste activated sludge (WAS), but its impact on PS is not known. I first evaluated the impacts of PEF pretreatment on energy recovery from PS by methanogenesis and fermentation to volatile fatty acids (VFAs) in Chapter 4. PEF treatment achieved successful microbial inactivation of PS and modestly enhanced conversion of PS chemical oxygen demand to methane (by ~8%) and to VFAs by fermentation (by ~7%) by increasing hydrolysis rates. Thus, the impact of PEF treatment was small for PS alone, compared to the much more significant increases in methane conversion from WAS or WAS+PS. This difference points to the value of optimizing ratios of PS:WAS for PEF treatment, whether the goal is methanogenesis or fermentation to VFAs.

In Chapter 5, I studied the combination of two technologies (PEF pretreatment and semi-continuous pre-fermentation of PS) that generate VFAs as electron donors in the MECs that I designed above (Chapter 4). Pre-fermentation with a 3-day solids retention time (SRT) led to the maximum generation of VFAs, with or without PEF pretreatment of the PS. PEF treatment before fermentation enhanced the accumulation of the preferred VFA, acetate, by 2.6-fold. Correspondingly, MEC anodes fed with centrate from 3-day pre-fermentation of PEF-treated PS had a maximum current density ~3.1 A m^{-2}, which was 2.4-fold greater than the control pre-fermented centrate. Over the full duration of batch MEC experiments, using pre-fermented centrate led to successful performance in terms of Coulombic efficiency, CE (95%), Coulombic recovery, CR (80%), and COD-removal efficiency (85%). However, overall energy conversion of PS to electrical current (or CR) through pre-fermentation and MEC, was just ~16% and volatile suspended solid (VSS) reduction was ~25%. The results suggest better energy recovery in direct PS-fed MEC.

Based on the results obtained from Chapter 5, I aimed to maximize CR by controlling operational conditions while achieving sludge reduction in an efficiently designed flat-plate MEC directly fed with PS (Chapter 6). I first evaluated the effect of HRT on CR in the range of 6-15 days in semi-continuous operation. Maximum current densities increased over 2 A m^{-2} at 6-and 9-day HRTs, while CR increased from 13% at 15-day HRT to 34% at 9-day HRT, becoming the main electron sink. High anodic pH (~8.1) significantly contributed to an increase in anode respiration, and a corresponding suppression of methanogenesis. PS-fed MECs yielded ~60% sludge reduction given the overall HRTs, indicating that lower HRT still enabled energy recovery and solids reduction using high-surface area anodes. Moreover, I showed that maintaining high pH improved sludge dewaterability by 7.3- and 3.3-fold compared to the influent PS and effluent PS values at neutral pH, respectively. As a first report of electron balances using PS in long-term MEC operation for ~300 days, this study demonstrated that Coulombic recovery and sludge treatment can be improved using an efficiently designed MXC and optimized operational conditions.

Armed with my knowledge that higher CR was achieved at a 9-day HRT in a direct PS-fed MEC, I designed a final study examining H_2O_2 production in an air-cathode microbial electrochemical cells (or H_2O_2 cell) and compared it with an MEC run at a 9-day anodic HRT. Both MXCs achieved ~30% of CRs. Similar microbial communities found in anode suspensions and biofilms from the two MXC modes corroborates that anode respiration has no effect, even in the air-cathode H_2O_2 cell. CE was higher by ~12% in H_2O_2 cell than MEC, resulting from lower PS-TCOD removal likely due to methanogen inhibition. Detection of aerobic bacteria in the membrane-side anode biofilm as well as no gas production in the H_2O_2 cell caused inhibition of methanogens and a consequent decrease in COD removal. H_2O_2 cell achieved ~230 mg/L of maximum H_2O_2 concentration during 6 hours of batch operation. However, I observed H_2O_2

gradually decaying with time with a decrease of H_2O_2 production efficiency (PPE). Two important features of this study are 1) it is the first demonstration of H_2O_2 production using PS in an H_2O_2 cell and 2) the energy requirement for H_2O_2 production is very low (~0.87 kWh per kg H_2O_2) compared to previous literature (2.5-78 kWh per kg H_2O_2).

In conclusion, my dissertation study has focused on anaerobic conversion processes to maximize energy recovery as electrical current in efficiently designed MXCs. The studies in Chapter 3 reveal that overpotentials in MECs could be reduced through improved design, operation, and electrochemical characterization (Ki et al., 2016). As shown in Chapter 4, PEF pretreatment provided a modest improvement in PS conversion by methanogenesis and fermentation as compared to conversion from WAS or WAS+PS. This suggests that further optimization of PS:WAS ratios is needed in order for PEF treatment to maximize methane or VFA production (Ki et al., 2015a). Chapters 5 and 6 show how many electrons from PS can be converted to electrical current by optimizing operational conditions such as two-stage (pre-fermented, PS-fed MEC) versus single-stage (direct PS-fed MEC) sludge input, HRTs, and pH control (Ki et al., 2015). Last but not least, Chapter 7 demonstrates that H_2O_2 producing microbial electrochemical cells (H_2O_2 cells) generate H_2O_2 successfully through bio- and electro-chemical energy conversion processes in MXC system. In the following section, I suggest some promising and relevant approaches as recommended future research.

8.2 Recommendations for future research

8.2.1 Variation of organic loading rates by increasing COD or decreasing HRT

In my dissertation research, I fixed PS-COD as ~7-9 g L^{-1}; diluting with DI water for MXC experiments (Chapter 5-7). Typical PS concentrations are higher than the value that I have used. The reasons for PS dilution were that 1) we proposed using PS as a forward operating bases (FOBs) blackwater surrogate and needed a known concentration of organic material, and 2) we needed to dilute to meet the conductivity requirement for PEF treatment while diluting PS with water. An important next step will be to study energy recovery performance in MXCs with higher concentrations of PS, since applying raw PS without dilution is more realistic and we need to know whether the electron balances are similar or not. During semi-continuous long-term operation in Chapter 7, the organic loading rates (OLRs) as COD and VSS at 6-15 day HRTs were 0.536-1.341 kgCOD m^{-3} d^{-1} and 0.242-0.606 kgVSS m^{-3} d^{-1}, respectively. The overall energy recoveries to Coulombs and methane at the all SRTs were high, >41% by $TCOD_{in}$ as well as >55% of sludge reduction by VSS_{in}.

To evaluate and show the limiting condition of PS hydrolysis, I propose to further test even higher OLRs by applying lower HRT (e.g. 2 or 3 day) with the same concentration range that I tested or by increasing PS concentrations to raw, undiluted levels. Higher PS-COD concentrations used for methanogenesis, fermentation, and MXCs in (semi-) continuous operation were reported in the literature, as shown in Table 8.1. Higher organic loading will provide larger net electron capture at the anode, and more opportunities to produce higher concentrations of H_2O_2 when using H_2O_2 cells.

Table 8.1 PS organic loading on methanogenesis, fermentation, and MXC in the literature.

Reference	COD or VSS ($g\ L^{-1}$)*	OLR (kgCOD or VSS $m^{-3}\ d^{-1}$)	Retention time (day)	Recovery (%)**
Miron et al. (2000)	27 (C) and 18 (V)	1.8-8.9 (C) and 1.2-6 (V)	3-15 (SRT)	~55% (M) by COD
Bouzas et al. (2002)	6.4-30.7 (V)	1.1-5.1 (V)	4-10 (SRT)	~10% (F) by VSS
Elefsiniotis et al. (1996)	2.710 (V)	4.3-10 (V)	0.25-0.625 (HRT)	~25% (F) by VSS
Yuan et al. (2010)***	25 (C) and 15 (V)	6.2 (C) and 3.7 (V)	4 (SRT=HRT)	~13% (F) by COD
Ge et al. (2013)	14.2-78 (C) and 6.1-44.8	1.58-11 (C) and 0.68-4.1 (V)	7-9 (HRT)	~0.87% (C) by COD and more methane****

* C – COD, V – VSS

**M – methane in methanogenesis, F – volatile fatty acids in fermentation, C – electrical current in MXC or anode respiration

***Mixture of PS and WAS by 1:1 to 1:3

****CR was calculated based on the COD removal and CE given the paper but methane recovery data was not provided even though more energy on methane was produced in MXC.

8.2.2 Other high-strength organic waste streams

I chose PS as the high-strength organic waste input in all of my dissertation research, but there are many other opportunities to extract useful energy and resources from wastes (WAS, swine wastewater, brewery wastewater, palm oil mill effluent, algae biomass, etc.) in MXCs. I propose to applying mixed sludges with PS and WAS to MXCs.

Pulsed-electric-field (PEF) treatment can be optimized using my research parameters as starting references. Given the results that I obtained in Chapter 4, PEF was not significantly beneficial to methanogenesis and fermentation using PS alone, as compared to WAS. However, PEF treatment can improve hydrolysis and fermentation by optimizing the ratio of PS:WAS . Quantification of hydrolysis and energy recovery rates in Biochemical Methane Potential (BMP) or fermentation reactors with varying ratios of PS:WAS is needed next. One could establish optimum MXC conditions for various sludge mixtures, that would dictate appropriate HRTs, similar to the two-stage or single-stage experiments that I conducted in Chapter 5 and 6. Using mixtures of two sludges (PS and WAS) is more realistic for MXC applications applied in wastewater treatment plants (WWTPs). Such studies will elucidate the dual benefits of PEF and MXC processing in the context of anaerobic energy recovery from energy-rich organics in WWTPs.

8.2.3 H_2O_2 application – H_2S removal

H_2O_2 produced in the cathode chamber of a H_2O_2 cell can be used to disinfect low-strength wastewater (or graywater) and for pre- or post-treatment of high-strength wastewater (or blackwater) as explained in Chapter 1. H_2O_2 produced in MXCs can also be studied to determine whether it would be an effective odor control mediator by removing hydrogen sulfide (H_2S) formed in anaerobic sludge treatment. Odor management is an important issue of wastewater treatment facilities. Many municipal wastewater treatment plants have concerns about H_2S generation during sludge processing. This is the same situation in sludge-fed MXCs. Beyond the obnoxious odor problems of H_2S gas emission, there are equipment and concrete corrosion issues as well as sulfide gas toxicity risks to sewer workers (Zhang et al., 2008). For control of H_2S gas, inhibition and elimination methods have been considered. Sulfate-reducing bacteria (SRB) thrive in anaerobic conditions, producing a characteristic rotten-egg odor. SRB

can be inhibited by controlling pH (Jayaraman et al., 1999; Nemati et al., 2001) and/or by adding other electron acceptors that stimulate bacteria having more favorable thermodynamics than SRB (Lovley and Phillips, 1986; Hobson and Yang, 2000). To eliminate H_2S, addition of iron salts (Fe^{2+}, Fe^{3+}) and chemical oxidants such as H_2O_2, chlorine (Cl_2), potassium permanganate ($KMnO_4$) etc. has been used (US EPA, 1991). Among them, the chemical scrubbing tower is considered one of the most popular and effective processes. H_2O_2 has been the preferred chemical for treating H_2S because its oxidation does not produce toxic byproducts, as compared to chlorine (Couvert et al, 2006).

In order to achieve a safer and better quality of air and water, an enhanced, post-treatment chemical scrubbing tower type should be designed and tested. After treating sludge in the anode chamber of an H_2O_2 cell, the effluent containing aqueous sulfide can be treated with the effluent containing aqueous H_2O_2 from the cathode chamber. Also, the potentially odorous gas (H_2S) emanating from the packed media will be efficiently removed if sprayed with high pH H_2O_2 from the top of the treatment system. Since sulfuric acids are formed during the reaction between H_2S and H_2O_2, the resulting alkaline condition enhances the H_2S removal efficiency. The H_2O_2 produced in the MEC cathode has a pH higher than 10 which is an ideal H_2S removal condition requiring no further application of additional chemicals. Complete control of odor-causing compounds (sulfide [H_2S, HS^-, S^{2-}]) requires that a mass balance of total sulfide and elemental sulfur be determined along with the flow rates of influents into the post-treatment system.

8.2.4 Recalcitrant organic removal by fungi in MXCs

I have seen fungi growing on the membrane side of the anode while operating acetate- and PS-fed H_2O_2 cells. Even though the microbial biofilm and suspension communities were distinctive compared to the membrane side of the anode, I still

achieved sufficient Coulombic recovery to produce H_2O_2 at the cathode, as shown in Chapter 7. However, the community analysis yielded mostly bacteria and a little bit of archaea with the given primer set. If fungi do exist on the membrane side of the anode, we may be observing a new syntrophic relationship in MXCs, specific to H_2O_2-producing MECs. Fungi are capable of excreting extracellular enzymes (Nakayama and Amachi, 1999; Kersten et al., 1990; Cajthaml et al., 2009). One possible enzyme that may significantly impact H_2O_2 cells is peroxidase. Interestingly, this enzyme can catalyze the oxidation of a variety of recalcitrant compounds by H_2O_2 (Nakayama and Amachi, 1999). Thus, various biotechnological applications have been deployed in the field of soil remediation, biobleaching, biopulping, biological material manufacturing, and endocrine disrupting compound (EDCs) removal (Aust, 1990; Higson, 1991; Karam and Nicell, 1997; Kirk and Farrell, 1987; Cajthaml et al., 2009). If fungi and peroxidase are shown to favor H_2O_2 cells, we can expect many promising research avenues to develop. Or, we might indirectly prove that H_2O_2 is not able to diffuse all the way from the cathode to the anode chamber to impact anode respiration of ARB because it is consumed by fungi.

An appropriate fungal primer set must be used to conduct Illumina MiSeq to identify fungal population on the existing DNA extracted from my H_2O_2 cell, used in Chapter 7, to see if there are any common fungi such as *Aspergillus niger, Phanerochaete chrysosporium,* and *Trametes versicolor*, able to produce efficient peroxidases (Conesa et al., 2000; Kersten et al., 1990; Cajthaml et al., 2009). To explore the ability of peroxidase to remove recalcitrant organic compounds, I propose that my reactor should be modified with the addition of a liquid chamber between the anode and membrane. The volume should be very small, to minimize Ohmic loss. Peroxidase activity can be measured using a commercial assay kit (Peroxidase Activity Assay Kit, Sigma-Aldrich or Worthington Biochemical Corporation) under a wide range of buffer pH conditions as activity has been shown to vary with pH in the literature (Kersten et al.,

1990). Target recalcitrant compounds such as methoxybenzene and 17α-ethinylestradiol (EE2) (Kersten et al., 1990; Cajthaml et al., 2009) can then be applied and their removal rates quantified. Based on the removal capacity, the middle chamber may be operated in batch or continuous mode in the H_2O_2 cell.

REFERENCES

American Public Health Association (APHA). 2012. *Standard Methods for the Examination of Water and Wastewater*, Washington, D.C.

Abourached, C., Lesnik, K.L., Liu, H. 2014. Enhanced power generation and energy conversion of sewage sludge by CEA-microbial fuel cells. *Bioresource Technology*, **166**, 229-234.

Alami, E., Levy, H., Zana, R., Skoulios, A. 1993. Alkanediyl-alpha,omega-bis(dimethylalkylammonium bromide) surfactants. 2. Structure of the lyotropic mesophases in the presence of water. *Langmuir*, **9**(4), 940-944.

Alcaide, F., Brillas, E., Cabot, P.L. 1998. Electrogeneration of hydroperoxide ion using an alkaline fuel cell. *Journal of the Electrochemical Society*, **145**(10), 3444-3449.

Alder, J.M., Lee, I.-S., Parameswaran, P., Rittrnann, B.E., Lopez, R., Banaszak, J.E. 2009. Making Waste Biosolids a Sustainable Organic Electron Donor for Denitrification Using Focused Pulsed Technology, in: Water Environment Federation. pp. 780–789.

An, J., Lee, H.-S. 2013. Implication of endogenous decay current and quantification of soluble microbial products (SMP) in microbial electrolysis cells. *Rsc Advances*, **3**(33), 14021-14028.

Angelidaki, I., Alves, M., Bolzonella, D., Borzacconi, L., Campos, J.L., Guwy, A.J., Kalyuzhnyi, S., Jenicek, P., van Lier, J.B. 2009. Defining the biomethane potential (BMP) of solid organic wastes and energy crops: a proposed protocol for batch assays. *Water Science and Technology*, **59**(5), 927-934.

Angosto, J.M., Fernandez-Lopez, J.A., Godinez, C. 2015. Brewery and liquid manure wastewaters as potential feedstocks for microbial fuel cells: a performance study. *Environmental Technology*, **36**(1), 68-78.

Apul, O.G., Atalar, I., Zorba, G.T., Sanin, F.D. 2010. The Dewaterability of Disintegrated Sludge Samples Before and After Anaerobic Digestion. *Drying Technology*, **28**(7), 901-909.

Arends, J.B.A., van Denhouwe, S., Verstraete, W., Boon, N., Rabaey, K. 2014. Enhanced disinfection of wastewater by combining wetland treatment with bioelectrochemical H2O2 production. *Bioresource Technology*, **155**, 352-358.

Arends, J.B.A., Verstraete, W. 2012. 100 years of microbial electricity production: three concepts for the future. *Microbial Biotechnology*, **5**(3), 333-346.

Aust, S.D. 1990. Degradation of environmental pollutants by Phanerochaete chrysosporium. *Microbial Ecology,* **20**,197–209.

Baras, A.S., Solomon, A., Davidson, R., Moskaluk, C.A. 2011. Loss of VOPP1 overexpression in squamous carcinoma cells induces apoptosis through oxidative cellular injury. *Laboratory Investigation*, **91**(8), 1170-1180.

Belafi-Bako, K., Vajda, B., Bakonyi, P., Nemestothy, N. 2014. Removal of COD by Two-Chamber Microbial Fuel Cells. In: Chin-Tsan Wang (Ed.), Technology and Application of Microbial Fuel Cells. INTECH, pp. 77–87.

Bhattacharya, S.K., Madura, R.L., Walling, D.A., Farrell, J.B. 1996. Volatile solids reduction in two-phase and conventional anaerobic sludge digestion. *Water Research*, **30**(5), 1041-1048.

Bolzonella, D., Fatone, F., Pavan, P., Cecchi, F. 2005. Anaerobic fermentation of organic municipal solid wastes for the production of soluble organic compounds. *Industrial & Engineering Chemistry Research*, **44**(10), 3412-3418.

Bond, D.R., Holmes, D.E., Tender, L.M., Lovley, D.R. 2002. Electrode-reducing microorganisms that harvest energy from marine sediments. *Science*, **295**(5554), 483-485.

Bond, D.R., Lovley, D.R. 2003. Electricity production by Geobacter sulfurreducens attached to electrodes. *Applied and Environmental Microbiology*, **69**(3), 1548-1555.

Bond, D.R., Lovley, D.R. 2005. Evidence for involvement of an electron shuttle in electricity generation by Geothrix fermentans. *Applied and Environmental Microbiology*, **71**(4), 2186-2189.

Bond, D.R., Strycharz-Glaven, S.M., Tender, L.M., Torres, C.I. 2012. On Electron Transport through Geobacter Biofilms. *Chemsuschem*, **5**(6).

Borole, A.P., O'Neill, H., Tsouris, C., Cesar, S. 2008. A microbial fuel cell operating at low pH using the acidophile Acidiphilium cryptum. *Biotechnology Letters*, **30**(8), 1367-1372.

Borole, A.P., Reguera, G., Ringeisen, B., Wang, Z.-W., Feng, Y., Kim, B.H. 2011. Electroactive biofilms: Current status and future research needs. *Energy & Environmental Science*, **4**(12), 4813-4834.

Bouzas, A., Gabaldon, C., Marzal, P., Penya-Roja, J.M., Seco, A. 2002. Fermentation of municipal primary sludge: Effect of SRT and solids concentration on volatile fatty acid production. *Environmental Technology*, **23**(8), 863-875.

Bretschger, O., Obraztsova, A., Sturm, C.A., Chang, I.S., Gorby, Y.A., Reed, S.B., Culley, D.E., Reardon, C.L., Barua, S., Romine, M.F., Zhou, J., Beliaev, A.S., Bouhenni, R., Saffarini, D., Mansfeld, F., Kim, B.-H., Fredrickson, J.K., Nealson, K.H. 2007. Current production and metal oxide reduction by Shewanella oneidensis MR-1 wild type and mutants. *Applied and Environmental Microbiology*, **73**(21), 7003-7012.

Brown, R.E., Jarvis, K.L., Hyland, K.J. 1989. Protein measurement using bicinchoninic acid - Elimination of interfering substances. *Analytical Biochemistry*, **180**(1), 136-139.

Buswell, A.M.; Hatfield, W.D. 1936. Bulletin 32, Anaerobic Fermentations. Urbana, IL: State of Illinois Department of Registration and Education.

Caccavo, F., Lonergan, D.J., Lovley, D.R., Davis, M., Stolz, J.F., McInerney, M.J. 1994. Geobacter sulfurreducens sp-nov, a hydrogen-oxidizing and acetate-oxidizing dissimilatory metal-reducing microorganism. *Applied and Environmental Microbiology*, **60**(10), 3752-3759.

Cajthaml, T., Kresinova, Z., Svobodova, K., Sigler, K., Rezanka, T. 2009. Microbial transformation of synthetic estrogen 17 alpha-ethinylestradiol. *Environmental Pollution*, **157**(12), 3325-3335.

Campos-Martin, J.M., Blanco-Brieva, G., Fierro, J.L.G. 2006. Hydrogen peroxide synthesis: An outlook beyond the anthraquinone process. *Angewandte Chemie-International Edition*, **45**(42), 6962-6984.

Cao, Y., Pawlowski, A. 2012. Sewage sludge-to-energy approaches based on anaerobic digestion and pyrolysis: Brief overview and energy efficiency assessment. *Renewable & Sustainable Energy Reviews*, **16**(3), 1657-1665.

Caporaso, J.G., Kuczynski, J., Stombaugh, J., Bittinger, K., Bushman, F.D., Costello, E.K., Fierer, N., Pena, A.G., Goodrich, J.K., Gordon, J.I., Huttley, G.A., Kelley, S.T., Knights, D., Koenig, J.E., Ley, R.E., Lozupone, C.A., McDonald, D., Muegge, B.D., Pirrung, M., Reeder, J., Sevinsky, J.R., Tumbaugh, P.J., Walters, W.A., Widmann, J., Yatsunenko, T., Zaneveld, J., Knight, R. 2010. QIIME allows analysis of high-throughput community sequencing data. *Nature Methods*, **7**(5), 335-336.

Caporaso, J.G., Lauber, C.L., Walters, W.A., Berg-Lyons, D., Huntley, J., Fierer, N., Owens, S.M., Betley, J., Fraser, L., Bauer, M., Gormley, N., Gilbert, J.A., Smith, G., Knight, R. 2012. Ultra-high-throughput microbial community analysis on the Illumina HiSeq and MiSeq platforms. *Isme Journal*, **6**(8), 1621-1624.

Chae, K.-J., Choi, M.-J., Kim, K.-Y., Ajayi, F.F., Park, W., Kim, C.-W., Kim, I.S. 2010. Methanogenesis control by employing various environmental stress conditions in two-chambered microbial fuel cells. *Bioresource Technology*, **101**(14), 5350-5357.

Chandran, K. 2012. Shifting from Resource Removal to Resource Recovery. Special issue of Columbia Engineering Magazine. http://engineering.columbia.edu/web/newsletter/fall_2012/shifting_resource_removal_resource_recovery

Chaudhuri, S.K., Lovley, D.R. 2003. Electricity generation by direct oxidation of glucose in mediatorless microbial fuel cells. *Nature Biotechnology*, **21**(10), 1229-1232.

Chauzy, J., Cretenot, D., Bausseron, A. & Gokelaere, X. 2007. Thermal hydrolysis to increase sludge biodegradability or how to turn mesophilic anaerobic digestion of biological sludge into an attractive process. WEFTEC 2007, 80th Annual Water Environment Federation Technical Exhibition and Conference, San Diego, CA, October 13–17.

Chen, J. 2013. Recent Progress in Advanced Materials for Lithium Ion Batteries. *Materials*, **6**(1), 156-183.

Chen, J.-y., Li, N., Zhao, L. 2014. Three-dimensional electrode microbial fuel cell for hydrogen peroxide synthesis coupled to wastewater treatment. *Journal of Power Sources*, **254**, 316-322.

Chen, J.-Y., Zhao, L., Li, N., Liu, H. 2015. A microbial fuel cell with the three-dimensional electrode applied an external voltage for synthesis of hydrogen peroxide from organic matter. *Journal of Power Sources*, **287**, 291-296.

Cheng, S., Logan, B.E. 2011. Increasing power generation for scaling up single-chamber air cathode microbial fuel cells. *Bioresource Technology*, **102**(6), 4468-4473.

Cho, S.K., Shin, H.S., Kim, D.H. 2012. Waste activated sludge hydrolysis during ultrasonication: Two-step disintegration. *Bioresource Technology*, **121**, 480-483.

Choi, H., Jeong, S.W., Chung, Y.J. 2006. Enhanced anaerobic gas production of waste activated sludge pretreated by pulse power technique. *Bioresource Technology*, **97**(2), 198-203.

Choi, J., Ahn, Y. 2014. Increased power generation from primary sludge in microbial fuel cells coupled with prefermentation. *Bioprocess and Biosystems Engineering*, **37**(12), 2549-2557.

Choi, Y., Kim, N., Kim, S., Jung, S. 2003. Dynamic behaviors of redox mediators within the hydrophobic layers as an important factor for effective microbial fuel cell operation. *Bulletin of the Korean Chemical Society*, **24**(4), 437-440.

Cokgor, E.U., Oktay, S., Tas, D.O., Zengin, G.E., Orhon, D. 2009. Influence of pH and temperature on soluble substrate generation with primary sludge fermentation. *Bioresource Technology*, **100**(1), 380-386.

Cole, J.R., Wang, Q., Cardenas, E., Fish, J., Chai, B., Farris, R.J., Kulam-Syed-Mohideen, A.S., McGarrell, D.M., Marsh, T., Garrity, G.M., Tiedje, J.M. 2009. The Ribosomal Database Project: improved alignments and new tools for rRNA analysis. *Nucleic Acids Research*, **37**, D141-D145.

Conesa, A., van den Hondel, C., Punt, P.J. 2000. Studies on the production of fungal peroxidases in Aspergillus niger. *Applied and Environmental Microbiology*, **66**(7), 3016-3023.

Couper, A.M., Pletcher, D., Walsh, F.C. 1990. Electrode materials for electrosynthesis. *Chemical Reviews*, **90**(5), 837-865.

Couvert, A., Charron, I., Laplanche, A., Renner, C., Patria, L., Requieme, B. 2006. Treatment of odorous sulphur compounds by chemical scrubbing with hydrogen peroxide - Application to a laboratory plant. *Chemical Engineering Science*, **61**(22), 7240-7248.

Danino, D., Talmon, Y., Zana, R. 1995. Alkanediyl-alpha,omega-bis(dimethylalkylammonium bromide) surfactants (dimeric surfactants). 5. Aggregation and microstructure in aqueous-solutions. *Langmuir*, **11**(5), 1448-1456.

De Vrieze, J., Gildemyn, S., Arends, J.B.A., Vanwonterghem, I., Verbeken, K., Boon, N., Verstraete, W., Tyson, G.W., Hennebel, T., Rabaey, K. 2014. Biomass retention on electrodes rather than electrical current enhances stability in anaerobic digestion. *Water Research*, **54**, 211-221.

DeSantis, T.Z., Hugenholtz, P., Larsen, N., Rojas, M., Brodie, E.L., Keller, K., Huber, T., Dalevi, D., Hu, P., Andersen, G.L. 2006. Greengenes, a chimera-checked 16S rRNA gene database and workbench compatible with ARB. *Applied and Environmental Microbiology*, **72**(7), 5069-5072.

Ditzig, J., Liu, H., Logan, B.E. 2007. Production of hydrogen from domestic wastewater using a bioelectrochemically assisted microbial reactor (BEAMR). *International Journal of Hydrogen Energy*, **32**(13), 2296-2304.

Dubois, M., Gilles, K.A., Hamilton, J.K., Rebers, P.A., Smith, F. 1956. Colorimetric method for determination of sugars and related substances. *Analytical Chemistry*, **28**(3), 350-356.

Elbeshbishy, E., Nakhla, G., Hafez, H. 2012. Biochemical methane potential (BMP) of food waste and primary sludge: Influence of inoculum pre-incubation and inoculum source. *Bioresource Technology*, **110**, 18-25.

Eskicioglu, C., Kennedy, K.J., Droste, R.L. 2006. Characterization of soluble organic matter of waste activated sludge before and after thermal pretreatment. *Water Research*, **40**(20), 3725-3736.

Eurostat. 2013. http://epp.eurostat.ec.europa.eu/portal/page/portal/waste/introduction/

Ferreiro, N., Soto, M. 2003. Anaerobic hydrolysis of primary sludge: influence of sludge concentration and temperature. *Water Science and Technology*, **47**(12), 239-246.

Ferry J.G. 1993. Methanogenesis: Ecology, Physiology, Biochemistry, and Genetics. London: Chapman Hall.

Fornero, J.J., Rosenbaum, M., Cotta, M.A., Angenent, L.T. 2010. Carbon Dioxide Addition to Microbial Fuel Cell Cathodes Maintains Sustainable Catholyte pH and Improves Anolyte pH, Alkalinity, and Conductivity. *Environmental Science & Technology*, **44**(7), 2728-2734.

Frankel, R.B., Bazylinski, D.A. 2003. Biologically induced mineralization by bacteria. *Biomineralization*, **54**, 95-114.

Frost & Sullivan. 2011. Key opportunities in waste to energy plant market (technical insights).

Fu, L., You, S.-J., Yang, F.-l., Gao, M.-m., Fang, X.-h., Zhang, G.-q. 2010. Synthesis of hydrogen peroxide in microbial fuel cell. *Journal of Chemical Technology and Biotechnology*, **85**(5), 715-719.

Ge, Z., Zhang, F., Grimaud, J., Hurst, J., He, Z. 2013. Long-term investigation of microbial fuel cells treating primary sludge or digested sludge. *Bioresource Technology*, **136**, 509-514.

Ghosh, S. 1987. Improved sludge gasification by two-phase anaerobic digestion. *Journal of Environmental Engineering*, **113**,1265-1284.

Ghosh, S., Buoy, K., Dressel, L., Miller, T., Wilcox, G., Loos, D. 1995. PILOT-SCALE AND FULL-SCALE 2-PHASE ANAEROBIC-DIGESTION OF MUNICIPAL SLUDGE. *Water Environment Research*, **67**(2), 206-214.

Ghyoot, W., Verstraete, W. 1997. Anaerobic digestion of primary sludge from chemical pre-precipitation. *Water Science and Technology*, **36**(6-7), 357-365.

Graf, E., Penniston, J.T. 1980. Method for determination of hydrogen-peroxide, with its application illustrated by glucose assay. *Clinical Chemistry*, **26**(5), 658-660.

Güler, E. 2014. Anion exchange membrane design for reverse electrodialysis.

Harnisch, F., Schroeder, U. 2010. From MFC to MXC: chemical and biological cathodes and their potential for microbial bioelectrochemical systems. *Chemical Society Reviews*, **39**(11), 4433-4448.

Haug, R.T., Stuckey, D.C., Gossett, J.M., Mccarty, P.L. 1978. Effect of thermal pretreatment on digestibility and dewaterability of organic sludges. *Journal of Water Pollution Control Federation*, **50**(1), 73-85.

Hegar, S.F. High strength wastewater literature review. http://standards.nsf.org/apps/group_public/download.php/27220/Heger_HSW_literature%20review.pdf.

Heidrich, E.S., Dolfing, J., Scott, K., Edwards, S.R., Jones, C., Curtis, T.P. 2013. Production of hydrogen from domestic wastewater in a pilot-scale microbial electrolysis cell. *Applied Microbiology and Biotechnology*, **97**(15), 6979-6989.

Hernandez, M.E., Newman, D.K. 2001. Extracellular electron transfer. *Cellular and Molecular Life Sciences*, **58**(11), 1562-1571.

Higson, F.K. 1991. Degradation of xenobiotics by white rot fungi. *Reviews of Environmental Contamination and Toxicology*, **122**, 111-152.

Hobson, J., Yang, G. 2000. The ability of selected chemicals for suppressing odour development in rising mains. *Water Science and Technology*, **41**(6), 165-173.

Holmes, D.E., Bond, D.R., Lovley, D.R. 2004. Electron transfer by Desulfobulbus propionicus to Fe(III) and graphite electrodes. *Applied and Environmental Microbiology*, **70**(2), 1234-1237.

Holmes, D.E., Nicoll, J.S., Bond, D.R., Lovley, D.R. 2009. Potential Role of a Novel Psychrotolerant Member of the Family Geobacteraceae, Geopsychrobacter electrodiphilus gen. nov., sp. nov., in Electricity Production by a Marine Sediment Fuel Cell (vol 70, pg 6023, 2004). *Applied and Environmental Microbiology*, **75**(3), 885-885.

Hoskins, D.L., Zhang, X., Hickner, M.A., Logan, B.E. 2014. Spray-on polyvinyl alcohol separators and impact on power production in air-cathode microbial fuel cells with different solution conductivities. *Bioresource Technology*, **172**, 156-161.

Hu, H., Fan, Y., Liu, H. 2009. Hydrogen production in single-chamber tubular microbial electrolysis cells using non-precious-metal catalysts. *International Journal of Hydrogen Energy*, **34**(20), 8535-8542.

Hu, H., Fan, Y., Liu, H. 2010. Optimization of NiMo catalyst for hydrogen production in microbial electrolysis cells. *International Journal of Hydrogen Energy*, **35**(8), 3227-3233.

Jantrania, A. 1991. Dealing with Oil and Grease in Restaurant Wastewater, Small Flows Journal, Vol. 5 (1), January.

Jayaraman, A., Mansfeld, F.B., Wood, T.K. 1999. Inhibiting sulfate-reducing bacteria in biofilms by expressing the antimicrobial peptides indolicidin and bactenecin. *Journal of Industrial Microbiology & Biotechnology*, **22**(3), 167-175.

Jeremiasse, A.W., Hamelers, H.V.M., Saakes, M., Buisman, C.J.N. 2010. Ni foam cathode enables high volumetric H(2) production in a microbial electrolysis cell. *International Journal of Hydrogen Energy*, **35**(23), 12716-12723.

Jia, J., Tang, Y., Liu, B., Wu, D., Ren, N., Xing, D. 2013. Electricity generation from food wastes and microbial community structure in microbial fuel cells. *Bioresource Technology*, **144**, 94-99.

Jones, R., Parker, W., Khan, Z., Murthy, S., Rupke, M. 2008. Characterization of sludges for predicting anaerobic digester performance. *Water Science and Technology*, **57**(5), 721-726.

Karam, J., Nicell, J.A. 1997. Potential applications of enzymes in waste treatment. *Journal of Chemical Technology and Biotechnology*, **69**(2), 141-153.

Kern, F., Lequeux, F., Zana, R., Candau, S.J. 1994. Dynamic Properties of Salt-Free Viscoelastic Micellar Solutions. *Langmuir*, **10**, 1714.

Kersten, P.J., Kalyanaraman, B., Hammel, K.E., Reinhammar, B., Kirk, T.K. 1990. Comparison of lignin peroxidase, horseradish-peroxidase and laccase in the oxidation of methoxybenzenes. *Biochemical Journal*, **268**(2), 475-480.

Khanal, S.K., Grewell, D., Sung, S., Van Leeuwen, J. 2007. Ultrasound applications in wastewater sludge pretreatment: A review. *Critical Reviews in Environmental Science and Technology*, **37**(4), 277-313.

Ki, D., Parameswaran, P., Popat, S.C., Rittmann, B.E., Torres, C.I. 2015a. Effects of pre-fermentation and pulsed-electric-field treatment of primary sludge in microbial electrochemical cells. *Bioresource Technology*, **195**, 83-88.

Ki, D., Parameswaran, P., Rittmann, B.E., Torres, C.I. 2015b. Effect of pulsed electric field (PEF) pretreatment on primary sludge for enhanced bioavailability and energy capture. *Environmental Engineering Science*, **32**, 831-837.

Ki, D., Park, J., Lee, J., Yoo, K. 2008. Microbial diversity and population dynamics of activated sludge microbial communities participating in electricity generation in microbial fuel cells. *Water Science and Technology*, **58**(11), 2195-2201.

Ki, D., Popat, S.C., Torres, C.I. 2016. Reduced overpotentials in microbial electrolysis cells through improved design, operation, and electrochemical characterization. *Chemical Engineering Journal*, **287**, 181-188.

Kiely, P.D., Rader, G., Regan, J.M., Logan, B.E. 2011. Long-term cathode performance and the microbial communities that develop in microbial fuel cells fed different fermentation endproducts. *Bioresource Technology*, **102**(1), 361-366.

Kim, B.H., Kim, H.J., Hyun, M.S., Park, D.H. 1999. Direct electrode reaction of Fe(III)-reducing bacterium, Shewanella putrefaciens. *Journal of Microbiology and Biotechnology*, **9**(2), 127-131.

Kim, J., Park, C., Kim, T.H., Lee, M., Kim, S., Kim, S.W., Lee, J. 2003. Effects of various pretreatments for enhanced anaerobic digestion with waste activated sludge. *Journal of Bioscience and Bioengineering*, **95**(3), 271-275.

Kim, K.K., Jin, L., Yang, H.C., Lee, S.-T. 2007a. Halomonas gomseomensis sp nov, Halomonas janggokensis sp nov, Halomonas salaria sp nov and Halomonas denitrificans sp nov, moderately halophilic bacteria isolated from saline water. *International Journal of Systematic and Evolutionary Microbiology*, **57**, 675-681.

Kim, T.-H., Kim, T.-H., Yu, S., Nam, Y.K., Choi, D.-K., Lee, S.R., Lee, M.-J. 2007b. Solubilization of waste activated sludge with alkaline treatment and gamma ray irradiation. *Journal of Industrial and Engineering Chemistry*, **13**(7), 1149-1153.

Kim, T.-H., Lee, S.-R., Nam, Y.-K., Yang, J., Park, C., Lee, M. 2009. Disintegration of excess activated sludge by hydrogen peroxide oxidation. *Desalination*, **246**(1-3), 275-284.

Kirk, T.K., Farrell, R.L. 1987. Enzymatic combustion - the microbial-degradation of lignin. *Annual Review of Microbiology*, **41**, 465-505.

Koch, C., Kuchenbuch, A., Kretzschmar, J., Wedwitschka, H., Liebetrau, J., Mueller, S., Harnisch, F. 2015. Coupling electric energy and biogas production in anaerobic digesters - impacts on the microbiome. *Rsc Advances*, **5**(40), 31329-31340.

Koners U. H.; Toepfl, S.; Heinz, V.; Camacho, P.; Ginestet, P.; Knorr, D. 2004. Application of Pulsed Electric Field Treatment for Sludge Reduction on Wastewater Treatment Plants. Proceedings of the 2nd European Pulsed Power Symposium (EPPS); International Society on Pulsed Power Applications e.V.: Gelsenkirchen, Germany.

Kopplow, O., Barjenbruch, M., Heinz, V. 2004. Sludge pre-treatment with pulsed electric fields. *Water Science and Technology*, **49**(10), 123-129.

Krstajic, N.V., Gajic-Krstajic, L., Lacnjevac, U., Jovic, B.M., Mora, S., Jovic, V.D. 2011. Non-noble metal composite cathodes for hydrogen evolution. Part I: The Ni-MoOx coatings electrodeposited from Watt's type bath containing MoO3 powder particles. *International Journal of Hydrogen Energy*, **36**(11), 6441-6449.

Lai, Y.S., Parameswaran, P., Li, A., Aguinaga, A., Rittmannl, B.E. 2016. Selective Fermentation of Carbohydrate and Protein Fractions of Scenedesmus, and Biohydrogenation of its Lipid Fraction for Enhanced Recovery of Saturated Fatty Acids. *Biotechnology and Bioengineering*, **113**(2), 320-329.

Lai, Y.S., Parameswaran, P., Li, A., Baez, M., Rittmann, B.E. 2014. Effects of pulsed electric field treatment on enhancing lipid recovery from the microalga, Scenedesmus. *Bioresource Technology*, **173**, 457-461.

Lalaurette, E., Thammannagowda, S., Mohagheghi, A., Maness, P.C., Logan, B.E. 2009. Hydrogen production from cellulose in a two-stage process combining fermentation and electrohydrogenesis. *International Journal of Hydrogen Energy*, **34**(15), 6201-6210.

Lee, H.H.B., Park, A.-H., Oloman, C. 2000. Stability of hydrogen peroxide in sodium carbonate solutions. *TAPPI Journal*, **83**(8), 94-101.

Lee, H.-S., Parameswaran, P., Kato-Marcus, A., Torres, C.I., Rittmann, B.E. 2008. Evaluation of energy-conversion efficiencies in microbial fuel cells (MFCs) utilizing fermentable and non-fermentable substrates. *Water Research*, **42**(6-7).

Lee, H.-S., Rittmann, B.E. 2010. Characterization of energy losses in an upflow single-chamber microbial electrolysis cell. *International Journal of Hydrogen Energy*, **35**(3), 920-927.

Lee, H.-S., Torres, C.I., Parameswaran, P., Rittmann, B.E. 2009. Fate of H-2 in an Upflow Single-Chamber Microbial Electrolysis Cell Using a Metal-Catalyst-Free Cathode. *Environmental Science & Technology*, **43**(20).

Lee, H.-S., Vermaas, W.F.J., Rittmann, B.E. 2010a. Biological hydrogen production: prospects and challenges. *Trends in Biotechnology*, **28**(5), 262-271.

Lee, I.S., Parameswaran, P., Alder, J.M., Rittmann, B.E. 2010b. Feasibility of Focused-Pulsed Treated Waste Activated Sludge as a Supplemental Electron Donor for Denitrification. *Water Environment Research*, **82**(12), 2316-2324.

Lee, I.S., Rittmann, B.E. 2011. Effect of low solids retention time and focused pulsed pre-treatment on anaerobic digestion of waste activated sludge. *Bioresource Technology*, **102**(3), 2542-2548.

Lee, S.A., Choi, Y., Jung, S.H., Kim, S. 2002. Effect of initial carbon sources on the electrochemical detection of glucose by Gluconobacter oxydans. *Bioelectrochemistry*, **57**(2), 173-178.

Li, H., Jin, Y., Mahar, R., Wang, Z., Nie, Y. 2008. Effects and model of alkaline waste activated sludge treatment. *Bioresource Technology*, **99**(11), 5140-5144.

Li, N., An, J., Zhou, L., Li, T., Li, J., Feng, C., Wang, X. 2016. A novel carbon black graphite hybrid air-cathode for efficient hydrogen peroxide production in bioelectrochemical systems. *Journal of Power Sources*, **306**, 495-502.

Li, W.-W., Yu, H.-Q., Rittmann, B.E. 2015. Reuse water pollutants. *Nature*, **528**(7580), 29-31.

Lim, S.Y., Lim, K.M., Yoo, S.H. 2014. External benefits of waste-to-energy in Korea: A choice experiment study. *Renewable & Sustainable Energy Reviews*, **34**, 588-595.

Liu, H., Cheng, S.A., Logan, B.E. 2005. Production of electricity from acetate or butyrate using a single-chamber microbial fuel cell. *Environmental Science & Technology*, **39**(2), 658-662.

Liu, H., Logan, B.E. 2004. Electricity generation using an air-cathode single chamber microbial fuel cell in the presence and absence of a proton exchange membrane. *Environmental Science & Technology*, **38**(14), 4040-4046.

Liu, H., Ramnarayanan, R., Logan, B.E. 2004. Production of electricity during wastewater treatment using a single chamber microbial fuel cell. *Environmental Science & Technology*, **38**(7), 2281-2285.

Liu, H.H., H.Chignell, J.Fan Y. 2010. Microbial electrolysis: novel technology for hydrogen production from biomass. *Biofuels*, **1**, 129-142.

Liu, J., Zhang, F., He, W., Yang, L., Feng, Y., Logan, B.E. 2014. A microbial fluidized electrode electrolysis cell (MFEEC) for enhanced hydrogen production. *Journal of Power Sources*, **271**, 530-533.

Loeffler, M.; Schmidt, W.; Schuhmann, R.; Rottering, A.; Neumann, J.; Dreesen, C. 2001. Treatment of Sewage Sludge with Pulsed Electric Fields. Proceedings of the International Conference on Pulsed Power Applications, Number B.04, March 27–29, Gelsenkirchen, Germany; International Society on Pulsed Power Applications e.V.: Gelsenkirchen, Germany.

Logan, B.E. 2009. Exoelectrogenic bacteria that power microbial fuel cells. *Nature Reviews Microbiology*, **7**(5), 375-381.

Logan, B.E., Hamelers, B., Rozendal, R.A., Schrorder, U., Keller, J., Freguia, S., Aelterman, P., Verstraete, W., Rabaey, K. 2006. Microbial fuel cells: Methodology and technology. *Environmental Science & Technology*, **40**(17), 5181-5192.

Lovley, D.R., Nevin, K.P. 2013. Electrobiocommodities: powering microbial production of fuels and commodity chemicals from carbon dioxide with electricity. *Current Opinion in Biotechnology*, **24**(3), 385-390.

Lovley, D.R., Phillips, E.J.P. 1986. Organic-matter mineralization with reduction of ferric iron in anaerobic sediments. *Applied and Environmental Microbiology*, **51**(4), 683-689.

Lovley, D.R., Ueki, T., Zhang, T., Malvankar, N.S., Shrestha, P.M., Flanagan, K.A., Aklujkar, M., Butler, J.E., Giloteaux, L., Rotaru, A.-E., Holmes, D.E., Franks, A.E., Orellana, R., Risso, C., Nevin, K.P. 2011. Geobacter: The Microbe Electric's Physiology, Ecology, and Practical Applications. *Advances in Microbial Physiology, Vol 59*, **59**, 1-100.

Lowe, K.S., N. Rothe, J. Tomaras, K. DeJong, M. Tucholke, J. Drewes, J. McCray, and J. Munakata-Marr. 2007. Influent Constituent Characteristics of the Modern Waste Stream from Single Sources: Literature Review. Water Environment Research Foundation. 04-DEC-1. PDF available at: www.ndwrcdp.org/publications.

Lukicheva, I., Pagilla, K., Rohloff, G., Kunetz, T. 2009. To Do Class A or Not? What To Do To Enhance Sludge Processing? WEFTEC, Session 21-30, pp. 1256-1273.

Madigan, M. T., Martinko, J. M. & Parker, J. 2003. Brock Biology of Microorganisms. Prentice Hall, Upper Saddle River, NJ.

Mahmoud, M., Parameswaran, P., Torres, C.I., Rittmann, B.E. 2014. Fermentation pre-treatment of landfill leachate for enhanced electron recovery in a microbial electrolysis cell. *Bioresource Technology*, **151**, 151-158.

Malvankar, N.S., Vargas, M., Nevin, K.P., Franks, A.E., Leang, C., Kim, B.-C., Inoue, K., Mester, T., Covalla, S.F., Johnson, J.P., Rotello, V.M., Tuominen, M.T., Lovley, D.R. 2011. Tunable metallic-like conductivity in microbial nanowire networks. *Nature Nanotechnology*, **6**(9), 573-579.

Matejcek, B., S. Erlsten, and Bloomquist, D. 2000. Determination of Properties and Long Term Acceptance Rate of Effluents from Food Service Establishments that Employ Onsite Sewage Treatment, Department of Environmental Engineering Sciences and Civil & Coastal Engineering, University of Florida.

Mavropoulos, A. 2012. International Scenario in Waste and e-Waste Management, D-waste.

McCabe, J; Eckenfelder, W. eds. 1958. Biological Treatment of Sewage and Industrial Wastes. Two volumes. New York, Reinbold Publishing.

McCarty, P.L., Bae, J., Kim, J. 2011. Domestic Wastewater Treatment as a Net Energy Producer-Can This be Achieved? *Environmental Science & Technology*, **45**(17), 7100-7106.

McCarty, P.L., Smith, D.P. 1986. Anaerobic wastewater treatment. *Environmental Science & Technology*, **20**(12), 1200-1206.

McInerney, M.J., Bryant, M.P., Hespell, R.B., Costerton, J.W. 1981. Syntrophomonas-wolfei gen-nov sp-nov, an anaerobic, syntrophic, fatty-acid oxidizing bacterium. *Applied and Environmental Microbiology*, **41**(4), 1029-1039.

McInerney, M.J., Bryant, M.P., Pfennig, N. 1979. Anaerobic bacterium that degrades fatty-acids in syntrophic association with methanogens. *Archives of Microbiology*, **122**(2), 129-135.

McInerney, M.J., Hoehler, H., Gunsalus, R.P., Schink, B. 2010. Introduction to microbial hydrocarbon production: bioenergetics. In: Kenneth N. Timmis (Ed.), Handbook of Hydrocarbon and Lipid Microbiology. Springer Berlin Heidelberg, pp. 319-335.

McLean, G.F., Niet, T., Prince-Richard, S., Djilali, N. 2002. An assessment of alkaline fuel cell technology. *International Journal of Hydrogen Energy*, **27**(5), 507-526.

Metcalf & Eddy, I., Tchobanoglous, G., Burton, F.L., Stensel, H.D. 2003 *Wastewater Engineering: Treatment and Reuse. 4th ed. ed.* McGraw-Hill, Boston.

Meynell, P-J. 1976. Methane: Planning a Digester. New York: Schocken Books. pp. 3.

Miceli, J.F., III, Parameswaran, P., Kang, D.-W., Krajmalnik-Brown, R., Torres, C.I. 2012. Enrichment and Analysis of Anode-Respiring Bacteria from Diverse Anaerobic Inocula. *Environmental Science & Technology*, **46**(18).

Min, S., Evrendilek, G.A., Zhang, H.Q. 2007. Pulsed electric fields: Processing system, microbial and enzyme inhibition, and shelf life extension of foods. *Ieee Transactions on Plasma Science*, **35**(1), 59-73.

Miron, Y., Zeeman, G., Van Lier, J.B., Lettinga, G. 2000. The role of sludge retention time in the hydrolysis and acidification of lipids, carbohydrates and proteins during digestion of primary sludge in CSTR systems. *Water Research*, **34**(5), 1705-1713.

Modin, O., Fukushi, K. 2012. Development and testing of bioelectrochemical reactors converting wastewater organics into hydrogen peroxide. *Water Science and Technology*, **66**(4), 831-836.

Modin, O., Fukushi, K. 2013. Production of high concentrations of H2O2 in a bioelectrochemical reactor fed with real municipal wastewater. *Environmental Technology*, **34**(19), 2737-2742.

Nakayama, T., Amachi, T. 1999. Fungal peroxidase: its structure, function, and application. *Journal of Molecular Catalysis B-Enzymatic*, **6**(3), 185-198.

Nam, J.-Y., Logan, B.E. 2012. Optimization of catholyte concentration and anolyte pHs in two chamber microbial electrolysis cells. *International Journal of Hydrogen Energy*, **37**(24), 18622-18628.

Nemati, M., Mazutinec, T.J., Jenneman, G.E., Voordouw, G. 2001. Control of biogenic H2S production with nitrite and molybdate. *Journal of Industrial Microbiology & Biotechnology*, **26**(6), 350-355.

Nevin, K.P., Hensley, S.A., Franks, A.E., Summers, Z.M., Ou, J., Woodard, T.L., Snoeyenbos-West, O.L., Lovley, D.R. 2011. Electrosynthesis of Organic Compounds from Carbon Dioxide Is Catalyzed by a Diversity of Acetogenic Microorganisms. *Applied and Environmental Microbiology*, **77**(9), 2882-2886.

Nickel, K., Neis, U. 2007. Ultrasonic disintegration of biosolids for improved biodegradation. *Ultrasonics Sonochemistry*, **14**(4), 450-455.

Oh, S.E., Logan, B.E. 2005. Hydrogen and electricity production from a food processing wastewater using fermentation and microbial fuel cell technologies. *Water Research*, **39**(19), 4673-4682.

Otsuka, K., Yamanaka, I. 1998. Electrochemical cells as reactors for selective oxygenation of hydrocarbons at low temperature. *Catalysis Today*, **41**(4), 311-325.

Otsuka, K., Yamanaka, I. 1990. One-step synthesis of hydrogen-peroxide through fuel-cell reaction. *Electrochimica Acta*, **35**(2), 319-322.

Owen, W.F., Stuckey, D.C., Healy, J.B., Young, L.Y., McCarty, P.L. 1979. Bioassay for monitoring biochemical methane potential and anaerobic toxicity. *Water Research*, **13**(6), 485-492.

O'Hayre, R.C., S.W. Colella, W. Prinz, F.B. 2006. *Fuel Cell Fundamentals*. Wiley, New York.

Parameswaran, P., Torres, C.I., Lee, H.S., Krajmalnik-Brown, R., Rittmann, B.E. 2009. Syntrophic Interactions Among Anode Respiring Bacteria (ARB) and Non-ARB in a Biofilm Anode: Electron Balances. *Biotechnology and Bioengineering*, **103**(3), 513-523.

Parameswaran, P., Torres, C.I., Lee, H.S., Rittmann, B.E., Krajmalnik-Brown, R. 2011. Hydrogen consumption in microbial electrochemical systems (MXCs): The role of homo-acetogenic bacteria. *Bioresource Technology*, **102**(1), 263-271.

Park, B., Ahn, J.H., Kim, J., Hwang, S. 2004. Use of microwave pretreatment for enhanced anaerobiosis of secondary sludge. *Water Science and Technology*, **50**(9), 17-23.

Park, D.H., Kim, B.H., Moore, B., Hill, H.A.O., Song, M.K., Rhee, H.W. 1997. Electrode reaction of Desulfovibrio desulfuricans modified with organic conductive compounds. *Biotechnology Techniques*, **11**(3), 145-148.

Park, D.H., Zeikus, J.G. 1999. Utilization of electrically reduced neutral red by Actinobacillus succinogenes: Physiological function of neutral red in membrane-driven fumarate reduction and energy conservation. *Journal of Bacteriology*, **181**(8), 2403-2410.

Park, H.S., Kim, B.H., Kim, H.S., Kim, H.J., Kim, G.T., Kim, M., Chang, I.S., Park, Y.K., Chang, H.I. 2001. A novel electrochemically active and Fe(III)-reducing bacterium phylogenetically related to Clostridium butyricum isolated from a microbial fuel cell. *Anaerobe*, **7**(6), 297-306.

Pavlostathis, S.G., Giraldogomez, E. 1991. Kinetics of anaerobic treatment - a critical-review. *Critical Reviews in Environmental Control*, **21**(5-6), 411-490.

Pham, C.A., Jung, S.J., Phung, N.T., Lee, J., Chang, I.S., Kim, B.H., Yi, H., Chun, J. 2003. A novel electrochemically active and Fe(III)-reducing bacterium phylogenetically related to Aeromonas hydrophila, isolated from a microbial fuel cell. *Fems Microbiology Letters*, **223**(1), 129-134.

Pham, T.H., Boon, N., Aelterman, P., Clauwaert, P., De Schamphelaire, L., Vanhaecke, L., De Maeyer, K., Hoefte, M., Verstraete, W., Rabaey, K. 2008. Metabolites produced by Pseudomonas sp enable a Gram-positive bacterium to achieve extracellular electron transfer. *Applied Microbiology and Biotechnology*, **77**(5), 1119-1129.

Pham, T.H., Rabaey, K., Aelterman, P., Clauwaert, P., De Schamphelaire, L., Boon, N., Verstraete, W. 2006. Microbial fuel cells in relation to conventional anaerobic digestion technology. *Engineering in Life Sciences*, **6**(3), 285-292.

Pickworth, B., Cranshaw, I., Abraham, K., Coleman, P., Walley, P. & Solheim, O. E. 2005. Large scale reality of sewage sludge pasteurisation and thermal hydrolysis. WEFTEC 2005, 78th Annual Water Environment Federation Technical Exhibition and Conference, Washington, DC, October 29–November 2.

Pilli, S., Bhunia, P., Yan, S., LeBlanc, R.J., Tyagi, R.D., Surampalli, R.Y. 2011. Ultrasonic pretreatment of sludge: A review. *Ultrasonics Sonochemistry*, **18**(1), 1-18.

Pirbadian, S., El-Naggar, M.Y. 2012. Multistep hopping and extracellular charge transfer in microbial redox chains. *Physical Chemistry Chemical Physics*, **14**(40), 13802-13808.

Pletcher, D. 1999. Indirect oxidations using electrogenerated hydrogen peroxide. *Acta Chemica Scandinavica*, **53**(10), 745-750.

Popat, S.C., Ki, D., Rittmann, B.E., Torres, C.I. 2012. Importance of OH- Transport from Cathodes in Microbial Fuel Cells. *Chemsuschem*, **5**(6).

Popat, S.C., Torres, C.I. 2016. As fast as an electron: Critical transport rates that limit the performance of microbial electrochemistry technologies. *Bioresource Technology*. Submitted.

Prasad, D., Arun, S., Murugesan, A., Padmanaban, S., Satyanarayanan, R.S., Berchmans, S., Yegnaraman, V. 2007. Direct electron transfer with yeast cells and construction of a mediatorless microbial fuel cell. *Biosensors & Bioelectronics*, **22**(11), 2604-2610.

Pratt, S., Liew, D., Batstone, D.J., Werker, A.G., Morgan-Sagastume, F., Lant, P.A. 2012. Inhibition by fatty acids during fermentation of pre-treated waste activated sludge. *Journal of Biotechnology*, **159**(1-2), 38-43.

Rabaey, K., Angenent, L.T., Schröder, U., Keller, J. 2010. Bioelectrochemical Systems: from extracellular electron transfer to biotechnological application, International Water Association London, UK.

Rabaey, K., Boon, N., Siciliano, S.D., Verhaege, M., Verstraete, W. 2004. Biofuel cells select for microbial consortia that self-mediate electron transfer. *Applied and Environmental Microbiology*, **70**(9), 5373-5382.

Rabaey, K., Butzer, S., Brown, S., Keller, J., Rozendal, R.A. 2010. High Current Generation Coupled to Caustic Production Using a Lamellar Bioelectrochemical System. *Environmental Science & Technology*, **44**(11), 4315-4321.

Rabaey, K., Clauwaert, P., Aelterman, P., Verstraete, W. 2005. Tubular microbial fuel cells for efficient electricity generation. *Environmental Science & Technology*, **39**(20), 8077-8082.

Rabaey, K., Rozendal, R.A. 2010. Microbial electrosynthesis - revisiting the electrical route for microbial production. *Nature Reviews Microbiology*, **8**(10), 706-716.

Raposo, F., Banks, C.J., Siegert, I., Heaven, S., Borja, R. 2006. Influence of inoculum to substrate ratio on the biochemical methane potential of maize in batch tests. *Process Biochemistry*, **41**(6), 1444-1450.

Rhoads, A., Beyenal, H., Lewandowski, Z. 2005. Microbial fuel cell using anaerobic respiration as an anodic reaction and biomineralized manganese as a cathodic reactant. *Environmental Science & Technology*, **39**(12), 4666-4671.

Ringeisen, B.R., Ray, R., Little, B. 2007. A miniature microbial fuel cell operating with an aerobic anode chamber. *Journal of Power Sources*, **165**(2), 591-597.

Rismani-Yazdi, H., Carver, S.M., Christy, A.D., Yu, Z., Bibby, K., Peccia, J., Tuovinen, O.H. 2013. Suppression of methanogenesis in cellulose-fed microbial fuel cells in relation to performance, metabolite formation, and microbial population. *Bioresource Technology*, **129**, 281-288.

Ristow, N.E., Sotemann, S.W., Wentzel, M.C., Loewenthal, R.E., Ekama, G.A. 2005. Hydrolysis of Primary Sewage Sludge under Methanogenic , Acidogenic and Sulfate-reducing Conditions, Water Research Commission Report No. 1216/1/05.

Rittmann, B.E., Lee, H.S., Zhang, H.S., Alder, J., Banaszak, J.E., Lopez, R. 2008a. Full-scale application of focused-pulsed pre-treatment for improving biosolids digestion and conversion to methane. *Water Science and Technology*, **58**(10), 1895-1901.

Rittmann, B.E., McCarty, P.L. 2001. *Environmental Biotechnology: Principles and Applications*. McGraw-Hill, New York.

Rittmann, B.E., Torres, C.I., Marcus, A.K. 2008b. Understanding the Distinguishing Features of a Microbial Fuel Cell as a Biomass-Based Renewable Energy Technology. *Emerging Environmental Technologies*, 1-28.

Rosenbaum, M., Agler, M.T., Fornero, J.J. Venkataraman, A., Angenent, L.T. 2010. Integrating BES in the wastewater and sludge treatment line, In: Korneel Rabaey, Largus Angenent, Uwe Schröder and Jürg Keller (Ed.), Bioelectrochemical Systems: From Extracellular Electron Transfer to Biotechnological Application. IWA Publishing, London, UK, pp. 393-408.

Rozendal, R.A., Hamelers, H.V.M., Euverink, G.J.W., Metz, S.J., Buisman, C.J.N. 2006. Principle and perspectives of hydrogen production through biocatalyzed electrolysis. *International Journal of Hydrogen Energy*, **31**(12), 1632-1640.

Rozendal, R.A., Hamelers, H.V.M., Rabaey, K., Keller, J., Buisman, C.J.N. 2008a. Towards practical implementation of bioelectrochemical wastewater treatment. *Trends in Biotechnology*, **26**(8), 450-459.

Rozendal, R.A., Leone, E., Keller, J., Rabaey, K. 2009. Efficient hydrogen peroxide generation from organic matter in a bioelectrochemical system. *Electrochemistry Communications*, **11**(9), 1752-1755.

Rozendal, R.A., Sleutels, T.H.J.A., Hamelers, H.V.M., Buisman, C.J.N. 2008b. Effect of the type of ion exchange membrane on performance, ion transport, and pH in biocatalyzed electrolysis of wastewater. *Water Science and Technology*, **57**(11), 1757-1762.

Rulkens, W. 2008. Sewage sludge as a biomass resource for the production of energy: Overview and assessment of the various options. *Energy & Fuels*, **22**(1), 9-15.

Salerno, M.B., Lee, H.S., Parameswaran, P., Rittmann, B.E. 2009. Using a Pulsed Electric Field as a Pretreatment for Improved Biosolids Digestion and Methanogenesis. *Water Environment Research*, **81**(8), 831-839.

Sasaki, K., Hirano, S.-i., Morita, M., Sasaki, D., Matsumoto, N., Ohmura, N., Igarashi, Y. 2011. Bioelectrochemical system accelerates microbial growth and degradation of filter paper. *Applied Microbiology and Biotechnology*, **89**(2), 449-455.

Sasaki, K., Sasaki, D., Morita, M., Hirano, S.-i., Matsumoto, N., Ohmura, N., Igarashi, Y. 2010. Bioelectrochemical system stabilizes methane fermentation from garbage slurry. *Bioresource Technology*, **101**(10), 3415-3422.

Schleheck, D., Weiss, M., Pitluck, S., Bruce, D., Land, M.L., Han, S., Saunders, E., Tapia, R., Detter, C., Brettin, T., Han, J., Woyke, T., Goodwin, L., Pennacchio, L., Nolan, M., Cook, A.M., Kjelleberg, S., Thomas, T. 2011. Complete genome sequence of Parvibaculum lavamentivorans type strain (DS-1(T)). *Standards in Genomic Sciences*, **5**(3), 298-310.

Schroder, U., Niessen, J., Scholz, F. 2003. A generation of microbial fuel cells with current outputs boosted by more than one order of magnitude. *Angewandte Chemie-International Edition*, **42**(25), 2880-2883.

Selembo, P.A., Merrill, M.D., Logan, B.E. 2010. Hydrogen production with nickel powder cathode catalysts in microbial electrolysis cells. *International Journal of Hydrogen Energy*, **35**(2), 428-437.

Sheng, J., Vannela, R., Rittmann, B.E. 2011. Evaluation of Cell-Disruption Effects of Pulsed-Electric-Field Treatment of Synechocystis PCC 6803. *Environmental Science & Technology*, **45**(8), 3795-3802.

Shizas, I., Bagley, D.M. 2004. Experimental determination of energy content of unknown organics in municipal wastewater streams. *Journal of Energy Engineering-Asce*, **130**(2), 45-53.

Siegrist, R.D., Anderson, D.L., and J.C. Converse. 1984. Commercial Wastewater On-Site Treatment and Disposal, ASAE On-Site Wastewater Treatment Proceedings, December, pp. 210–219. St. Joseph, Michigan.

Sim, J., An, J., Elbeshbishy, E., Ryu, H., Lee, H.-S. 2015. Characterization and optimization of cathodic conditions for H2O2 synthesis in microbial electrochemical cells. *Bioresource Technology*, **195**, 31-36.

Sleutels, T.H.J.A., Hamelers, H.V.M., Rozendal, R.A., Buisman, C.J.N. 2009a. Ion transport resistance in Microbial Electrolysis Cells with anion and cation exchange membranes. *International Journal of Hydrogen Energy*, **34**(9), 3612-3620.

Sleutels, T.H.J.A., Lodder, R., Hamelers, H.V.M., Buisman, C.J.N. 2009b. Improved performance of porous bio-anodes in microbial electrolysis cells by enhancing mass and charge transport. *International Journal of Hydrogen Energy*, **34**(24), 9655-9661.

Sleutels, T.H.J.A., Ter Heijne, A., Buisman, C.J.N., Hamelers, H.V.M. 2013. Steady-state performance and chemical efficiency of Microbial Electrolysis Cells. *International Journal of Hydrogen Energy*, **38**(18), 7201-7208.

Sorokin, D.Y., Tourova, T.P., Mussmann, M., Muyzer, G. 2008. Dethiobacter alkaliphilus gen. nov sp nov., and Desulfurivibrio alkaliphilus gen. nov sp nov.: two novel representatives of reductive sulfur cycle from soda lakes. *Extremophiles*, **12**(3), 431-439.

Spinosa, L., Vesilind, P.A. 2001. *Sludge Into Biosolids: Processing, Disposal, Utilization*. IWA Publishing.

Stadie, M. 2015. A sustainable approach to wastewater treatment using microbial fuel cells with peroxide production. Barrett, the Honors College Honors Thesis, Arizona State University.

Stryer, L. 1988. Biochemistry. W.H. Freeman and Company, New York, USA.

Sun, D., Call, D.F., Kiely, P.D., Wang, A., Logan, B.E. 2012. Syntrophic interactions improve power production in formic acid fed MFCs operated with set anode potentials or fixed resistances. *Biotechnology and Bioengineering*, **109**(2), 405-414.

Tartakousky, B., Mehta, P., Santoyo, G., Guiot, S.R. 2011. Maximizing hydrogen production in a microbial electrolysis cell by real-time optimization of applied voltage. *International Journal of Hydrogen Energy*, **36**(17), 10557-10564.

Tartakovsky, B., Guiot, S.R. 1997. Modeling and analysis of layered stationary anaerobic granular biofilms. *Biotechnology and Bioengineering*, **54**(2).

Taylor, B. and Gardner, T. 2007. Southeast Queensland recycled water aspects and soil impacts, In Proceedings of the AWA Queensland 2007 Regional Conference: 9–11 November; Sunshine Coast, Australia, Australian Water Association.

Tchobanoglous, G., Burton, F.L., Stensel, H.D. 2003. *Wastewater engineering: Treatment and Reuse. 4th ed.* McGraw-Hill, Boston.

Tezel, U., Tandukar, M., Pavlostathis, S.G. 2011. *Anaerobic biotreatment of municipal sewage sludge. 2nd ed. ed.* Elsevier, Amsterdam, The Netherlands.

Thurston, C.F., Bennetto, H.P., Delaney, G.M., Mason, J.R., Roller, S.D., Stirling, J.L. 1985. Glucose-metabolism in a microbial fuel-cell - stoichiometry of product formation in a thionine-mediated proteus-vulgaris fuel-cell and its relation to coulombic yields. *Journal of General Microbiology*, **131**(JUN), 1393-1401.

Töpfl, S. 2006. Pulsed electric fields (PEF) for permeabilization of cell membranes in food and bioprocessing: applications, process and equipment design and cost analysis. PhD Thesis. Department of Food Process Engineering and Food Biotechnology, Berlin University of Technology, Berlin.

Torres, C.I. 2014. On the importance of identifying, characterizing, and predicting fundamental phenomena towards microbial electrochemistry applications. *Current Opinion in Biotechnology*, **27**, 107-114.

Torres, C.I., Kato Marcus, A., Rittmann, B.E. 2007. Kinetics of consumption of fermentation products by anode-respiring bacteria. *Applied Microbiology and Biotechnology*, **77**(3).

Torres, C.I., Krajmalnik-Brown, R., Parameswaran, P., Marcus, A.K., Wanger, G., Gorby, Y.A., Rittmann, B.E. 2009. Selecting Anode-Respiring Bacteria Based on Anode Potential: Phylogenetic, Electrochemical, and Microscopic Characterization. *Environmental Science & Technology*, **43**(24).

Torres, C.I., Lee, H.-S., Rittmann, B.E. 2008a. Carbonate Species as OH(-) Carriers for Decreasing the pH Gradient between Cathode and Anode in Biological Fuel Cells. *Environmental Science & Technology*, **42**(23).

Torres, C.I., Marcus, A.K., Lee, H.-S., Parameswaran, P., Krajmalnik-Brown, R., Rittmann, B.E. 2010. A kinetic perspective on extracellular electron transfer by anode-respiring bacteria. *Fems Microbiology Reviews*, **34**(1).

Torres, C.I., Marcus, A.K., Parameswaran, P., Rittmann, B.E. 2008b. Kinetic experiments for evaluating the Nernst-Monod model for anode-respiring bacteria (ARB) in a biofilm anode. *Environmental Science & Technology*, **42**(17).

Torres, C.I., Marcus, A.K., Rittmann, B.E. 2008c. Proton transport inside the biofilm limits electrical current generation by anode-respiring bacteria. *Biotechnology and Bioengineering*, **100**(5).

Tyagi, V.K., Lo, S.-L. 2013. Sludge: A waste or renewable source for energy and resources recovery? *Renewable & Sustainable Energy Reviews*, **25**, 708-728.

UNEP, UN-Habitat. 2010. Sick water? The central role of wastewater management in sustainable development.

U.S. EPA. 1979. Process Design Manual Sludge Treatment and Disposal, U.S. Environmental Protection Agency.

U.S. EPA. 1991. Hydrogen sulphide corrosion in wastewater collection and treatment system. Technical Report. 430/09-91-010.

U.S. EPA. 2000. Guide to field storage of biosolids. EPA/832-B-00-007.

Ursua, A., Gandia, L.M., Sanchis, P. 2012. Hydrogen Production From Water Electrolysis: Current Status and Future Trends. *Proceedings of the Ieee*, **100**(2), 410-426.

Vavilin, V.A., Fernandez, B., Palatsi, J., Flotats, X. 2008. Hydrolysis kinetics in anaerobic degradation of particulate organic material: An overview. *Waste Management*, **28**(6), 939-951.

Veeken, A., Kalyuzhnyi, S., Scharff, H., Hamelers, B. 2000. Effect of pH and VFA on hydrolysis of organic solid waste. *Journal of Environmental Engineering-Asce*, **126**(12), 1076-1081.

Vega, C.A., Fernandez, I. 1987. Mediating effect of ferric chelate compounds in microbial fuel-cells with lactobacillus-plantarum, streptococcus-lactis, and erwinia dissolvens. *Bioelectrochemistry and Bioenergetics*, **17**(2), 217-222.

Velasquez-Orta, S.B., Yu, E., Katuri, K.P., Head, I.M., Curtis, T.P., Scott, K. 2011. Evaluation of hydrolysis and fermentation rates in microbial fuel cells. *Applied Microbiology and Biotechnology*, **90**(2), 789-798.

Venkateswaran, K., Moser, D.P., Dollhopf, M.E., Lies, D.P., Saffarini, D.A., MacGregor, B.J., Ringelberg, D.B., White, D.C., Nishijima, M., Sano, H., Burghardt, J., Stackebrandt, E., Nealson, K.H. 1999. Polyphasic taxonomy of the genus Shewanella and description of Shewanella oneidensis sp. nov. *International Journal of Systematic Bacteriology*, **49**, 705-724.

Vijayaraghavan, K., Sagar, G.K. 2010. Anaerobic Digestion and In situ Electrohydrolysis of Dairy Bio-sludge. *Biotechnology and Bioprocess Engineering*, **15**(3), 520-526.

Vlyssides, A.G., Karlis, P.K. 2004. Thermal-alkaline solubilization of waste activated sludge as a pre-treatment stage for anaerobic digestion. *Bioresource Technology*, **91**(2), 201-206.

Vologni, V., Kakarla, R., Angelidaki, I., Min, B. 2013. Increased power generation from primary sludge by a submersible microbial fuel cell and optimum operational conditions. *Bioprocess and Biosystems Engineering*, **36**(5), 635-642.

Vyas, P.V., Shah, B.G., Trivedi, G.S., Ray, P., Adhikary, S.K., Rangarajan, R. 2001. Characterization of heterogeneous anion-exchange membrane. *Journal of Membrane Science*, **187**(1-2), 39-46.

Wang, X., Feng, Y.J., Wang, H.M., Qu, Y.P., Yu, Y.L., Ren, N.Q., Li, N., Wang, E., Lee, H., Logan, B.E. 2009. Bioaugmentation for Electricity Generation from Corn Stover Biomass Using Microbial Fuel Cells. *Environmental Science & Technology*, **43**(15), 6088-6093.

Wang, Y., Chen, K.S., Mishler, J., Cho, S.C., Adroher, X.C. 2011. A review of polymer electrolyte membrane fuel cells: Technology, applications, and needs on fundamental research. *Applied Energy*, **88**(4), 981-1007.

Wang, Z., Lee, T., Lim, B., Choi, C., Park, J. 2014. Microbial community structures differentiated in a single-chamber air-cathode microbial fuel cell fueled with rice straw hydrolysate. *Biotechnology for Biofuels*, **7**.

Wang, Z., Ma, J., Xu, Y., Yu, H., Wu, Z. 2013. Power production from different types of sewage sludge using microbial fuel cells: A comparative study with energetic and microbiological perspectives. *Journal of Power Sources*, **235**, 280-288.

Water Environmental Research Foundation. 2010. Sustainable Treatment: Best Practices from the Strass im Zillertal Wastewater Treatment Plant, Stock No.: OWSO4R07b.

Weber, K.A., Achenbach, L.A., Coates, J.D. 2006. Microorganisms pumping iron: anaerobic microbial iron oxidation and reduction. *Nature Reviews Microbiology*, **4**(10), 752-764.

Weld, R.J., Singh, R. 2011. Functional stability of a hybrid anaerobic digester/microbial fuel cell system treating municipal wastewater. *Bioresource Technology*, **102**(2), 842-847.

Wett, B., Buchauer, K., Fimml, C. 2007. Energy self-sufficiency as a feasible concept for wastewater treatment systems. Proc. IWA Leading Edge Technology Conference, Singapore, Asian Water, Sept.2007, 21-24.

Wolff, H.J., Nickel, K., Houy, A., Lunden, A., Neis, U. 2007. Two years experience on a large German STP with acoustic disintegration of waste activated sludge for improved anaerobic digestion. 11th IWA World Congress on Anaerobic Digestion, Session PP9C-Biosolids, Brisbane, Australia, September 23–27.

World Bank. 2012. What a waste: a global review of solid waste management. Urban development series knowledge papers.

World Energy Council. 2013. World Energy Resources: Waste to Energy. 4184478.

Wrighton, K.C., Agbo, P., Warnecke, F., Weber, K.A., Brodie, E.L., DeSantis, T.Z., Hugenholtz, P., Andersen, G.L., Coates, J.D. 2008. A novel ecological role of the Firmicutes identified in thermophilic microbial fuel cells. *Isme Journal*, **2**(11), 1146-1156.

Xiao, B., Han, Y., Liu, X., Liu, J. 2014. Relationship of methane and electricity production in two-chamber microbial fuel cell using sewage sludge as substrate. *International Journal of Hydrogen Energy*, **39**(29), 16419-16425.

Xing, D., Zuo, Y., Cheng, S., Regan, J.M., Logan, B.E. 2008. Electricity generation by Rhodopseudomonas palustris DX-1. *Environmental Science & Technology*, **42**(11), 4146-4151.

Yamanaka, I., Hashimoto, T., Ichihashi, R., Otsuka, K. 2008. Direct synthesis of H2O2 acid solutions on carbon cathode prepared from activated carbon and vapor-growing-carbon-fiber by a H-2/O-2 fuel cell. *Electrochimica Acta*, **53**(14), 4824-4832.

Yamanaka, I., Murayama, T. 2008. Neutral H2O2 synthesis by electrolysis of water and O-2. *Angewandte Chemie-International Edition*, **47**(10), 1900-1902.

Yamanaka, I., Otsuka, K. 1991. The partial oxidations of cyclohexane and benzene on the fecl3-embedded cathode during the o-2-h-2 fuel-cell reactions. *Journal of the Electrochemical Society*, **138**(4), 1033-1038.

Yamanaka, I., Tazawa, S., Murayama, T., Iwasaki, T., Takenaka, S. 2010. Catalytic Synthesis of Neutral Hydrogen Peroxide at a CoN2Cx Cathode of a Polymer Electrolyte Membrane Fuel Cell (PEMFC). *Chemsuschem*, **3**(1), 59-62.

Yang, F., Ren, L., Pu, Y., Logan, B.E. 2013. Electricity generation from fermented primary sludge using single-chamber air-cathode microbial fuel cells. *Bioresource Technology*, **128**, 784-787.

Yoho, R.A., Popat, S.C., Torres, C.I. 2014. Dynamic Potential-Dependent Electron Transport Pathway Shifts in Anode Biofilms of *Geobacter sulfurreducens*. *Chemsuschem*, **7**(12), 3413-3419.

You, S.J., Zhao, Q.L., Jiang, J.Q., Zhang, J.N., Zhao, S.Q. 2006. Sustainable approach for leachate treatment: Electricity generation in microbial fuel cell. *Journal of Environmental Science and Health Part a-Toxic/Hazardous Substances & Environmental Engineering*, **41**(12), 2721-2734.

Yuan, Q., Baranowski, M., Oleszkiewicz,J.A. 2010. Effect of sludge type on the fermentation products. *Chemosphere*, **80**, 445-449.

Yuan, Y., Chen, Q., Zhou, S., Zhuang, L., Hu, P. 2012. Improved electricity production from sewage sludge under alkaline conditions in an insert-type air-cathode microbial fuel cell. *Journal of Chemical Technology and Biotechnology*, **87**(1), 80-86.

Zaman, A.U. 2009. Life Cycle Environmental Assessment of Municipal Solid Waste to Energy Technologies. EESI, School of Architecture and the Built Environment, KTH Royal Institute of Technology, Stockholm, Sweden, Global Journal of Environmental Research 3 (3): 155-163, 2009.

Zhang, F., Saito, T., Cheng, S., Hickner, M.A., Logan, B.E. 2010a. Microbial Fuel Cell Cathodes With Poly(dimethylsiloxane) Diffusion Layers Constructed around Stainless Steel Mesh Current Collectors. *Environmental Science & Technology*, **44**(4), 1490-1495.

Zhang, H., Banaszak, J.E., Parameswaran, P., Alder, J., Krajmalnik-Brown, R., Rittmann, B.E. 2009. Focused-Pulsed sludge pre-treatment increases the bacterial diversity and relative abundance of acetoclastic methanogens in a full-scale anaerobic digester. *Water Research*, **43**(18), 4517-4526.

Zhang, J.N., Zhao, Q.L., You, S.J., Jiang, J.Q., Ren, N.Q. 2008a. Continuous electricity production from leachate in a novel upflow air-cathode membrane-free microbial fuel cell. *Water Science and Technology*, **57**(7), 1017-1021.

Zhang, L., De Schryver, P., De Gusseme, B., De Muynck, W., Boon, N., Verstraete, W. 2008b. Chemical and biological technologies for hydrogen sulfide emission control in sewer systems: A review. *Water Research*, **42**(1-2), 1-12.

Zhang, L., Zhou, S., Zhuang, L., Li, W., Zhang, J., Lu, N., Deng, L. 2008c. Microbial fuel cell based on Klebsiella pneumoniae biofilm. *Electrochemistry Communications*, **10**(10), 1641-1643.

Zhang, T., Cui, C.Z., Chen, S.L., Ai, X.P., Yang, H.X., Ping, S., Peng, Z.R. 2006. A novel mediatorless microbial fuel cell based on direct biocatalysis of Escherichia coli. *Chemical Communications*(21), 2257-2259.

Zhang, Y., Merrill, M.D., Logan, B.E. 2010b. The use and optimization of stainless steel mesh cathodes in microbial electrolysis cells. *International Journal of Hydrogen Energy*, **35**(21), 12020-12028.

Zhang, Y., Wang, Y., Angelidaki, I. 2015. Alternate switching between microbial fuel cell and microbial electrolysis cell operation as a new method to control H2O2 level in Bioelectro-Fenton system. *Journal of Power Sources*, **291**, 108-116.

Zhao, F., Harnisch, F., Schroerder, U., Scholz, F., Bogdanoff, P., Herrmann, I. 2006. Challenges and constraints of using oxygen cathodes in microbial fuel cells. *Environmental Science & Technology*, **40**(17), 5193-5199.

Zhao, F., Rahunen, N., Varcoe, J.R., Chandra, A., Avignone-Rossa, C., Thumser, A.E., Slade, R.C.T. 2008. Activated carbon cloth as anode for sulfate removal in a microbial fuel cell. *Environmental Science & Technology*, **42**(13), 4971-4976.

Zhou, X., Jiang, G., Wang, Q., Yuan, Z. 2014. A review on sludge conditioning by sludge pre-treatment with a focus on advanced oxidation. *Rsc Advances*, **4**(92), 50644-50652.

Zhu, X., Siegert, M., Yates, M.D., Logan, B.E. 2015. Alamethicin Suppresses Methanogenesis and Promotes Acetogenesis in Bioelectrochemical Systems. *Applied and Environmental Microbiology*, **81**(11), 3863-3868.

Zhuang, L., Chen, Q., Zhou, S., Yuan, Y., Yuan, H. 2012a. Methanogenesis Control using 2-Bromoethanesulfonate for Enhanced Power Recovery from Sewage Sludge in Air-cathode Microbial Fuel Cells. *International Journal of Electrochemical Science*, **7**(7), 6512-6523.

Zhuang, L., Yuan, Y., Wang, Y., Zhou, S. 2012b. Long-term evaluation of a 10-liter serpentine-type microbial fuel cell stack treating brewery wastewater. *Bioresource Technology*, **123**, 406-412.

Zhuang, L., Zhou, S., Li, Y., Yuan, Y. 2010. Enhanced performance of air-cathode two-chamber microbial fuel cells with high-pH anode and low-pH cathode. *Bioresource Technology*, **101**(10), 3514-3519.

Zuo, Y., Xing, D., Regan, J.M., Logan, B.E. 2008. Isolation of the exoelectrogenic bacterium Ochrobactrum anthropi YZ-1 by using a U-tube microbial fuel cell. *Applied and Environmental Microbiology*, **74**(10), 3130-3137.

APPENDIX A

SUPPLEMENTARY DATA FOR CHAPTER 6

A.1 Calculation of anode projected area with assumptions

Before designing the reactor, I tried to calculate anode projected areas with the assumptions of PS-$TCOD_{in}$, solid retention time, anode volume, and expected current density. The values for calculation are as below,

- PS-$TCOD_{in}$: 8 gCOD/L, but I count 50% of TCOD as bioavailable fraction: 4 gBOD/L
- Hydraulic retention time: 9-day
- Anode volume: 500 mL
- Expected current density: 1.5 A/m^2

I calculated the anode projected area with the above assumption values.

Anode projected area

$$= \frac{4\ gBOD}{L} \times 0.5L \times \frac{1}{9\ day} \times \frac{1\ e^-}{8\ gBOD} \times \frac{96485\ C}{1\ e^-} \times \frac{1\ day}{24 \times 60 \times 60 sec} \times \frac{m^2}{1.5\ A}$$

$$= 0.02\ m^2 = 200\ cm^2$$

A.2 PS fed batch MEC operation

A.2.1 Results and discussion

I performed batch experiments fed with PS twice consecutively for 30 and 45 days of 1st and 2nd batch, respectively. Input and output characteristics of the 1st and 2nd batch MECs are shown in Table A.1. Average of input PS-TCOD was ~8.6 g COD L^{-1}, which is equivalent to ~51,800 Coulombs. BOD_5 was about 43% of $TCOD_{in}$ and the VSS/TSS ratio was 90%, for both batch operations.

I show in Figure A.1a that the maximum current density was ~2 and 1 A m^{-2} for 1st and 2nd batch, respectively. Current density represents the rate of electron capture and varied with time probably corresponding to different hydrolysis of PS components (protein, carbohydrate, and lipid), and differences in ARB utilization rate of the volatile fatty acids produced from upstream microbial processes. In Figure A.1b, I show mass

balance of PS diverted to each fraction: electrical current, methane, effluent, and unaccounted electrons (others). While electrons recovered as currents were similar in both batch operations (56% and 53%), there was greater COD and VSS removals in the 2nd batch, likely due to the greater retention time for the solids in the MEC anode, leading to greater accumulation and retention (as evidenced by the higher fraction of unaccounted electrons in the 2nd batch). Moreover, the ARB could have been more primed in the 1st batch operation to oxidize VFAs from PS after acetate depletion, while the 2nd batch likely decreased compared to the initial condition of the 1st batch. Correspondingly, less electrons in the 2nd batch went to electrical current despite of 15 days' longer operation. Decrease of maximum current density from 2 to 1 A m^{-2} was likely due to the less favorable ARB conditions, which might stem from competition for space for existing ARB and other microbes from accumulated PS, or other transport limitation due to the accumulated solid layers.

Table A.1. Characteristics of PS input and output for batch MEC experiments

Parameter	1st batch for 30 days		2nd batch for 45 days	
	Input PS	**Output PS**	**Input PS**	**Output PS**
TCOD (mg/L)	8827 (±779)	2827 (±65)	8400 (±579)	2099 (±17)
SSCOD (mg/L)	323 (±1.4)	635 (±7)	276 (±4.9)	581 (±1)
BOD_5 (mg/L)	3498 (±111)	1554 (±27)	3864 (±409)	967 (± 180)
TSS (mg/L)	5911 (±168)	2100 (±0)	5600 (±67)	1478 (±96)
VSS (mg/L)	5311 (±135)	1722 (±0)	4967 (±67)	1178 (±38)
VSS/TSS (%)	90	82	89	80
NH_3-N (mg/L)	44.5 (±0.4)	121.8 (±1.1)	58.8 (±0.4)	61.3 (±1.1)
Alkalinity (mg/L as $CaCO_3$)	270 (±16)	2515 (±7)	457 (±19)	2583 (±25)
Carbs (mg/L as Glucose)	3417 (±430)	398 (±51)	2289 (±193)	199 (±14)
Protein (mg/L as BSA)	3093 (±203)	764 (±20)	3409 (±77)	398 (±3)
Lipid (mg/L as FAME)	269 (±55)	91 (±5)	267 (±29)	15

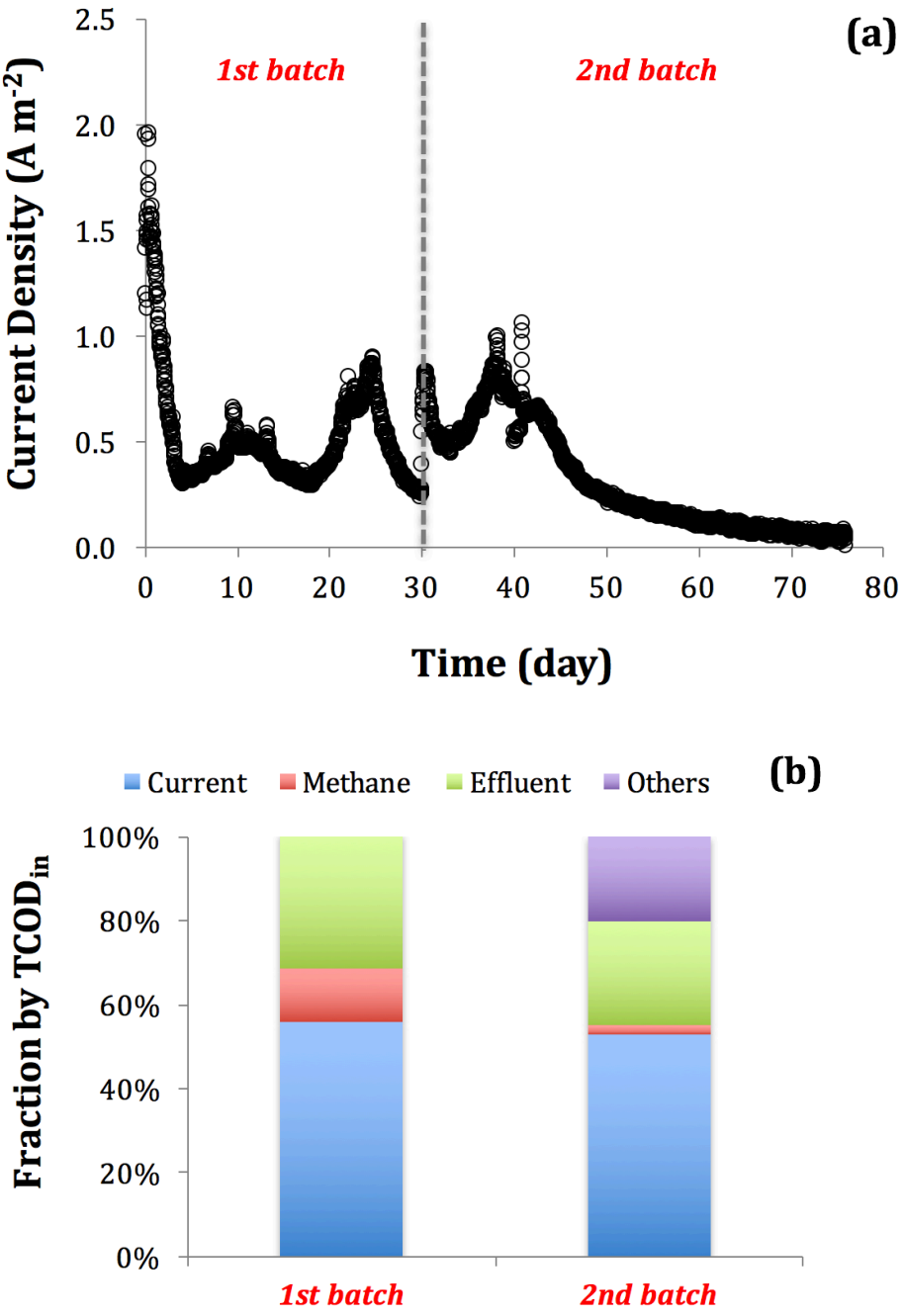

Figure A.1. Performance of consecutive batch MECs fed with PS for 30 and 45 days (1st and 2nd batch, respectively) - (a) current density and (b) mass balance at the end of batch runs.

Both 1st and 2nd batch MECs fed with PS achieved Coulombic recovery (CR) more than 50% (Figure A.2), which is significantly higher than pre-fermented PS centrate fed

MEC (Ki et al., 2015). Optimum condition of two-stage system with pre-fermentation and MEC enabled to convert ~16% of PS-$TCOD_{in}$ into soluble COD at 3-day HRT in pre-fermentation stage which was followed by ~13% CR in the centrate-fed batch MEC stage, again based on PS-$TCOD_{in}$. The major advantage of the two-stage centrate fed MEC was a higher rate of electron recovery due to the selective availability of volatile fatty acids in the centrate. On the other hand, direct PS fed MECs in the 1st and 2nd batch operation achieved CR of ~16% and ~45% of PS-$TCOD_{in}$ in ~7 days and 45 days, respectively (Figure A.2), a clear benefit compared to the two-stage approach.

Although the direct PS batch experiments have a significant CR and VSS destruction, the CR might be overestimated due to endogenous current from the biofilms on the anode surface during longer batch experiments compared to the pre-fermented PS centrate fed MECs (> 30 days versus ~ 3 days). Decayed microbes from anodes (total geometric area of 200 cm^2) could serve as electron donors for active ARBs after hydrolysis and fermentation. This bias from a large decay current on the CR could be minimized during long term (semi-) continuous MEC operation fed with PS could be more reliable and practical to represent the PS conversion to electrical energy.

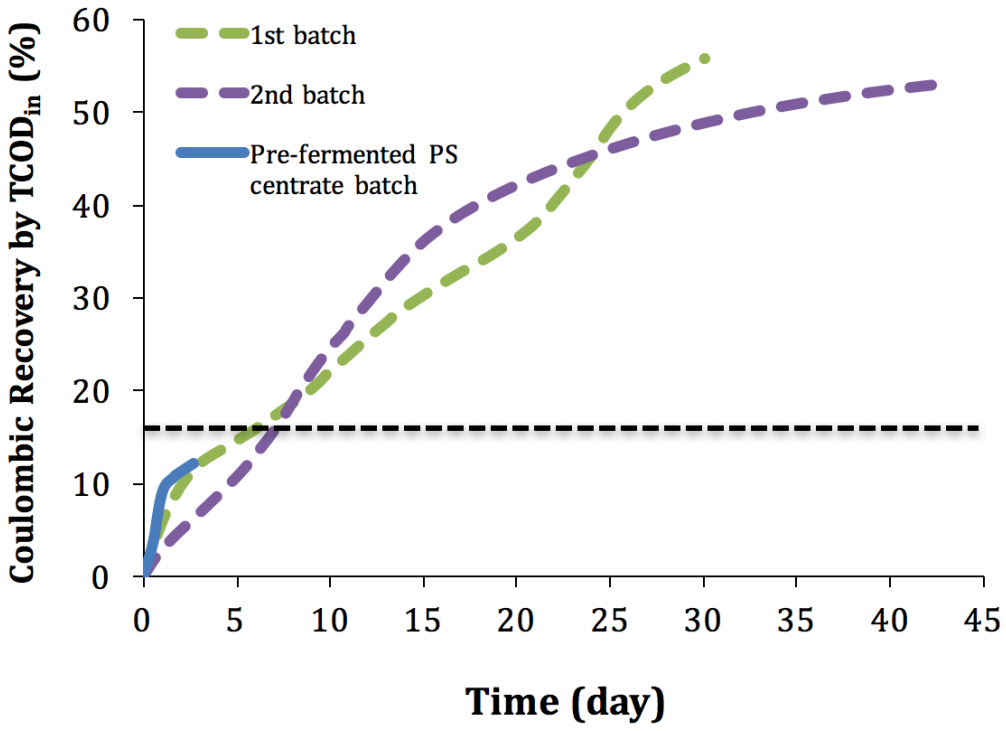

Figure A.2. Comparisons of Coulombic recoveries between pre-fermented PS centrate (Ki et al., 2015) and direct PS fed MEC. The dotted line (black) is the maximum recovery (~16% of PS-TCOD$_{in}$) as semi-soluble COD after pre-fermentation of PS in optimum condition of two-stage system from Ki et al., 2015.

A.2.2 Materials and Methods

For PS batch operation, I used a stirrer plate for mixing PS in the anode of the MEC with ~150 rpm. After 30-day batch operation, I replaced substrate with new PS for the following 45-day batch operation. I maintained pH in the anode chamber between 6.5 and 8.5 during the batch runs while adjusting with sodium hydroxide (2.5 M).

PS characterization included measurement of total chemical oxygen demand (TCOD), semi-soluble COD (SSCOD), biochemical oxygen demand (BOD), total suspended solids (TSS), volatile suspended solids (VSS), ammonia (NH_3-N), total phosphorus (T-P), alkalinity, carbohydrate, protein, and lipid. COD, NH_3-N, T-P, and

alkalinity were measured using spectrophotometric methods by HACH kit and spectrophotometer (DR2700, HACH, Loveland, CO). Semi-soluble COD was measured on the permeate after filtration through a 1.2-μm glass-fiber filter (Whatman™, UK), as described in Ki et al. (2015). TSS, VSS and BOD_5 were measured according to Standard Methods (APHA, 2012). Carbohydrates were measured by a colorimetric method (DuBois et al., 1956). Proteins were analyzed by the bicinchoninic acid (BCA) method (Brown et al. 1989). To measure the total proteins of PS, I separated PS to solids and soluble after centrifugation for 5 min. I extracted solids proteins by heat treatment at 90 °C with 0.1 N NaOH for 30 min, described in Lee et al. (2008), cooled down, centrifuged the lysate, and used the supernatant for the BCA assay. I used a spectrophotometer (Varian Cary 50 Bio, Varian Inc., Walnut Creek, CA) for carbohydrate and protein at a wavelength of 485 and 562 nm, with glucose and bovine serum albumin (BSA) as standards, respectively. Lipids measurement was followed by the method of Lai et al. (2015). Biogas production during batch MEC mode was collected using a gas tedlar bag and the total gas volume was measured with a gas-tight syringe.

Electron-equivalent mass balances for MEC batch and semi-continuous operation were based on PS-COD equivalents:

$$TCOD_{influent} = Coulombs\ circuited + methane + TCOD_{effluent} + Others$$

where $TCOD_{influent}$ is the measured mg COD of the input PS, Coulombs circuited is the COD equivalent of the Coulombs accumulated during the batch and semi-continuous operations, 1 Coulomb of current = 0.083 mg COD, as described in Ki et al. (2015b), methane is the COD equivalent of the methane gas (mL) produced, 1 mL of CH_4 = 2.57 mg COD at 30 °C, as decribed in Ki et al. (2015), $TCOD_{effluent}$ is the measured mg COD at the end of batch MEC or effluent PS during the semi-continuous operations at each HRT, and Others is any unaccounted COD in $TCOD_{influent}$ of PS.

A.3 Open circuit potential analysis in semi-continuous operation

Open circuit potential or voltage (OCP or OCV) is the cell potential or voltage that can be measured without current in an electrochemical cell (Logan et al., 2006). OCP values are an indicator of the thermodynamic equilibrium of the electrochemical cell. The theoretical reaction potential and, correspondingly, the OCP change as the concentration of reactants and products are varied. When acetate medium (5 mM of acetate and 5 mM of bicarbonate at pH 7 and 30°C) is used in the anode, the theoretical potential is -0.304 V vs SHE, which corresponded to -0.574 V vs Ag/AgCl. If I changed the acetate concentration to 125 mM to match with a similar PS concentration (~8 g COD of PS L^{-1}),

$$\frac{8\ \text{gCOD}}{\text{L}} \times \frac{1\ \text{mol of acetate}}{64\ \text{g COD}} \times \frac{1000\ \text{mmol}}{1\ \text{mol}} = 125\ \text{mM}$$

the theoretical potential slightly changed and became -0.584 V vs Ag/AgCl. Also, pH provides a bigger impact on the potential, ~60 mV decrease per every one pH unit. Compared to acetate, PS is comprised of very complex organic solids which are then converted into several simple and intermediate volatile fatty acids. Thus, it is difficult to calculate the exact theoretical potential for a given PS sample. In our study, I measured OCP at the anode as a working electrode for each operating condition with PS (Table A.2). In the semi-continuous experiments, the OCP decreased with the lower HRTs, indicating a higher concentration of the readily available substrate (VFAs) with higher pH. This also partly affected in higher maximum current density, thus it could be a good indication of the MEC maintenance with lower OCPs.

Table A.2. Maximum current densities, open circuit potential, and pH in the batch and semi-continuous experiments

HRTs	Maximum current density (A m^{-2})[1]	Open circuit potential at anode (V)[2]	pH[3]
Batch	1.5 (± 0.71)	-0.383 (± 0.090)	6.5 ~ 8.5
15 day	0.35 (± 0.06)	-0.360 (± 0.026)	7.32 (± 0.24)
12 day	1.08 (± 0.22)	-0.403 (± 0.017)	7.24 (± 0.30)
9 day	2.21 (± 0.28)	-0.498 (± 0.009)	7.49 (± 0.33)
6 day	2.08 (± 0.14)	-0.515 (± 0.013)	8.13 (± 0.29)
12 day neutral pH	1.34 (± 0.11)	-0.467 (± 0.015)	7.30 (± 0.17)
12 day high pH	1.40 (± 0.04)	-0.523 (± 0.008)	8.08 (± 0.11)

[1]Average value on the steady-state condition at each HRT. In the case of batch operations, the value was averaged with two consecutive runs

[2]Open circuit potentials at anode are all versus Ag/AgCl.

[3]pHs in the semi-continuous operation were all measured at the end of everyday feeding cycle

A.4 Additional electrochemical analysis data for pH importance

The following two figures shows the effect of pH on *j-V* curves (Figure A.3) and chronoamperometries (Figure A.4).

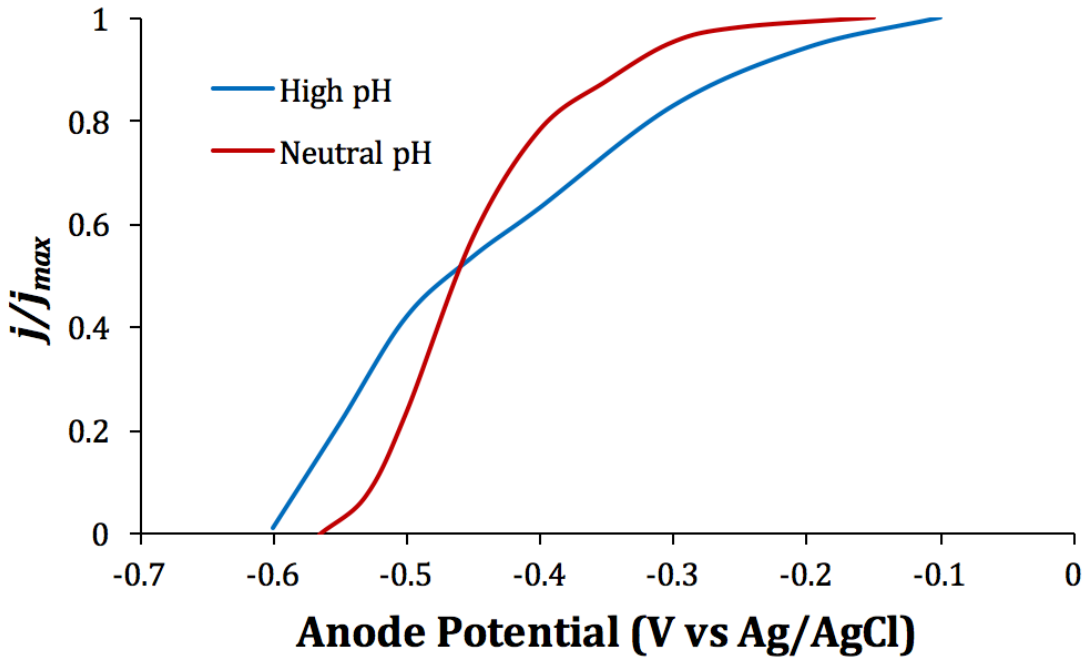

Figure A.3. Effect of pH on the *j-V* response. *j-V* from Figure 6.3b normalized to the maximum current density at each condition.

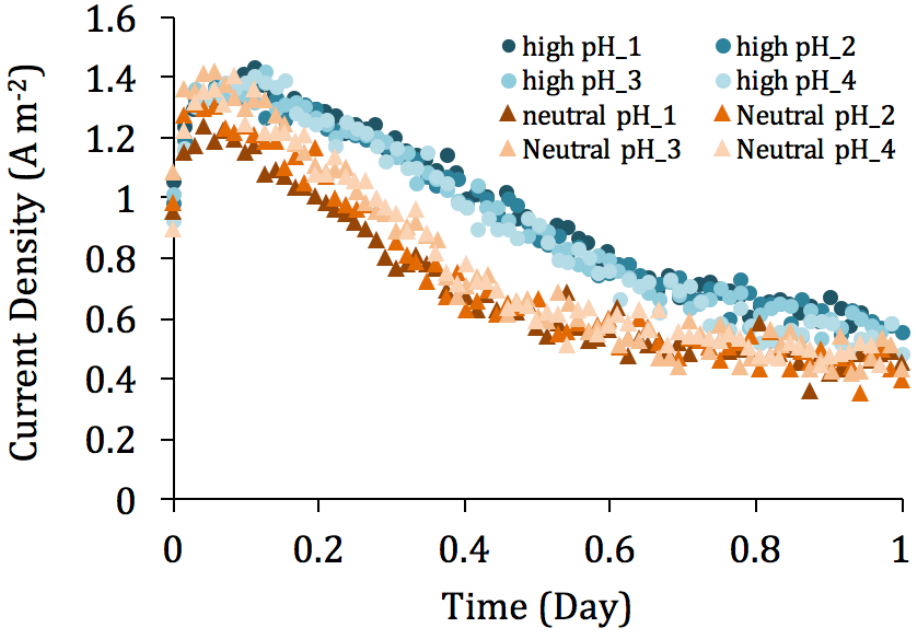

Figure A.4. Comparisons of current densities at different pHs with 4 representative sets on each condition

A.5 Microbial community analysis

A.5.1 Results and discussion

The qualified sequences for the microbial samples were 61,214 to 110,156 (Table A.1). The sequences were clustered to represent operational taxonomic units (OTUs) with 97% nucleotide similarity by Greengene database (DeSaints et al., 2006). Since it is necessary to compare the number of OTUs correctly, 60,000 sequences, which is the close to the minimum number of sequences of 4 samples, were randomly selected to calculate the number of OTUs in each sample. Alpha diversity analysis showed biofilm have formed slightly more diverse microbial community than suspension, see the index of alpha diversities of Phylogenetic diversity and Shannon Index in Table A.3 and Figure A.5. This may result from large surface area of carbon fiber used as anode, which could provide sufficient space for microbial resident with rich organic wastes as growth medium. Also, microbial richness in suspension was much higher in high pH condition compared to neutral pH indicating better environmental condition in MXC anode chamber, see Chao1 and Shannon Index (Table A.3 and Figure A.5). Compared to influent PS diversity, I could clearly see that effluent PS and biofilm had lower diversity in stabilized condition. Beta diversity showed that effluent suspension samples formed a cluster in the result of unweighted principle coordinate analysis (PCoA) (e.g., based on the presence or absence of microbial phylotype) with the sequences obtained for all samples (Figure A.6). The PC1 vector explained 56% of the variance, while PC2 accounts for 23%. The PC1 vector appeared driven by PS characteristics, which was completely different between the influent and effluent or biofilm. The grouping and separation of high pH and neutral pH on the PC2 vector seems to correspond with the different pH conditions.

Table A.3. Summary of alpha diversity of microbial communities of the influent PS, effluent suspension at neutral and high pH, and biofilm on the anode

	Influent PS	Effluent Suspension Neutral pH	Effluent Suspension High pH	Biofilm High pH
# of sequences	102,853	61,214	110,156	75,528
subsamples	60,000	60,000	60,000	60,000
Observed OTUs	3046 (± 9)	1526 (± 2)	1819 (± 7)	2048 (± 5)
Chao1	4003 (± 29)	2343 (± 13)	3108 (± 61)	3161 (± 45)
Phylogenetic diversity	182	96	104	109
Evenness	0.630	0.491	0.477	0.483
Shannon Index	7.29	5.20	5.17	5.32
Simpson	0.975	0.920	0.894	0.913

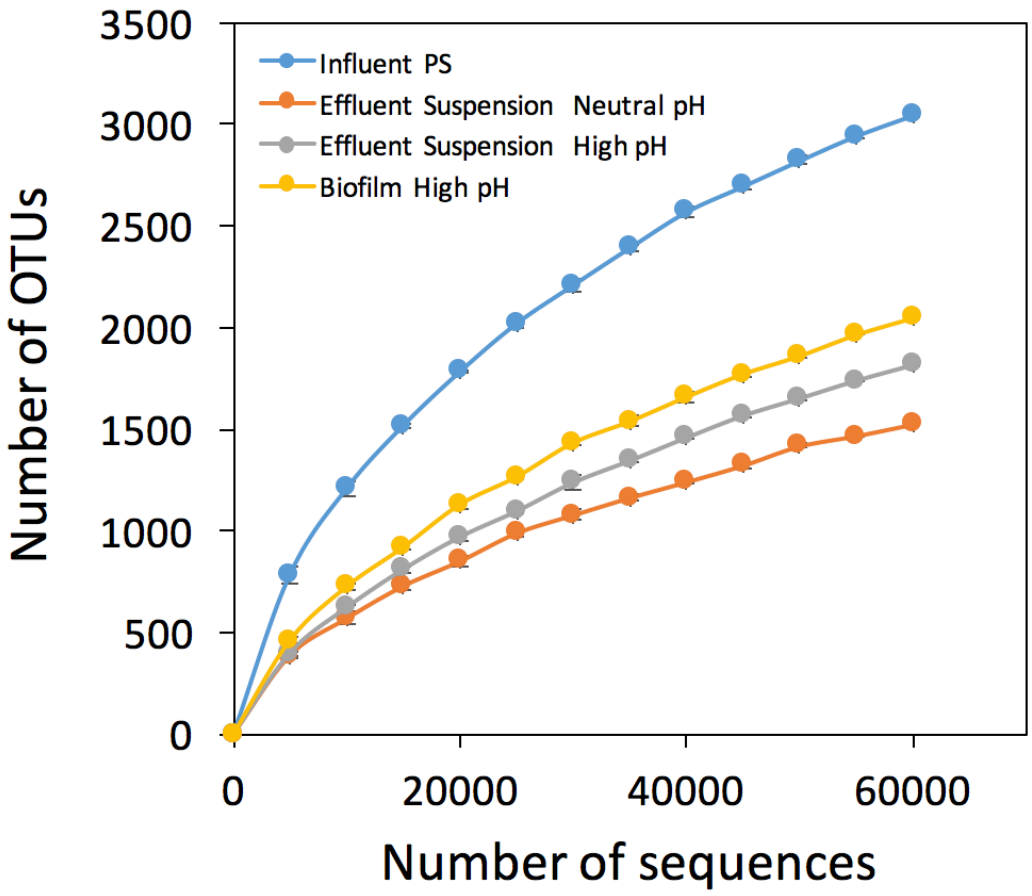

Figure A.5. Rarefaction curves based on Illumina MiSeq of microbial communities.

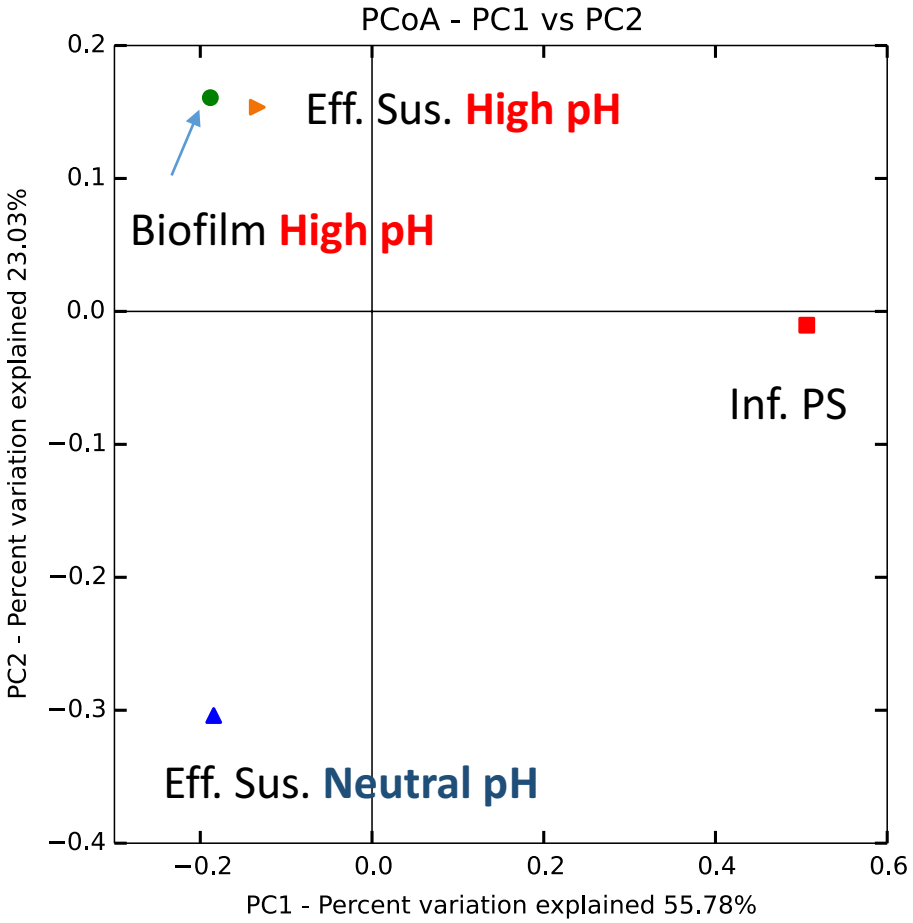

Figure A.6. Principle Coordinate Analysis (PCoA) based on the unweighted UniFrac analyses. While PC1 and PC2 axes represent ~56 and 23% of the variance within the microbial community, PC3 (not shown) has a 21% variance.

Figure A.7a shows the taxonomy at class level of the influent and effluent PS samples as well as biofilm sample at the end of long-term operation. The most well-known phylotype of ARB is *Deltaproteobacteria*. I could see the highest fraction of *Deltaproteobacteria* were detected in biofilm, followed by effluent suspension at high pH and neutral pH. Detail analysis in genus level in Figure A.7b shows more *Geobacter* (19%) was detected in biofilm, while relatively more unclassified *Desulfuromonadales* was detected in effluent suspension, though unclassified *Desulfuromonadales* also were dominant in biofilm. Next dominant classes were affiliated with *Bacteroidia* (24%) and *Clostridia* (10%). *Bacteroidia* are well-known bacteria for hydrolysis and fermentation of complex organic molecules including cellulose (Rismani-Yazdi et al., 2013), and also were found significantly (39%) in MFC-anode biofilm fed with food wastes (Jia et al., 2013). *Bacteroidetes* group (phylum) are typically found in the human gut microbiome, and they break down large organic molecules to obtain energy and nutrients in the human body. This support the results aforementioned in that maintaining hydrolytic and fermentative bacteria as well as ARB is crucial especially when fed with complex molecules, PS, for efficient energy recovery. Especially, more *Bacteroidia* were detected in suspension samples (over 40%) indicating suspended microbes functionally worked more degradation of PS to small pieces when PS firstly inserted into the MEC.

Between two suspension effluents (high and neutral pH), three predominant classes were different each other. *Deltaproteobacteria* (21%) and *Clostridia* (20%) were more abundant in high pH than in neutral pH (12 and 7%, respectively). On the other hand, *Gammaproteobacteria* (23%) was higher fraction in neutral pH than in high pH (3%). More *Deltaproteobacteria*, especially more *Geobacter* and unclassified *Desulfuromonadales*, were likely to actively grow and detach in better environmental condition at high pH. *Clostridia* were primarily comprised of the genus

Syntrophomonas (9%) at high pH, which was 9-fold more abundant than neutral pH. *Syntrophomonas* is known as fermenter having the ability to break down intermediate chain fatty acids (C4~C8) and several unsaturated fatty acids, such as caproate, caprylate, valerate, or heptanoate (McInerney et al., 1979; 1981; 2010). At high pH those bacteria could work efficiently to generate short chain fatty acids (C2~C3, e.g. acetate or butyrate) syntrophically with other hydrolytic and fermentative bacteria. *Pseudomonas* is well known aerobic bacteria for biodegradation of pollutants. However, in the absence of oxygen, they can utilize nitrate as an electron acceptor instead of oxygen. Predominance of *Pseudomonas* at neutral pH could possibly drive in more biodegradation of degradation-tolerant organics in PS, which may be lower SSCOD in the effluent suspension (Table A.4). Hence, synergetic relationships among ARB, hydrolytic and fermentative bacteria seem to have played an important role for energy recovery as electrical current and methane in the PS-fed MXC.

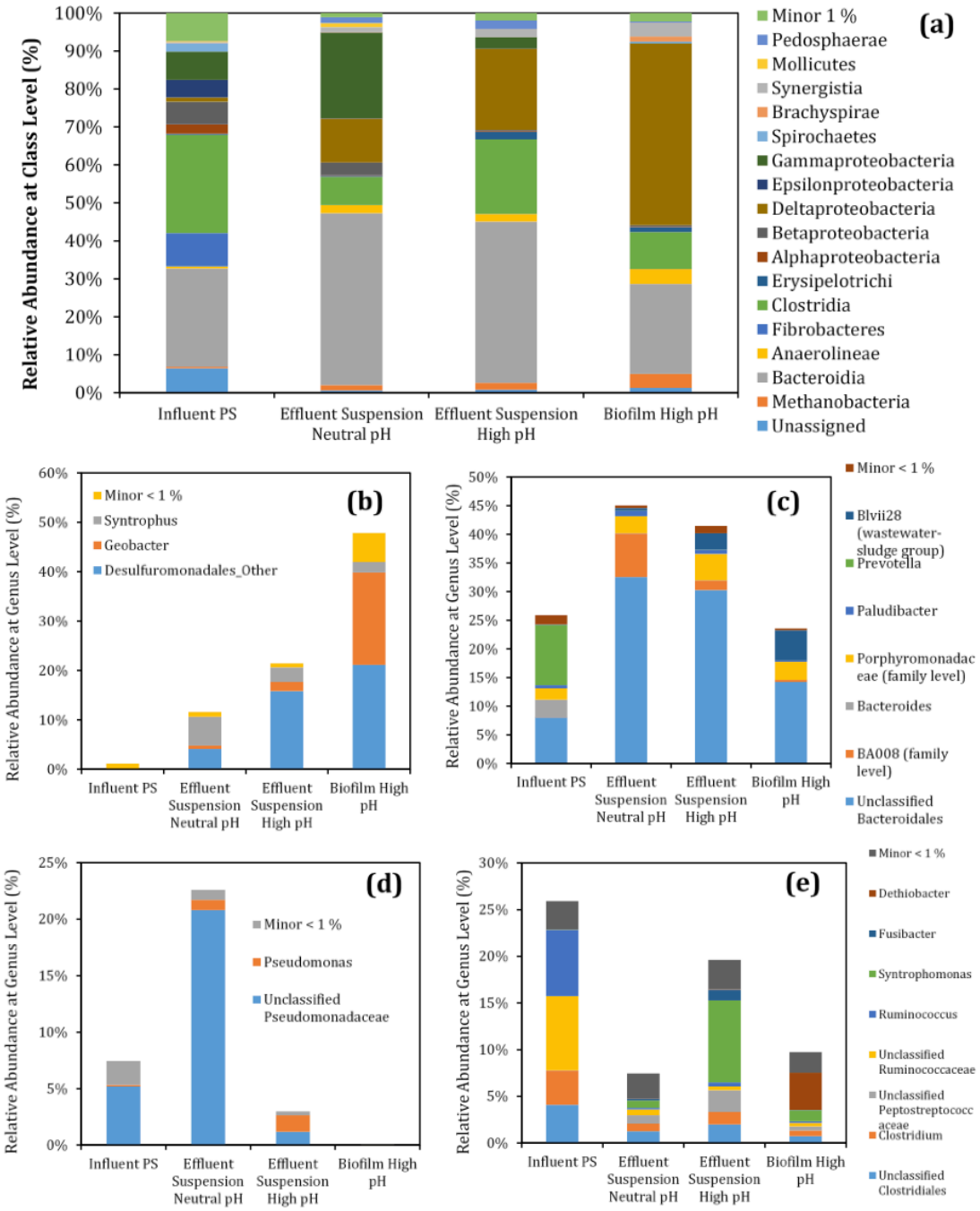

Figure A.7. Microbial community structures at phylum level (a). Predominant community analyzed at genus level: *Deltaproteobacteria* (b), *Bacteroidia* (c), *Gammaproteobacteria* (d), *Clostridia* (e).

A.5.2 Materials and methods

The DNAs were sent to the Microbiome Analysis Laboratory (http://krajmalnik.environmentalbiotechnology.org/microbiome-lab.html) for Illumina MiSeq at Arizona State University. Amplicon sequencing of the V4 region of the 16SrRNA gene was performed with the barcoded primer set 515f/806r designed by Caporaso et al. (2012). Data received from the testing laboratory were analyzed using QIIME (Caporaso et al., 2010) after discarding sequences shorter than 25 bp, longer than 450 bp, or labeled as chimeric sequences. After screening, primer sequences were trimmed off, and taxonomic classification was performed using RDP classifier (Cole et al., 2009) at the 80%-confidence threshold. The total number of sequence reads for each sample after screenings were: influent PS=102,853, effluent suspension of neutral pH=61,214, effluent suspension of high pH=110,156, and biofilm of high pH=75,528.

A.6 Quantitative PCR (qPCR) analysis

A.6.1 Results and discussion

I analyzed microbial diversity and community in PS influent, effluent suspension at neutral and high pHs of 12 day HRT, and anode biofilm at high pH of 12 day HRT, and provided above section. However, since *Archaea*, especially, methanogens cannot be reliably detected with Illumina MiSeq with the primers (V4 region) of choice, I conducted qPCR for general *Archaea* and *Bacteria* to see how pH affected methanogenesis in the MEC (Table A.4). Between neutral and high pH suspension, total *Archaea* gene copies decreased by ~30% at high pH, indicating decrease of methanogens with the inhibited condition, and consistent with a decrease in the methane fraction (26%) at high pH compared to neutral pH as shown in Figure 6.3b.

Table A.4. The number of 16S rRNA gene copies of total *Archaea* and *Bacteria* in effluent suspension of neutral and high pH

	Effluent Suspension Neutral pH	Effluent Suspension High pH
Total *Archaea* (copies per g pellet)	7.22 (± 0.31) x 10^7	5.65 (± 0.30) x 10^7
Total *Bacteria* (copies per g pellet)	1.74 (± 0.15) x 10^{11}	1.17 (± 0.19) x 10^{11}

A.6.2 Results and discussion

Four samples were collected for microbial community analysis: influent PS, neutral and high pH suspension at the end of 12-day HRT operation, and biofilm on the carbon fiber electrodes at the end of 12-day HRT. I centrifuged the samples to obtain pellets for DNA extraction. Around 0.25g of biomass was inserted into the bead tubes provided by a Powersoil DNA extraction kit (MoBio laboratories, Inc., Carlsbad, CA), quantified the DNA with a nanodrop spectrophotometer, and documented their yield and purified at 260 and 280 nm (Lai et al., 2014). The extracted DNAs were stored at -20 °C until sending for Illumina MiSeq and quantitative real-time PCR (qPCR).

To quantify total *Archaea* and *Bacteria* with the extracted DNA samples, I performed 16S rRNA gene-targeted quantitative real-time PCR (qPCR) with TaqMan detection. The *Archaea*- and *Bacteria*-specific primers and probes were used in the previous study (Parameswaran et al., 2009) - Arc787f, Arc1059r, Arc915probe, Bac1055f, Bac1392r, and Bac1115probe. Plasmid DNA standards for *Archaea* and *Bacteria* were prepared from representative 16S rRNA gene clones of *Methanosaeta* KB-1 (AN, AY 570685) and *Prevotella copri* (DSM18205), respectively. I performed the reactions in an Eppendorf Realplex gradient cycler with an initial denaturation at 94 °C for 2 min,

followed by 45 cycles of denaturation at 94 °C for 10 s and combined annealing and extension at 60 °C for 30 s for total *Archaea*. I conducted the reactions with an initial denaturation at 95 °C for 2 min, followed by 40 cycles of denaturation at 95 °C for 10 s, annealing at 56 °C for 20 s, and extension at °C for 20 s for total *Bacteria*. I set up the qPCR reactions using Eppendorf epmotion 5070 and 5075 for precision and reproducibility. A 10-μL PCR contained 4 μL of 2.5x Realmastermix probe solution (5 Prime, MD), 0.5 μL of each primer (500 nM final concentration), 0.03 μL of FAM-labeled probe (300 nM final concentration, TaqMan, Applied Biosystems), 0.97 μL of PCR water, and 4 μL of template DNA. I calculated the copy number of the 16S rRNA gene per gram wet sludge pellets as follows: # per mL = $q/4$ x D x (50 μL)/(g pellet), where q is the detected copy numbers from 4 μL of diluted template, D is the dilution factor, 50 μL is the elution volume in genomic DNA extraction, and g pellet is the wet weight of sludge pellets for DNA extraction (0.23~0.28 gram).

A.7 Filtrate quality of PS influent and effluent

Filtrate quality including SSCOD, alkalinity, ammonia, total phosphorus, conductivity, and TTF of PS influent and effluents are presented in Table A.5. Increasing alkalinity (from 240 to ~2500 mg/L as $CaCO_3$) and conductivity (from 0.9 to ~3.3 mS/cm) in the filtered PS effluent might result from organic oxidation, cell decay and added hydroxide ions. The neutral pH effluent PS has a common alkalinity observed in anaerobic digesters, 2000-5000 mg/L as $CaCO_3$ (APHA, 2012).

Table A.5. Filtrate quality comparisons of PS characteristics between influent and effluent (neutral and high pHs) at 12-day HRT

Parameter	Unit	PS influent	PS effluent neutral pH	PS effluent high pH
SSCOD	mgCOD/L	1046 (± 78)	319 (± 33)	434 (± 49)
Alkalinity	mg/L as $CaCO_3$	238 (± 9)	2367 (± 106)	2720 (± 79)
Ammonia	mg NH_3-N/L	39 (± 0.4)	66 (± 0.9)	71 (± 0.5)
Total P	mg PO_4^{3-}-P/L	25.6 (± 0.5)	25.4 (± 0.5)	30.4 (± 0.6)
Conductivity	mS/cm	0.9	2.73	3.83
TTF	min	3.64 (± 0.83)	1.66 (± 0.35)	0.50 (± 0.05)

A.8 Long-term operation of PS-fed MEC

Following two figures (Figure A.8-A.9) shows the anodes and membranes after long-term operation (~300 days) without changing the materials.

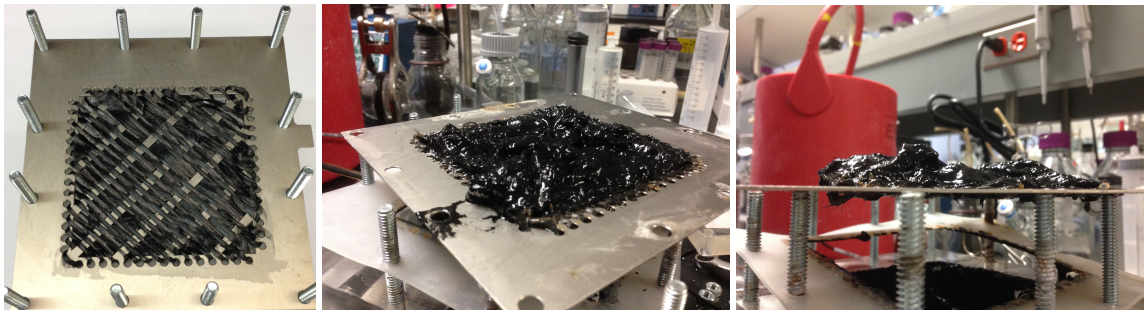

Figure A.8. Photos of anode fibers: i) initial (left) and ii) after 12-day HRT at high pH (right).

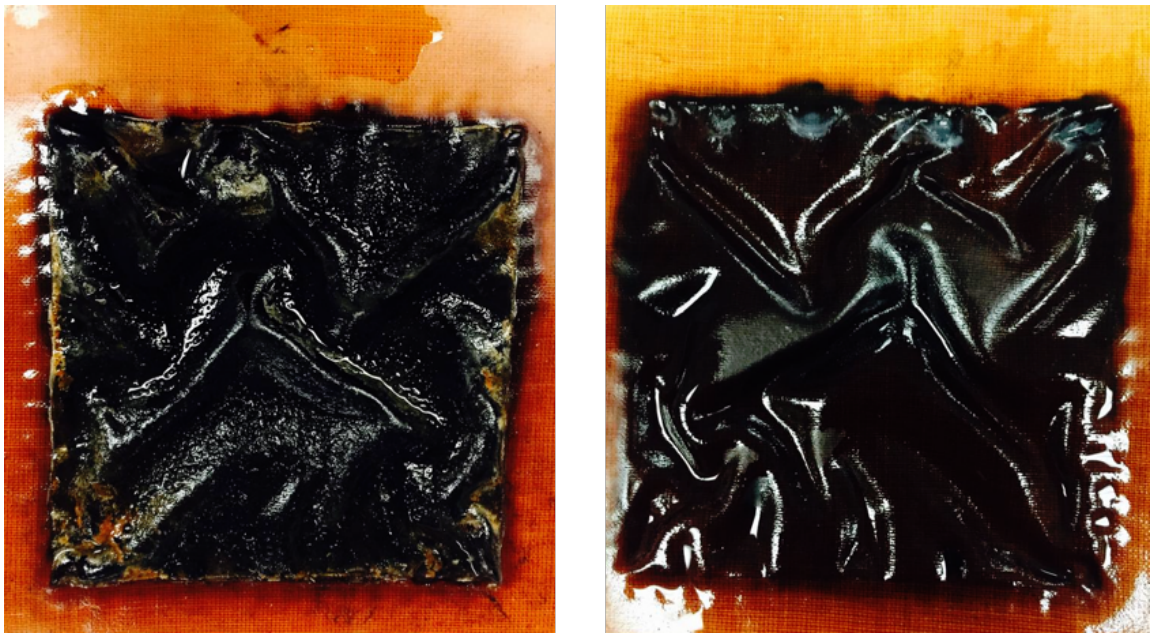

Figure A.9. Photos of the membrane at the end of the long-term operation for ~300 days: anode side (left) and cathode side (right).

APPENDIX B

SUPPLEMENTARY DATA FOR CHAPTER 7

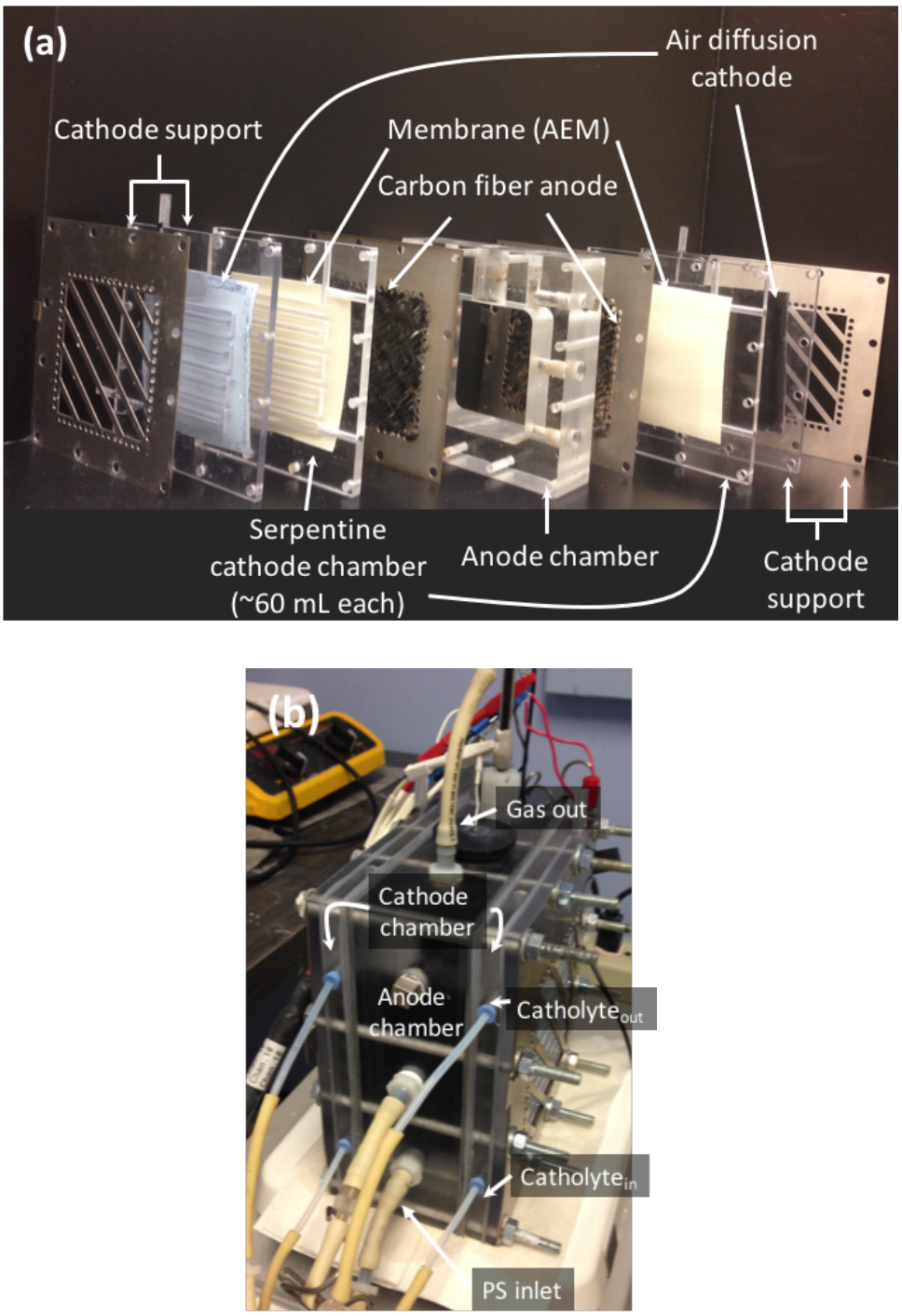

Figure B.1. H_2O_2-producing MEC design. Each part of the reactor components (a) and the assembled one (b).

Table B.1. Gas production in anode-chamber after steady-state

	MEC	H_2O_2 cell
Biogas (mL)	27 (± 4)	2 (± 4)

MEC

Chamber side of anode	Membrane side of anode
	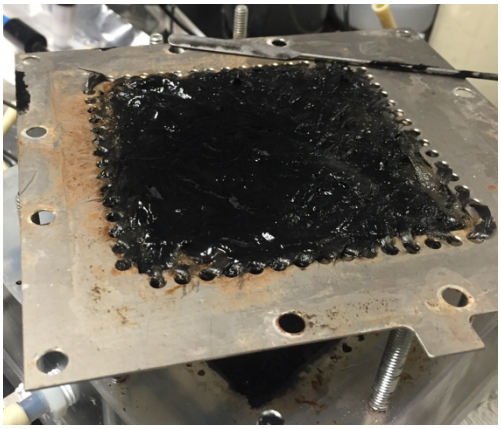

H_2O_2 cell

Chamber side of anode	Membrane side of anode
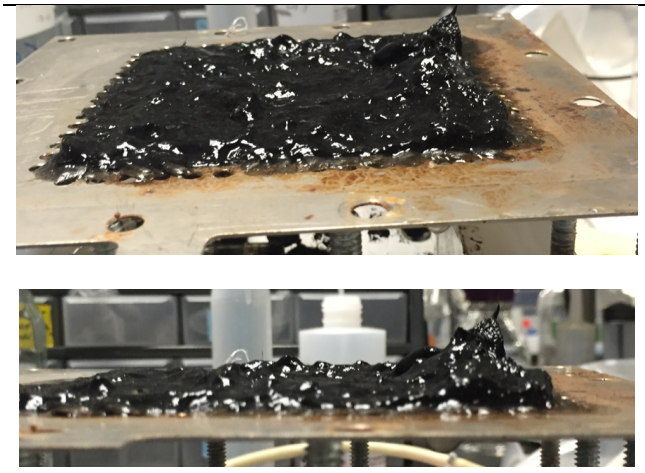	

Figure B.2. Comparisons of solid biomass on carbon fiber anodes towards chamber and membrane in MEC (top) and H_2O_2 cell (bottom) operation

Live and dead cell analysis

I analyzed live and dead cells of samples: AnS, BfC, and BfM from MEC and H_2O_2 cell. I used 26.2 mg of biomass samples suspended in 1.5 mL of 100 mM phosphate buffer solution. Then, I followed the manufacturer's instructions with the LIVE/DEAD BacLight Bacterial Viability Kit (L7012, Invitrogen) for staining. In brief, I prepared samples in 1.5 mL tubes, added 3 μL of the prepared dye, mixed thoroughly and incubated at room temperature for 15 minutes in the dark. To quantify the number of cells in each prepared sample, 5 μL of the stained cell solution were added to a Petroff-Hausser Counting Chamber (Hausser Scientific, Catalog # 3900). Imaging was carried out using fluorescence microscopy [Microscope: Olympus BX 61, Camera: Olympus DP70, Filters: FITC-3540B, Cy5-4040A, Light Source: Mercury Bulb]. Cell counting calculation is based manufacturer's instructions (Hausser Scientific, Catalog # 3900). Briefly, the counting chamber depth is 1/50 mm. Each side of the entire counting grid is 1mm. This makes the total conversion: #cells counted x dilution (if applicable) x 50,000. The # cells counted refers to the total number of cells in the entire 1mm x 1mm x 1/50mm chamber. A representative sample of 5/25 boxes were counted. Total counts were then extrapolated to the full grid. The captured digital images were processed by ImageJ (NIH) image processing software. According to the previous protocol (Baras et al., 2011), I counted live and dead cells, and calculated cell densities, which is the number of cells per added sample volume in the cell counting slide.

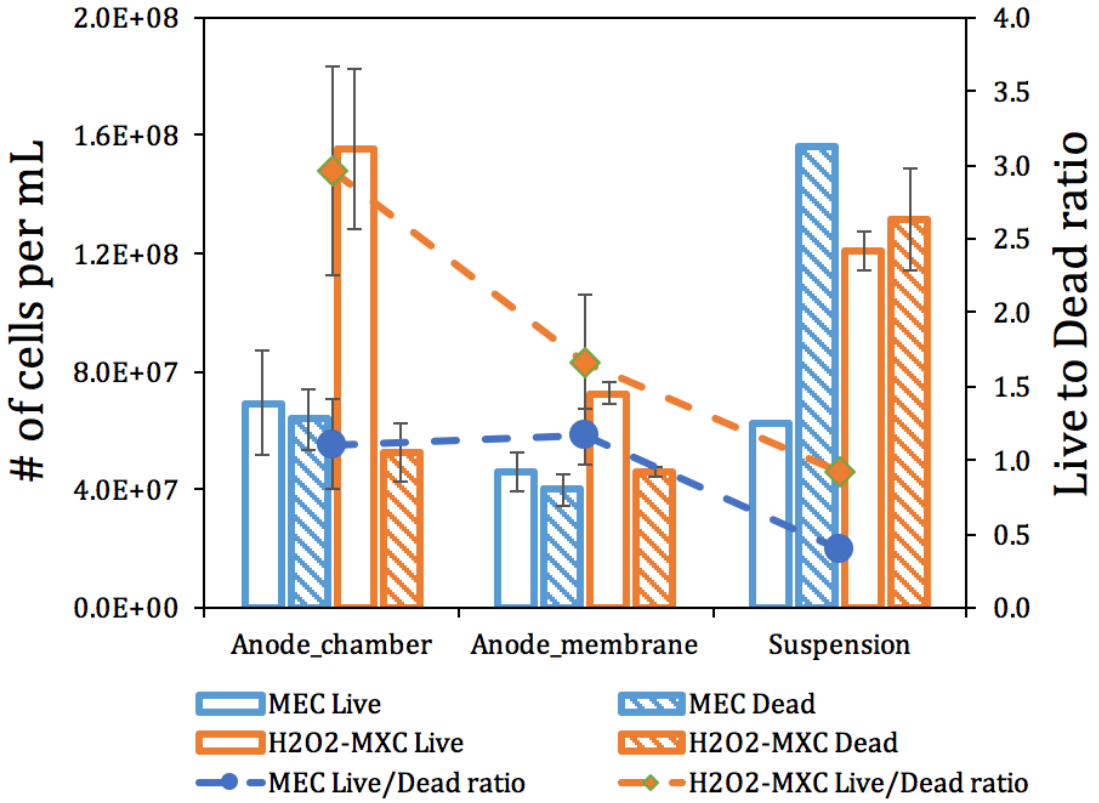

Figure B.3. Ratio of live/dead ratio and cell densities of live/dead bacteria on the carbon fiber anode: toward anode chamber and membrane, and in suspension. Cell counts were normalized by the volume added in the cell counting slide for each sample.

Figure B.3 shows the ratio of live-to-dead in each sample (anode biofilm of the chamber side, anode biofilm of the membrane side, and anode suspension) of two conditions: MEC and H_2O_2 cell. Before changing reactor mode from MEC to H_2O_2 cell, the MEC operated around 4 months aforementioned. Cell (live and dead) numbers of biofilms on the anode at both side of anode chamber and membrane are similar to the MEC mode, but the dead cells in suspension was much higher than the live cells, resulting in the low live-to-dead ratio, 0.4. On the other hand, after changing to H_2O_2 cell mode, live cells increased on the anode at both sides of anode chamber and membrane. Despite of the increased live cells in suspension, dead cells were still high

fraction, resulting in lower live-to-dead ratio, 0.9. Lower live-to-dead ratios in suspension (or high fraction of dead cells) at both cases indicate that cells decayed from biofilm might flow toward suspension in the anode chamber. Our original hypothesis of H_2O_2 inhibition to anode biofilm and thus limiting performance seems incorrect because of 1) slow diffusion of H_2O_2 from cathode to anode, 2) low concentration of H_2O_2 produced, and 3) strong, thick and healthy biofilm formation. Interestingly, the number of live cells and the ratio of live to dead are increased in H_2O_2 cell mode, compared to MEC mode. The most probable reason would be long-term operation in MEC mode, where dead cells might be deposited with time on the fiber. At the end of MEC operation, I scraped off solids attached on the fiber for collecting biofilm samples for microbial community and live/dead cell assay, possibly resulting in physical elimination of dead cells at the time. One difference between MEC and H_2O_2 cell is the ratio of live-to-dead on two difference side of the anode (chamber and membrane). In MEC, the ratio was similar, while I can clearly see much lower value of the ratio in membrane side of anode, which is statistically significance ($p<0.05$). Also the color of biofilm and solids were significantly different at the end of H_2O_2 cell operation, compared to MEC operation (Figure B.2). It indicates that H_2O_2 or O_2 diffusion might affect the phenomenon. Microbial community analysis then could be important as described in the next section.

Principal Coordinate Analysis

The Principal Coordinate Analysis (PCoA) shows that the community composition of suspension and biofilm samples were clearly distinct from each other (Figure B.4). AnS and BfC grouped together having relatively high value of PC1 and PC2, respectively. The separation of BfM in MEC and H_2O_2 cell on PC1 and PC2 seem to

correspond with differences of the microbial community structure. In addition, among the top-nine genera in the suspension and biofilm communities, I can clearly see the key phylotypes at the genus level in each sample.

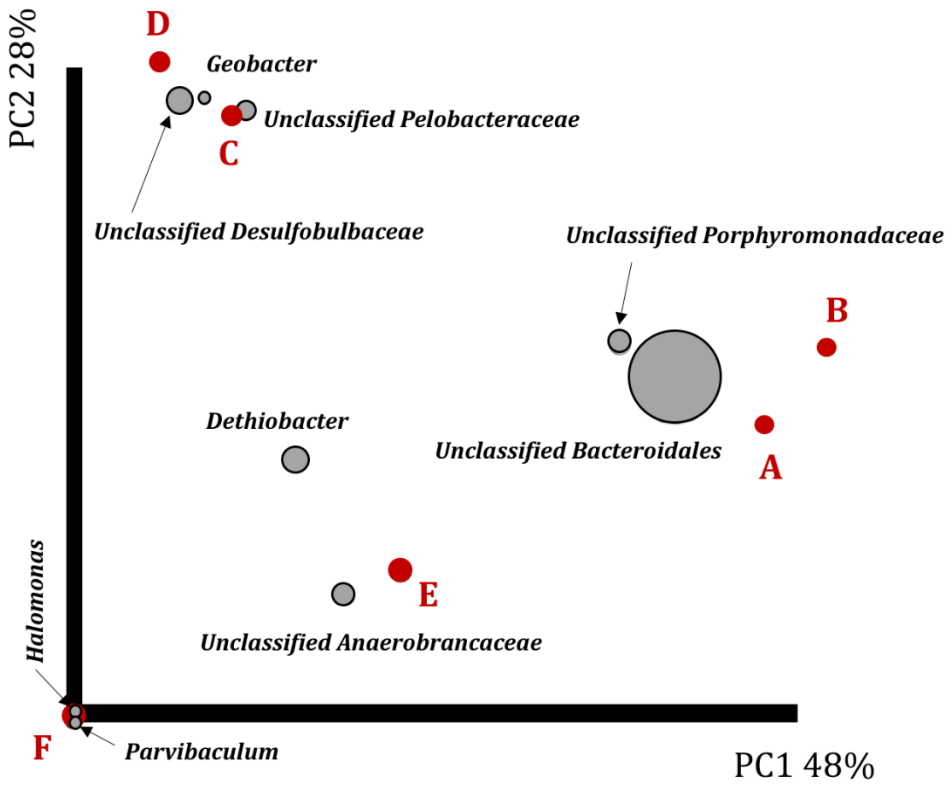

Figure B.4. Principal Coordinate Analysis (PCoA) bi-axis plot based on weighted UniFrac analysis for 6 samples (A-F) from MEC and H_2O_2 cell: MEC AnS (A), H_2O_2 cell AnS (B), MEC BfC (C), H_2O_2 cell BfC (D), MEC BfM (E), and H_2O_2 cell BfM (F). These samples (A-F) are represented by red circles. The most abundant genera are superimposed on the PCoA as dark-gray circles. The size of the dark-gray circles represents mean abundances of those taxons across reactor samples (A-F). While unclassified *Bacteroidales* pull the anode suspension samples (A and B) away from others on PC1, *Geobacter* and unclassified *Desulfobulbaceae* separate biofilms of chamber side from others on PC2.

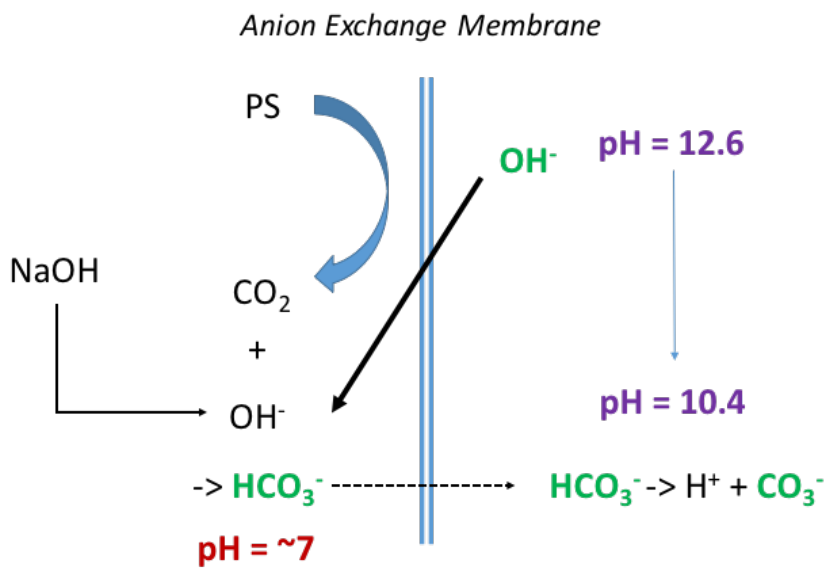

Figure B.5. Possible mechanisms ions migration and diffusion across the anion exchange membrane between anode can cathode

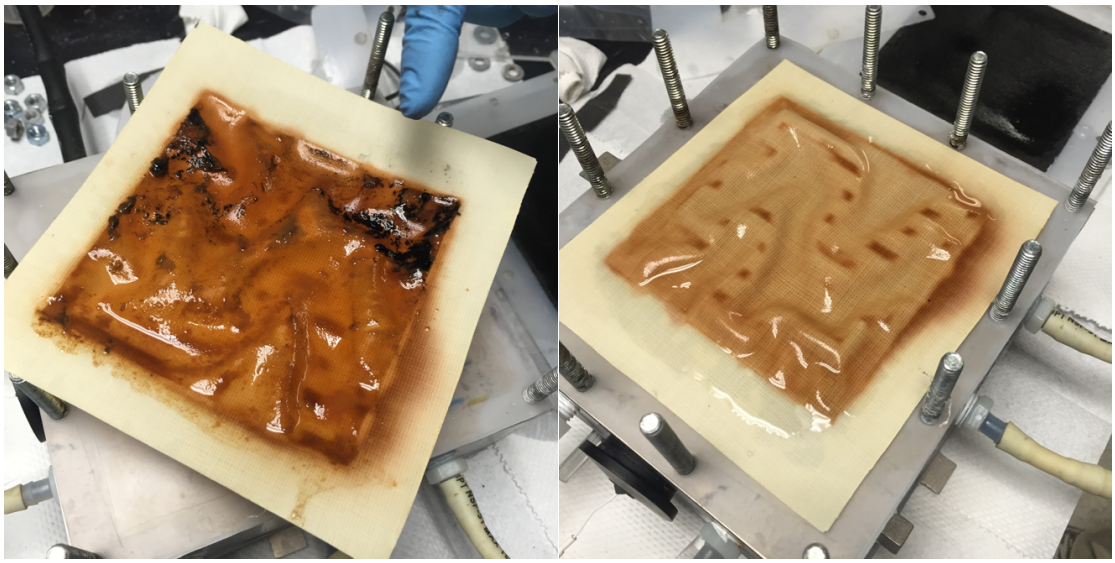

Figure B.6. Anion exchange membrane used during H_2O_2 cell fed with PS for 27 days. Left (anode side) and Right (cathode chamber side).

I performed H_2O_2 decay tests in 100 mM solutions of sodium carbonate, sodium bicarbonate, and sodium hydroxide with ~2700 mg L^{-1} of H_2O_2. Although pH was maintained stable during ~1 day operation, H_2O_2 in sodium carbonate decreased very rapidly and 99% removed in 23 hours, while H_2O_2 in positive control with deionized water was very stable and H_2O_2 in sodium hydroxide and sodium bicarbonate were relatively stable with 9 and 28% removal in 23 hours.

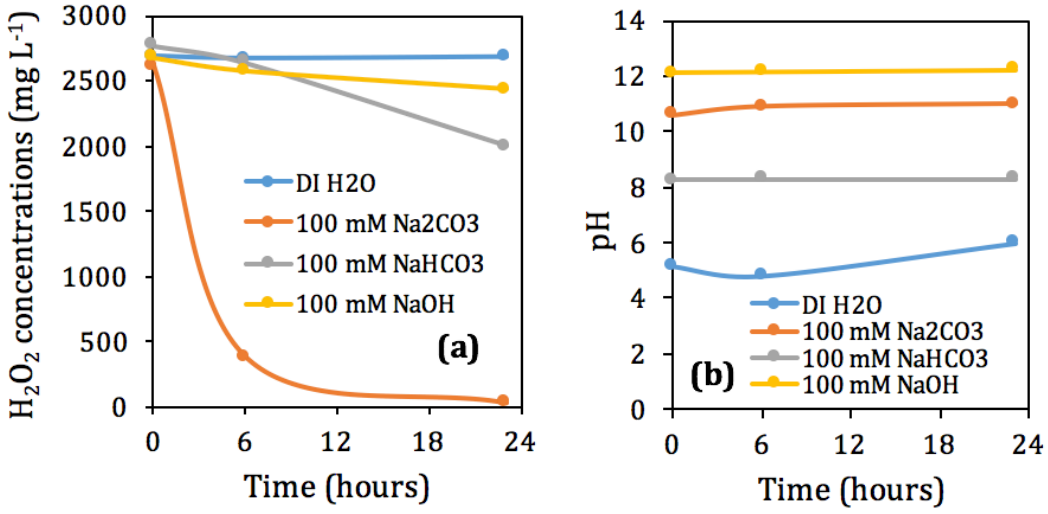

Figure B.7. H_2O_2 decay with time in different solutions: 100 mM sodium carbonate, sodium bicarbonate, and sodium hydroxide. (a) H_2O_2 concentration and (b) pH.

Table B.2. H_2O_2 producing microbial electrochemical cell studies using real wastewater

Authors	Anolyte	Anode HRT	Membrane type	Catholyte	Maximum H_2O_2 conc. (wt %)	Maximum current & voltage applied	Energy input (kWh/kg H_2O_2)	PPE (%)*
Arends et al. (2014)	Wetland effluent	Batch	AEM	50 mM NaCl	0.056%	10 A/m² at 0.6 V	2.5	~40
Modin & Fukushi (2012)	Domestic wastewater	6 min HRT	CEM	50 mM NaCl	0.008%	0.2 A/m² at 0.6 V	18.2	4.8
Modin & Fukushi (2013)	Domestic wastewater	15 min HRT	CEM	50 mM NaCl	0.23%	0.5 A/m² at 1 V	8.3	37-66
Sim et al. (2015)	Raw domestic wastewater	2-10 hr HRT	CEM	Deionized water	0.001%	0.56 A/m² at 12 V	78	~10-70
This study	Primary sludge	9 day HRT	AEM	50 mM NaOH	0.023%	1 A/m² at 0.2 V	0.87	4-72

* PPE: H_2O_2 production efficiency

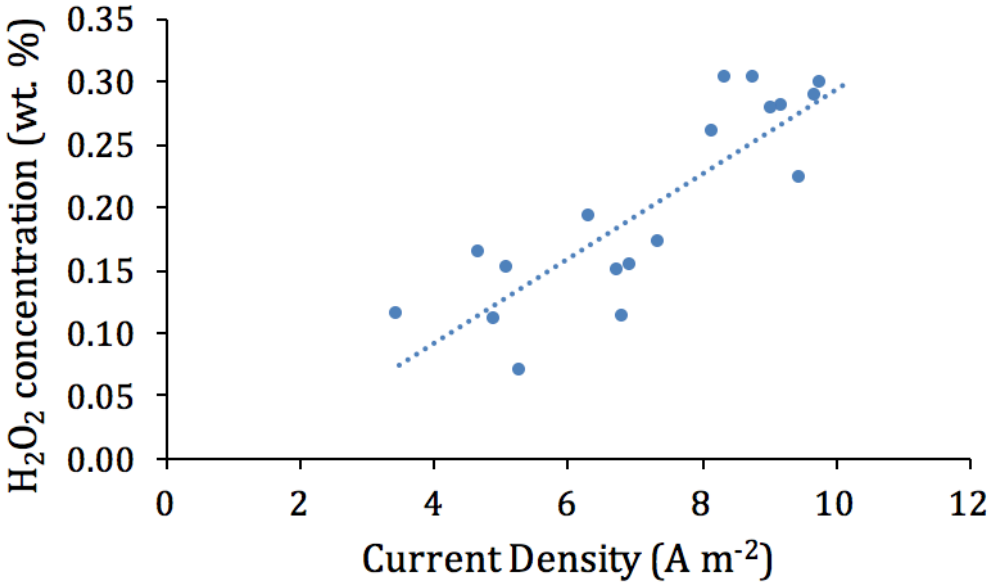

Figure B.8. A linear relationship between H_2O_2 concentration and current density at values up to 10 A m^{-2}. This result was from the experiment in H_2O_2 cell fed with 50 mM acetate medium.

Table B.4. Summary of alpha diversity of microbial communities of the influent PS, anode surface toward chamber and membrane in MEC and H_2O_2 cell

	MEC			H_2O_2 cell		
	Influent PS	Anode-chamber	Anode-membrane	Influent PS	Anode-chamber	Anode-membrane
# of sequences	58,557	64,681	56,365	35,928	58,902	55,570
subsamples	35,500	35,500	35,500	35,500	35,500	35,500
Observed OTUs	1393 (± 3)	1576 (± 3)	1386 (± 1)	1384 (± 2)	1180 (± 0)	1250 (± 2)
Chao1	1964 (± 18)	2419 (± 25)	1862 (± 6)	1663 (± 10)	1798 (± 19)	1588 (± 6)
Phylogenetic diversity	108	110	109	114	93	94
Evenness	0.506	0.495	0.466	0.535	0.430	0.529
Shannon Index	5.29	5.26	4.86	5.58	4.39	5.45
Simpson	0.907	0.917	0.879	0.900	0.842	0.933